NUMERICAL INVESTIGATION AND MODELLING OF SOLAR PHOTOVOLTAIC/THERMAL SYSTEMS

AFROZA NAHAR

INSTITUTE OF GRADUATE STUDIES
UNIVERSITY OF MALAYA
KUALA LUMPUR

2017

NUMERICAL INVESTIGATION AND MODELLING OF SOLAR PHOTOVOLTAIC/THERMAL SYSTEMS

AFROZA NAHAR

THESIS SUBMITTED IN FULFILMENT OF THE REQUIREMENTS FOR THE DEGREE OF DOCTOR OF PHILOSOPHY

INSTITUTE OF GRADUATE STUDIES
UNIVERSITY OF MALAYA
KUALA LUMPUR

2017

UNIVERSITY OF MALAYA

ORIGINAL LITERARY WORK DECLARATION

Name of Candidate: **Afroza Nahar**

Registration/Matric No: **HHD 110001**

Name of Degree: **Doctor of Philosophy**

Title of Thesis ("this work"): **Numerical Investigation and Modelling of Solar Photovoltaic/Thermal Systems**

Field of Study: **Solar Thermal**

I do solemnly and sincerely declare that:

(1) I am the sole author/writer of this Work;
(2) This Work is original;
(3) Any use of any work in which copyright exists was done by way of fair dealing and for permitted purposes and any excerpt or extract from, or reference to or reproduction of any copyright work has been disclosed expressly and sufficiently and the title of the Work and its authorship have been acknowledged in this Work;
(4) I do not have any actual knowledge nor do I ought reasonably to know that the making of this work constitutes an infringement of any copyright work;
(5) I hereby assign all and every right in the copyright to this Work to the University of Malaya ("UM"), who henceforth shall be owner of the copyright in this Work and that any reproduction or use in any form or by any means whatsoever is prohibited without the written consent of UM having been first had and obtained;
(6) I am fully aware that if in the course of making this Work I have infringed any copyright whether intentionally or otherwise, I may be subject to legal action or any other action as may be determined by UM.

Candidate's Signature Date:

Subscribed and solemnly declared before,

Witness's Signature Date:

Name:

Designation:

ABSTRACT

Solar energy is the most promising resource among all other renewable energy, because of its inexhaustible supply, environmental friendly notion and options for harnessing the energy directly from the Sun. Solar energy may be harvested as thermal energy by solar thermal collector (STC) as well as electrical energy through solar photovoltaic (PV) module. Hybrid photovoltaic thermal (PV/T) module is combination both of these solar thermal and PV which is a well-engineered solar co-generation system in one physical profile. One of the major shortcomings of PV technology is its poor energy conversion efficiency; commercially available solar cells have efficiency from 4 to 17%. Moreover, traditional silicon solar cells suffer from a drop in efficiency by 0.4–0.65% per degree increase in cell temperature. The heat produced in the PV cells which would otherwise be wasted, is taken away to make use in different thermal applications. The main problem of PV/T is the effectual removal of heat from the module and transfers heat to end users for making efficient utilization. In the present research, attempt has been made to design and develop several configurations of thermal collector with the novel concept of excluding absorber plate. This elimination of absorber plate from thermal collector is done with a view to make the design simple and ensuring well integration with PV module. In addition, elevation head has been employed to maintain the circulation of water inside the flow channel in order to save the power that would otherwise be consumed in pumping. A three-dimensional mathematical model of PV/T module based on the above concept is developed and simulated in finite element based (FEM) based software COMSOL Multiphysics®. The validation of the model has been ascertained through outdoor experimentation for a representative design. In numerical simulation, effect of various parameters like inlet velocity, water inlet temperature and environment conditions like irradiation, ambient temperature have been investigated to evaluate the performance of PV/T module. All of the investigations are made with two

channel materials: aluminum and copper. The numerical results with the representative design were found to be in well agreement with the corresponding experimental outcomes. Based on this validated mathematical model, performance of the other designs has been evaluated by numerical simulation. Also, numerical results show that thermal performance without absorber plate was found as good as that with absorber plate. Maximum overall efficiency of the PV/T has been obtained with parallel plate flow configuration. For aluminum and copper flow channels, the overall efficiencies are 86% and 89%, respectively. The highest output power of 129.2 W and the maximum electrical efficiency of 12.6% are achieved with copper channel of same flow design. Regarding the effect of channel materials on PV/T performance, no significant dominance of any of the material aluminum or copper was found. In the present research, a new concept of thermal collector without absorber plate has been proposed and the performance of PV/T is found acceptable using this collector. This type of thermal collector reduces the weight and cost of the system.

ABSTRAK

Tenaga solar adalah pilihan yang paling menjanjikan di antara sumber tenaga yang boleh diperbaharui, kerana bekalan yang tidak putus, mesra alam sekitar dan pilihan untuk memanfaatkan tenaga secara langsung dari matahari. Tenaga solar boleh dituai sebagai tenaga haba oleh pengumpul haba matahari (STC) dan juga tenaga elektrik melalui modul solar fotovoltaik (PV). Hibrid fotovoltan terma (PV/T) adalah gabungan kedua-dua solar haba dan PV merupakan sistem penjanaan solar baik-kejuruteraan dalam satu profil fizikal. Salah satu kelemahan utama teknologi PV adalah kecekapan penukaran tenaga; secara komersial sel-sel solar mempunyai kecekapan daripada 4 hingga 17%. Selain itu, sel-sel solar silikon tradisional mengalami penurunan dalam kecekapan dengan 0.4 – 0.65% pada setiap peningkatan darjah dalam suhu sel. Haba yang dihasilkan dalam sel-sel PV yang disia-siakan, akan diambil untuk digunakan dalam aplikasi haba yang berbeza.Masalah utama PV/T adalah penyingkiran berkesan haba dari modul dan pemindahan haba kepada pengguna akhir untuk membuat penggunaan yang cekap. Dalam kajian ini, percubaan telah dibuat untuk mereka bentuk dan membangunkan beberapa konfigurasi pengumpul haba dengan konsep novel tidak termasuk plat penyerap. Penghapusan plat penyerap daripada pengumpul haba dilakukan dengan tujuan untuk membuat reka bentuk yang mudah dan memastikan integrasi yang baik dengan modul PV. Di samping itu, turus aras telah dilaksanakan untuk mengekalkan peredaran air di dalam saluran aliran untuk menjimatkan kuasa yang sebaliknya akan digunakan di dalam pam. Tiga dimensi model matematik PV/T modul berdasarkan konsep di atas dibangunkan dan disimulasi dalam dasar elemen terhad (FEM) berasaskan perisian COMSOL Multiphysics®. Pengesahan model yang telah ditentukan melalui eksperimen luar untuk wakil reka-bentuk. Dalam simulasi berangka, pelbagai kesan parameter seperti halaju masuk, suhu masukan air dan keadaan alam sekitar seperti sinaran, suhu ambien telah dikaji untuk menilai prestasi

PV/T modul. Semua penyiasatan dibuat dengan dua bahan saluran: aluminium dan tembaga. Keputusan berangka yang diwakili oleh reka bentuk didapati sepadan dengan hasil eksperimen tersebut. Berdasarkan model matematik yang sah, prestasi reka bentuk yang lain telah dinilai oleh simulasi berangka. Keputusan berangka juga menunjukkan bahawa prestasi terma tanpa plat penyerap didapati bagus seperti dengan menggunakan plat penyerap. Kecekapan maksimum keseluruhan untuk PV/T telah diperolehi dengan konfigurasi aliran plat selari. Untuk saluran aliran aluminium dan tembaga, kecekapan keseluruhan adalah 86% dan 89% masing-masing. Kuasa keluaran tertinggi adalah 129.2 W dan kecekapan maksimum elektrik adalah 12.6% dicapai dengan saluran reka-bentuk tembaga yang sama. Mengenai kesan bahan-bahan saluran pada prestasi PV/T, tiada dominasi kepentingan mana-mana daripada bahan aluminium atau tembaga ditemui. Dalam kajian ini, satu konsep baru pengumpul haba tanpa plat penyerap telah dicadangkan dan prestasi PV/T dengan pengumpul terma ini didapati memuaskan. Jenis pengumpul haba ini akan mengurangkan berat dan sistem kos.

ACKNOWLEDGEMENTS

The sole gratitude and thanks is only for the almighty Allah (s.w.t) for the help and divine guidance that He bestowed upon me in course of the research work.

I would like to express my earnest reverence and gratitude to my supervisors Professor Dr. Nasrudin Abd. Rahim and Dr. Md. Hasanuzzaman for their sincere supervision, valuable suggestions, professional directives and compassionate support all the way through this research work.

Special thanks to all the staffs of the UM Power Energy Dedicated Advanced Centre (UMPEDAC) of University of Malaya for their support during this research work.

My deepest gratitude goes to my family for the pain they endured because of my obsessive engagement in research. Without their continual encouragement and support I would not have been able to reach my goal.

TABLE OF CONTENTS

Abstract iii

Abstrak v

Acknowledgements vii

Table of Contents viii

List of Figures xiv

List of Tables xvii

List of Symbols and Abbreviations xviii

CHAPTER 1: INTRODUCTION 1

1.1 World Energy Scenario 1

1.2 Renewable Energy Sources 5

1.2.1 Bioenergy 6

1.2.2 Geothermal Energy 6

1.2.3 Hydropower 7

1.2.4 Ocean or Marine Energy 8

1.2.5 Wind Energy 8

1.2.6 Solar Energy 9

1.3 Solar Energy Technologies 10

1.3.1 Solar Photovoltaic Technology 11

1.3.2 Solar Thermal Technology 14

1.3.2.1 Solar thermal heat 14

1.3.2.2 Solar thermal electricity 16

1.3.3 Hybrid Photovoltaic Thermal Technology 18

1.4 Problems Statement 19

1.5 Objectives of the Research Work 20

1.6 Scope of the Research Work 21
1.7 Research Methodology 21
1.8 Organization of the Thesis 22

CHAPTER 2: LITERATURE REVIEW 24

2.1 Introduction 24
2.2 Photovoltaic Thermal Technology: Historical Overview 24
2.3 Photovoltaic Thermal Collectors: Overview on Classification 26
2.4 Classification Based on Design Geometry 27
2.4.1 Flat-Plate PV/T 27
2.4.2 Concentrator PV/T 29
2.4.3 Building-integrated PV/T 31
2.5 Classification Based on HTF 33
2.5.1 Air Based PV/T Collectors 34
2.5.2 Water Based PV/T Collectors 39
2.5.2.1 Sheet-and-tube PV/T collectors 40
2.5.2.2 Channel PV/T collectors 40
2.5.2.3 Free-flow PV/T collectors 41
2.5.2.4 Two-absorber PV/T collectors 42
2.5.3 Heat Pipe Based PV/T Collectors 44
2.5.4 Refrigerant Based PV/T 46
2.6 Summary of Research Works 47
2.7 Performance Evaluation Criteria for PV/T 52
2.7.1 Mass Flow Rate 52
2.7.2 Effect of Temperature 54
2.7.3 Collector Geometry 55
2.7.4 Effect of Glazing 56

2.7.5 Packing Factor 56
2.7.6 Absorber and Thermal Collector Materials 58
2.7.7 PV Cell Materials 59
2.8 Improvement Techniques and Relevance of the Present Research 61

CHAPTER 3: THEORETICAL BACKGROUND 65

3.1 Photovoltaic Thermal System: An Optimized Solar PV 65
3.2 Photovoltaic Thermal System Overview 66
3.2.1 Construction of a PV/T Module 66
3.2.2 Working Principle of PV/T 68
3.2.3 Application Areas of PV/T 68
3.2.3.1 Household applications 69
3.2.3.2 Hospitals and hotels 70
3.2.3.3 Space heating 70
3.2.3.4 Industrial applications 70
3.2.3.5 Agricultural application 71
3.2.3.6 Building integrated PV/T 71
3.2.3.7 Solar desalination 72
3.2.4 Advantages of PV/T Technology 72
3.2.5 Limitations of PV/T Technology 73
3.3 PV/T Related Heat Transfer and Fluid Flow Parameters 74
3.3.1 Conduction Heat Transfer 74
3.3.2 Convection Heat Transfer 74
3.3.3 Radiation Heat Transfer 75
3.3.4 Convection Heat Transfer Coefficient 76
3.3.5 Thermal Conductivity and Specific Heat Capacity 76
3.3.6 Nusselt Number, Grashof Number and Prandtl Number 77

3.3.7 Laminar vs. Turbulent Flow: Reynolds Number 78
3.3.8 Conjugate Heat Transfer 80
3.3.9 Steady and Unsteady Analysis 81

CHAPTER 4: RESEARCH METHODOLOGY 82

4.1 Introduction 82
4.2 Mathematical Modelling and Numerical Simulation 83
4.2.1 Finite Element Method 84
4.2.2 COMSOL Multiphysics® 86
4.3 PV/T Layers 87
4.3.1 Glass Layer 87
4.3.2 Ethylene Vinyl Acetate Layer 88
4.3.3 Polycrystalline Silicon Cell Layer 88
4.3.4 Poly Vinyl Fluoride or Tedlar Layer 88
4.3.5 Adhesive Layer 88
4.3.6 Flow Channel Wall Layer 89
4.3.7 Heat Transfer Fluid Layer 89
4.4 Mathematical Modelling 89
4.4.1 Governing Equations 89
4.4.2 Boundary Conditions 90
4.4.3 Mesh Generation 91
4.5 Mathematical Modelling for Proposed Design 94
4.5.1 Heat Transfer Correlations 96
4.5.2 Energy Analysis 98
4.5.3 Thermo-Physical Properties and Design Parameters 100
4.6 Experimental Investigations 101
4.6.1 Experimental Set Up 101

4.6.1.1 PV module 102
4.6.1.2 Thermal collector for experimental study 103
4.6.1.3 Thermal collectors for numerical study 105
4.6.2 Instrumentation and Control 108
4.6.2.1 I-V tracer 109
4.6.2.2 Pyranometer 109
4.6.2.3 Flow meter 110
4.6.2.4 Thermocouple 111
4.6.2.5 Data logger 112
4.6.3 Experimental Procedure 112

CHAPTER 5: RESULTS AND DISCUSSION 115

5.1 Introduction 115
5.2 Justification of Exclusion of Absorber Plate 116
5.3 Experimental Validation 118
5.4 Performance Evaluation of PV/T with Parallel Plate Flow Channel 121
5.4.1 Numerical Simulation Results 121
5.4.2 Experimental Results 125
5.4.2.1 Effect on inlet velocity 127
5.4.2.2 Effect of irradiation 133
5.5 Numerical Simulation Results with Different Collector Designs 136
5.5.1 Effect of Inlet Velocity on Temperature Distribution Throughout the Flow Channel 136
5.5.2 Effect of Inlet Velocity on Temperature Distribution Throughout the PV/T Module 144
5.5.3 Effect of Inlet Velocity 148
5.5.3.1 On cell temperature and water outlet temperature 148

5.5.3.2 On PV/T performance 151
5.5.4 Effect of Inlet Temperature on Overall Performance of PV/T Module . 155
5.5.5 Effect of Cell Temperature on Electrical Performance of PV Module .. 157
5.5.6 Effect of Ambient Temperature on the Performance of PV/T 159
5.5.7 Effect of Absorbed Solar Radiation on the Performance of PV/T 163
5.6 A Compendium on Different Flow Channel Design 166

CHAPTER 6: CONCLUSIONS AND RECOMMENDATIONS 170
6.1 Conclusions 170
6.2 Recommendations for Further Works 171
References 173
List of Publications and Presented Papers 188

LIST OF FIGURES

Figure 1.1: Global energy consumption by sources up to 2040 2

Figure 1.2: Energy related CO_2 emission by fuel types, 1990-2040 3

Figure 1.3: Share of renewable energies in global final energy consumption, 2014 4

Figure 1.4: Renewable energy share in world electricity generation, End-2015 5

Figure 1.5: Comparison of the other energy resources with solar energy 9

Figure 1.6: Solar energy conversion technologies 11

Figure 1.7: The photovoltaic effect 12

Figure 1.8 : Spectral content of incident solar radiation 13

Figure 1.9: Optical and thermal losses of a flat-plate collector 15

Figure 1.10: Heat pipe based collector 16

Figure 1.11: Applications of concentrating solar collector 17

Figure 1.12: Solar thermal power plant 18

Figure 2.1: Schematic of a typical flat-plate PV/T 28

Figure 2.2: Schematic of a concentrator PV/T 30

Figure 2.3: PV/T classification based on HTF 33

Figure 2.4: (a) Unglazed PV/T air collector (i) without tedlar (ii) with tedlar. (b) Glazed PV/T air collector (i) without tedlar (ii) with tedlar 34

Figure 2.5: Various PV/T air collector designs 36

Figure 2.6: Single-pass and double-pass PV/T air collectors 37

Figure 2.7: Water based PV/T collectors; (a) sheet-and-tube, (b) channel, (c) free- flow, (d) two-absorber 42

Figure 2.8: Schematic of refrigerant based PV/T collector 47

Figure 3.1: Construction of a PV/T module 67

Figure 3.2: Water temperature requirement for various purposes 69

Figure 4.1: Three-dimensional finite element mesh 85

Figure 4.2: Cross section of PV/T module 87

Figure 4.3: PV/T collector meshed in COMSOL Multiphysics® using the physics controlled mesh sequence 92

Figure 4.4: Schematic diagram of the experimental set up 101

Figure 4.5: Poly-crystalline PV module 102

Figure 4.6: Parallel plate flow channel 104

Figure 4.7: Pancake flow channel 106

Figure 4.8: Parallel square pipe flow channel 107

Figure 4.9: Serpentine flow channel 108

Figure 4.10: *I-V* tracer 109

Figure 4.11: Pyranometer (LI-COR, Model: PY82186) 110

Figure 4.12: Flow meter (Model: LZB-10B) 111

Figure 4.13: K-type thermocouple 111

Figure 4.14: Data Taker DT80 112

Figure 4.15: Instrumentation of the experimental set up 114

Figure 5.1: Comparison of PV/T performance with and without absorber plate 117

Figure 5.2: Validation of the experimental results by (a) thermal efficiency, (b) overall efficiency 119

Figure 5.3: Attainment of steady state conditions in the simulation study 122

Figure 5.4: 3D surface plot of temperature for flow channel at steady state 123

Figure 5.5: 3D surface plot of temperature distribution throughout PV module 124

Figure 5.6: PV module top and bottom surface temperature and ambient temperature as a function of daytime (May 9, 2016) 126

Figure 5.7: Electrical power output of the PV as a function of daytime (May 9, 2016) 126

Figure 5.8: Thermal energy gain of PV/T module as a function of daytime (May 9, 2016) 127

Figure 5.9: Effect of inlet velocity on the performance of PV/T at irradiation 1000 W/m^2 129

Figure 5.10: Effect of cell temperature on PV performance (a) output power, (b) electrical efficiency at irradiation level 1000 W/m^2 132

Figure 5.11: Effect of irradiation on PV performance (a) output power (b) electrical efficiency at inlet velocity 0.0007 m/s 135

Figure 5.12: Effect of inlet velocity on temperature distribution throughout the pancake flow channel 139

Figure 5.13: Effect of inlet velocity on temperature distribution throughout the parallel square pipe flow channel 141

Figure 5.14: Effect of inlet velocity on temperature distribution throughout the sepentine flow channel 143

Figure 5.15: Effect of inlet velocity on temperature distribution throughout panel 145

Figure 5.16: Effect of inlet velocity on temperature distribution throughout panel 146

Figure 5.17: Effect of inlet velocity on temperature distribution throughout panel 147

Figure 5.18: Effect of inlet velocity on (a) cell temperature and (b) water outlet temperature of the PV/T module for all designs with Al and Cu flow channels 150

Figure 5.19: Effect of inlet velocity on the performance of PV panel for all designs with both Al and Cu flow channels 153

Figure 5.20: Effect of inlet temperature on PV/T performance for both Al and Cu flow channels 156

Figure 5.21: Effect of cell temperature (a) output power (b) electrical efficiency for both Al and Cu flow channels under cooling system 158

Figure 5.22: Effect of ambient temperature on the performance of PV/T panel for both Al and Cu flow channels 161

Figure 5.23: PV/T performance variation with absorbed radiation for both Al and Cu flow channels 164

LIST OF TABLES

Table 1.1: Merits, demerits and applications of solar energy 10

Table 2.1: Comparison of the efficiency of PV, STC and PV/T air collector 39

Table 2.2: Comparison of air and water as heat transfer fluid (HTF) for PV/T 44

Table 2.3 Highlights of the research works by different researchers..... 48

Table 2.4: Mass flow rate ranges adopted by different researchers..... 53

Table 2.5: Characteristics of absorptive coatings 58

Table 2.6: PV cell material types - merits, demerits and efficiency level 60

Table 2.7: Effect of control parameters on PV/T system efficiency..... 63

Table 4.1: Statistic of mesh generation by COMSOL Multiphysics® 93

Table 4.2: PV/T collector materials and thermal properties 100

Table 4.3: Thermal collector specification 100

Table 4.4: The values of design parameters used in the numerical simulation 100

Table 4.5: Specifications of the PV module 103

Table 4.6: Measuring range and least count of the measuring instruments..... 114

Table 5.1: Increment in electrical efficiency and output power per 1^{o}C decrement in cell temperature 133

Table 5.2: Change in PV performance parameters per 100 W/m^2 increase in radiation 134

Table 5.3: Increase in electrical efficiency and output power per 1^{o}C increase of cell temperature 159

Table 5.4: Comparison in performance of PV/T with different collector designs..... 167

Table 5.5: Increase in electrical efficiency and output power per 1^{o}C decrease in cell temperature (R = 1000 W/m^2, T_{in} = 27^{o}C and T_{amb} = 27^{o}C) 168

Table 5.6: Change in electrical efficiency and output power per 100 W/m^2 increase in radiation (T_{in} = 27^{o}C and T_{amb} = 27^{o}C) 169

LIST OF SYMBOLS AND ABBREVIATIONS

A_c	:	Total PV cell area (m^2)
A_f	:	Cross-sectional area of the duct (m^2)
C_p	:	Specific heat at constant pressure (J/kg.K)
E_c	:	Total solar energy rate into the cell (W)
E_{el}	:	Electrical energy rate (W)
E_{th}	:	Thermal energy rate extracted by water (W)
g	:	Accelaration due to gravity (m/s^2)
h	:	Heat transfer coefficient ($W/m^2.K$)
k	:	Thermal conductivity (W/m.K)
L	:	Length (m)
$\dot{m}$	:	Mass flow rate (kg/s)
Nu	:	Nusselt number
p	:	Pressure (Pa)
Pe	:	Perimeter (m)
P_c	:	Packing factor
Pr	:	Prandtl number
q	:	Inward heat flux (W/m^2)
R	:	Solar irradiance (W/m^2)
Ra	:	Rayleigh number
Re	:	Reynolds number
T	:	Temperature (^oC/K)
t	:	Time (s)
u,v,w	:	Velocity components along axes x, y and z
U	:	Overall heat transfer coefficient ($W/m^2.K$)

U_o : Inlet water velocity (m/s)

V : Wind speed (m/s)

Greek symbols

α : Absoptivity

β_{ref} : Temperature coefficient at reference temperature of 25^{o}C

μ : Dynamic viscosity (Pa.s)

ν : Kinematic viscosity (m^2/s)

ρ : Density (kg/m^3)

η : Efficiency (%)

$\overline{\eta_{el}}$: Average electrical efficiency (%)

τ : Transmissivity

ε : Emissivity

σ : Stefan-Boltzmann constant $W/(m^2.K^4)$

δ : Thickness (m)

Subscript

amb : Ambient

c : PV cell

el : Electrical

d : Duct

f : Fluid

g : Glass

in : Inlet

out	:	Outlet
ref	:	Reference
s	:	Sky
S	:	Solid/Surface
td	:	Tedlar
th	:	Thermal
tol	:	Total
w	:	Water

Abbreviation

Al	:	Aluminum
BE	:	Boundary element
BV	:	Boundary volume
BIPV	:	Building integrated photovoltaics
BIPV/T	:	Building integrated photovoltaic thermal
CFD	:	Computational fluid dynamics
CHP	:	Combined heat and power
CHT	:	Conjugate heat transfer
CPC	:	Compound parabolic collector
CPV	:	Concentrator photovoltaics
CPV/T	:	Concentrator photovoltaic thermal
CSP	:	Concentrating solar power
Cu	:	Copper
DC	:	Direct current
DSSC	:	Dye sensitized solar cell
DSWH	:	Domestic solar water heater

EIA	:	Energy information administration
ESTELA	:	European Solar Thermal Electricity Association
EVA	:	Ethyl vinyl acetate
FD	:	Finite difference
FE	:	Finite element
FEM	:	Finite element method
FV	:	Finite volume
GEA	:	Geothermal Energy Association
GHG	:	Greenhouse gas
GWEC	:	Global Wind Energy Council
HTF	:	Heat transfer fluid
IEA	:	International Energy Agency
IHA	:	International Hydropower Association
PV	:	Photovoltaic
PVF	:	Poly vinyl fluoride
PV/T	:	Photovoltaic thermal
REN21	:	Renewable Energy Policy Network for the 21st Century
STC	:	Standard testing condition
STE	:	Solar thermal electricity
WBA	:	World Bioenergy Association

CHAPTER 1: INTRODUCTION

1.1 World Energy Scenario

Energy is the keystone of modern civilization and one of the principal driving factors for the overall socio-economic growth of a country. Per capita energy consumption ranks the level of economic development of a country. Demand for energy is growing up day by day with increasing population and also with the level of gross domestic product (GDP). While the global GDP will rise by 3.3% per year between 2012 and 2040, the total world energy consumption will rise from 160,895.43 to 238,852.05 Terawatt-hour (TWh) during the same period, almost doubling the number (EIA, 2016).

The energy resources of the world consist of conventional fossil fuels like coal, oil, gas and contemporary solar energy and nuclear energy. Fossil fuels are hydrocarbons that represent stored solar energy formed from the remains of prehistoric plants and animals and accumulated during the past 300 to 400 million years (Hubbert, 2016). Fossil fuels afford most of the energy demand as these are relatively cheap and convenient to explore and exploit and will remain the dominant form of energy providing around 60% of the additional energy in 2035 (BP, 2016). The global energy consumption trend, as shown in Figure 1.1, predicts that the contribution of non-fossil fuels (oil, gas, coal) in the energy mix in 2040 will be 78% despite of the faster growing trend of the non-fossil fuels (renewable and nuclear energy) (EIA, 2016).

However, the problem with fossil fuels is that they contribute highly to global warming by emitting tons of carbon dioxide (CO_2) and other pollutants from their combustion. By 2040 world energy related CO_2 emissions, as predicted in Figure 1.2, is likely to reach 43.2 billion metric tons (EIA, 2016). Moreover, fossil fuel based power generation system is non-renewable in nature, that is, the consumed reserves are not

replenished naturally. The amount of accessible energy resources in this planet is very much limited and the principal energy sources like coal, mineral oil and natural gas all are depleting rapidly due to the ever increasing consumption.

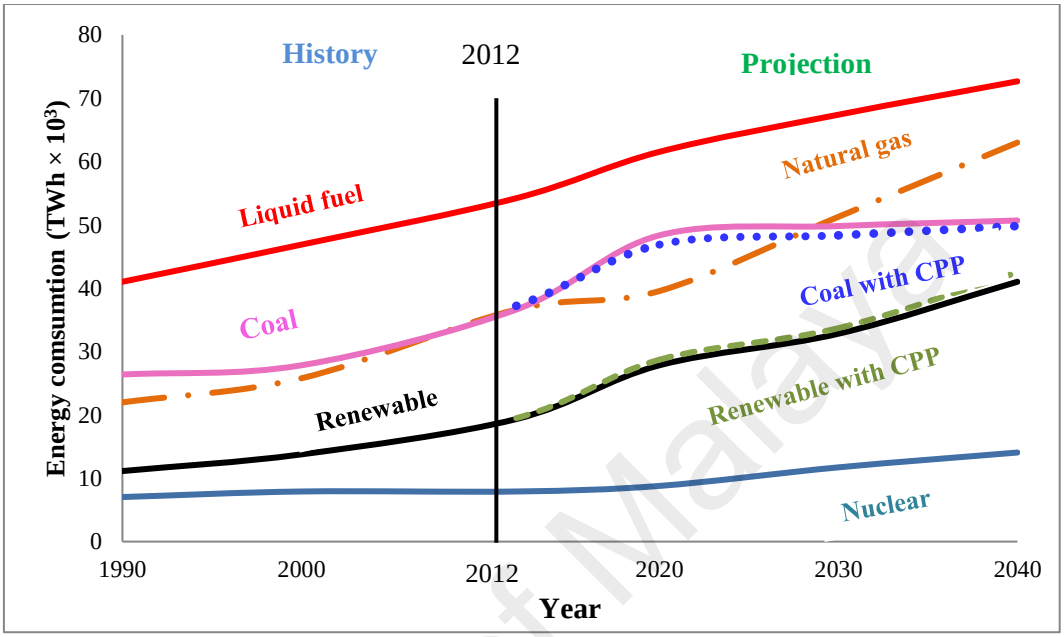

Figure 1.1: Global energy consumption by sources up to 2040 (EIA, 2016)

In addition, fossil fuel sources are being spent out in a non-sustainable manner. Also this sector is most incentivized by governments all around the world to keep the price low which builds pressure on the economy. Since clean energy is a pre-requisite for sustainable development, it has become exigent to expand technologies to ensure efficient use of renewable energy sources to solve the problem with fossil fuels.

With the present situation of growing energy demand, ascending energy prices, and strengthening the countermeasures for global warming, renewable energy sources have got the limelight of the energy market. In the last decade, renewable energy has emerged as world's fastest-growing energy source and its consumption will increase by 2.6% per annum between 2012 and 2040, whereas nuclear power will rise at a rate of 2.3% per annum over the same period (EIA, 2016).

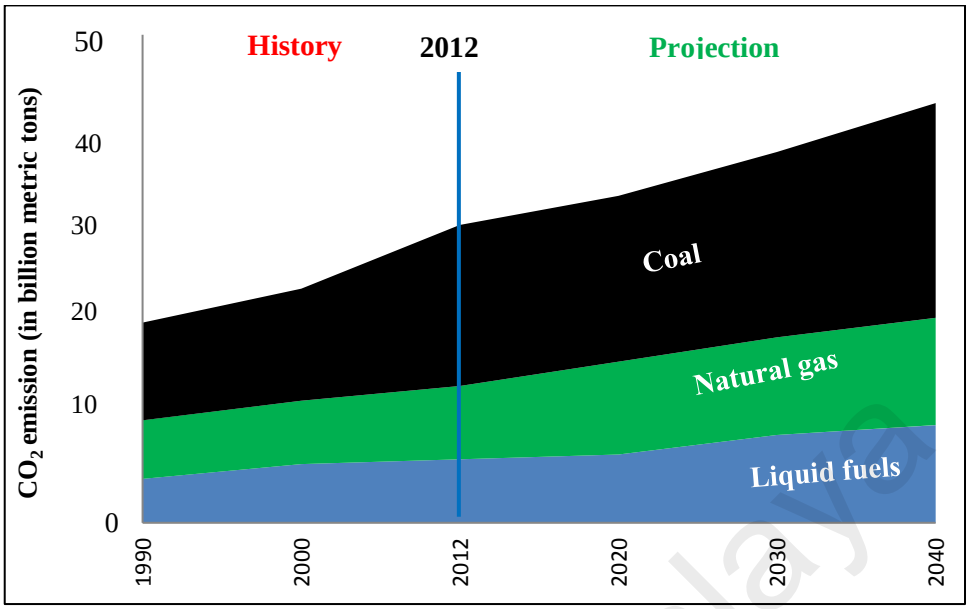

Figure 1.2: Energy related CO_2 emission by fuel types, 1990-2040 (EIA, 2016)

Renewables are now established as the mainstream energy source all around the world. The rapid growth of renewable energy is the resultant of issues like cost-competitiveness of these technologies, concern over energy security, climate change and thriving energy demand in developing and emerging economies. The estimated contribution of the renewable energy sources as final energy in 2014 was 19.2% (Figure 1.3) which means about 20% of the world energy demand is now met by the renewables. In terms of electricity generation, this share is rather more which is about 23.7% at the end of 2015 due to the addition of 147 Giga-watts (GW) renewable power capacity. In the same period, renewable heat capacity has increased by 38 Gigawatts-thermal (GWth) (REN 21, 2016).

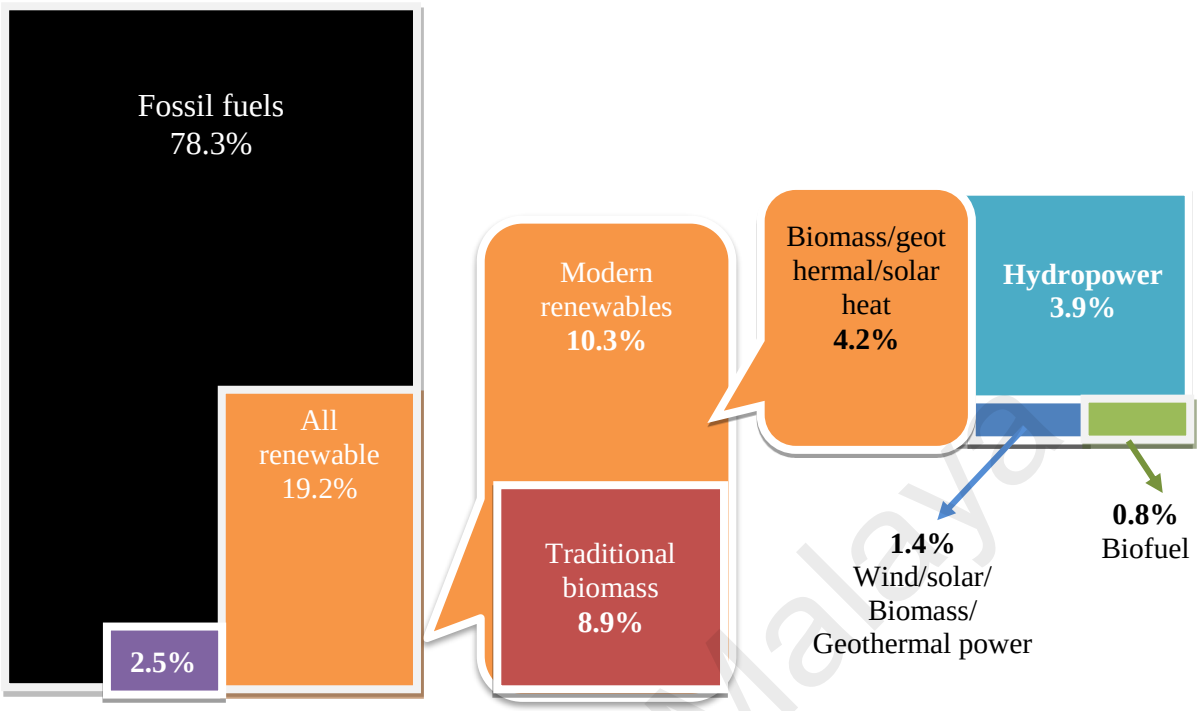

Figure 1.3: Share of renewable energies in global final energy consumption, 2014 **(**REN 21, 2016**)**

Although there are many sources of renewable energy like bioenergy, wind energy, ocean energy etc. which are all solar in origin, but the energy directly available and harvested from the solar radiation, especially termed as 'solar energy' is the main accessible source of carbon-neutral energy supply. The energy incident on the Earth through solar radiation in one hour is more than that consumed worldwide in a whole year. Solar energy is cleaner and greener compared to other forms of renewable energies in the sense that it causes almost no environmental pollution from production to supply. So, it has been recognized as one of the most promising alternatives that can alleviate the dependence on fossil fuels (Bouroussis & Topalis, 2004). The solar PV capacity has increased from 177 GW in 2014 to 227 GW in 2015 worldwide, while the solar thermal capacity during that period has increased from 409 GWth to 435 GWth

(REN 21, 2016). The contribution of renewable energy sources in electricity generation, as shown in Figure 1.4, was 23.7% at the end-2015.

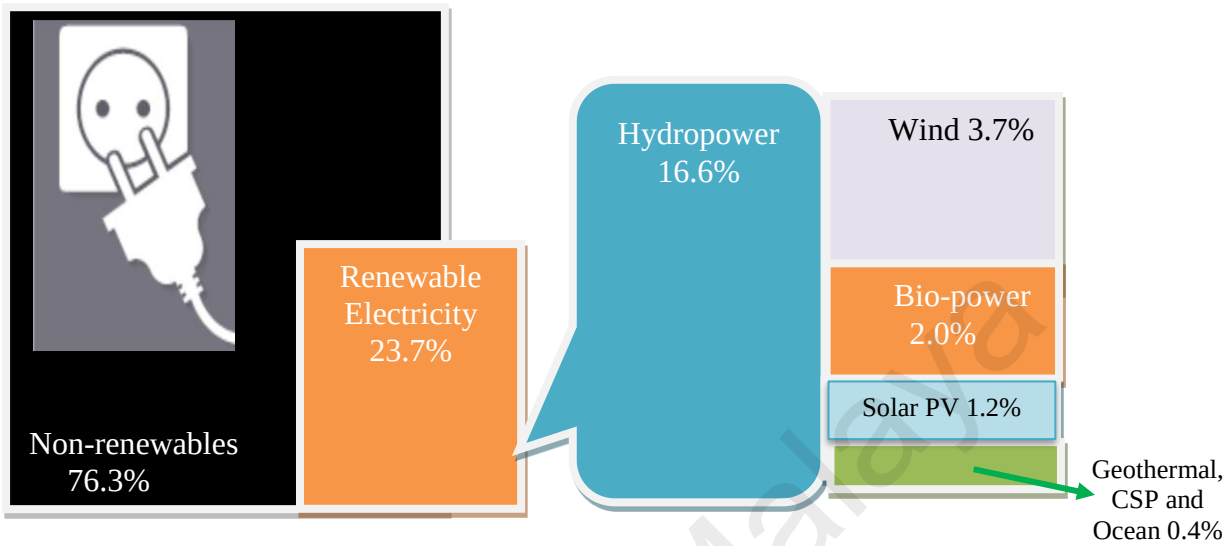

Figure 1.4: Renewable energy share in world electricity generation, End-2015 **(**REN 21, 2016**)**

Unfortunately, due to the lack of apt technology to harness energy from the sun in an efficient manner, solar energy presently provides only a minor part of the global energy utilization. Other drawbacks with solar energy are its intermittent nature, very low efficiency of the photovoltaic (PV) devices, and lack of apposite storage facility for extended period of energy availability. The search for an appropriate technology for harvesting and storing solar energy to ensure its continuous supply and sustainable use is a major concern worldwide. Extensive studies and investigations are still required to find better methods to utilize this inexhaustible source of energy.

1.2 Renewable Energy Sources

Defining renewable energy and distinguishing it from non-renewables is not always easy. However, in general, renewable energy is considered as energy that is derived from resources which are replenished naturally within a human timescale. The major

sources of renewable energy are sunlight, wind, rain, tides, waves and geothermal heat (Ellabban et al., 2014). Bioenergy, geothermal energy, hydropower, ocean or marine energy, wind energy and solar energy are the six major categories of renewable energy technologies. (IEA, 2016).

1.2.1 Bioenergy

Bioenergy is the energy stored in the form of biomass which is any organic matter of recently living plant or animal origin. It is derived from sources like agricultural products, forestry products, municipal solid waste and other waste. Bioenergy is available in various forms, such as biogas, landfill gas, ethanol, biodiesel, etc. This renewable energy source is being used increasingly to generate electricity and heat or to produce liquid fuels for transport. Historically, the very first source of fire for humankind was wood. Biomass still meets the household energy requirement in many underdeveloped and developing countries. Acoording to World Bioenergy Association (WBA), bioenergy is the third major renewable electricity-generating source, while it is the largest renewable source for direct heat, derived heat and transportation. In 2015, the production of biofuel reached 133 billion liters providing 13.9% of the final energy consumption worldwide. In 2013, 462 TWh of bio-electricity was generated which was a 6% increase over the previous year, while 0.9 EJ of derived bio-heat was generated globally during the same period (Shankar, 2016).

1.2.2 Geothermal Energy

Geothermal energy is thermal energy generated and stored in the Earth's crust that was originated from the original formation of the planet and from radioactive decay of materials (Dye, 2012). This energy is available from the shallow ground to hot water springs and hot rocks and stones found a few miles underneath the Earth's surface or

down, even deeper to the extremely high temperatures of molten rock called magma. Geothermal energy technologies include geothermal power generation, geothermal direct use and geothermal heat pump. Again, geothermal power plants may be of three types: dry steam power plant, flash steam power plant and binary cycle power plant; out of these three flash steam power plants are most common. The global geothermal power generation is at about 13.3 GW of operating capacity in January 2016, installed across 24 countries. It is expected that the generation capacity will reach 18.4 GW by 2021 (GEA, 2016). In direct-use systems, a draw-well is bored into geothermal basin from where hot mass is brought up through piping and a heat exchanger facilitates controlled transfer of heat to application end. The cooled geothermic mass is then reinjected underground. Geothermal hot water can be used for space heating, crops drying, raising plants in greenhouses, supplying warm water at fish hatchery, pasteurization process of milk and providing process heat in industries. At the end of 2014, the direct utilization of geothermal heat reached 70,885 Megawatt thermal (MWth), while the thermal energy was used at a rate of 164,635 Gigawatt-hour per year (GWh/year) (Lund & Boyd, 2016).

1.2.3 Hydropower

Hydropower refers to the energy of falling or fast running stream of water, which may be harnessed for by means of different water turbines, namely Kaplan turbine (for low water head), Francis turbine (for medium water head) or Pelton wheel (for high water head) to generate electricity. Hydropower is viewed worldwide as a means for economic development that adds the minimum possible amount of carbon to the atmosphere (Schneider, 2013). However, dams built to harness the running water may cause adverse impacts on social and environmental milieu (Nikolaisen & Ukeblad, 2015). In 2015, an estimated 33.7 GW of hydroelectric power plant were brought into

operation, taking the global installed capacity of hydropower up to 1,212 GW. The average hydropower generation in the same year was 3,975 Terrawatt-hour (TWh) (IHA, 2016).

1.2.4 Ocean or Marine Energy

Ocean or marine energy refers to the energy carried by ocean waves, currents and swells, movement of tides, salt content and ocean temperature differences. The term ocean or marine energy covers both wave power, i.e., the power from surface waves and tidal power derived from the kinetic energy of huge bulk of flowing water. The perpetual movement of water in the oceans creates a vast storage of kinetic energy. Ocean energy, if harnessed properly, has the potential to provide a large-scale of energy demand around the world (Carbon trust, 2006). The estimated potential to generate electricity by utilizing ocean energy is around 20,000–80,000 TWh (IEA, 2015).

1.2.5 Wind Energy

Wind energy is the kinetic energy of flowing air stream that can be employed for electricity generation by wind turbines. Wind power offers the unique advantage of no water requirement for power generation which is a growing concern in case of thermal power plants. In addition, wind turbine does not emit greenhouse gas (GHG) or any other pollutant gases, such as oxides of sulphur and nitrogen. Moreover, it entails no risk of fuel price hike that helps to improve energy security. Wind turbines are categorized by two groups: onshore or land-based wind that are installed on the land and offshore wind which have been deployed in the sea. Offshore wind had a global installed capacity of over 8800 MW. Offshore technology is growing substantially with an increase in the installed capacity by 37.6% in 2015, reaching to a mark of 12,105

MW. However, it is still a minor share (less than 3%) in the global cumulative installed wind power capacity, which was 4,32,419 MW at the end of 2015 (GWEC, 2016).

1.2.6 Solar Energy

Solar energy is radiant light and heat from the Sun that is harnessed as photovoltaic electricity or solar thermal energy. The solar resource is abundant and it is virtually inexhaustible. It is the most potential alternative to meet the global energy demand in a sustainable manner and ensure the energy security while reducing the GHG emission significantly. The energy received per annum from the Sun, as depicted in Figure 1.5, far exceeds the total energy anticipated from fossil and nuclear based resources.

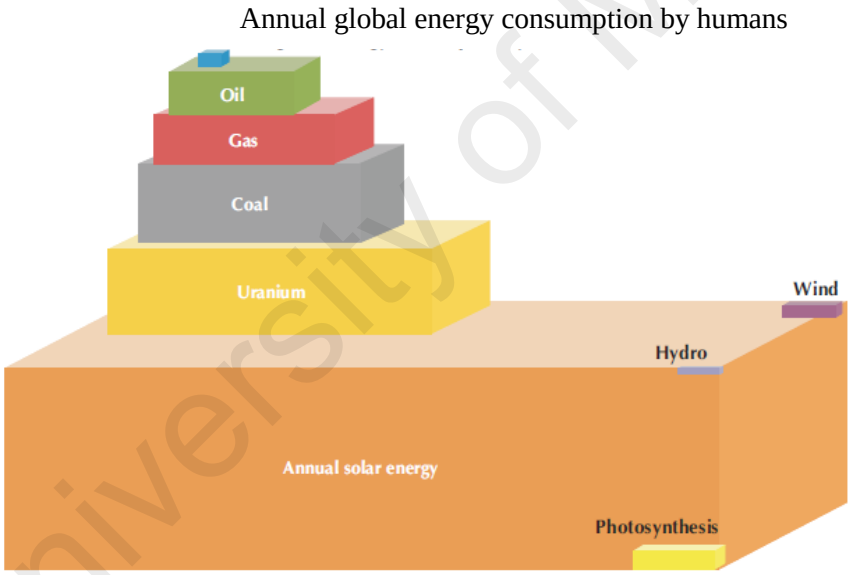

Figure 1.5: Comparison of the other energy resources with solar energy (IEA, 2011)

The estimated incident energy from the Sun to the Earth surface per year is about 885 million TWh which is about 4200 times the primary commercial energy that would be consumed worldwide in 2035 (IEA, 2011). Despite of so many adjuvant benefits, there are several limitations of this technology. Solar energy is not available at night time and the amount and availability also depends on the location and weather

condition. Moreover, large land areas are required to capture the adequate amount of solar energy. In addition, solar collectors and associated equipment are manufactured in factories that in turn create some pollution. A summary of the merits, demerits and applications of the solar energy has been summarized in Table 1.1.

Table 1.1: Merits, demerits and applications of solar energy

Merits	Demerits	Applications
• Free, clean, renewable, inexhaustible, and versatile • Usable anywhere, especially isolated areas • No fuel cost • Pollution free • No waste production • Electricity bill reduction • Easy installation and maintenance • Long life	• Weather dependent • High primary cost • Difficulty in energy storage • Need a lot of space • Longer payback period • Solar thermal power plants require huge amount of water supply	• Space cooling and heating • Cooking and household hot water supply • Process heat supply in industries. • Desalination process for supplying drinkable water in coastal regions. • Electricity generation

1.3 Solar Energy Technologies

Solar energy based technologies have drawn attention of both policy makers and consumers as a feasible solution to growing energy demands (Modi et al., 2017). Energy from the sun can be captured in two basic ways, namely heat and photoreaction. The harnessed solar energy may be characterized according to the application domains, such as solar heat, solar thermal electricity; photovoltaic electricity and solar fuel manufacture (IEA, 2011). Among the above four, the most common solar technologies are photovoltaics (PV), where sunlight is directly converted into electricity; concentrating solar power (CSP), where thermal energy from the sun is used to run

utility-scale turbines to produce electricity; and solar thermal (ST), where solar heat is directly used to produce hot water. Apart from these conventional methods for harvesting solar energy, a rather new hybrid technology that combines both solar PV and solar thermal in a single unit (known as photovoltaic thermal, PV/T) is getting popular day by day. The solar energy conversion technologies and their interrelation is illustrated in Figure 1.6.

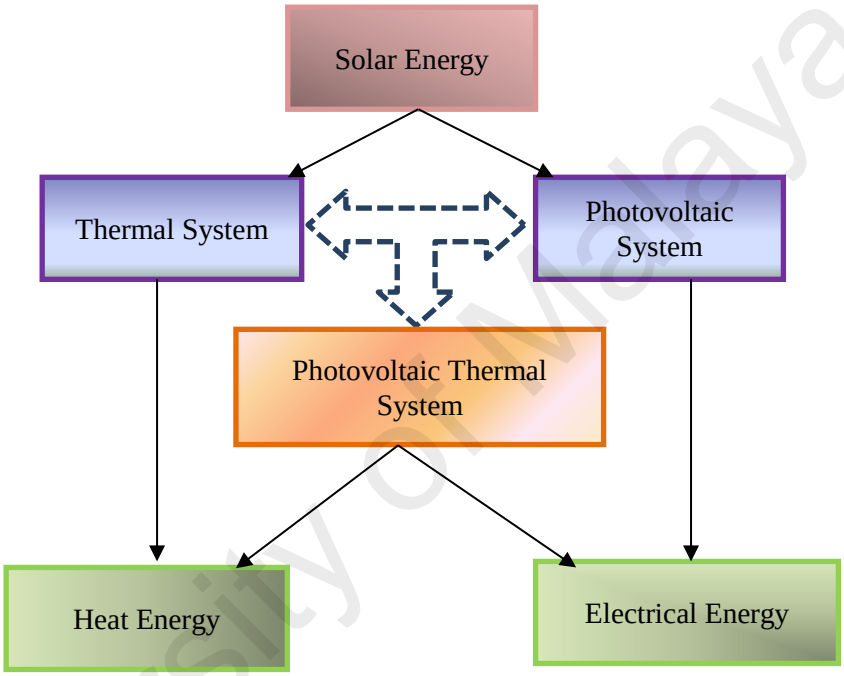

Figure 1.6: Solar energy conversion technologies (Zhang et al., 2012)

1.3.1 Solar Photovoltaic Technology

Solar photovoltaic refers to power system designed to supply usable solar electricity by means of photovoltaic effect. Photovoltaic technology is based on the photoelectric effect discovered by French physicist Edmond Becquerel in 1839 which was explained and stated as law of photoelectric effect in 1905 by Albert Einstein. Photovoltaic (PV) cells are made of semiconductor materials comprising of a p-n junction. Upon the absorption of incident photons of sunlight in PV cells, a meta-stable electron-hole pair is created that exists only for a short period before recombining. The

recombination of the light-generated carriers is prevented by spatially separating them by a p-n junction, which if connected, causes the electrons and holes to gather a n-type and p-type poles, respectively. This gives rise to a voltage difference that drives the light-generated carriers to flow through an external circuit producing direct current (DC) electricity (Figure 1.7). Photovoltaic power systems employ solar panels (also known as PV module), each consisting of a certain number solar cells interconnected so as to produce desired power.

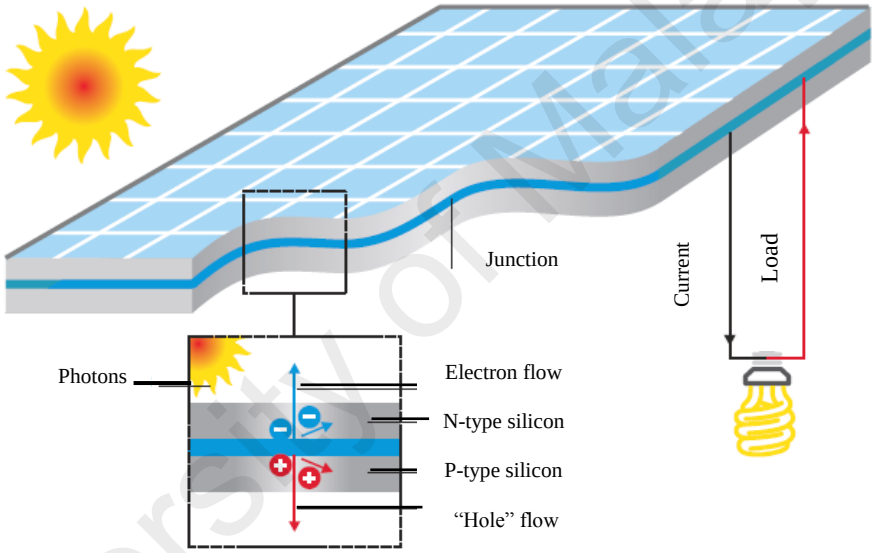

Figure 1.7: The photovoltaic effect (IEA, 2011)

Sunlight is a type of electromagnetic radiation and the range of electromagnetic energy radiated by the sun is called the solar spectrum. Solar spectrum comprises of three major regions: ultraviolet (UV), visible, and infrared (IR). Solar spectrum ranges from 290 nm in the longer wavelengths of the UV region to about 3,200 nm in the far IR region (Figure 1.8) (NASA, 1980).

The semiconductor material silicon (Si) of traditional PV cells responds to a narrow range of light wavelengths. Photovoltage cannot be generated by the light having energy less than band gap of semiconductor, because photons with an energy smaller

than band gap are not absorbed and their energy is not used for carrier generation. Solar radiation with wavelengths of 380 nm to 750 nm hit the Si semiconductor with energy sufficient to extricate electrons from their weak bonds and generate electricity. However, photons with energy larger than band gap are absorbed, but the excess energy is lost due to thermalization of the generated electrons. The maximum conversion efficiency of such a cell is 31% which is called the Shockley-Queisser limit (van Sark, 2012).

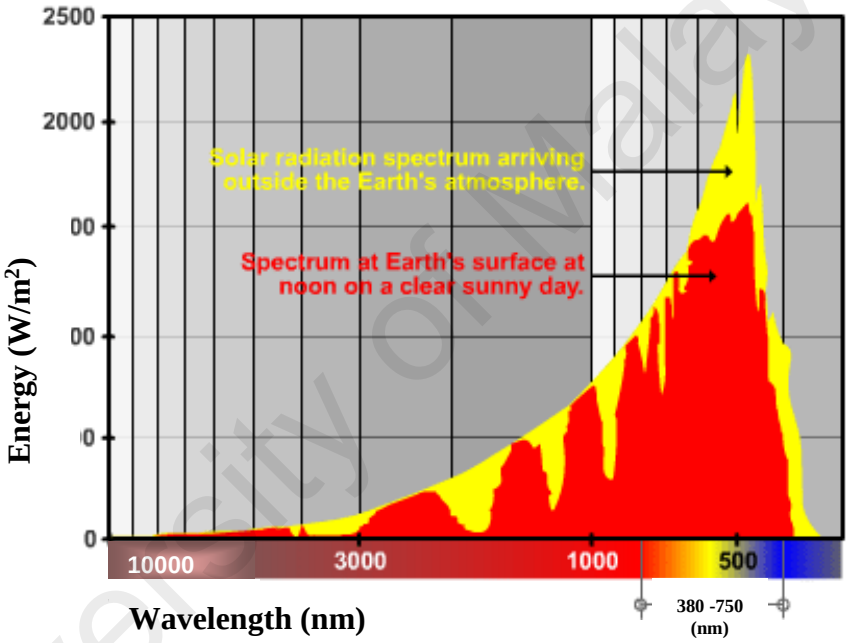

Figure 1.8 : Spectral content of incident solar radiation (Marsh, 2011)

Solar cells may be of many types based on the material and structure. However, the major two categories: crystalline silicon (c-Si) cells and thin film solar cells are wafer-based. Crystalline silicon cells are made by growing a single crystal of silicon (Si), thereby called monocrystalline (m-Si) solar cells, or by high purity multi-crystalline form of silicon that are called ploy-crystalline (p-Si) or polysilicon (poly-Si) solar cells. Monocrystalline cells have slightly higher electrical conversion efficiency (14–22%) than polysilicon cells (12–19%), when the values being measured under standard testing

conditions (STC) of AM 1.5 and 25°C ambient temperature. The major drawback of crystalline silicon cells is that they have a negative temperature coefficient, i.e., their efficiency level decrease with rise in temperature. Thin-film solar cells are constructed by the deposition of thin layers of different photovoltaic materials on substrates like glass, plastic or metal. Commercial thin-film solar cells are made mostly with amorphous silicon (a-Si), cadmium-telluride (CdTe) and copper-indium-gallium-(di) selenide (CIGS). Thin film modules, especially CIGS thin films, can be manufactured as flexible sheets and offer a great diversity of sizes, shapes and colors which make this technology apt for building-integrated photovoltaic (BIPV) application. Although thin-film cells are cheaper, the problem with these devices is their lower efficiency than conventional crystalline silicon cells. The emerging third generation solar cells, most of which are at their nascent stage, include organic solar cell, dye-sensitized solar cells (DSSC), polymer solar cells, perovskite solar cells, etc.

1.3.2 Solar Thermal Technology

1.3.2.1 Solar thermal heat

Solar thermal technology employs sun ray to generate heat. In the face of the recent rapid growth of solar PV technology, solar heat is still the largest solar contributor to our energy needs. In 2015, the use of solar thermal collector (glazed and unglazed) around the world has increased by more than 6%. The global capacity of solar water collectors at the end of 2015 touched 435 GWth, while air collectors provided 1.6 GWth, collectively which is equivalent to an annual heat generation of 357 TWh (REN21, 2016).

Solar thermal collectors are basically of two types, viz., flat-plate collectors and evacuated tube collectors. Flat-plate collectors (Figure 1.9) are capable of supplying heat at 80°C to 160°C with efficiencies as high as 60%. Water is primarily used as the

heat transfer fluid (HTF) in flat-plate collectors. If required, glycol can be added as anti-freezing agent. Air is also employed as HTF, especially in case of space heating or crop drying applications.

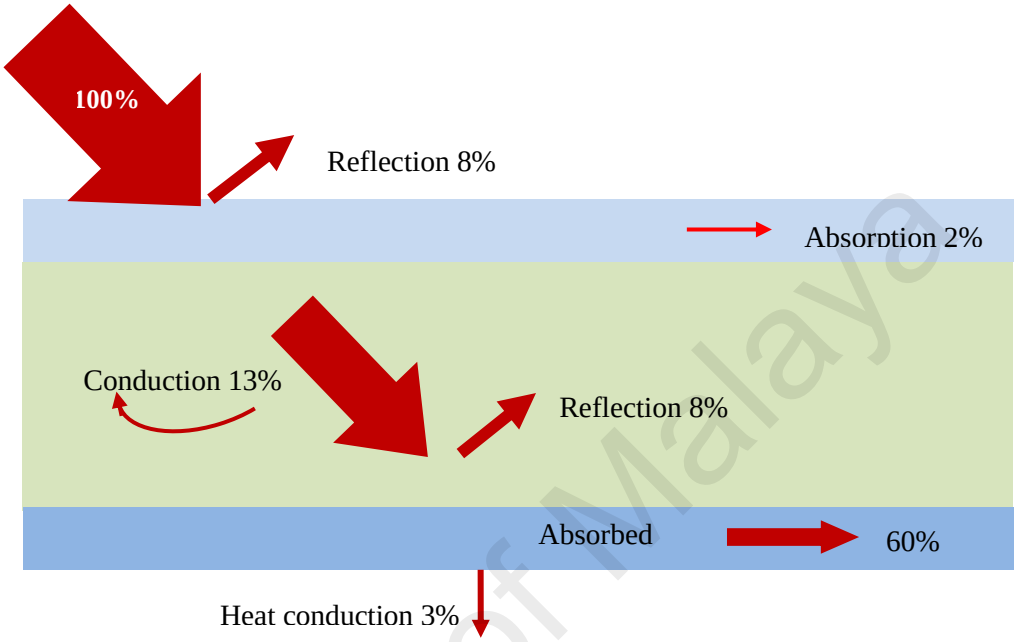

Figure 1.9: Optical and thermal losses of a flat-plate collector (IEA, 2011)

Evacuated tube collectors are comprised of vacuum glass tubes connected in parallel that facilitate to eliminate the convection and radiation heat loss. The temperature gain by these collectors may range between 77°C to 170°C. Although evacuated tube collectors are costlier than conventional flat-plate collectors, they offer efficiency enough for commercial and industrial heating applications as well as several cooling processes. There are two different technologies in evacuated tube collector: direct-flow tube collector and heat pipe tube collector. In direct-flow tubes, the fluid circulates through rows of glass tubes inside each of which there is a plain or curved aluminum fin bonded to a metal. On the other hand, in heat pipe based collectors (Figure 1.10), the collected heat is conveyed by means of heat pipe without direct contact with the fluid.

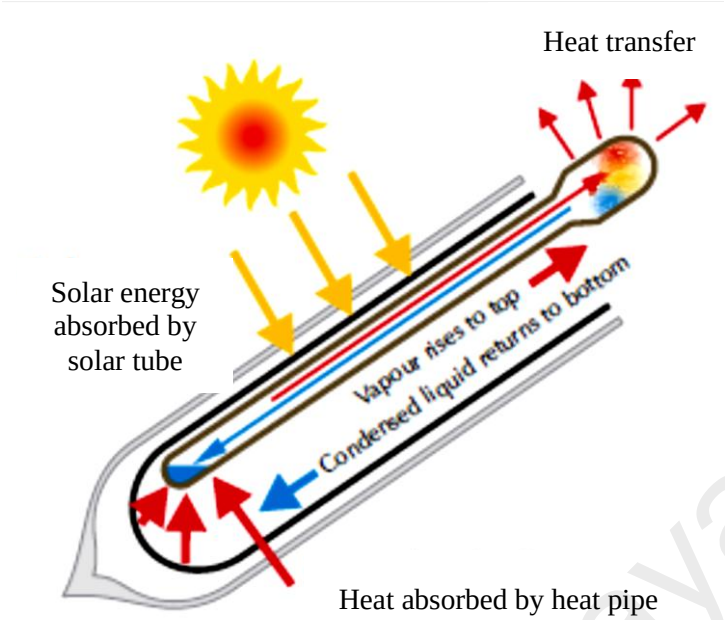

Figure 1.10: Heat pipe based collector (IEA, 2011)

1.3.2.2 Solar thermal electricity

Concentrator solar collectors are the third category of collector that uses mirrors, lens and tracking devices to concentrate sun ray onto a small area to produce intense heat which is specifically suitable for high temperature applications like producing process heat or generating steam to run steam turbines. Solar thermal electricity (STE) plants, also called concentrating solar power (CSP) plants, employ concentrator collectors with concentration ratio as high as 100 to 1500 and produce fluid to temperature 450^{o}C and above. Concentrating collectors, generating heat at temperatures between 150°C and 300°C, are apt for solar cooling and for combined heat and power (CHP) generation. On the other hand, collectors working between 250°C and 450°C are appropriate for solar thermal power plants (Heimsath et al., 2009).

These collectors perform best in regions where direct solar irradiation is available almost all the year round. There are several types of concentrating collectors, such as parabolic trough, parabolic dish and solar tower. Parabolic troughs are long parabola shaped reflectors with a receiver pipe placed at the focal line of the parabola. The usual

concentration ratio of parabolic troughs range is from 30 to 100, enough to achieve temperatures around 350^{o}C. Solar dish or engine is very large mirrored dish, generally equipped with tracking device to intercept maximum irradiation all day long. With much higher concentration ratio than solar troughs, solar dishes can achieve temperatures around 750^{o}C. In solar power tower (also known as central receiver), a heat exchanger is mounted on a tower surrounded by hundreds to thousands of flat, sun-tracking mirrors called heliostats which reflect and concentrate sun ray onto the heat exchanger. In this way, energy can be magnified by about 1500 times the incident energy (EIA, 2015). Figure 1.11 presents applications of concentrating solar collector with corresponding operating temperatures. Compound parabolic collectors (CPC) are special type to concentrator collector designed in the shape of two meeting parabolas so as to concentrate solar irradiation. The temperature of these collectors ranges from 100^{o}C to 170^{o}C.

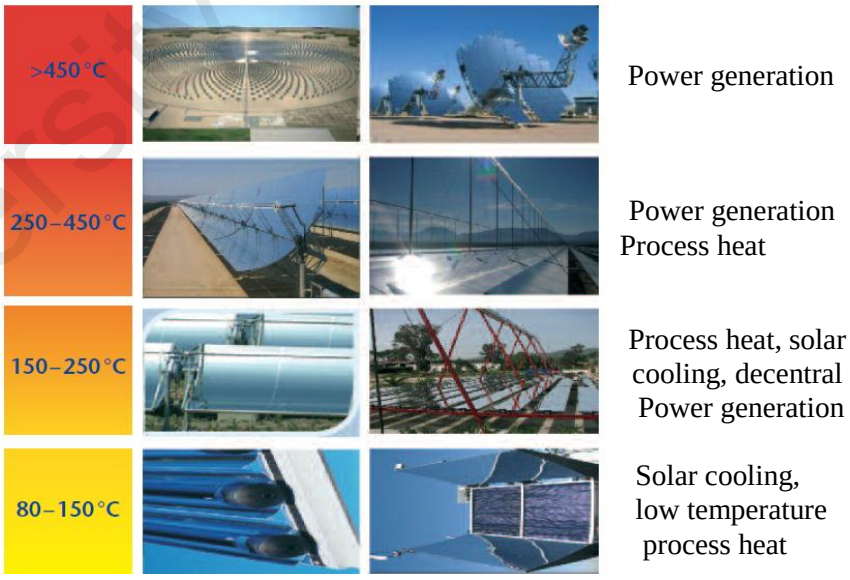

Figure 1.11: Applications of concentrating solar collector (Heimsath et al., 2009)

Solar thermal plants, as shown in Figure 1.12, work essentially on the same principle as conventional fossil fueled steam turbine power plants. In this case, highly concentrated solar energy heats up the heat exchanger fluid. The hot fluid then exchange heat with water to generate steam. The steam runs a turbine through generator which produces electricity. The capacity of STE plants may be as high as several hundred megawatts. The global installed capacity of STE toady is about 5 GW (ESTELA, 2016).

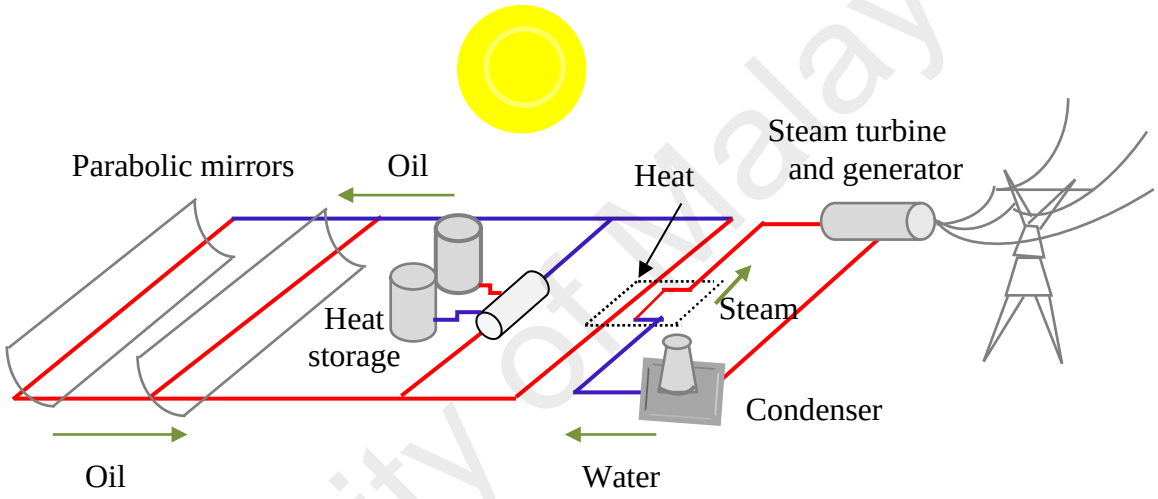

Figure 1.12: Solar thermal power plant (ESTELA, 2016)

1.3.3 Hybrid Photovoltaic Thermal Technology

Hybrid photovoltaic thermal (PV/T) technology is a well-engineered co-generation technology that integrates photovoltaic (PV) modules and solar thermal collector in a single unit (Riffat et al., 2005). The combi-panel produces both electricity and heat concurrently from the absorbed solar radiation offering a cogeneration efficiency of as high as 80%. The efficiency of solar cells is austerely affected by temperature rise. Due to increased temperature, heat is generated in PV cells which can be extracted by heat exchanger through heat transfer media, then the collected heat can be used in home, industries and others commercial purposes. PV/T collector is a solar energy system that provides both of electricity and heat with higher efficiency than separate PV and solar

thermal systems. Besides, fabrication and installation cost of this hybrid collector is less. Both air and water are used as heat transfer fluid in PV/T. The water based PV/T collector may be covered or uncovered. In uncovered PV/T collectors, a heat pipe is attached on the PV module backside; whereas if the same unit is placed inside flat-plate solar heat collectors, then it is termed as covered PV/T. The covered PV/T can raise outlet temperatures of the fluid relatively higher than the uncovered one due to additional insulation from transparent glass cover (van Helden et al., 2004). On the other hand, the best electrical performance is attained with uncovered hybrid collectors (Fraisse et al., 2007).

1.4 Problems Statement

Photovoltaic thermal (PV/T) system is the optimized solar energy system with both heat and electricity as its yield. The key factors for achieving better performance from this system include PV cell material, design of thermal collector, collector material and heat transfer fluid. However, the performance of PV/T system is mostly dependent on the efficient design and integration of the thermal collector with PV module. Although the main theme of using thermal collector is to accumulate heat from PV module in order to reduce the cell temperature for achieving better electrical performance, but there is material limit for electrical gain. However, the thermal efficiency of the module can be maximized to a significant extent and more heat can be harvested from the module by making use of efficient heat exchanger and effective heat transfer technology. In order to improve the performance of PV/T system, it is important to understand the complex phenomenon of conjugate heat transfer along with flow characteristics inside the thermal collector for which numerical analysis is the appropriate technique. Although several numerical studies have been carried out to understand the thermo-fluid phenomenon and thereby improve PV/T performance, but

almost all of those analyses are one and two dimensional. However, heat transfer from the PV cell to the coolant takes place through a number of layers, viz., cell encapsulant EVA (ethyl vinyl acetate), back surface coating poly vinyl fluoride (PVF) commercially named as tedlar, absorber plate and collector material. So, one and two dimensional analyses are not enough to predict the complex phenomenon of conjugate heat transfer.

Therefore, the following specific problems with PV/T system have been identified:

1. There is a lack of three dimensional (3D) numerical analysis which is of the utmost importance for better understanding of the real time information regarding temperature distribution inside the PV/T system with more accuracy.
2. Investigation on apposite and efficient thermal collector design for PV/T systems is not enough.
3. Well integration of the thermal collector with PV module backside is still a major problem which is very much important to maximize the amount and rate of heat removal.
4. Another major problem with PV/T system is the pumping power required to maintain the circulation of heat transfer fluid (HTF) which consumes a portion of the PV yield.

1.5 Objectives of the Research Work

In order to address and accomplish the problems mentioned above the following principal objectives have been set up as follows:

1. To design and develop novel configurations for thermal collector of photovoltaic thermal (PV/T) systems in order to acquire better thermal as well as electrical performance.

2. To develop a comprehensive three dimensional mathematical model that is able to predict the real time conjugate heat transfer and fluid flow characteristics inside the thermal collector (flow channel).
3. To identify the numerical model of representative configuration among the thermal collectors designed and validate it through experimental investigation.
4. To investigate the effect of different control parameters on the performance of other designs of PV/T collector based on the validated numerical model.
5. To compare the performance of all the PV/T collectors in order to authenticate the best design.

1.6 Scope of the Research Work

The detail objectives of the present research work are those as mentioned in previous section. However, the focus will be contemplated on the following particular points:

1. To design and develop thermal collectors with different geometries and configurations and compare their relative merits and contribution in enhancing the overall efficiency of the PV/T system.
2. To develop an appropriate technique for the effective integration of the thermal collector with PV module.
3. To eliminate the pumping power required to maintain the flow of HTF through the PV/T system.

1.7 Research Methodology

The research methodology of the present research has been detailed in chapter 4; however, a brief outline is presented here to give a primary notion.

The basic objective of this research is to develop a three-dimensional mathematical model for PV/T with different designs of thermal collector excluding the absorber plate and validate the model through experimentation. The first step of the research work has been accomplished by employing the basic laws for continuous media, i.e., principles of conservation of mass, momentum and energy to develop the mathematical model. The model is then used in finite element method (FEM) based software COMSOL Multiphysics® for carrying out simulation study. In the next step, among the collector designs one is selected for experimental validation, wherein the experiments were performed outdoor in the typical ambient condition of Malaysia. Once the model is validated, it has been employed to evaluate numerically the performance of PV/T with the other collector designs. The research concludes with a comparative performance appreciation of PV/T with all the developed collector designs.

1.8 Organization of the Thesis

The thesis comprises of six chapters wherein chapter 1 is the introduction of the thesis. The contents of the other chapters are organized as follows:

Chapter 2 contains a literature review on PV/T systems including the historical development of the conceptual framework of the PV/T technology, different methods of classification, issues related to their performance and different techniques proposed so far to enhance the performance. The all-inclusive overview ends with the recognition of the research gap as identified.

Chapter 3 provides a theoretical background on the heat transfer and fluid flow involved with PV/T system. Theory includes some basics of heat transfer and fluid flow with main focus being on the thermal performance analysis of the PV/T system. The basics of the electrical performance of the system have also been enumerated.

Chapter 4 describes the methodology, including both numerical and experimental procedure that has been adopted in the present research. The detail features of the experimental set up and instrumentation have been elaborated to provide a clear view about the experimentation.

Chapter 5, which is the nucleus episode of this thesis, presents the discussion and critical analysis on the results and findings of the present research. The circumstantial investigation includes decisive reasoning regarding the effect of control parameters on PV/T performance as well as contains hints for forthcoming works.

Chapter 6 puts forward a general conclusion on the present research including the major findings in brief. In addition, a future outlook in course of this work has also been added in this chapter in the form of specific recommendations for further research.

CHAPTER 2: LITERATURE REVIEW

2.1 Introduction

Photovoltaic thermal (PV/T) is relatively a budding technology. Many aspects regarding PV/T are still under research and development. In the present chapter, attempt has been made to put forward a detailed overview on PV/T technology along with their historical development, types, performance and approaches for further improvement of these systems. Although the review focus is mainly on the different types and design of thermal collectors, the parameters affecting PV/T performance such as mass flow rate, temperature (of ambient, fluid and cell), packing factor, cell material, absorber plate material, glazing, etc. are also discussed extensively. The sources of the literature review are articles published in reputed journal, websites and personal communication.

2.2 Photovoltaic Thermal Technology: Historical Overview

A photovoltaic thermal system essentially assembles the features of a solar thermal collector and a photovoltaic (PV) system in a single module to translate solar radiation directly into both electrical and thermal energies. The concept of PV/T emerged in mid 1970s when researchers were trying to solve the problem of efficiency drop with increasing solar cell temperature. Wolf (1976) is reported to fabricate the first flat-plate PV/T liquid-based system for residential heating. Author mounted a PV module on a non-concentrating thermal collector equipped with a battery for electrical storage and a water tank to collect hot water. The merger system was found technically viable and cost effective. Florschuetz (1975) developed a mathematical model of this combination system using TRNSYS software. Later the same researcher applied the Hottel-Whillier thermal model based on the decreasing cell efficiency with temperature to analyze the performance of a flat-plate PV/T collector which made the foundation of the PV/T model TYPE 50 in TRNSYS.

Kern & Russell (1978) developed and tested hybrid PV/T collectors according to ASHRAE standards at the Lincoln Laboratory of the University of Texas for the U.S. Department of Energy, Conservation and Solar Application. Authors concluded that the effective energy yield per unit area by hybrid collectors is more than the individual PV module and the thermal collector. In 1979, Hendrie (1979) theoretically analyzed and experimentally assessed the thermal and electrical performance of PV/T solar collector with both air and liquid as heat transfer fluid. The experimental results were found to have close correspondence with the theoretical results. It was observed for both liquid and air collector that thermal efficiencies fall (from 42.5% to 40.4% for liquid and from 40% to 32.9% for air collector) when electrical power is taken as an output. The maximum electrical efficiency obtained was 6.8%.

In 1980s, the emerging technology of combining two different solar conversion methods attracted many researchers' interest and studies on the performance of this hybrid technology were carried out using different types of cell materials to ascertain which one is best suited for PV/T application, mono-, poly- or amorphous silicon. Cox and Raghuraman (1985) carried out a computer simulation study to explore the design features of PV/T collectors with a view to improve their efficiency. In order to attain optimum performance, authors suggested the use of a high transmissivity/low-emissivity cover above the PV cells, the cells being gridded-back with nonselective secondary absorber.

Lalovic et al. (1986) fabricated a PV/T by gluing amorphous silicon (a-Si) cells with an average efficiency of 4% over a fin-and-tube solar thermal collector. The hybrid collector performed aright as a thermal collector raising water temperature up to 65°C with a slight variation in PV performance.

Due to the unaffordable price of isolated PV/T collectors, the trend of these systems turned to building integrated applications which experienced rapid developments in recent years. The Hottel–Whillier model, which was initially developed for the analysis of flat-plate solar collectors has been customized for analyzing BIPV/T systems. Studies on BIPV/T included the development of computational fluid dynamics (CFD) model, performance evaluation using exergy analysis and cost and economic analysis (Ibrahim et al., 2014).

Although PV/T technology has already passed four decades of research and development and its technical cogency is already established, but commercialization of these collectors is still very limited. So, much focus is needed to improve the availability and effective use of this hybrid panel for which historical trail of this combination technology will be a helpful means.

2.3 Photovoltaic Thermal Collectors: Overview on Classification

The demand for thermal and electrical energy is often complementary. Photovoltaic thermal system is a solar cogeneration scheme, merging photovoltaic module and solar thermal collector in one unit to provide both electricity and heat simultaneously. Several researchers have used the term ‘solar cogeneration’ while some other used the phrase ‘photo thermo conversion’ to express this innovative technology. The initiatory drive behind the integration of PV with solar thermal technology was that PV efficiency was found to deteriorate with the increase in temperature; this diminution in PV performance may be compensated to some extent by removing the heat from the module and exploiting the waste heat in useful heating applications which lead to the hybrid technology of PV/T. The major advantage of hybrid PV/T systems is that they present dual outturns, that is electricity and heat with a bit extra cost, but saving

valuable space. Moreover, it is an efficient and flexible technology which can be used for both heating and cooling purpose (Kumar et al., 2015).

The PV/T collectors may be of different types and classification has been made from diverse perspectives. Researchers have classified PV/T in different ways. Based on design geometry there are flat plate PV/T, concentrator PV/T and BIPV/T; on the basis cooling method, there are liquid based PV/T, air based PV/T and heat pipe based PV/T; based on HTF used PV/Ts may be PV/T-water (PV/T-w), PV/T-air (PV/T-a), PV/T-nano fluid and PV/T-oil. Again, PV/T may be glazed or unglazed and the HTF circulation may be by natural or forced convection. There are also some special types of PV/T, viz., micro-channel based PV/T, jet impingement based PV/T, heat spreader based PV/T, etc.

2.4 Classification Based on Design Geometry

The design geometry of PV/T collectors may be flat plate structure or concentrator type. Building integrated PV/T is also a special configuration in which geometry is dictated by the architecture of the building.

2.4.1 Flat-Plate PV/T

Flat-plate PV/T is the most popular variety of PV/T collectors due to its simplicity in design (Besheer et al., 2016). This design primarily is suitable for residential applications such as hot water supply and space heating. In domestic solar water heaters (DSWH), flat-plate collectors are generally connected in parallel and run automatically using thermosiphon process, while the industrial water heating systems employ a number of flat plate collectors in series which requires pump to maintain water flow through the collector (Erdil et al. 2008). The side faces and bottoms are generally insulated and a glass cover minimizes its heat loss. Figure 2.1 illustrates the key features

of a flat-plate PV/T collector. The collector absorbs waste heat from the solar cells and transfers to a heat transfer fluid (HTF) which in most cases are air or water.

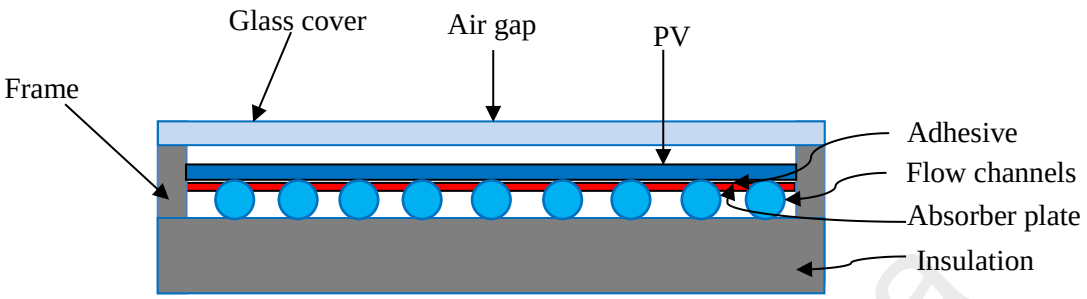

Figure 2.1: Schematic of a typical flat-plate PV/T (Ibrahim et al., 2011)

Flat-plate PV/T can capture both beam and diffuse irradiation. Because of their simple design, flat-plate PV/Ts are not so expensive. Some of the important research works on flat plate PV/T are discussed in this section.

Dupeyrat et al. (2011) investigated the thermal and electrical performances of single glazed flat-plate PV/T water collectors both numerically and experimentally. At zero reduced temperature, authors found thermal and electrical efficiencies of 79% and 8.8%, respectively.

Dubey and Tiwari (2009) assessed the performance of partly shrouded flat-plate water collectors connected in series by means of theoretical modeling. As the number of collector increases from four to ten, authors found an increase in water outlet temperature from 60 to 86 °C, thermal energy gain from 4.17 to 8.66 kWh and electrical energy gain from 0.052 to 0.123 kWh. Dubey and Tiwari (2008) designed and tested a flat-plate PV/T solar water heater under the climatic condition of New Delhi. With the increase in glazing area, the instantaneous efficiency was found to rise from 33% to 64%.

Zondag et al. (2003) evaluated the performance of nine different designs of flat plate PV/T which were classified into four groups, namely sheet-and-tube PV/T collector, channel PV/T collector, free-flow PV/T collector, and two-absorber PV/T collector. Thermal efficiency of the uncovered collector was found 52%, whereas for sheet-and-tube configuration it was 58% and for channel above PV design this figure was 65%.

2.4.2 Concentrator PV/T

Concentrating PV/T (CPV/T) systems are employed to produce higher temperatures than flat-plate collectors. CPV/T originates from the concentrator PV (CPV) which employs Fresnel lenses and mirrors to focus sun's ray onto some small, highly efficient solar cells that produce very high temperature and needs dedicated cooling; the heat thereby carried away by the coolant may be utilized in relatively high temperature thermal applications. This approach is promising as very small area of solar cell is required for CPV/T and cost of the reflectors is significantly lower than the solar cells. A tracking system is needed to focus to the Sun to capture maximum solar energy all day round. CPV/T performs well under shiny clear sky and dusty environment affect the performance significantly. A schematic diagram of CPV/T is shown in Figure 2.2. An advanced configuration of CPV/T known as Spectral Beam Splitting CPV/T has been developed to ensure full-fledged utilization of solar insolation over the entire spectrum (Xing et al., 2017).

Calise et al. (2015) developed an Organic Rankine Cycle (ORC) working in conjunction with a concentrating photovoltaic/thermal (CPV/T) solar collector that produces electricity and heats diathermic oil simultaneously. The authors used TRNSYS software to evaluate the performance of the hybrid CPV/T collector and ORC system and found CPV/T only system to be more economical.

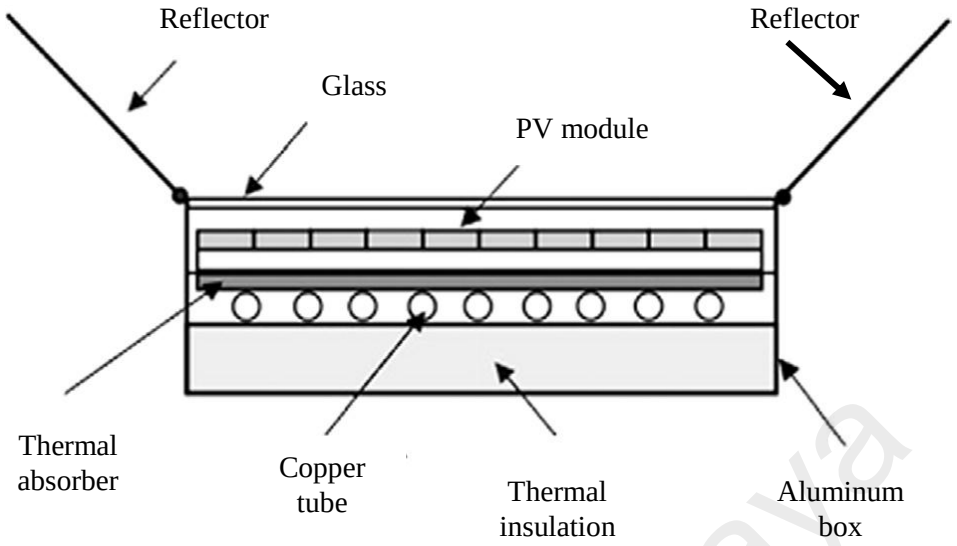

Figure 2.2: Schematic of a concentrator PV/T (Kumar et al., 2015)

Li et al. (2015) performed a numerical and experimental investigation on building integrated PV/T system with static miniature solar concentrators. The maximum thermal efficiency, as reported by the authors, was 37.2% with a water outlet temperature of 56.9^{o}C in the month of September.

Renno (2014) fabricated high concentration PV/T system using point-focus parabolic mirror concentrators and triple-junction cells (InGaP/InGaAs/Ge) governed by a dual axis tracker. The water outlet temperature obtained was about 90^{o}C which is enough to run an auxiliary heat pump.

Liu et al. (2014) proposed a CPV/T hybrid system that employs beam splitter and linear Fresnel reflector to attain high concentration. The authors reported an overall power generation and efficiency of 1367.0 W and 26.5% under the solar cell operating temperature of 25^{o}C, and 1319.5 W and 25.6% under 50^{o}C.

2.4.3 Building-integrated PV/T

Energy consumption in residential and commercial buildings is increasing day by day, especially in the urbanized developed countries. Employing PV/T as an integrated part of building envelop is getting increasingly popular in recent years (Nemati et al., 2016). Because, building integrated PV/T (BIPV/T) is one of the most operative ways to achieve net-zero objective in buildings.

Yang and Athienitis (2015) studied the thermal features of an open loop bi-inlet BIPV/T air system using a full-scale solar simulator. Experimental study reveals that compared to a single inlet system, the double inlet collector upsurge the thermal efficiency by 5%. The authors also reported a 7.6% higher thermal efficiency using BIPV/T system with semi-transparent PV than with transparent ones.

Yang and Athienitis (2014) carried out experimental investigation on an open loop air-based BIPV/T system with a single inlet. A 10% increase in thermal efficiency was noticed with wire mesh packing in the collector, while vertical glazed collectors improved efficiency by about 8%. A BIPV/T rooftop fabricated in accordance with the developed model exhibited a 7% increase in thermal efficiency.

Hailu et al. (2014) carried out a simulation study of a BIPV/T system using finite element analysis (FEA) based software COMSOL Multiphysics®. The authors studied the forced convection through the collector where they considered turbulent flows with Reynolds number ranging from 5199 to 9392. The simulation outcome proved practicable to develop mathematical models for the design and optimization of different components of a BIPV/T system.

Yang and Athienitis (2012) carried out a numerical study on BIPV/T systems including glazed air collector and wire mesh to obtain high air outlet temperature. The

results showed that heat transfer enhancement depends on wire mesh geometry and inclusion of wire net favors performance at air flows less than 0.03 kg/s. The efficiency using wire mesh was obtained 8.5% higher than that excluding wire mesh, and the outlet air temperature was raised by 4°C to 11°C.

Shahsavar et al. (2011) developed a building integrated PV/T setup that employed the cooling potential of ventilation and exhaust air to chill PV panels, which in turn heats up the ventilation air. The cooling effect of the 10 m^2 PV panels was found to increase the electricity generation up to 10.1%, which is equivalent to129.2 kilowatt-hour (kWh) in a year. Energy recovered through this scheme was estimated to be 3400.4 kWh per year.

Agrawal and Tiwari (2010) codified a one-dimensional transient model of an air based BIPV/T system to be used as the roof top of a building. The annual estimated electrical and thermal exergies of a 65 m^2 roof top BIPV/T was found 16,209 kWh and 1531 kWh, respectively, while the thermal efficiency was 53.7%.

Davidsson et al. (2010) devised a simulation model for PV/T solar window that provides electricity and hot water. The authors claimed a 35% more electrical output on annual basis in one solar window compared to a vertical PV panel. This scheme requires fewer PV panels and thermal absorber and less glazed area, but the mechanism is rather complex.

Anderson et al. (2009) proposed a one-dimensional, steady-state thermal model based on Hottel-Whillier-Bliss equations to investigate BIPV/T performance for both glazed and unglazed system. The authors suggested to increase the tube width to tube spacing ratio to obtain an improved thermal efficiency.

Chow et al. (2008) presented an experimentally validated dynamic simulation model of a BIPV/T system based on finite difference method. In experimental study under thermosyphon test, the highest thermal and electrical efficiencies were obtained 26.8% and 7%, whereas in case of pump-operated test, these figures were 28.8% and 9.1%, respectively.

2.5 Classification Based on HTF

Heat transfer fluid (HTF) used to carry away the heat from the PV/T module constitutes a major range of classification of the PV/T systems. Currently, HTF used by different researchers are air, water, refrigerant, nanofluid, heat transfer oil and heat-pipe fluid. However, the mostly employed fluids in PV/T system are air and water. Figure 2.3 gives a detail classification of PV/T based HTF.

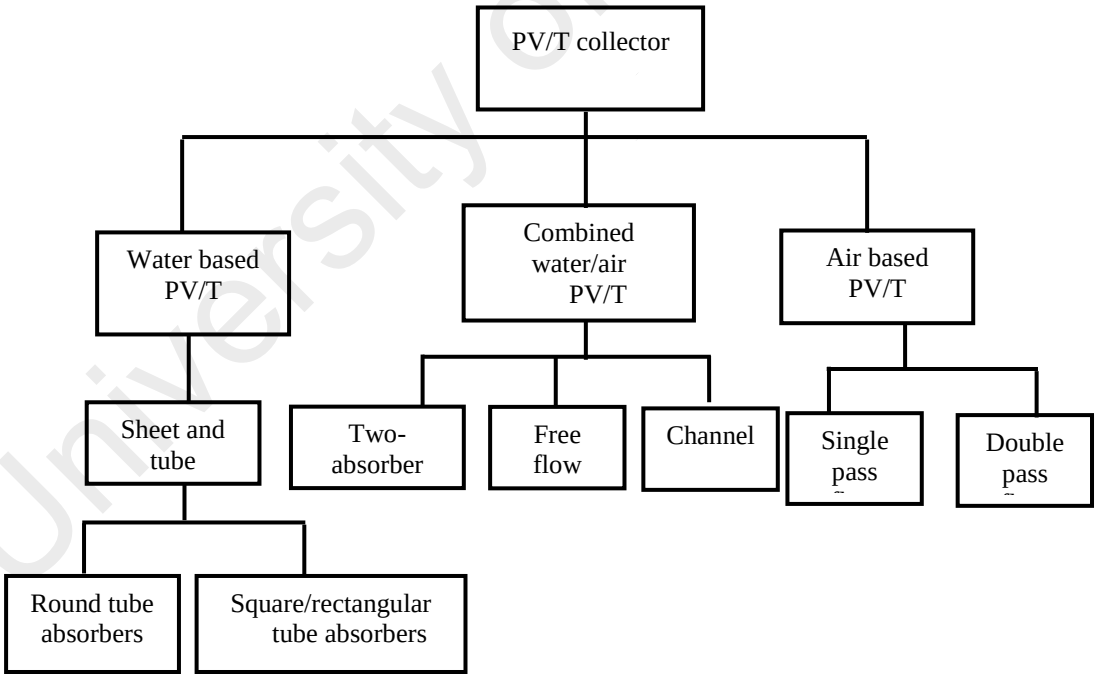

Figure 2.3: PV/T classification based on HTF (Ibrahim et al., 2011)

2.5.1 Air Based PV/T Collectors

Air based PV/T collectors exploit air as the medium of energy transfer and are mainly used for space heating and crop drying. PV/T air collectors are simple in design and require little maintenance. Moreover, they are less prone to leakage and corrosion as compared to liquid based systems. However, low thermal capacity and heat-transfer coefficient of air makes PV/T-air systems less efficient. The PV/T-air collector developed at University of Delaware, USA in 1973 is considered as one of the earliest ventures in photovoltaic thermal technology (Boer & Tamm, 2003).

Coventry and Lovegrove (2003) developed a range of ratios independent of time and location to apprise the comparative electrical to thermal yield from a household scale PV/T system through 'equivalent electrical levelized energy cost'. The authors reported that when the energy value ratio is less than 4.5, a-Si cells require lower levelized energy cost than c-Si cells.

Tiwari and Sodha (2006) investigated experimentally on the performance of PV/T-air collector using four different configurations, viz., glazed with or without tedlar, unglazed with or without tedlar (Figure 2.4). The glazed PV/T without tedlar was found to perform the best.

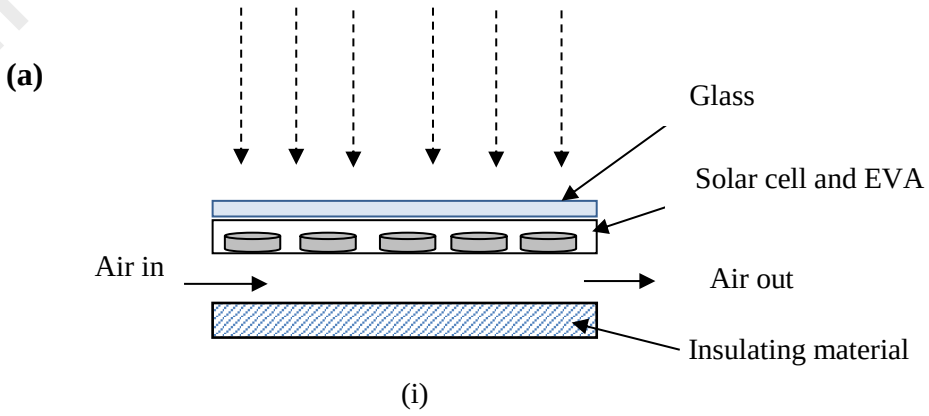

Figure 2.4: (a) Unglazed PV/T air collector (i) without tedlar (ii) with tedlar. (b) Glazed PV/T air collector (i) without tedlar (ii) with tedlar (Tiwari & Sodha, 2006)

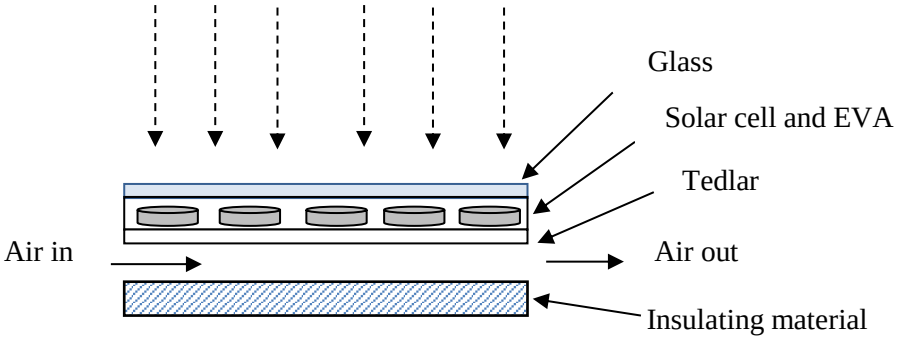

(ii)

(b)

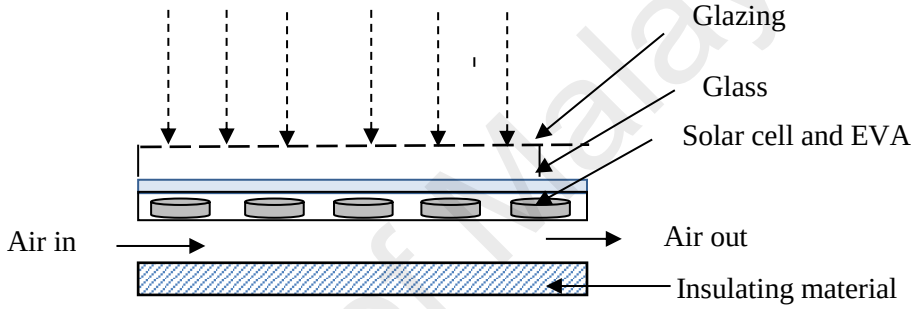

(i)

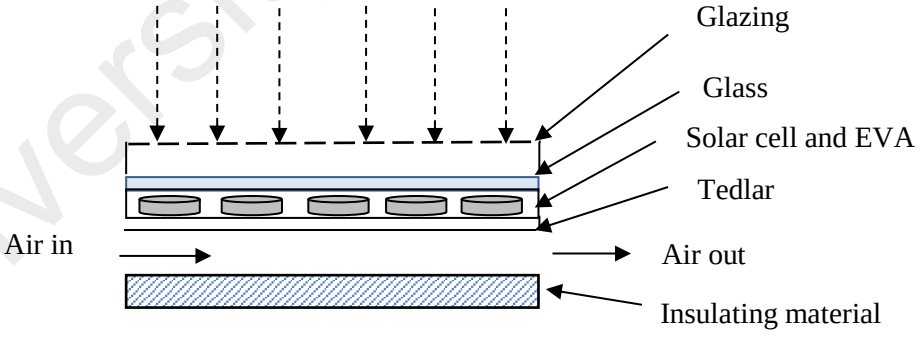

(ii)

Figure 2.4, continued

Zhang et al. (2012) designed several types of air-based PV/Ts for space heating, herb drying or to improve ventilation. These designs included unglazed, single glazed and double glazed configuration and air could be delivered in single pass or double pass mode (Figure 2.5).

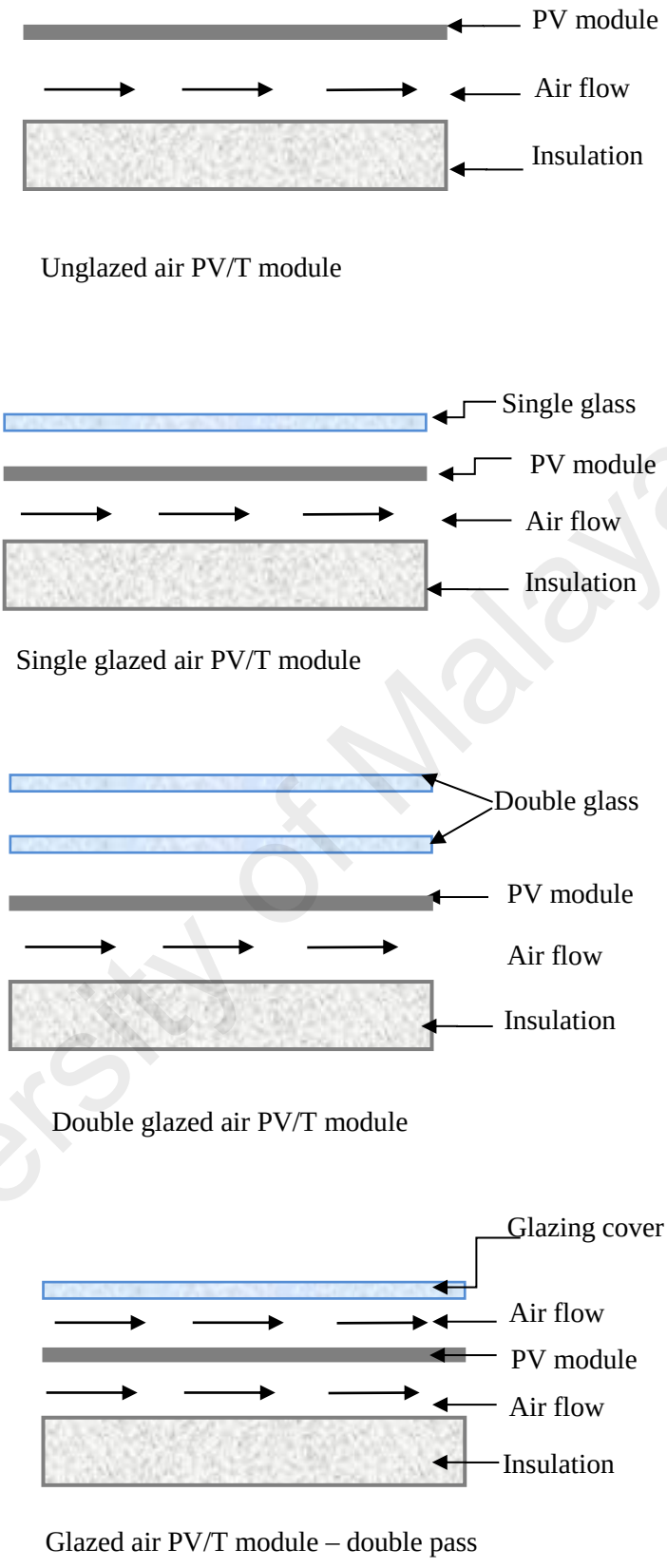

Figure 2.5: Various PV/T air collector designs (Zhang et al., 2012)

On the basis of the number of run of air flow passage, the PV/T-air collectors are classified into single pass flow and double pass flow collectors. Hegazy (2000) listed the common models of single glazed PV/T air collector as illustrated in Figure 2.6. The three single pass air collectors include Model I in which air may flow over absorber, Model II where air flow beneath the absorber and Model III wherein air flows on both sides of the absorber. In model IV air is flown in double pass mode. The conventional design in single pass air collector is the model II although model I offer the simplest configuration.

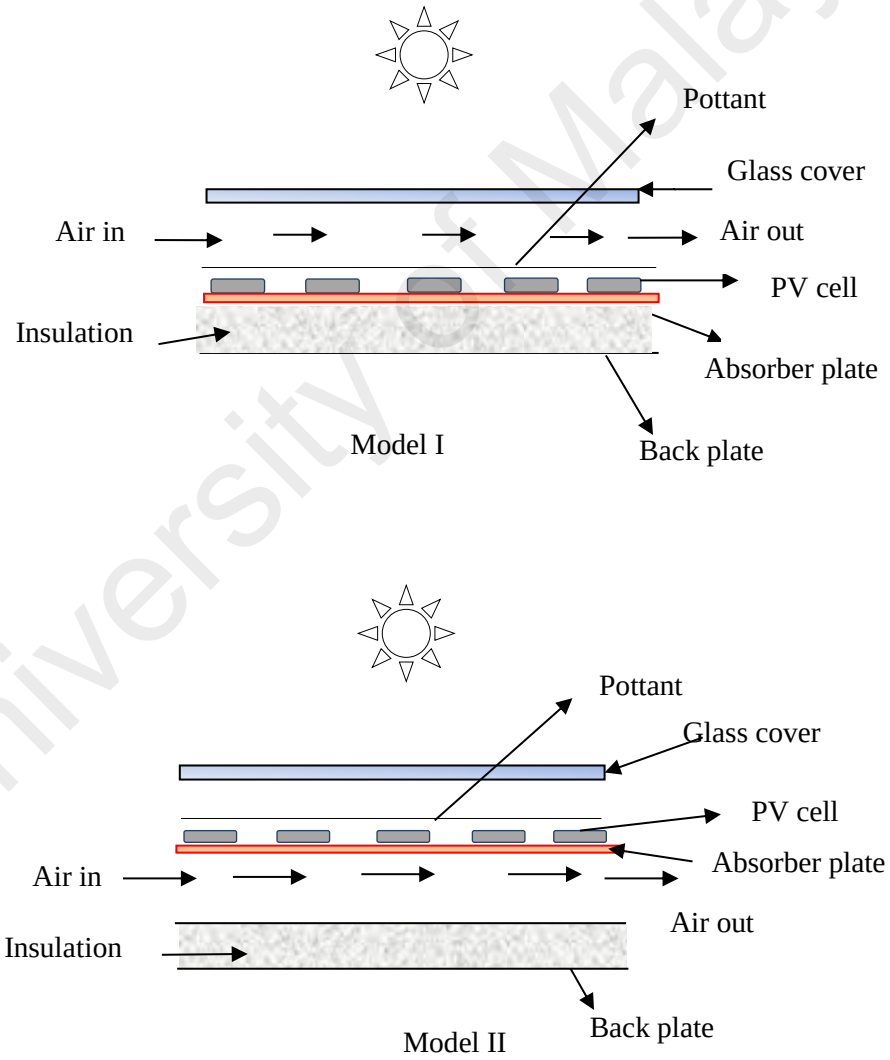

Figure 2.6: Single-pass and double-pass PV/T air collectors (Hegazy, 2000)

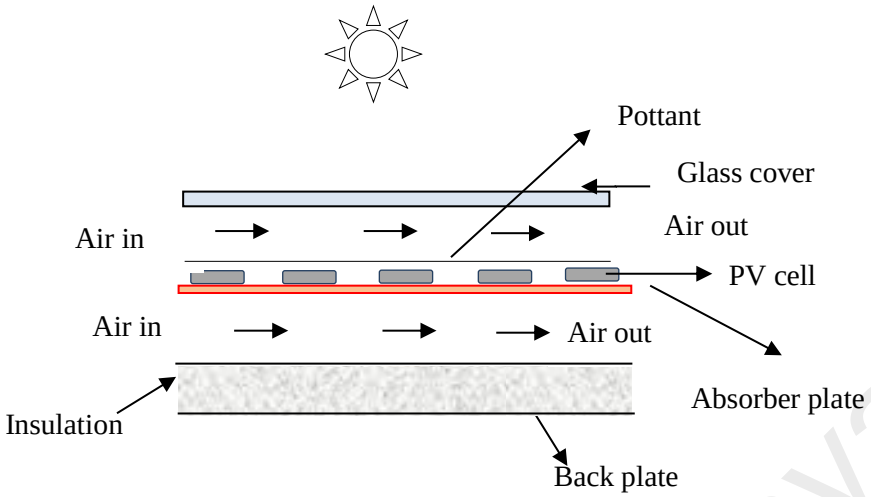

Model III

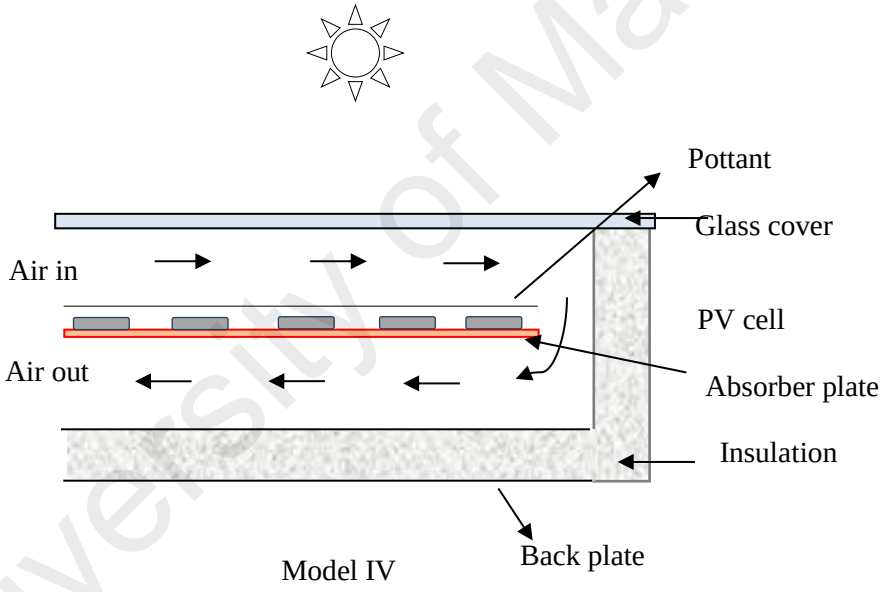

Model IV

Figure 2.6, continued

A numerical study on various performance parameters of PV/T air heater using single and double glass configurations was performed by Garg and Adhikari (1997). The authors suggested that the use of single or double glass closure is contingent to the projected temperature range.The single glass system was observed to accumulate more heat than double glass system beyond a critical temperature.

Sopian et al. (1996) examined the performance of a double-pass PV/T-air collector (model IV, Figure 2.6) that is suited for solar drying of crops and herbs. The performance of the double pass configuration was found better than the conventional single pass design and the authors suggested that besides solar drying, this configuration would be appropriate for building applications. Table 2.1 shows the efficiency performance of single-pass and double pass PV/T air collectors.

Table 2.1: Comparison of the efficiency of PV, STC and PV/T air collector (Charalambous et al., 2007)

Efficiency	Single-pass	Double-pass
PV	6-7%	8-9%
STC	24-28%	32-34%
PV/T	30-35%	40-45%

2.5.2 Water Based PV/T Collectors

Water has higher thermal capacity than air. Moreover, it possesses better optical properties in near infrared radiation (Palmer & Williams, 1974). Therefore, water is more effective as a heat transfer fluid in photovoltaic thermal collectors. Early research on PV/T-water system was carried out from mid 1970s to early 1980s. Smith et al. modified a flat-plate thermal collector by pasting 104 solar cells over it. The authors noticed that the efficiency-temperature relationship was independent of the temperature gradient (Smith et al., 1978). Wolf (1976) examined the performance of PV/T collectors in producing hot water based on the Hottel-Whillier model (Hottel & Whillier, 1955) and found these systems economically feasible. Kern and Russell (1978) proposed the basic idea of PV/T water and air collectors. The Lincoln laboratory of Massachusetts Institute of Technology (MIT) and Sandia Laboratory jointly developed three full-size prototypes of flat plate PV/T collector (Hendrie, 1979).

Like PV/T air, PV/T water collectors also fall into four basic categories as depicted in Figure 2.7. Each category may have several variations in design, but all configurations follow these four basic concepts (Zondag et al., 2003). One notable point here is that air also contributes in the heat transfer process in each design of the PV/Ts. However, as water acts the main heat transfer fluid (HTF), so these collectors are categorized as PV/T-water collector.

2.5.2.1 Sheet-and-tube PV/T collectors

Sheet and tube collector (Figure 2.7 (a)) is one of the simplest design for PV/T water collectors. The tubes may be of circular, rectangular or square geometry. Florschuetz (1979) extended the Hottel-Whillier (H-W) method of performance study of sheet-and-tube collectors with glazing to adapt it in conjunction with PV laminate. A physical model of a hybrid PV/T based on heat transfer through conduction, convection, and radiation was developed by Bergene and Løvvik (1995). The authors opined that the fin width to tube diameter ratio is a key control factor for sheet and tube collectors. Zondag et al (2003) studied different types of PV/T-water collector and found sheet and tube concept slightly less effective than all other collectors. The use of multiple glass cover for sheet-and-tube PV/T collector has been examined by researchers with a view to enhance the PV/T performance. However, using more than two glass covers was found to render much reduced electrical efficiency.

2.5.2.2 Channel PV/T collectors

Channel PV/T collector consists of two separate channels for water and air flow, both above the PV laminate and partitioned by a glass cover (Figure 2.7(b)). In this configuration, as the coolant flows over the PV, selection of fluid becomes a factor, too. If the absorption spectrum of the fluid and that of PV is similar, it may hamper the

incoming radiation absorption capacity of the solar cells. Although this design is simple to construct, a conceivable problem may occur with wide channels where glass plate of sufficient thickness would be required to withstand the water pressure and there remains a risk of fragile structure (Bakkar et al., 2002). An alternate design in channel PV/T is to allow the water to flow beneath the PV module. Tiwari and Sodha (2006) numerically carried out a parametric study on such a design with four configurations, viz., unglazed with tedlar, glazed with tedlar, unglazed without tedlar and glazed without tedlar. The same authors performed a performance evaluation of the same designs on the basis of energy balance of each consecutive layer of the PV/T system (Tiwari & Sodha, 2006a). The authors found the simulation predicted daily thermal efficiency (58%) at good compliance with that obtained experimentally (61.3%) by Huang et al. (2001).

2.5.2.3 Free-flow PV/T collectors

Vaxman and Sokolov (1985) proposed the first free-flow model for water based PV/T system (Figure 2.7(c)). Unlike channel type collector, the flow of air and water is not separated by glass layer, which reduces the losses due to reflection as well as the material cost. However, there is twofold limitation with this design of PV/T collector. In one hand, evaporation is likely to occur as air flows directly in contact with water which may cause a reduction in thermal efficiency. On the other hand, condensation on top of the glass layers reduces transmission of sunlight A highly absorbing fluid with a high evaporation temperature may alleviate these problems to a good extent. Hence, water is not an appropriate choice for this design as in other cases; however, increased evaporation rate of water with rising temperature facilitate in preventing the overheating of the system.

2.5.2.4 Two-absorber PV/T collectors

In two-absorber configuration, a transparent PV laminate is employed as the primary absorber and a high absorptivity black metal sheet is used as a secondary absorber (Figure 2.7 (d)). There are two flow passages of water separated by an air flow passage. Water enters through the upper channel (primary flow) and returns (secondary flow) through the lower one. This distinct design was investigated under PV/T development program at Massachusetts Institute of Technology (MIT) and a high thermal efficiency was observed (Hendrie, 1979). Several adaptations are possible in two-absorber PV/T collector design, viz. inclusion of a transparent insulating layer between the primary and secondary channel and replacing the water channel beneath the secondary metallic absorber by a sheet-and-tube. The former configuration was proved effective in abating further heat loss.

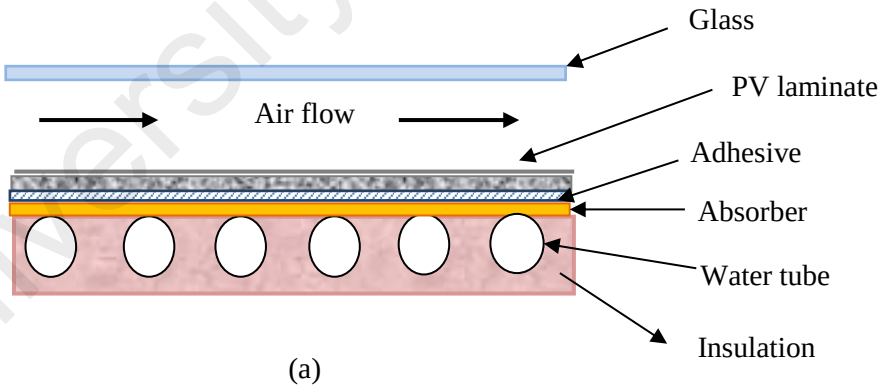

Figure 2.7: Water based PV/T collectors; (a) sheet-and-tube, (b) channel, (c) free-flow, (d) two-absorber (Zondag et al., 2003)

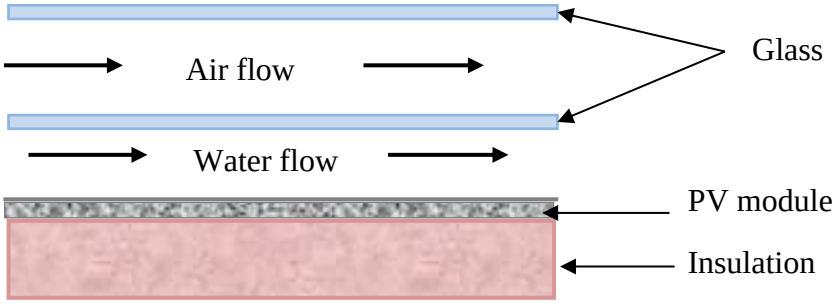

(b)

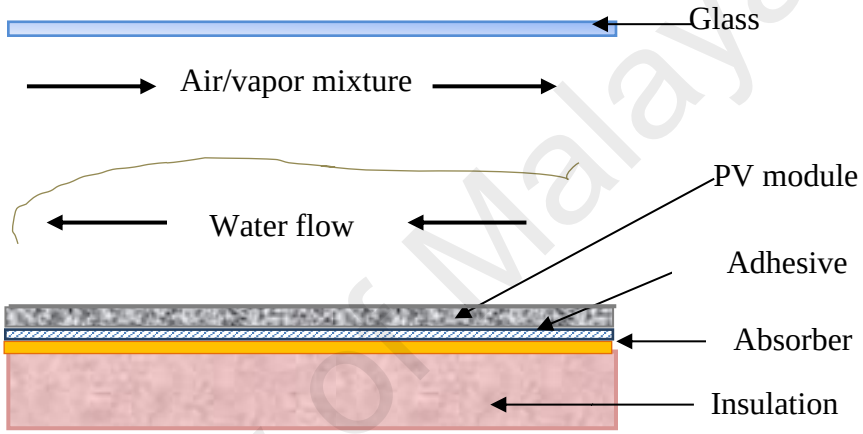

(c)

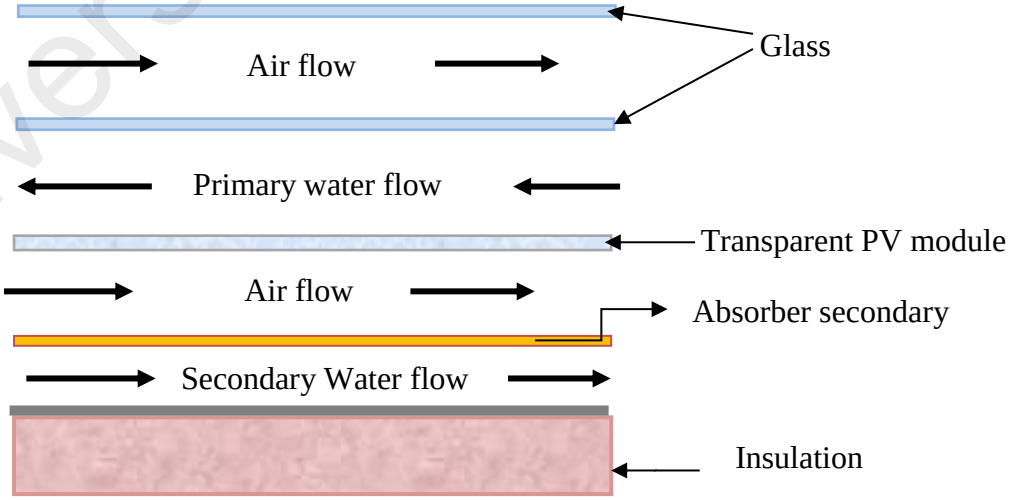

(d)

Figure 2.7, continued

Both PV/T-air and PV/T-water collectors have their own merits and demerits. A comparative merits and demerits of these two types of PV/T have been tabulated in Table 2.2.

Table 2.2: Comparison of air and water as heat transfer fluid (HTF) for PV/T

HTF	Merits	Demerits
Air	• Free from freezing or stagnation • Simple in design and less expensive with minimal uses of materials • Appropriate for preheating of air for building applications • No risk of damage whenever it leaks • Free from environmental or health hazards	• Low heat transfer due to low heat capacity • Larger channels are necessary to attain considerable performance due to the low density of air • Second solar circuit is required for closed loop systems • Open systems suffer from low temperature range and noise due to the use of fan
Water	• Simplest way to construct PV/T system • Excellent heat transfer fluid medium due to its thermal capacity and viscosity. • Low cost	• Freezing problem in cold regions. • Incessant rise temperature of water during operation that affect the efficiency and cause poor heat removal • Increased heat loss due to evaporation. • Evaporation problems at high temperatures.

2.5.3 Heat Pipe Based PV/T Collectors

A heat pipes is a highly efficient heat-dissipating device that employs evaporative cooling technique to transfer heat at large-scale with very small drop in temperature. It is a sealed evaporator-condenser pair made of a metallic tube internally lined with capillary structure or wick to facilitate the reversion the condensed liquid from condenser to evaporator. The thermal conductivity of heat pipe depends on its length

and can be as high as 100 kW/(m.K) for long heat pipes. Among many other use, heat pipes find important application in solar thermal area, too. Recently, attempts have been made to employ this heat dissipation technology in PV/T systems.

Makki and Omer (2015) analytically investigated a hybrid system comprising of a Heat Pipe-based Photovoltaic-Thermoelectric Generator (HP-PV/TEG) which employs a PV panel for direct power generation, a heat pipe to absorb excessive heat from the PV cells and assist uniform temperature distribution on the surface of the panel, and a thermoelectric generator (TEG) to perform direct heat-to-electricity conversion. The authors reported that the combination of TEG modules with PV cells improved the performance of the PV cells through utilizing the waste-heat available, leading to higher output power.

Zhang et al. (2013) introduced the concept of solar photovoltaic/loop-heat-pipe (PV/LHP) heat pump scheme for supplying warm to hot water. The authors developed a computer simulation model of the system to assess system performance and carried out experimental investigation to verify the results obtained from numerical study. Authors reported to achieve thermal and electrical efficiencies of proposed system as 10% and 40%, respectively; whilst the coefficient of performance of the system ($COP_{PV/T}$) was found 8.7.

Gang et al. (2011) designed and constructed an innovative heat-pipe photovoltaic/thermal system for employing in cold regions without freezing. The electrical and thermal efficiencies of the system were found 9.4% and 41.9% with an average electrical and thermal gain of 62.3 and 276.9 W/m^2, respectively. The exergy efficiency of the system was found 6.8%.

Fu et al. (2012) constructed and investigated two heat pipe based PV/T collectors, with 80 and 140 mm tube spacing. Outdoor tests were carried out to compare the performance of the two systems with PV/T collectors placed at tilt angles of 32 and 45º. Results showed that an 80-mm tube space for the heat pipes improved both the thermal and electrical efficiency better than that with 140-mm tube space.

Wu et al. (2011) investigated the effect of various parameters, such as water inlet temperature, mass flow rate, packing factor and heat loss coefficient on the performance of a heat pipe photovoltaic/thermal hybrid system. The overall thermal electrical and exergy efficiencies were obtained 63.65%, 8.45% and 10.26%, respectively. The authors recommended heat pipe-PV/T hybrid system as potential over other conventional BIPV/T systems.

2.5.4 Refrigerant Based PV/T

The heat that is recovered from PV/T system has been utilized for desiccant cooling and dehumidification applications (Guo et al., 2017). Tsai (2015) developed a photovoltaic/thermal assisted heat pump water heater (PV/TA–HPWH) system where the PV/T provides thermal energy to run the evaporator of the HPWH system and generates electricity as well. The main goal of this research was to develop a user friendly computational model for PVTA–HPWH system and to study its dynamic behavior. Experimental validation was also performed and the results showed well agreements between simulation and experimental measurement with adequate poise.

Zhao et al. (2011) designed a photovoltaic/evaporation-coil (PV/e) module integrated with the building as a roof element and acts as an electricity generator as well as evaporator of a heat pump system. Authors suggested an operating temperature of 10°C for evaporation and 60°C for condensation. The predicted performance under typical

Nottingham, UK climate were 55% of thermal efficiency and 19% of electrical efficiency, while the overall efficiency estimate of the heat pump system was 70%. The schematic of a refrigerant-based PV/T system is shown in Figure 2.8.

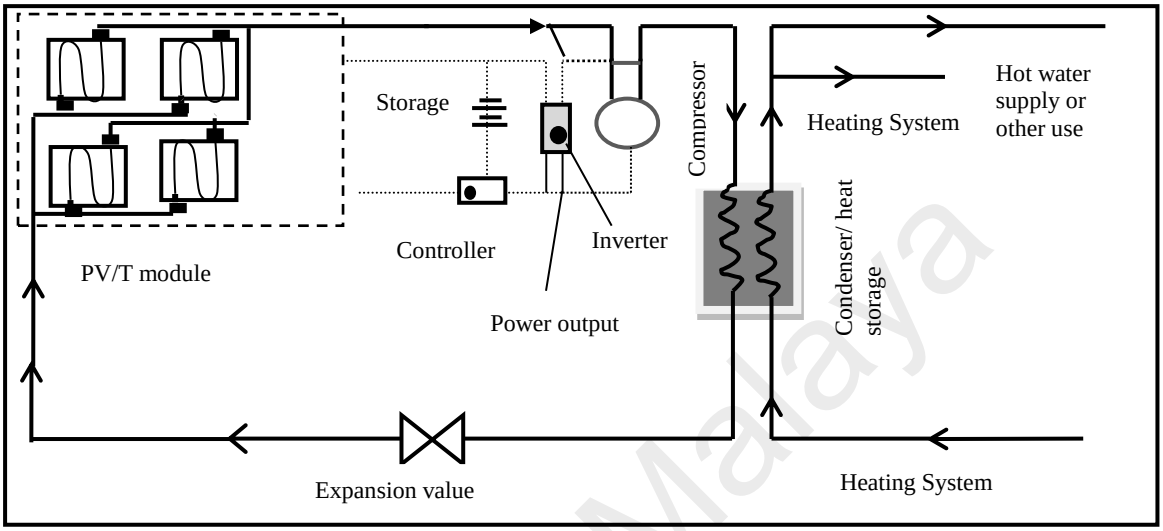

Figure 2.8: Schematic of refrigerant based PV/T collector (Zhao et al., 2011)

In PV/T collectors, refrigerants are tried as HTF, specially to run heat pumps. Kern and Russell (1978) designed a refrigerant based PV/T that is attached to a heat pump and tested according to ASHRAE standards. Authors concluded that hybrid systems are economically viable for small houses with considerable heating loads.

2.6 Summary of Research Works

In literature, there is found three types of research works on PV/T, viz., theoretical studies to analyze its basic physical and technical aspects, numerical studies to optimize system design and performance and experimental studies to verify the theoretical and numerical observation in real-world condition. Some of the important works have been summarized in Table 2.3.

Table 2.3 Highlights of the research works by different researchers

Authors	Highlights	Findings
Florschuetz (1975)	• First mathematical model for hybrid PV/T system • Extension of Hottel–Whillier thermal model for solar thermal collector • Used TRNSYS software	• Electrical efficiency as well as module system efficiency of PV/T reduce linearly with increasing cell temperature
Wolf (1976)	• First physical model of PV/T • Expeimental study on liquid based PV/T	• Able to supply warm water for residential application along with electricity generation
Kern & Russell (1978)	• Fabricated and experimentally tested PV/T based on ASHRAE standards	• Effective energy yield per unit area of hybrid PV/T is greater than separate PV and STC
Hendrie (1979)	• Analyzed thermal and electrical performance of air and liquid based PV/T • Analytical as well as experimental investigation	• Thermal efficiencies was found to drop when elctricity is taken as an output. • Thermal efficiency of the air based and liquid based collectors was 42.5% and 40%, respectively. • Maximum electrical efficiency obtained was 6.8%
Raghuraman (1981)	• Studied both air and water based flat-plate PV/T	• A thermal efficiency of about 42% was attained with air as a heat transfer media
Cox and Raghuraman (1985)	• Computer simulation of PV/T design aspects	• High transmissive and low emissive PV cell cover helps to improve performance
Vaxman and Sokolov (1985)	• Free-flow configuration • Both air and water used as HTF in the same PV/T	• Reduces reflective losses • Drop in thermal efficiency due to evaporation • Condensation on top glass surface reduce transmissivity of incident radiation
Lalovic et al. (1986)	• Attcahed a-Si cells over fin- and -tube STC	• Provide hot water with a temperature of 65^{o}C
Bergene and Løvvik (1995)	• Sheet-and-tube type PV/T water collector with fins over the tube • Studied heat transfer features of PV/T	• Fin width to tube diameter ratio is the key parameter to control the performance • The result shows 60%-80% overall PV/T collector efficiency.
Sopian et al. (1996)	• Experimental study on double-pass PV/T air collector	• Double-pass PV/T air collector was found to provide better thermal efficiency than conventional single-pass design
Garg & Adhikari (1997)	• Numerical study PV/T air collector • Both single- and double-glass configurations were studied	• Beyond a critical temperature, single glass system collected more heat • Increasing duct depth decreases the efficiency of both configurations

Table 2.3, continuied

Authors	Highlights	Findings
Sopian et al. (2000)	• Double-pass PV/T collector • Variable packing factor	• Electrical efficiency increases with packing factor and mass flow rate
Kumar & Prasad (2000)	• Effect of solar irradiation intensity and Reynolds number on thermal performance was studied	• Performance improves with solar radiation intensity. • Best performance for Re < 12 000
Sandnes & Rekstad (2002)	• Relation between irradiance and ambient temperature is studied • Numerical simulation and experimental validation	• Electrical efficiency reduces due to some parameters such as module temperature and packing factor
Zondag et al. (2003)	• Sheet-and-tube PV/T collector, • Channel PV/T collector, • Free-flow PV/T collector, • Two-absorber PV/T collector	Thermal efficiency • The uncovered collector was found 52%, • Sheet-and-tube configuration was 58% • Channel above PV design was 65%.
Coventry & Lovegrove (2003)	• Economic analysis of household PV/T • Equivalent electrical levelized energy cost	• When energy value ratio is less than 4.5, a-Si cells require lower levelized energy cost than c-Si cells
He et al. (2006)	• Water based PV/T collector with a polycrystalline PV module	• The maximum thermal efficiency could reach 40%
Othman et al. (2006)	• Double pass PV/T collector with fins, • Parabolic concentrator (CPC), • V-groove absorber	• The collector with fins only performed poorly than the one with CPC and fins. • Increasing the flow rate increases the heat transfer coefficient, increasing the collector's electrical efficiency.
Ji et al. (2006)	• BIPV/T • Effect of mass flow rate • Effect of packing factor	• Thermal efficiency increases with mass flow rate increases
Tiwari & Sodha (2006)	• PV/T air collectors • Tested the system by forced convection	• Glazed hybrid PV/T collector without tedlar perform the best.
Tiwari & Sodha (2006a)	• Analytical study of PV/T air through energy balance method	• Daily thermal efficiency 58%
Dubey & Tiwari (2008)	• Flat-plate PV/T water heater • Effect of increasing glazing area	• With the increase in glazing area, the instantaneous efficiency was found to rise from 33% to 64%.
Tonui et al.(2008)	• Flat plate air-based PV/T • Glazed and unglazed • Mathematical model	• Investigated on the effect of parameters such as mass flow rate, ambient temperature, and tilt angle • validated it against experiment data
Chow et al. (2008)	• Dynamic simulation model of BIPV/T based on FDM • Experimental validation	• Thermal efficiency 26.8% with thermosyphon and 28.8% with pumps • Electrical efficiency 7% with thermosyphon and 9.1% with pumps

Table 2.3, continuied

Authors	Highlights	Findings
Dubey et al. (2009)	• Analytical model and experimentation on four PV configurations	• The electrical efficiency of glass-to-glass PV module with duct is the highest among the four designs
Dubey & Tiwari (2009)	• Semi shrouded flat-plate PV/T water collector • A number of collector connected in series • Theoretical modelling	• As the number of collector increases from 4 to 10 • outlet temperature increases from 60 to 86ºC • thermal energy gain increases from 4.17 to 8.66 kWh • electrical energy gain increases from 0.052 to 0.123 kWh
Anderson et al. (2009)	• BIPV/T – glazed & unglazed • 1D steady-state thermal model based on H-W-B model	• Thermal efficiency improves as the tube width to spacing is incresaed
Sarhaddi et al.(2010)	• Flat plate PV/T air collector	• Thermal, electrical and overall energy efficiency is about 17.18%, 10.01% and 45%, respectively • Overall and thermal efficiency decreases as inlet air temperature or wind speed or duct length increase.
Agarwal & Tiwari (2010)	• Air based BIPV/T • 1D transient model	• Thermal exergy per year 1531 kWh • Electrica lexergy per year 16209 kWh • Thermal efficiency 53.7%
Davidsson et al. (2010)	• Simulation model for PV/T solar window	• Annual electrical output is 35% more than a PV panel
Dupeyrat et al. (2011)	• Single glazed flat-plate PV/T water collector • Electrical performance was evaluated numerically and experimentally	• Thermal efficiency 79% • Electrical efficiency 8.8%
Shahsavar et al. (2011)	• BIPV/T • Used the cooling potential of ventilation and exhaust air to cool PV panels	• Electricity generation increased up to 10.1%, equivalent to 129.2 kWh per year • Energy recovery 3400.4 kWh per year
Gang et al. (2011)	• Heat pipe PV/T system without freezing • Effect of water inlet temperature, mass flow rate, packing factor and heat loss coefficient on system performance was studied	• Thermal efficiency 63.65% • Electrical efficiency 8.45% • Exergy efficiency 10.26% • Better for building applications than conventional BIPV/T
Wu et al. (2011)	• Heat pipe PV/T	• Thermal efficiency 41.9% • Electrical efficiency 9.4% • Exergy efficiency 6.8% • Thermal gain 276.9 W/m^2 • Electrical gain 62.3 W/m^2

Table 2.3, continuied

Authors	Highlights	Findings
Yang & Athienitis (2012)	• BIPV/T air collector with wirw mesh • Numerical study	• Efficiency with wire mesh is 8.5% higher than that without mesh • Outlet temperature rise by 4° to 11°C by using wire mesh
Zhang et al. (2012)	• PV/T air heater • Unglazed, single glazed, double glazed configurtaion	• Space heating • Herb drying
Zhang et al. (2013)	• Photovoltaic/Loop Heat Pipe (PV/LHP) • Simulation model and experimental validation	• Thermal efficiency 10% • Electrical efficiency 40% • System COP 8.7
Hailu et al. (2014)	• Forced convection in BIPV/T • Used FEM based software COMSOL Multiphysics®.	• Simulation reults employed to develop models for design and optimization
Liu et al. (2014)	• CPV/T with beam splitter and linear Fresnel refelctor	Power generation and efficiency – • 1367.0 W and 26.5% at cell temperature of 25°C • 1319.5 W and efficiency 25.6% at cell temperature of 50°C
Yang & Athienitis (2014)	• One-loop BIPV/T air collector with wirw mesh • Numerical and experimental study	• By using wire mesh thermal efficiency increased by 10% numerically and 7% experimentally. • Electrical efficiency incresaed by 8%
Renno (2014)	• CPV/T with point focus parabolic mirror and triple junction cells (InGaP/InGaAs/Ge) • Dual-axis tracking	• Water outlet temperature 90°C
Yang & Athienitis (2015)	• One-loop double inlet BIPV/T air collector • Used full-scale solar simulator for experimental study	• Thermal efficiency improves 5% by using double inlet compared to a single inlet system • Thermal efficiency is 7.6% higher with sei-transperant Pv than with transperant one
Makki and Omer (2015)	• Heat pipe based PV thermoelectric generator (HP-PV/TEG)	• Combination of TEG with PV ensures better utilization of waste heat
Tsai (2015)	• PV/T assisted heat pump water heater system (PV/T-HPWH) • Computational model to study dynamic behavior and experimental validation	• PV/T provides thermal energy to run the ecaporator of the heat pump
Calise et al. (2015)	• Organic Rankine Cycle (ORC) in conjuction with CPV/T • Used TRNSYS software	• Used to heat dithermic oil along with producing electricity • CPV/T only system is more economical
Li et al. (2015)	• Building integrated CPV/T • Numerical and experimental study	• Thermal efficiency 37.2% • Water outlet temperature 56.9°C

2.7 Performance Evaluation Criteria for PV/T

The performance of a PV/T module is mainly dependent on climate, design and operational conditions (Elbreki et al., 2016). Metrological parameters like direct and diffused radiation, ambient temperature, wind speed, etc., design parameters of the collector, viz., collector geometry and materials and flow parameters such as mass flow rate and mode of flow have got immense effect on PV/T performance. In addition, factors like cell materials, glazing, and use of cover influence the PV/T system performance to some extent.

2.7.1 Mass Flow Rate

Mass flow rate is the most influential parameter in PV/T performance as convection heat transfer coefficient is directly related to mass flow rate variations. Fluid type (gas or liquid), magnitude of the flow velocity and collector geometry are the main factors that control the mass flow rate (Kumar et al., 2015). Increasing mass flow rate increases heat transfer rate and decreases fluid outlet temperature, thereby improving the electrical and thermal efficiencies (Garg & Adhikari, 1997; Sopian et al., 2000).

Teo et al. (2011) observed that in PV/T-air system, thermal collector absorbs maximum heat from the PV module if air flow rate is 0.055 kg/s. Flow rate more than this limit no influence on thermal and electrical performance. Ji et al. (2006) numerically studied the effect of mass flow rate and packing factor on the performance of a wall-mounted BIPV/T. The authors found that thermal efficiency increased quiet sharply up to a mass flow rate of 0.05 kg/s.

Bhargava et al. (1991) carried out a numerical simulation of a PV/T-air collector to study the effect of mass flow rate, cell area and length of collector on performance. The authors noticed an increasing trend in air heater efficiency with the increase in mass flow rate of air and found the efficiency as high as around 50% at a flow rate near 500

kg/h. Othman et al. (2006) showed the effect of mass flow rate on collector efficiency. The authors observed that heat transfer coefficient increase with flow rate resulting in a reduction in PV panel temperature and enhancement in collector.

Bergene and Løvvik (1995) investigated the effect of tube spacing to diameter ratio *W/D* along with mass flow rate of water on flat-pate PV/T performance. The authors suggested that the most important factor in controlling cell temperature and improving collector efficiency are the mass flow rate and fluid inlet temperature. It was observed that at relatively lower flow rates, increasing the *W/D* ratio produces higher flow velocity leading to a considerable drop in fluid outlet temperature and the corresponding efficiency enhancement. Results also indicate that increasing the flow rate beyond 0.001 kg/s does not further improve the efficiency. A summary of the minimum and maximum mass flow as adopted by different researchers have been tabulated in Table 2.4.

Table 2.4: Mass flow rate ranges adopted by different researchers

Authors	**Mass flow rate (kg/s)**		**Type of fluid**
	Minimum	**Maximum**	
Garg et al. (1997)	0.01	0.09	Air
Sopian et al. (1996)	0	0.083	Air
Hegazy (2000)	0.0005	0.04	Air
Chow et al. (2003)	0.002	0.004	Water
Zondag et al. (2003)	0	0.21	Water
Tiwari et al. (2006a)	0.005	0.075	Water/air
Tonui et al. (2007)	0	0.05	Air
Dubey and Tiwari (2008)	0.005	0.08	Water
Shasavar et al. (2011)	0.0122	0.3182	Air
Kumar and Rosen (2011)	0.03	0.15	Air
Wu et al. (2011)	0.03	0.07	Water

2.7.2 Effect of Temperature

Photovoltaic/thermal modules, like all other semiconductor devices, are sensitive to temperature change and temperature has got a profound effect on PV/T performance. Most of the solar PV (except amorphous silicon solar cells) has negative temperature coefficient which means power generation decrease with the rise in module temperature. Electrical efficiency of mono- and polycrystalline silicon solar cells is found to decrease at rate of - 0.4 to - 0.65% per Kelvin, when the cell temperature increases (Davis et al., 2001; Teo et al., 2011).

Rahman et al. (2015) experimentally investigated the effect of temperature on PV performance at indoor conditions. A reduction in module temperature by 22.4^{o}C causes an increase in electrical efficiency by 1.23% at indoor,

Ray (2010) conducted an experiment on PV cell efficiency at a high temperature using polymer, copper indium diselenide (CIS), and a-Si type solar modules. Authors suggested CIS and a-Si cells suitable for solar power generation under high temperature.

Fesharaki et al. (2011) observed that electrical efficiency decreases linearly with the increase in temperature. Radziemska (2003) studied the effect of temperature and wavelength on electrical performance of crystalline silicon solar cell. The author detected a drop in fill factor by - 0.2% and that in conversion efficiency by - 0.08% per Kelvin as the cell temperature increases.

Power generation by PV cell depends on its operating temperature. Short circuit current (I_{sc}) increases slightly, while the open circuit voltage (V_{oc}) drops significantly with increasing temperature. Krauter and Ochs (2003) showed that open circuit voltage decrease at a rate of - 2.3 mV for every Kelvin increment in cell temperature.

Thermal performance of the PV/T collectors is also dependent on temperature change. Kim et al. (2014) showed that thermal efficiency decreases moderately as the temperature difference between collector fluid and ambient temperature is increased. The maximum value of thermal efficiency at zero reduced temperature was found 29%, but the value decreased to about 22% with increased temperature difference. Tiwari and Sodha (2007) observed that the instantaneous efficiency of a glazed PV/T-air collector without tedlar drops at greater rate than that of glazed PV/T with tedlar. Dubey and Tiwari (2008) noticed that the instantaneous efficiency of a PV/T-water system decreased almost linearly with growing temperature difference between the water inlet and ambient temperatures.

2.7.3 Collector Geometry

Collector geometry and dimension has great influence on PV/T performance. Tonui et al. (2008) investigated the effect of collector length and channel depth on the collector efficiency. The authors found the thermal efficiency increases noticeably while the electrical efficiency decreases slightly with the increment in collector length. On the other hand, Koech et al. (2012) noted a considerable decline in electrical efficiency with the increment collector length. Regarding the effect of channel depth, Tonui et al. (2008) noticed that there is an optimum channel depth, which allows the maximum mass flow rate as well as thermal efficiency. After that value, the efficiency does not vary that much. Bergene and Løvvik (1995) studied the impact of tube spacing to diameter ratio (*W/D*) on performance of PV/T. The authors reported that thermal efficiency falls by around 50% when *W/D* ratio is increased from 1 to 10, keeping *W* as constant. Increasing *W/D* also decreases the outlet fluid temperature.

2.7.4 Effect of Glazing

In order to reduce convective heat losses in PV/T collectors, some researchers proposed the use of glass cover (glazed) over the PV module (Chow et al., 2009; Fujisawa & Tani, 1997; de Veries, 1998). Fujisawa and Tani (1997) performed exergy analysis of PV/T collectors with and without glass cover, i.e., glazed and unglazed PV/T. Thermal energy gain was found to be greater for PV/T with single-cover (glazed); however, in terms of exergy, unglazed design showed slightly better performance than the glazed design. de Vries (1998) studied different types of sheet-and-tube combi-panel (PV/T collector), viz., uncovered (unglazed), single-covered (glazed), double-covered (glazed) and narrow channel combi-panel. The author found that the electrical efficiency of the uncovered combi-panel is higher than that of the single-covered combi-panel, whereas its thermal efficiency is much lower. The thermal efficiency of double-cover combi-panel was also found to be lower due to its lower optical efficiency.

Tripanagnostopoulos et al. (2002) compared the performance of glazed and unglazed PV/T collectors and found the thermal output improves by using extra glazing. Again, by using a booster diffuse reflector both electrical and thermal output can be enhanced. Zondag et al. (2003) reported a poor performance of sheet-and-tube PV/T collectors without glazing and indicated the cause as large heat losses due to the absence of glass-cover. Kim and Kim (2012) found that glazed PV/T collectors show better thermal performance than the unglazed PV/T collectors, whilst electrical performance of the unglazed collector was found higher than that of the glazed one.

2.7.5 Packing Factor

Packing factor is the fraction of absorber plate area covered by the solar cells. It is an important parameter to control the performance of a PV/T system, especially in case of

building integrated ones. Electrical output is directly related to packing factor. However, increased packing factor increasing PV module temperature and thus decrease electrical efficiency.

Vats et al. (2012) studied the effect of packing factor on the room and module temperature and electrical efficiency of roof-mount PV/T system with semitransparent PV module. The authors carried out energy and exergy analysis of the system using three different packing factors, viz., 0.42, 0.62 and 0.83 of various types of cells. It was noticed that PV temperature decreases with low packing factor resulting in an improvement in efficiency. Kumar and Rosen (2011) performed a parametric study on PV/T air heater with and without fin. The authors reported that higher packing factor increases the electrical output and they claimed a 17% enhancement in overall efficiency. Wu et al. (2011) carried out a parametric study on heat piped based PV/T wherein the effect of packing factor along with several other parameters were observed. The authors found a very minor effect of varying packing factor on PV cell temperature, the disparity being less than 2^{o}C. In addition, the electrical efficiency was observed to increase moderately (from 6.45 to 8.33% against packing factors from 0.7 to 0.9) and thermal efficiency was found to decrease slightly (from 60.6 to 59.2% against packing factors from 0.7 to 0.9) with increasing packing factor.

Sopian et al. (2000) developed a double-pass PV/T collector for solar drying applications wherein the packing factor could be altered in accordance with the electricity requirement. Dunlop et al. (1998) reported to obtain a 25% thermal and 11% electrical efficiency for a PV module with a packing factor of 0.85 when the irradiation was 380 W/m^2 and the flow velocity was 0.4 m/s. Sopian et al. (1996) noticed an increasing trend in thermal and overall efficiencies with reduced packing factor.; on the other hand, electrical efficiency showed a slight decrease.

2.7.6 Absorber and Thermal Collector Materials

As one of the major focus of the PV/T system is its thermal output, the material of absorber and thermal collector plays a key role in its performance. Copper has been considered as the best absorber plate material due to its high thermal conductivity and low emissivity. However, copolymer as absorber material has also been investigated. Chow et al. (2003) tried different materials for absorber plate and thermal collector – aluminum for absorber and copper for collector tubes. The reported maximum overall efficiency was over 70%. Sandnes and Rekstad (2002) used a polymer absorber sheet instead of conventional metallic plate. Huang et al. (2001) used corrugated polycarbonate absorber sheet in PV/T water collector. The authors reported an attainment of 38% thermal efficiency along with 9% PV efficiency.

Apart from good thermal conductivity, especially for thermal collector, the material should be corrosion resistant, durable and light weight. On the other hand, the absorber material should have high absorption coefficient of incident irradiation, and thermal stability at the operating temperature (Ekechukwu & Norton, 1999). Kreider and Kreith (1989) proposed the use of different types of coating on absorber plate to increase the absorption characteristics. Table 2.5 shows the characteristics of absorptive coatings.

Table 2.5: Characteristics of absorptive coatings (Kreider & Kreith, 1989)

Material	Absorptance (α)	Emittance (ε)	Break down temperature (^{o}C)	Comments
Black silicon paint	0.86-0.94	0.83-0.89	350	Silicone binder
Black silicon paint	0.9	0.5	-	Stable at high temperature
Black copper over copper	0.85-0.9	0.08-0.12	450	Patinates with moisture
Black chrome over nickel	0.92-0.94	0.07-0.12	450	Stable at high temperatures

2.7.7 PV Cell Materials

The electrical performance of a PV/T system has an outright relation with PV cell material. Solar cells are mainly made from silicon, either crystalline silicon (c-Si) or amorphous silicon (a-Si). The crystalline silicon may be of single or mono-crystal or they may be of poly-crystals. Solar cells produced from monocrystalline silicon (m-Si) offer higher efficiency (15 - 20%) and reliability in outdoor operation. On the other hand, polycrystalline silicon (p-Si) cells are stronger than their monocrystalline counterpart with slightly lower cost, but they are relatively inefficient (10 - 14%) in energy conversion. A compound semiconductor material gallium arsenide (GaAs), manufactured from two elements gallium (Ga) and arsenic (As), has its crystal structure resembling almost with that of silicon. GaAs cells possess high light absorptivity and greater efficiency (25 - 30%) than crystalline silicon cells. Moreover, this compound semiconductor has high thermal stability and good resistance to radiation. That is why, GaAs cells are best suited for concentrator photovoltaics and space applications. Thin film solar cells are manufactured by depositing a semiconductor material on a substrate like metal, glass or plastic foil. Thin film cells are made from amorphous silicon (a-Si), cadmium telluride (CdTe), copper indium gallium diselenide (CIGS), etc. These cells have higher light absorption capability than crystalline silicon cells, but their energy conversion efficiency is very poor (NSPRI, 1998).

Dobrzański et al. (2013) compared the effect of using mono- or polycrystalline silicon on PV performance. A better electrical efficiency (14.95%) was achieved with monocrystalline cells than polycrystalline cells (12.60%), while fill factor was found better in polysilicon cells. Radziemska (2003a) indicated that using semiconductors with wide band gap, e.g., gallium arsenide (GaAs) for PV cells allow extended operating temperature. Ji et al. (2003) reported a higher thermal efficiency of

amorphous silicon (a-Si) PV cells. However, Versluis et al. (1997) noticed an opposite consequence, the collector efficiency of a-Si cells is lower than that with c-Si cells.

Tripanagnostopoulos et al. (2002) investigated on PV/T-liquid and PV/T-air collector with both crystalline and amorphous silicon solar cells. Using crystalline silicon solar cells, the thermal efficiency of the liquid based and air based collectors were found to be 55% and 38%, respectively. With amorphous silicon cells, PV/T-liquid collector showed a thermal efficiency of 45%, whereas PV/T-air collector produced 60% thermal efficiency. The advantage and disadvantage of different PV cell materials with efficiency are shown in Table 2.6.

Table 2.6: PV cell material types - merits, demerits and efficiency level (Nahar et al., 2014)

Types of PV Cell	Advantages	Disadvantages	Efficiency
Crystalline Silicon (c-Si)	• Mature technology • Si is the most studied element on the Periodic Table • Abundant and available material • High electronic quality • High efficiency	• Slow, expensive processes • *c-Si = Czochralski (Cz)* • *pc-Si = Directional* • *Solidification (DS)* • Energy intensive processes (1410°C) • Indirect band gap (Thick Material)	**m-Si** 25.0% **p-Si** 20.4%
Amorphous Silicon (a-Si)	• Better "low-light" performance • Thin Film (< 1 micr • Cheap deposition techniques (PECVD, Sputter) • Abundant and available material	• Low efficiency • Poor hole mobility • Poor stability (Staebler-Wronski effect) • High band gap (1.7 eV)	12.5%
Cadmium Telluride (CdTe)	• Can be doped with both p-& n-type • High deposition rate • Low manufacturing cost • Absorber layer is impurity tolerant	• Lacking of basic understanding • No standardized deposition process *(CSS/Sputter/Ink Jet/Electroplating)* • Cadmium is a toxic element	16.7%
Copper Indium Gallium Diselenide (CIGS)	• Highest efficiency thin film • Stable performance over time • Potentially low manufacturing cost • High deposition rate of absorber materials	• Lacking of basic understanding • No standardized deposition process *(CSS/Sputter/Ink Jet/Electroplating)* • Big gap between lab and commercial efficiency	20%

Table 2.6, continued

Types of PV Cell	Advantages	Disadvantages	Efficiency
Multi-Junction Solar Cells	• High power density • Highest efficiency solar cells • Suitable for concentration > 300X • Individually optimized layers	• Complicated manufacturing process • Very high cost • *GaInP2/GaAs/Ge* Triple Junction • Transport across interfaces • ~50 ayers, lattice matched	41.6%
Dye Sensitized Solar Cells (DSSC)	• Low cost manufacturing • Artificial photosysthesis • Low light sensitivity • Designer cells for BIPV • Tolerant to impurities	• Low efficiency • Liquid electrolyte • Expensive ruthenium dye	11%
Organic Solar Cells	• Simplified fabrication • Potentially very low cost • Highly versatile (flexible) • Abundant materials as carbon-based	• Low efficiency • Life time performance degradation • Integration of organic with inorganic • Low mobility / exciton diffusion	8%

2.8 Improvement Techniques and Relevance of the Present Research

Photovoltaic thermal is a very promising technology as the system produce electricity and heat concurrently. This technology may serve to abate the dependency on conventional fossil fuels to a good extent. As the performance of PV/T system is dependent on both thermal and electrical efficiency, improvement schemes should focus on the PV cell as well as on the thermal capacity of the collector. Hence, PV/T performance enhancement can be achieved at cell level, thermal collector design level or total system design level.

Performance of photovoltaic cells is a function factors of various factor, viz., material, size (larger cells yield more electricity), and the intensity and mode of the solar insolation. Temperature is the key factor that affects cell performance the most. Crystalline silicon cells suffer from a negative temperature coefficient, that is, their efficiency drops with rising temperature. As solar irradiation increases, temperature also

increase, resulting in a reduction in electrical efficiency. Module temperature is also related to several other factors like lifespan of the minority charge carriers, diffusion length and saturation current. Modifying the PV structure help a little in improving its electrical performance; however, cooling of the PV cells could upsurge cell efficiency significantly.

In order to improve the overall efficiency of a PV/T system, enhancement in thermal efficiency is very important. Thermal efficiency can be improved by producing efficient designs of thermal collectors, employing appropriate HTF, controlling the mass flow rate of HTF and using heat transfer equipment.

Sopian et al. (2011) examined the performance characteristics of PV/T with three different types of thermal collectors, viz., direct flow, parallel flow, and split flow collector. The authors found split flow collector to perform the best. Ibrahim et al. (2009) investigated PV/T performance with seven different collector designs. The spiral flow design was proved to be the best with a thermal efficiency 50.12% and an electrical efficiency of 11.98%. Zondag et al. (2003) tested and compared the electrical and thermal efficiencies of nine designs for PV/T water based collectors that included sheet-and-tube collector, channel type collector, free flow collector along with several other designs. The authors noticed more consistency in the performance of channel type collectors than other designs. Free flow collector was found to lose thermal efficiency due to evaporation. On the other hand, they also suffered electrical efficiency drop due to the increase in reflectivity through the accumulation of condensate on glazing surface. Table 2.7 shows the effects of control parameters on PV/T system.

Table 2.7: Effect of control parameters on PV/T system efficiency (Moradi et al., 2013)

Efficiency	Increase with	Decreases with
Thermal efficiency	• Increasing mass flow rate until optimum mass flow rate • Increasing collector length • Increasing tilt angle • Increasing inlet velocity • Increases packing factor	• Increasing mass flow rate beyond the optimum point • Increasing ambient temperature • Increasing inlet temperature • Increasing heat loss coefficient
Electrical efficiency	• Increasing of mass flow rate • Decreasing solar cell temperature • Increasing packing factor • Increasing solar radiation up to specific limit • Decreasing mean PV temperature	• Collector length decreases • Increasing solar radiation beyond a specific limit • Increasing absorber plate length • Increasing inlet water temperature
Overall efficiency	• Increasing mass flow rate • Increasing solar radiation up to specific limit • Decreasing mean PV temperature • Increasing packing factor	• Increasing inlet temperature • Increasing solar radiation intensities • Increasing absorber plate length

Performance of a PV/T system can be enhanced by working on two separate grounds. One is to reduce the loss in electrical efficiency of the PV cells and the other one is the effective harvest of the heat produced in the PV module, that is, to transfer the heat to the water cooling media effectively. However, there is a material limit in improving electrical performance. In order to improve the system efficiency, attention should be focused on the thermal collector, so that the maximum harvest of heat might be ensured.

From the above overview the following conclusion may be drawn: firstly, flat plate PV/T collectors are still the most promising option in photovoltaic thermal technology due to their simplicity in design, low cost, and easy application. Secondly, most of the researches on PV/T system were carried out to assess its performance and optimization of the geometric configuration of the thermal collector wherein the focus was primarily

on the effects of system's control parameters. Although some of these researches included experimental validation, numerical simulation is still considered as the effective and handy technique to explore the complex phenomenon of the conjugate heat transfer and corresponding fluid flow mechanism. However, literature review shows that most of the numerical studies performed so far are one or two dimensional and inadequate to portray the inner view of the thermo-fluid ambience inside the collector. Only three dimentional (3D) models can depict the real-time consequences that are going on inside a system. Three-dimensional mathematical model and numerical simulations are very much important to predict the performance parameters with more accuracy and faithfulness, which is important to design and device the experimental method. On the other hand, experimental justification of such a 3D model of particular geometrical design of a collector could establish the model as a standard to compare the performance of the other complex designs. This would alleviate the need for further experimentation for performance evaluation of new designs.

Therefore, in the present research work attempt has been made to develop an extensive 3D numerical model for the flow channel (thermal collector), which upon experimental validation might be extended for other flow channel designs with different geometries.

CHAPTER 3: THEORETICAL BACKGROUND

3.1 Photovoltaic Thermal System: An Optimized Solar PV

The traditional silicon based PV modules experience a drop in power production under elevated temperature and they produce more electricity the cooler they are. Solar cells have threshold photon energy conforming to the specific energy band gap below which electrical conversion does not take place. Photons with longer wavelength do not create electron-hole pairs; rather dissipate their energy as heat in the solar cell. Common PV modules convert only 4–17% of the incident solar radiation into electricity, the value being dependent on the type of the PV cell used. If the reflected energy is taken into account, it may be concluded that more than 50% of the solar energy received is transformed into heat which increase the cell temperature as high as 50^{o}C above the ambient temperature. This may lead to two unwanted consequences; first, a drop in the cell's energy conversion efficiency by 0.4 –0.65% per degree Celsius rise for crystalline silicon cells and secondly, permanent physical damage of the module if the thermal stress is prolonged (Chow, 2010). Hence, cooling of PV modules is essential not only for achieving enhanced performance, but also for improving the panel life span. However, this shortcoming may be transformed into an advantage by making wise use of the waste heat that would otherwise be dissipated from the PV module in vain. In order to improve the electrical efficiency and to ensure effective exploitation of incoming solar energy, the most effective way is to take away the heat accumulated in PV module and make suitable use thereby. This leads to the combination technology, now widely termed as PV/T system (Zhang et al., 2012). A PV/T system is a solar co-generation process wherein electricity and heat is produced simultaneously in a single module which enhances PV electrical efficiency as well. This integration of PV and thermal collector offers a new horizon in renewable heating and power generation (Kumar et al., 2015).

The demand for electricity and heat is often complementary and the potential heat generation from a given surface area is much greater than electricity. Thus, if designed aptly, PV/T systems are more effective than isolated solar thermal collector to serve as thermal energy source. The PV/T offers multi-dimensional benefits. The total area used to produce a given quantity of electricity and heat from a hybrid collector is less than for two separate systems, the material requirement for a PV/T system is obviously less, thereby the economy balance is better than that for individual units. PV/Ts have wide range of applications; the thermal energy can be used both for heating and cooling purpose depending on the season of application. In addition, these systems can be retrofitted to the building without major modification or replacing the roof materials (Danish, 2003).

3.2 Photovoltaic Thermal System Overview

There are different types of photovoltaic thermal (PV/T) systems available and each has its unique design feature. However, the basic construction and working principle of all the types is similar to each other. In addition, PV/T technology has its own vantage points as well as some limitations. This section provides a brief description of the construction of PV/T along with the advantages and limitations of this technology.

3.2.1 Construction of a PV/T Module

Hybrid photovoltaic thermal system is an amalgamation of solar PV and solar thermal technologies in one module. A PV/T module comprises of the two basic components, viz., a PV module and a thermal collector, the collector being coupled with the back of the PV module.

Structurally, PV/T modules consist of several layers, viz., from the top to bottom, a glass cover (in case of glazed PV/T), solar cells laid beneath the cover; an absorber

plate between thermal collector and the cell layer, thermal collector (or flow channel), and a thermal insulation covering the thermal collector. All the layers are secured into an aluminum frame using the connections and fasteners (Zhang et al., 2012). The structure of a common PV/T module is shown in Figure 3.1.

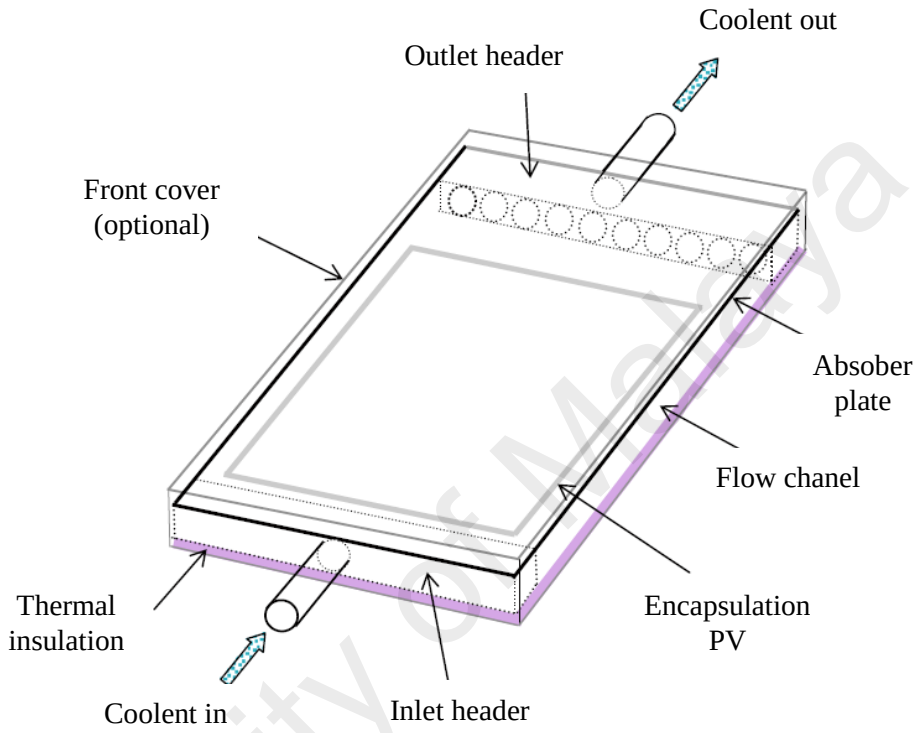

Figure 3.1: Construction of a PV/T module (Chow, 2010)

The PV part of the PV/T module is conventional mono crystalline or polycrystalline silicon cells. The absorber plate is mostly made of copper due to its high thermal conductivity. The flow channels may be constructed as an integrated part of the absorber or it may be fixed to the absorber by thermal paste. These two parts together constitute the thermal collector which is attached to the PV back surface by means of thermally conductive adhesive.

Photovoltaic technology is envisioned to increase effective usage of incoming solar energy by combining the photovoltaic module and solar thermal collector into a single system. Research works are ongoing to improve the constructional features of PV/T. In

the present study attempt has been made to discard the absorber plate in the thermal collector design. This will facilitate to reduce weight and cost of the module and it has been observed in this study that exclusion of the absorber plate does not make significant difference in the thermal performance of the PV/T system.

3.2.2 Working Principle of PV/T

The PV/T modules may be of two types; one design that generates electricity as primary output and heat as the secondary, and another design that offers heat as primary and electricity as secondary output. However, the working principle in both cases is almost the same. The incident solar radiation on the PV cells produce DC electricity which is fed to the load is the same as in the case of conventional PV modules. Regular PV modules' power conversion efficiency is around 12% and as the cell temperature rises, its efficiency is further reduced; the rest of the incoming solar energy produce heat in the module which may be extracted from its backside. For this purpose, a thermal collector composed of an absorber plate made of highly conductive metal like copper or aluminum along with flow channel is attached at the PV module backside. The dissipated heat is first accumulated in the absorber plate and then transferred to the HTF inside the flow channel. This permits a greater share of the solar energy falling on the collector to be converted into useful heat. The HTF flowing through the thermal collector takes heat away from the PV cells, ensuring for more efficient operation. (NREL, 2015).

3.2.3 Application Areas of PV/T

Similar to PV systems, the primary output from PV/T systems is also electricity which may be utilized like the conventional PV output. However, the thermal energy is the additional harvest of these hybrid systems, wherein the equivalent share of this form

of energy is much greater than the electrical output. The heat that is produced in PV/T may be utilized in household to industrial applications. Figure 3.2 presents the flow chart of the water temperature requirement for various purposes at domestic sector. Some of the major applications areas of PV/T systems are discussed in the subsequent sections.

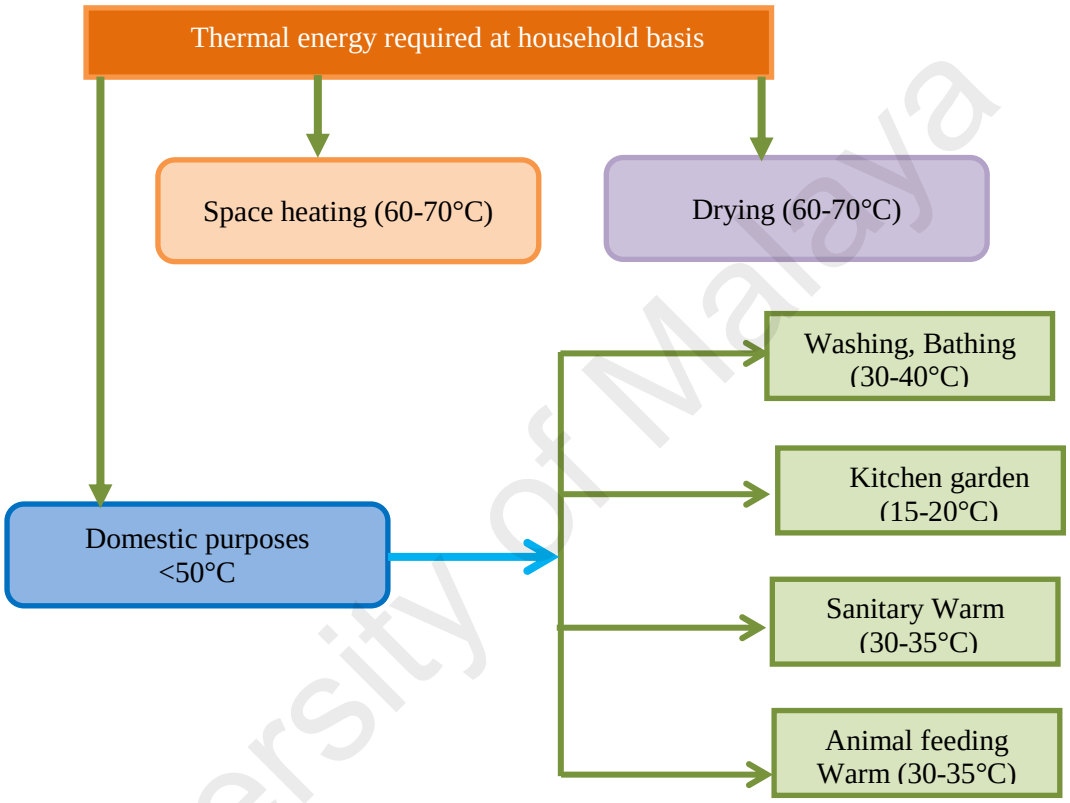

Figure 3.2: Water temperature requirement for various purposes (Kristual et al., 1994; Argiriou et al., 1997; Aktas et al., 2009)

3.2.3.1 Household applications

The demand for electricity and heat is often complementary; hence instead of PV only modules, PV/T modules may be installed that combines the domestic solar water heater (DSWH) with the PV in single physical profile. The water temperature raised by a solitary PV/T unit (45–70^{o}C, even higher) is enough to produce hot water for household applications like shower, laundry, dish washing, etc.

3.2.3.2 Hospitals and hotels

According to the World Health Organization (WHO) temperature affects the survival of legionella (the bacterium that causes legionnaries' disease) and more than 70ºC temperature that water is needed to kill these bacteria instantly. The PV/T systems may be optimized to supply such level of hot water to the hospitals. In the hotels, installation of PV/T system may help to double the benefit by providing electricity along warm water at a very little extra cost.

3.2.3.3 Space heating

Air based Building integrated PV/T (BIPV/T) may facilitate to reduce the air-condition load by supplying warm air into the conditioned space, the electricity comes as a bonus. The wall mounted BIPV/T provides much more energy than a conventional solar PV system in the form of electricity and heat. BIPV/Ts are also available as modular roof-top configuration which also serves the same purpose. In Concordia University, a 100 kW wall mounted BIPV/T has been installed that provides 25 kW of PV electricity and 75 kW of thermal energy (Wall, 2016).

3.2.3.4 Industrial applications

Almost all the industries currently depend on the fossil fuels for producing process heat. It has been reported in a study that about 13% of thermal applications require energy at temperatures up to 100°C, next 27% needs heat at temperatures up to 200°C and the rest which are mainly industrial application needs heat at higher temperatures (Mekhilef et al., 2011). The water outlet temperature from a PV/T may be augmented by connecting a number collector in series and systems may be designed to achieve higher temperatures as per requirement. The high temperature water may be used in process industries, textiles mills for preheating and direct heating purpose at a

negligible cost. The electricity produced from the panel may be sold to the utility grid or may be employed to reduce the internal electrical dependency on the utility source.

3.2.3.5 Agricultural application

Solar drying of crops, grains, herbs, fish and other agricultural products is an established technology. However, PV/T-air systems may serve the above purposes in a more efficient way. The electricity produced by the PV can be used to operate a DC fan to circulate air through the thermal collector to the drying chamber. The air gets hot by taking heat from the thermal collector and then this hot air dries up the crops or grains while passing through the drying chamber. A PV/T used in conjunction with a UV stabilized polyethylene greenhouse dryer was reported to lessen the moisture content of mint leaves from 80% to 11% (Nayak et al., 2011). A PV/T solar dryer coupled with an heat pump was reported to dry saffron with a maximum dryer efficiency of 72%. (Mortezapour et al., 2012).

3.2.3.6 Building integrated PV/T

Building integrated PV (BIPV) is already a well-established technology. The efficiency of these systems can be enhanced by 17 to 20 % by water cooling (Zdrowski et al., 2010). The thermal requirement of a residential or commercial building can be met to some extent by utilizing the heat taken away by water. Building integrated PV/T constitutes a part of the building envelop with suitable orientation and may also be simply mounted on rooftop of building. BIPV/T systems are installed as the replacement for rain screen and sun sheds. BIPV/T systems help to ensure better energy management leading to energy efficient buildings.

3.2.3.7 Solar desalination

Solar desalination is a process to reduce the salt content of saline sea water and make it drinkable. Photovoltaic thermal modules may be used in combination with the solar stills used for desalination process. Singh et al. (2011) developed a double slope PV/T solar still which could produce 7.54 kg/day fresh water with a daily mean energy efficiency of 17.4%. A standalone desalination plant running on reverse osmosis (RO) process and powered by a PV/T collector evinced economic and ecological advantage (Ammous & Chaabene, 2014).

3.2.4 Advantages of PV/T Technology

The advantages of PV/T technology may be enumerated as below:

- PV/T is a solar co-generation technology which is capable of providing low grade energy (heat) that is obtained along with high grade energy (electricity) from the same unit.
- This combination technology offers reduction in space requirement (Good, 2016); it saves at least 60% additional area needed to install a separate solar thermal collector;
- PV/T modules are aesthetic, uniform in structure and water tight. Thus, they can protect the roof with more longevity.
- PV/T systems may help to improve the environmental standard of a city. It has been estimated that in USA at least 1.17 million metric ton of carbon dioxide emission per year can be curtailed if only 10% of buildings install BIPV/T system. This will also save 1232 GWh electrical and 8.4 Btu thermal energy (UCTTO, 2011).

- PV/T is an economically viable technology. The cost and the payback period of a PV/T system is two-thirds that of an isolated PV and a thermal collector of equivalent specification (Annis & Baur, 2011).
- Above all, PV/T technology has the right potential to play an important role in achieving renewable targets set by different world organizations.

3.2.5 Limitations of PV/T Technology

Despite of many favorable features, PV/T systems still suffer from several shortcomings, which hold back commercialization of this technology.

- Careful design of PV/T, especially for electrical insulation and efficient heat transfer, is necessary since electrical and thermal devices are combined here to operate simultaneously.
- Poor thermal contact between the PV module and coolent fluid in the flow channel leads to a temperature difference of about 15^{o}C in case of unglazed PV/T (Saundnes & Rekstad, 2002). This is due to the increased resistance to heat transfer between the cell and absorber interface leading to poor heat removal rate. Search for appropriate thermal conductive adhesive is an important issue in PV/T manufacturing.
- The stagnation temperature of a PV/T system may reach as high as 150^{o}C, which is quite high than the standard operating temperature of a PV module and higher than the oxidizing temperature (135^{o}C) of EVA (Eisenmann & Zondag, 2005). At such high temperatures, electrical connection becomes brittle. Moreover, internal thermal shock between PV module and coolant fluid may occur if the temperature difference rises over 100^{o}C. The stagnation temperature for unglazed and glazed PV/T should be within 80^{o}C and 130^{o}C, respectively (Zondag et al., 2005).

3.3 PV/T Related Heat Transfer and Fluid Flow Parameters

3.3.1 Conduction Heat Transfer

Conduction is the transmission of energy between objects that are in physical contact. When a temperature gradient is produced in an object, there occurs a heat transfer from the high-temperature to the low-temperature end as a result of the interaction of hot vibrating atoms with the adjacent atoms and molecules. Heat transfer inside a solid and between solid boundaries in thermal contact takes place by means of conduction. Fluids, especially gases, are less conductive. Conduction heat transfer is of two types: steady-state conduction takes place when the temperature difference remains constant, while transient conduction happens when temperature difference is a function of time (Smith et al., 2005). The steady-state heat conduction is expressed by the Fourier's law as follows:

$$Q = -kA\frac{\partial T}{\partial x} \tag{3.1}$$

where Q is heat transfer rate and $\partial T/\partial x$ is temperature gradient in the direction of heat flow, A is the cross-sectional area and k is material's thermal conductivity in W/m.K in SI unit system. The minus sign has been used in order to comply with the second law of thermodynamics which states that heat must descent on the temperature scale.

3.3.2 Convection Heat Transfer

Convection, in general, means the movement of groups of molecules within fluids that takes place through advection, diffusion or both. Convection heat transfer (or convection for simplicity) is the transmission of heat by the movement of fluids, that is, convection essentially involves mass transfer (Çengel, 2003). The amount of convection is calculated using the Newton's law of cooling as:

$$Q = hA\left(T_W - T_\infty\right) \tag{3.2}$$

where the quantity *h* is called the convection heat transfer coefficient with SI unit $W/m^2.K$. Convection heat transfer is related to the fluid's thermal properties like thermal conductivity, specific heat and density. It also has some dependence on the flow property like viscosity, because viscosity dictates the velocity profile that in turn regulates the energy transfer rate in the region near the wall (Holman, 2010).

Convection heat transfer process may be self- driven due to density difference in fluid occurring due to temperature gradient, this is known as free or natural convection; or the heat transfer rate may be enhanced artificially by using fans or pumps in which case it is called forced convection. Convection heat transfer coefficient, free and forced convection has been elaborated in subsequent sections.

3.3.3 Radiation Heat Transfer

Conduction and convection heat transfer involves a material medium to convey the energy from one place to another. However, through a perfect vacuum heat transfer takes place by means of electromagnetic radiation which is propagated by due to temperature difference, thus called thermal radiation. All bodies emit energy in the form of photons moving in arbitrary directions with arbitrary phase and frequency. However according to Stefan-Boltzman equation, an ideal thermal radiator or black body emits energy at a rate directly proportional to its surface area and to the fourth power of the absolute temperature of the body (Holman 2010) as follows:

$$Q_{emitted} = \sigma A T^4 \tag{3.3}$$

where σ is the Stefan-Boltzman constant whose value is 5.669×10^{-8} $W/m^2.K^4$. When radiated photons reach another surface, they may be absorbed, reflected or transmitted following the relationship as below:

$$\alpha + \rho + \tau = 1 \tag{3.4}$$

where α is the absorptance, ρ is the reflectance and τ is the transmittance of the surface.

3.3.4 Convection Heat Transfer Coefficient

The proportionality constant between the heat flux and thermodynamic driving force (i.e.,temperature difference) is known as convection heat transfer coefficient (h). It is also known as film conductance due to its relation to the conduction process in the thin stationary layer of fluid at the wall surface and expressed as

$$h = \frac{Q}{A\Delta T} \tag{3.5}$$

Although this coefficient may be calculated analytically for simple systems, it must be determined experimentally for complex situations.

3.3.5 Thermal Conductivity and Specific Heat Capacity

Thermal conductivity expresses the capacity of a material to allow heat transmission from its hotter surface through the material to its cooler surface. It is generally denoted by k and in SI unit system, it is expressed in W/m.^{o}C or W/m.K. Thermal conductivity signifies how quick heat will propagate in a material under a given temperature difference. Generally, metals have high thermal conductivities with pure silver possessing thermal conductivity as high as 410 W/m.^{o}C, while pure copper and pure aluminum have thermal conductivities of 385 and 202 W/m.^{o}C, respectively.

Specific heat capacity is the amount of energy required to raise the temperature of a substance per unit mass. It is denoted by C_p and the SI unit is J/kg.K. The typical value of specific heat of liquid water at 25^{o}C is 4.1813 J/kg.K, while this value escalates to 2080 J/kg.K when water becomes steam at 100^{o}C. The specific heat capacity of air at

typical room condition is 1.012 J/kg.K. For aluminum and copper, the specific heat capacities are 0.897 and 0.385 J/kg.K, respectively.

3.3.6 Nusselt Number, Grashof Number and Prandtl Number

Forced convection heat transfer, as the name implies is enhanced heat transport mechanism affected artificially by fans or pumps. Generally, heat transfer in fluids occurs due to convection, but conduction also happens in a marginal magnitude. Nusselt number, named after Wilhelm Nusselt, is used to gauge the dominance of convection over conduction heat transfer in fluid. Nusselt number (Nu) is the ratio of convection to conduction occurring across a boundary within the fluid (Sanvicente, 2012). From another viewpoint, this is the traditional non-dimensional form of convection heat transfer coefficient (*h)* and expressed as follows:

$$\mathrm{Nu} = \frac{hl}{k} \tag{3.6}$$

where *l* is the width of fluid layer and *k* is the thermal conductivity of the fluid.

Larger values of Nusselt number represent very efficient convection; for example the values of Nu for turbulent pipe flow would be of the order of 100 to 1000.

On the other hand, the Grashof number (Gr) is the ratio of the buoyancy to viscous force acting on a fluid (Çengel, 2003). This dimensionless number is used to indicate the onset of turbulence in natural convection. The Grashof number for vertical flat plate and pipe are respectively as follows:

$$\mathrm{Gr} = \frac{g\beta\left(T_S - T_\infty\right)L^3}{\nu^2} \tag{3.7}$$

and

$$\mathrm{Gr} = \frac{g\beta\left(T_S - T_\infty\right)D^3}{\nu^2} \tag{3.8}$$

where g is the gravitational acceleration, β is the coefficient of thermal expansion and approximately equal to $1/T$ for ideal gases, T_s is the surface temperature, T_α is the bulk temperature, L is the surface length and D is the diameter.

Another dimensionless group or number that gauges the dominance of momentum over heat diffusion on a fluid is the Prandtl number, named after German physicist Ludwig Prandtl. Prandtl number (Pr) represents the ratio of diffusion of momentum to diffusion of heat in a fluid (Backhurst et al., 1999). In other words, it is the ratio between the rate of viscous diffusion to the rate of thermal diffusion.

$$\mathrm{Pr} = \frac{\text{viscous diffusion rate}}{\text{thermal diffusion rate}} = \frac{\mu/\rho}{k/\rho C_p} = \frac{\mu C_p}{k} \tag{3.9}$$

Prandtl number is a fluid property. Generally, liquid have high Prandtl number with values as high as 10^5 for some oils indicating that energy transfer by momentum diffusion in liquid is dominant. At room temperature, the value of Prandtl number for air is 0.71; most of the common gases have almost similar values. The value of Prandtl number at 17°C is 7.56.

3.3.7 Laminar vs. Turbulent Flow: Reynolds Number

In a flow field, laminar flow takes place when fluid flows in parallel layers in well-ordered manner without any interlayer disruption. At low velocities, fluid tends to flow without lateral mixing and layers of fluid (also called lamina) slide past each other. In laminar flow field, fluid particles always follow the streamlines; therefore this type flow is also called streamlined flow. In laminar flow, there is no mass or momentum transfer across the streamlines.

On the other hand, fluid experiences irregular fluctuations, or mixing in case of turbulent flow. The flow velocity at any point in the flow field continuously experiences

change both in magnitude and direction, and there occurs continuous mass and momentum transfer across the streamlines. In practice, most of the flows are turbulent. Laminar flow may occur at the edge of solids, moving relative to fluids or extremely close to solid surfaces, such as the inner wall of a pipe or in cases of highly viscous fluid flow through relatively small channel.

Reynolds number is a non-dimensional number that fixes whether the flow is laminar or turbulent. Reynolds number (Re) is the ratio of inertia force to viscous or friction force in a fluid flow; hence it quantifies the relative dominance of these two types of forces to drive a flow under certain given conditions (Reynolds, 1883). Laminar flow occurs when the viscous forces are dominant; so Reynolds numbers for laminar flow are low. On the other hand, turbulent flow takes place at high Reynolds number and is governed by inertial forces. The Reynolds number for laminar flow through circular pipe is less than 2100 and for turbulent flow it is greater than 4000. The expression for Reynolds number is:

$$\mathrm{Re} = \frac{\rho UD}{\mu} = \frac{UD}{\nu} \tag{3.10}$$

It is also interpreted as the ratio of dynamic pressure to shearing stress as follows:

$$\mathrm{Re} = \frac{\rho u^2}{\mu u / D} \tag{3.11}$$

where ρ, μ, ν are the fluid properties – density, dynamic viscosity and kinematic viscosity repectively, U is the flow velocity and D is the characteristic dimension along which the flow occurs.

Reynolds number helps to predict similar flow pattern in different flow situations. This parameter is frequently come up in case of carrying out scaling of fluid dynamics problems and hence employed to ascertain dynamic similarity among different fluid flows.

3.3.8 Conjugate Heat Transfer

Heat transfer in solid and fluids happen simultaneously in majority real world applications. This is due to the fact that fluids flow around solid or between solid walls, and solids are usually immersed in a fluid. In order to have a detail analysis of temperature field and heat transfer, it is essential to know a precise description of heat transfer modes, material properties, flow regimes and geometrical configurations. Such a description is possible if the combined effect of conduction and convection is taken into account. This consideration is very much important for numerical simulation that can be employed to predict accurately combined heat transfer effects or to test different configurations in order to improve thermal performance of some system.

The term conjugate heat transfer (CHT) corresponds to the combination of heat transfer in solids and fluids due to thermal interaction between the solids and fluids. Conduction often dominates in solids, whereas convection controls the heat transfer in fluids; however conjugate heat transfer augments the effect of both conduction and convection. Conjugate heat transfer allows the simulation of the heat transfer between solid and fluid domains by the exchange of thermal energy at their interface. The heat transfer in the solid occurs mainly by conduction, while in fluid it takes place due to the contribution of the transport of fluid which implies energy transport, the viscous effect of fluid flow which produces fluid heating and pressure work from density difference due to temperature difference. It requires a multi-region mesh to have a clear definition of the interfaces in the computational domain (Huc, 2014).

Conjugate heat transfer occurs in many situations, such as heat sinks wherein conduction takes place in the sink metal and convection in the surrounding fluid. Typical applications of CHT analysis include simulation of heat exchangers, cooling of electronic equipment and general-purpose cooling and heating system.

3.3.9 Steady and Unsteady Analysis

There are two types of approach in numerical simulation: one is steady-state flow where the flow conditions do not change over time; on the other hand, transient flow account for time-dependent effects. Steady-state simulations are computationally less demanding, while transient simulations are computationally challenging and expensive.

CHAPTER 4: RESEARCH METHODOLOGY

4.1 Introduction

The aim of the present research work is to design apt configurations of thermal collectors, excluding the absorber plate, develop a mathematical model for the PV/T system with the newly designed collector, validate the mathematical model through experimental investigation of one representative design and carry out performance evaluation of the other designs by numerical simulation based on the validated mathematical model. Therefore, the methodology of the present research work includes two major parts: numerical and experimental. The foremost part is the design and model development of new configurations of thermal collectors which has been carried out using commercial software COMSOL Multiphysics® that employs the finite element method to produce the complex three dimensional thermal features of the PV/T module. The subsequent task is to carry out experimental investigation of one of the proxy designs of thermal collector in order to validate the developed mathematical model. Then based on the validated model, performance of the other designs of thermal collector will be evaluated by numerical simulation. The concluding part of the research work is to carry out a comparative study on the performance of all of the PV/T systems developed.

In the present research, four different configurations of thermal collector has been developed, all excluding the absorber plate; that is, the only part of the collector in present designs is the flow channel. The four designs are named as Design 1 (D1): Parallel Plate Flow Channel; Design 2 (D2): Pancake Flow Channel; Design 3 (D3): Parallel Square Pipe Flow Channel and Design 4 (D4): Serpentine Flow Channel.

In this chapter, the numerical and experimental methods are elaborated in the subsequent sections.

4.2 Mathematical Modelling and Numerical Simulation

The basic purpose of engineering is to design devices, processes and systems. Mathematical models represent the behavior of a real device, process or physical system in terms of mathematics. Mathematical modeling is a structured process that follows particular logical meta-principles. The steps in modeling include recognizing the need of the model and identifying the information to be sought, gathering available information, identifying the circumstances and the governing physical law, constructing the equations, authenticating the model through validation and verifying the practicality of the model. There are some mathematical techniques to formulate models, such as dimensional homogeneity, abstraction and scaling, conservation principles, linearity, etc.

A numerical simulation is a computation process usually run on a single or network of computers to portray a physical phenomenon through appropriate mathematical model. Analyzing complicated physical behavior and solving the corresponding mathematical model numerical simulation is the most efficient tool that is capable of treating with large systems of equations and complex geometries which is often impracticable to solve analytically. Numerical simulations have become integral part of mathematical modelling of many natural phenomena. Sometimes experimental investigations become too much expensive and time-consuming like those in aerodynamics, and material sciences; sometimes experiments are prohibited like in case of nuclear tests or in medicine; even sometimes experiments are impossible to carry out like in case of weather forecast. Simulations are important to have insight of the above-mentioned phenomena and also of newly developed systems. Numerical simulation

facilitates to evaluate the performance of the systems which are too complex to solve analytically.

Partial differential equations (PDE) are generally employed to mathematically describe a physical phenomenon. These PDEs are converted into a "numerical analogue" which can be represented in the computer and then processed by a computer program built on some algorithm. In order to solve a mathematical model numerically, the physical model must be discretized. There are several discretization schemes, viz., finite difference method (FDM), finite volume method (FVM), finite element method (FEM) methods, boundary element method (BEM) method and boundary volume method (BVM). The present numerical computation has been performed by finite element method (FEM).

4.2.1 Finite Element Method

The space and time dependent physical laws are mathematically expressed by partial differential equations (PDE), most of which are not solvable in analytic method. An alternative way is to construct linear approximations of these PDEs based on different discretization method. Finite element method (FEM) or finite element analysis (FEA) is a numerical technique where the problem domain of interest is divided into a finite number of elements by suitable discretization scheme and from numerical model equations that are solvable numerically.

The discretized elements are connected to each other at some point called node, which lie on the element boundary where the adjacent element is connected. A collection of elements and nodes is called the finite element mesh. The nodal points represent the field variable defined in terms interpolating functions within each element. The behavior of the field variable within the elements depends on the nodal values of

that field variable and the interpolating functions for the elements. (Sandeep & Irudayaraj, 2008). Figure 4.1 presents the three-dimensional finite element mesh.

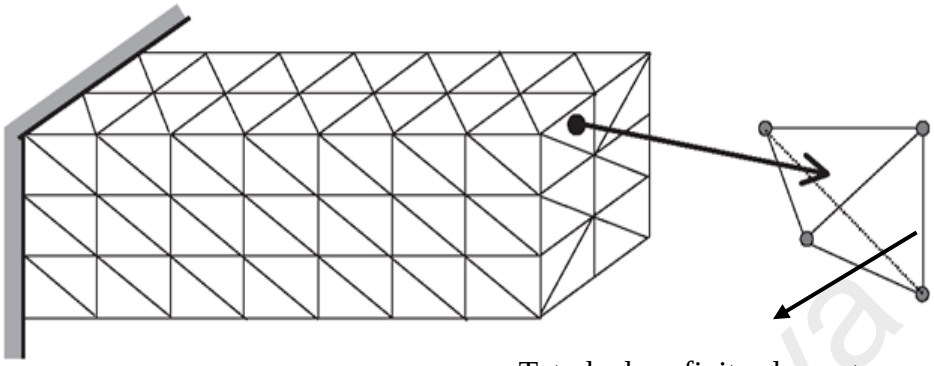

Figure 4.1: Three-dimensional finite element mesh

Richard Courant, in early 1940s, realized the importance of FEM in solving intricate equations that define complex real-world phenomena. Nowadays, finite element method (FEM) is considered as the best option for solving these problems. The theory of finite element analysis is well developed. In computer numerical solutions, FEM provides the error estimate or error bound which helps to predict the fidelity of the solution. It offers sufficient freedom in selecting discretization method.

Finite element analysis is increasingly used in in solar energy research. Rehena and Alim (2015) applied finite element method in a numerical study on forced convection through a flat-plate solar collector. A three-dimensional FEM model for non-uniform solar heat generation derived from heat flux profile was developed by Eck et al. (2010) that showed well agreement with experimental data. Finite element method has been adopted to develop mathematical model for innovative topologies of solar collectors. Alveraz et al. (2010) developed such a new serpentine configuration of solar collector, the mathematical model of which was based on finite element analysis. Eck et al. (2007) devised a FEM based two-dimensional plane stress model of a horizontal linear Fresnel collector by considering local non-uniform solar heat distribution outside of the tube.

4.2.2 COMSOL Multiphysics®

The PV simulation softwares available presently are either open source which mostly allow one-dimensional analysis or very costly with inexplicable functions. A handy and multipurpose simulation software in PV researchers field is eagerly awaited that is capable of optimizing existing technologies and save the time from concept to prototype for novel ones. COMSOL Multiphysics® software, with its Semiconductor Module, can be customized to provide and satisfy these requirements.

COMSOL Multiphysics® is a FEM based simulation software developed to solve physics and engineering problems, especially the coupled phenomena or multiphysics. This software offers more current features than ANSYS, NASTRAN, ABAQUS, complies well with MATLAB® and can use MATLAB® syntax, too. COMSOL Multiphysics® focuses on multiphysics, coupling different physics together as per requirement of the problem. The prime feature of this software is that it enables higher dimensional modeling with freedom enough to couple other relevant physics if necessary. In addition, this software is highly flexible allowing to program in user defined differential equations if they are not already employed. Moreover, with the time-dependent solver COMSOL Multiphysics® is capable of predicting both device performance and long-term reliability.

COMSOL Multiphysics® possess some distinguishable features, the most prominent of which is its capability to solve multi-physics problem. Besides, it facilitates the use of user specified partial differential equations. On one hand, this software has professional predefined modeling interfaces; on the other hand, it allows the direct use of CAD models.

4.3 PV/T Layers

Hybrid photovoltaic (PV/T) modules consist of a typical PV panel coupled with a solar thermal collector attached to its back side. The basic structure of the PV/T, as designed and developed in the present study, comprises of nine layers, namely, glass, polycrystalline silicon cell, ethyl vinyl acetate (EVA) as encapsulant on the both sides of the cell, poly vinyl fluoride (PVF) or Tedlar, thermal paste, heat transfer fluid (HTF) layer (water) and flow channel wall layer encompassing the water layer. The absorber plate has been excluded from the thermal collector in the present study and the flow channel is augmented to the backside of PV by means of thermal conductive adhesives only. Four different configurations of flow channel have been designed and investigated using 3D numerical simulation. The cross section PV/T layers are shown in Figure 4.2 and a brief detail of the layers is described as below:

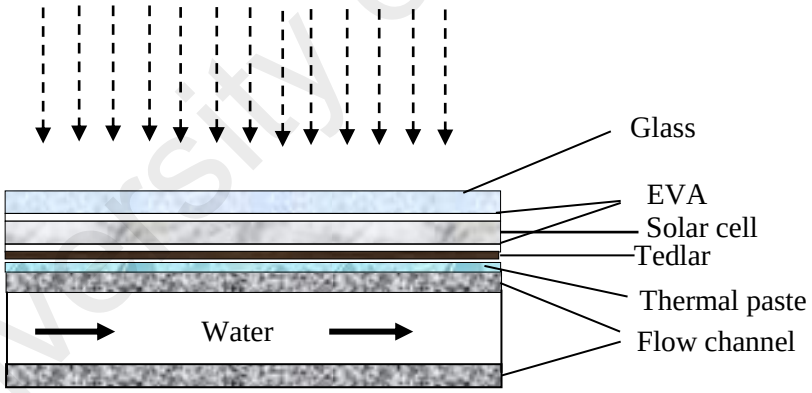

Figure 4.2: Cross section of PV/T module

4.3.1 Glass Layer

The first layer of the PV/T module is a protective cover of high transmittance textured tempered glass with maximum solar radiation transmissibility of about 95%.

4.3.2 Ethylene Vinyl Acetate Layer

Ethylene vinyl acetate (EVA) is a transparent and glossy copolymer of ethylene and vinyl acetate used to encapsulate silicon cells on both sides. Like glass cover EVA has also high optical transmittance with an ability to resist UV radiation. EVA encapsulation prevents cell damaging, module buckling caused difference among the thermal expansion coefficient of different module materials. It also saves from harm the solar cells from the adverse effect of moisture and high temperature.

4.3.3 Polycrystalline Silicon Cell Layer

Polycrystalline silicon or polysilicon (p-Si) is a high purity polycrystalline form of silicon consisting of multiple small crystals known as crystallites. It is the core layer of a PV/T module wherein the energy conversion takes place. A small portion of the (15-20%) the incident solar radiation is converted into electricity by photoelectric effect and the rest is dissipated as heat.

4.3.4 Poly Vinyl Fluoride or Tedlar Layer

Poly vinyl fluoride (PVF) is a thermoplastic flouro-polymer with repeating vinyl fluoride unit. This is widely familiar as Tedlar which is actually the commercial name of PVF film produced by DuPont^{TM}. It possesses low permeability to vapors, high dielectric strength and can resist weathering and staining or abrasion. Tedlar film has good adhesion to EVA encapsulant. That's why it is used as the back sheet for PV modules.

4.3.5 Adhesive Layer

Thermally conductive paste is used to couple the flow channel with PV module back surface. Although not near as good as copper, thermal paste is very high heat

conductive thixotropic adhesive that is used between two objects to ensure better conduction of heat. There are three types of thermal pastes; viz., metal based, ceramic based and silicon based thermal paste. Silicon based paste has been used in the present study.

4.3.6 Flow Channel Wall Layer

In the present study, a novel design of thermal collector without absorber plate has been introduced. So, there is only flow channel wall layer next to the adhesive layer. Aluminum and copper have been chosen as channel material in order make comparative assessment on their relative technical and economical merit.

4.3.7 Heat Transfer Fluid Layer

The fluid layer involved in the PV/T structure is the HTF layer flowing in between the aluminum or copper channel walls. Only water has been considered as HTF in the present research.

4.4 Mathematical Modelling

4.4.1 Governing Equations

In developing the mathematical model, the flow is considered laminar and incompressible and there is no viscous dissipation. The only force taken into account is the gravitational force acting vertically downward.

Heat transfer in solid domains of the PV/T collector has been considered to occur only by conduction heat transfer mechanism where thermal energy is transported through the body by means of vibrating particles. Heat transfer through PV cell surface to the flow channel is solved by the heat conduction equation as

$$\frac{\partial^2 T_S}{\partial x^2} + \frac{\partial^2 T_S}{\partial y^2} + \frac{\partial^2 T_S}{\partial z^2} = 0 \tag{4.1}$$

In fluid domain inside the flow channel the heat transfer mechanism has been considered as a conjugate heat transfer of conduction and convection. The fluid is considered as incompressible Newtonian and the flow is taken as steady. Therefore, the governing equations in the fluid domain are follows:

$$\frac{\partial u}{\partial x} + \frac{\partial v}{\partial y} + \frac{\partial w}{\partial z} = 0 \tag{4.2}$$

$$u\frac{\partial u}{\partial x} + v\frac{\partial u}{\partial y} + w\frac{\partial u}{\partial z} = -\frac{1}{\rho}\frac{\partial p}{\partial x} + \nu\left(\frac{\partial^2 u}{\partial x^2} + \frac{\partial^2 u}{\partial y^2} + \frac{\partial^2 u}{\partial z^2}\right) \tag{4.3}$$

$$u\frac{\partial v}{\partial x} + v\frac{\partial v}{\partial y} + w\frac{\partial v}{\partial z} = -\frac{1}{\rho}\frac{\partial p}{\partial y} + \nu\left(\frac{\partial^2 v}{\partial x^2} + \frac{\partial^2 v}{\partial y^2} + \frac{\partial^2 v}{\partial z^2}\right) \tag{4.4}$$

$$u\frac{\partial w}{\partial x} + v\frac{\partial w}{\partial y} + w\frac{\partial w}{\partial z} = -\frac{1}{\rho}\frac{\partial p}{\partial z} + \nu\left(\frac{\partial^2 w}{\partial x^2} + \frac{\partial^2 w}{\partial y^2} + \frac{\partial^2 w}{\partial z^2}\right)$$

(4.5)

$$u\frac{\partial T}{\partial x} + v\frac{\partial T}{\partial y} + w\frac{\partial T}{\partial z} = -\frac{1}{\rho}\frac{\partial p}{\partial x} + \frac{k}{\rho C_p}\left(\frac{\partial^2 T}{\partial x^2} + \frac{\partial^2 T}{\partial y^2} + \frac{\partial^2 T}{\partial z^2}\right) \tag{4.6}$$

4.4.2 Boundary Conditions

Appropriate boundary conditions were employed on the computational domain as per the physics of the problem. The boundary conditions are listed as follows:

At top surface, the inward heat flux:

$$-k_S\frac{\partial T_S}{\partial z} = q = h_c\left(T_{amb} - T_s\right) \tag{4.7}$$

At the wall, velocity components were set to zero in accordance with the no-slip condition as:

$$u = v = w = 0 \tag{4.8}$$

At the solid-fluid interface:

$$\left(\frac{\partial T_S}{\partial n}\right)_f = \frac{k_S}{k_f}\left(\frac{\partial T_S}{\partial n}\right)_S \tag{4.9}$$

At the inlet of flow channel:

For Design 1: $u = U_o, v = w = 0$

For Design 2: $v = -U_o, u = w = 0$

For Design 3: $v = -U_O, u = w = 0$

For Design 4: $v = U_O, u = w = 0$

At inlet for all designs

$$T = T_{in} \tag{4.10}$$

At outlet of the flow channel:

$$p = 0 \tag{4.11}$$

4.4.3 Mesh Generation

The purpose of mesh generation in finite element analysis is to subdivide a domain into a set of sub domains. The PVT module was meshed in COMSOL Multiphysics® using the built-in physics controlled mesh sequence setting, which is shown in Figure 4.3 (a - d), the number of mesh elements increase at each boundary so that the heat transfer and flow fields can be resolved accurately. To develop all models, free tetrahedral and free triangular mesh setting were used, which results are shown in Table

4.1 to decrease the physical time of running all of the required simulations in COMSOL Multiphysics®, while ensuring accurate results are obtained.

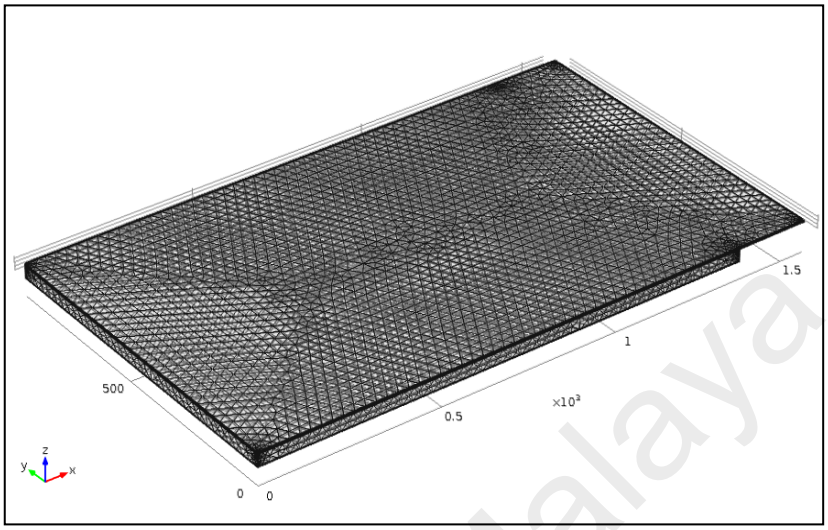

(a) PV/T with parallel plate flow channel

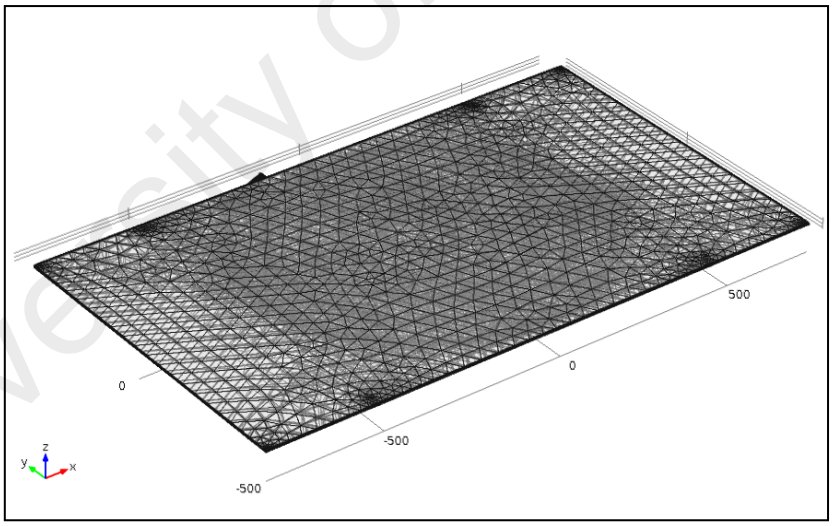

(b) PV/T with pancake flow channel

Figure 4.3: PV/T collector meshed in COMSOL Multiphysics® using the physics controlled mesh sequence

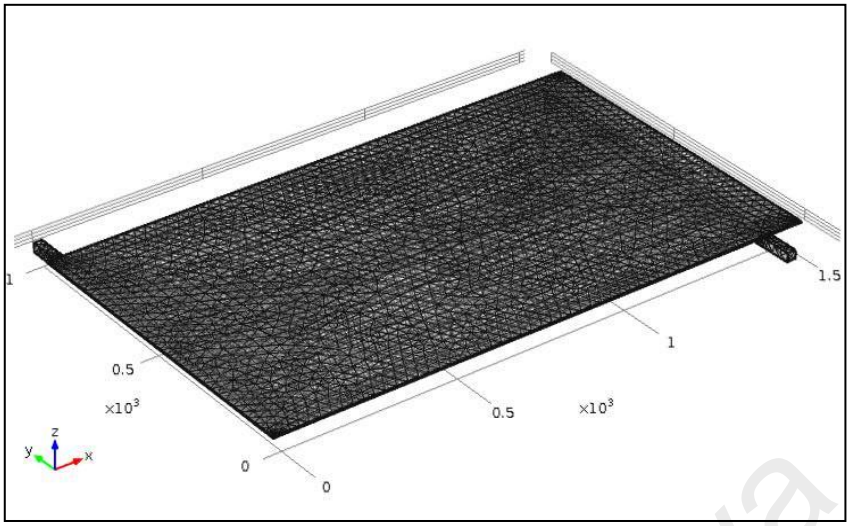

(c) PV/T with parallel square pipe flow channel

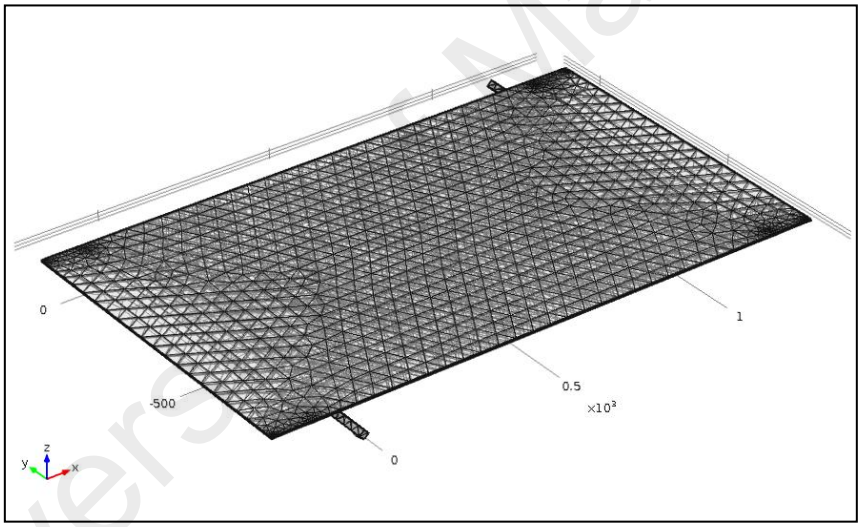

(d) PV/T with serpentine flow channel

Figure 4.3, continued

Table 4.1: Statistic of mesh generation by COMSOL Multiphysics®

Element type	Design 1	Design 2	Design 3	Design 4
Tetrahedral	130553	242075	176570	55738
Triangular	47802	89874	69097	26527
Edge	2183	10199	8389	5131
Vertex	42	49	372	346

4.5 Mathematical Modelling for Proposed Design

The heat transfer equations for different layers of the PV/T have been constructed according to the general energy equation applied for that particular layer. The energy equation states that the rate change of internal energy of a system is equal to the difference between rate of energy input and rate of energy output plus the rate of energy generated inside the system. The general three-dimensional energy balance equation is as follows:

$$\frac{dE(x,y,z)}{dt} = E_{in} - E_{out} + \dot{Q} \tag{4.12}$$

where

$\frac{dE}{dt}$ is the change in the internal energy

E_{in} is the heat transfer rate into the system

E_{out} is the heat transfer rate out of the system

$\dot{Q}$ is the heat generation rate into the system

For calculation of three-dimensional temperature distributions, the following assumptions are made:

- Transmissivity of ethyl vinyl acetate (EVA) is approximately 100%,
- No dust on surface will affect solar energy absorptivity,
- The flow is considered fully laminar and incompressible and the flow rate in uniform.
- The thermal-physical properties of the absorber tube are constant
- Loss of upper surface and back surface are same.
- The sky can be considered as a black body for long-wavelength radiation at an equivalent sky temperature.

Considering the above assumptions, the governing equation of the heat transfer in various layers of PV/T module are given as follows:

For the glass layer:

$$\rho_g \delta_g C_{pg} \frac{dT_g}{dt} = \alpha_g R - h_s (T_g - T_s) - h_{cv} (T_g - T_{amb}) - h_c (T_g - T_c) + k_g \delta_g \nabla^2 (T_g (x, y, z)) \tag{4.13}$$

where h_{cv} heat transfer coefficient from air to glass surface.

For PV module:

$$\rho_c \delta_c C_{pc} \frac{dT_c}{dt} = \alpha_c \tau_g \mathrm{P}_c R - E_{el} - h_c (T_c - T_g) - U_{td} (T_c - T_{td}) + k_c \delta_c \nabla^2 (T_c (x, y, z)) \tag{4.14}$$

For the tedlar layer:

$$\rho_{td} \delta_{td} C_{ptd} \frac{dT_{td}}{dt} = (1 - E_{el}) \alpha_{td} \alpha_c \tau_g \mathrm{P}_c R - U_{td} (T_{td} - T_{ch}) + k_{td} \delta_{td} \nabla^2 (T_{td} (x, y, z)) \tag{4.15}$$

where heat transfer coefficient from tedlar to channel, $U_{td} = \frac{k_{td}}{L_{td}}$

For parallel plate flow channel:

$$\rho_d \delta_d \mathrm{Pe}_\mathrm{d} dx C_{pd} \frac{dT_d}{dt} = (1 - E_{el}) (1 - \alpha_{td}) \alpha_c \tau_g \mathrm{P}_c R - U_{d \to f} \mathrm{Pe}_\mathrm{d} dx (T_d - T_f)$$
$$- U_{d \to amb} \mathrm{Pe}_\mathrm{d} dx (T_d - T_{amb}) + k_d \delta_d \mathrm{Pe}_\mathrm{d} dx \nabla^2 (T_d (x)) \tag{4.16a}$$

For pancake and parallel square pipe flow channel:

$$\rho_d \delta_d \mathrm{Pe}_\mathrm{d} dy C_{pd} \frac{dT_d}{dt} = (1 - E_{el}) (1 - \alpha_{td}) \alpha_c \tau_g \mathrm{P}_c R + U_{d \to f} \mathrm{Pe}_\mathrm{d} dy (T_d - T_f)$$
$$- U_{d \to amb} \mathrm{Pe}_\mathrm{d} dy (T_d - T_{amb}) + k_d \delta_d \mathrm{Pe}_\mathrm{d} dy \nabla^2 (T_d (y)) \tag{4.16b}$$

For sepentine flow channel:

$$\rho_d \delta_d \mathrm{Pe_d} dy\, C_{pd} \frac{dT_d}{dt} = (1-E_{el})(1-\alpha_{td})\,\alpha_c \tau_g \mathrm{P_c} R - U_{d\to f}\ \mathrm{Pe_d} dy\ (T_d - T_f) - U_{d\to amb}\ \mathrm{Pe_d} dy\ (T_d - T_{amb}) + k_d \delta_d \mathrm{Pe_d} dy \nabla^2 (T_d(y)) \quad (4.16c)$$

For the working fluid in the channel:

Parallel plate flow channel:

$$\rho_f A_f dx\, C_{pf} \frac{dT_f}{dt} = \mathrm{Pe_d} dx\, U_{d\to f} (T_d - T_f) - \dot{m} C_{pf} (T_d - T_f) \quad (4.17a)$$

Pancake, parallel square and serpentine flow channel:

$$\rho_f A_f dy\, C_{pf} \frac{dT_f}{dt} = \mathrm{Pe_d} dy\, U_{d\to f}\ (T_d - T_f) - \dot{m} C_{pf} (T_d - T_f) \quad (4.17b)$$

4.5.1 Heat Transfer Correlations

The heat transfer coefficients in the different energy balances equations are calculated using the following formulas:

The radiation heat transfer coefficient (h_s) between the glass and the sky can be calculated by assuming that the sky is a black body with a temperature T_s

$$h_S = \varepsilon_g \sigma (T_g^2 + T_s^2)(T_g + T_s) \quad (4.18)$$

where σ = 5.67 × 10^{-8} W/m^2.K^4

The sky temperature is calculated using Swinbank's formula

$$T_s = 0.0522\ T_{amb}^{1.5} \quad (4.19)$$

The convection heat transfer coefficient (h_{cv}) from air to glass surface is taken from McAdams (1954) which is valid for wind speed ranging from 0 to 10 m/s

$$h_{cv} = 5.67 + 3.86\,V \tag{4.20}$$

The convective heat transfer coefficient (h_c) between glass cover and PV is defined by considering the expression of Nusselt number:

$$h_c = \frac{\mathrm{Nu}_a\, k_a}{\delta_a} \tag{4.21}$$

where Nu_a, k_a, and δ_a represent Nusselt number, the thermal conductivity of air gap and the distance between glass and PV module. The Nusselt number is calculated using the formula giving by Hollands [1976].

$$\mathrm{Nu}_a = 1 + 1.44\left[1 - \frac{1708}{\delta_a \mathrm{Ra}\,\cos\theta}\right] \times \left[1 - \frac{1708\,(\sin\theta)^{1.66}}{\delta_a \mathrm{Ra}\,\cos\theta}\right] + \left[\frac{\left(\delta_a \mathrm{Ra}\,\cos\theta\right)^{0.33}}{5830} - 1\right]^{+} \tag{4.22}$$

This expression is valid for tilt angles from 0º to 75º. The notation in the above formula, the segments denoted by "+" shall be considered only when positive values are assumed. Otherwise they shall be replaced by zero value. The Rayleigh number is given by

$$\mathrm{Ra} = \frac{g\beta_a (T_c - T_g)\,\delta_a^3}{k_a \nu_a} \tag{4.23}$$

where β_a, ν_a is the thermal expansion coefficient and the kinematic viscosity of the air, respectively.

Heat transfer on the internal surface of the collector tube.

$$h_f = \frac{\mathrm{Nu}_f k_f}{D} \tag{4.24}$$

where D is the characteristic dimension of the channel.

The overall heat transfer coefficient from duct to water and duct to ambient is defined as follows:

$$U_{d \to f} = U_{d \to amb} = \left[\frac{L_d}{k_d} + \frac{1}{h_d} \right]^{-1} \tag{4.25}$$

4.5.2 Energy Analysis

The thermal energy extracted by coolant water is defined by

$$E_{th} = \dot{m} C_{p_w} \left(T_{out} - T_{in} \right) \tag{4.26}$$

where mass flow rate is calculated by the following equation

$$\dot{m} = \rho U_o A_f \tag{4.27}$$

As the peripheral velocity variation is more significant than the longitudinal change, the Reynolds number to characterize the flow is calculated using the following relation

$$\mathrm{Re} = \frac{U_o D_h}{\upsilon} \tag{4.28}$$

where D_h is the hydraulic diameter. For shapes such as squares, rectangular or circular ducts where the height and width are comparable, the characteristic dimension for internal flow situations is taken to be the hydraulic diameter.

The general expression for hydraulic diameter is

$$D_h = \frac{4A_f}{Pe_d} \tag{4.29}$$

where A_f is the flow area and Pe_d is the perimeter of flow channel

For flow through rectangular duct: $$D_h = \frac{2L\delta}{L+\delta} \quad (4.30a)$$

For flow through square duct: $$D_h = L \quad (4.30b)$$

For a circular pipe: $$D_h = D \quad (4.30c)$$

The electrical efficiency (η_{el}) is calculated by the following equation (Skoplaki & Palyvos, 2009)

$$\eta_{el} = \eta_{ref}\left[1-\beta_{ref}\left(T_C - T_{ref}\right)\right] \quad (4.31)$$

where η_{ref} is the reference efficiency at standard conditions (R = 1000 W/m^2 and T_{ref} = 25^{o}C), β_{ref} is the thermal coefficient of cell efficiency which is dependent on materials of PV module, here the value is taken 0.00045/K for silicon cell (Joshi et al., 2009).

The electrical efficiency of PV can also be expressed as below

$$\eta_{el} = \frac{V_{mp} I_{mp}}{E_c} \quad (4.32)$$

where V_{mp} and I_{mp} are voltage and current at maximum power point respectively. The total amount of energy (solar irradiance) absorbed by PV module can be calculated as

$$E_c = P_c \tau_g \alpha_c R A_c \quad (4.33)$$

The total efficiency of PVT collector is calculated as follows:

$$\eta_{tol} = \frac{E_{th} + E_{el}}{E_c} \quad (4.34)$$

where total amount of energy absorbed by PV cells that is converted into electrical energy can be written as,

$$E_{el} = \overline{\eta_{el}} E_C \quad (4.35)$$

4.5.3 Thermo-Physical Properties and Design Parameters

The design parameters and thermo-physical properties involved in the numerical model is shown in Tables 4.2, 4.3 and 4.4, respectively.

Table 4.2: PV/T collector materials and thermal properties

Materials	Layer	Density [kg/m^3]	Thermal Conductivity [W/(m.K)]	Heat capacity at constant pressure [J/(kg.K)]	Thickness (mm)
Glass	Top cover	2450	2	500	3
EVA	Encapsulant	950	0.311	2090	0.8
Silicon	Solar cell	2329	148	700	0.1
Tedlar	Bottom cover	1200	0.15	1250	0.05
Thermal paste	Conductor	2600	1.9	700	0.3

Table 4.3: Thermal collector specification

Materials	Dimension (mm)	Density [kg/m^3]	Thermal Conductivity [W/(m.K)]	Heat capacity at constant pressure [J/(kg.K)]	Wall thickness (mm)
Aluminum	1350 × 920 × 30	2700	237	900	1
Copper	1350 × 920 × 30	8700	400	385	1
Fluid	Water	998	0.68	4200	30

Table 4.4: The values of design parameters used in the numerical simulation

Parameters	Values
Transmissivity of glass	0.95
PV cell efficiency at standard test conditions	0.14
Absorptivity of solar cell	0.9
Packing factor of solar cell	0.95
Irradiation	200 W/m^2 – 1000 W/m^2
Ambient temperature	20 ^{o}C – 40^{o}C
Inlet velocity	0.0003 m/s – 0.05 m/s
Inlet temperature	20^{o}C – 40^{o}C

4.6 Experimental Investigations

In the present research, PV/T module with four different thermal collector designs has been designed and developed. The thermal collectors have been developed based on the novel concept of excluding the absorber plate. Experimental investigations have been carried out for PV/T with parallel plate flow channel only. The experiments have been performed under the typical meteorological conditions of Malaysia at the Solar Garden of UMPEDAC, University of Malaya, Malaysia. The experimental method along with the test set up and instrumentation has been elaborated in the following sections.

4.6.1 Experimental Set Up

The PV/T system basically consists of two components, a photovoltaic (PV) module and a thermal collector which is attached to back surface of PV and water is used as the heat transfer fluid. In experimental set up, the present research has two compornants, one is PV/T and the other components of the setup are instrumentation for measurement and control. The schematic of the basic experimental setup is shown in Figure 4.4.

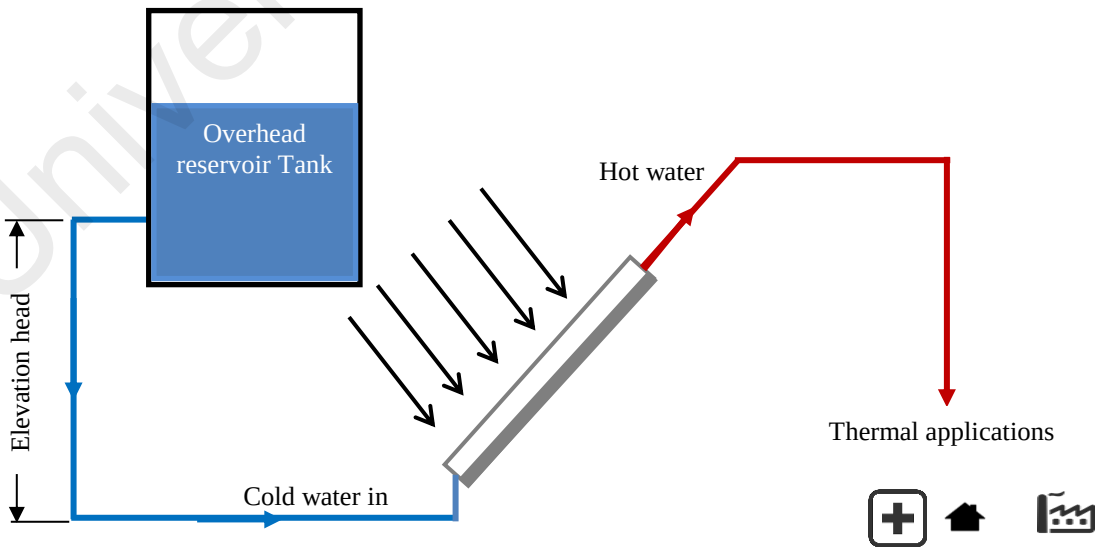

Figure 4.4: Schematic diagram of the experimental set up

Experimental investigations have been carried out using thermal collectors made of two different materials: aluminum and copper. Water supply and circulation to the PV/T modules is maintained by gravity from an overhead reservoir tank.

4.6.1.1 PV module

The electrical part of the PV/T system is a conventional solar PV module. Photovoltaic (PV) modules are interconnecting assembly of 4×9 or 6×10 or 6×12 solar cells designed to absorb sun ray to generate electricity by photovoltaic effect. The solar cells of a PV module may be crystalline silicon solar cells or thin film solar cells. Again, crystalline cells may be manufactured as single or mono crystalline silicon (sc-Si) or multi or poly crystalline silicon (mc-Si or p-Si) solar cells.

The PV module used in the present research is polycrystalline silicon (p-Si) PV module (Figure 4.5) of brand EPV, model LB250QM-60 manufactured by Endau PV Industries Sdn. Bhd. This module consists of 6×10 cells with short circuit current and voltage of 37.8A and 8.73V, respectively under the standard operating condition of 1000 W/m^2 irradiation and 25°C cell temperature. The detail specification of PV module is given in Table 4.5.

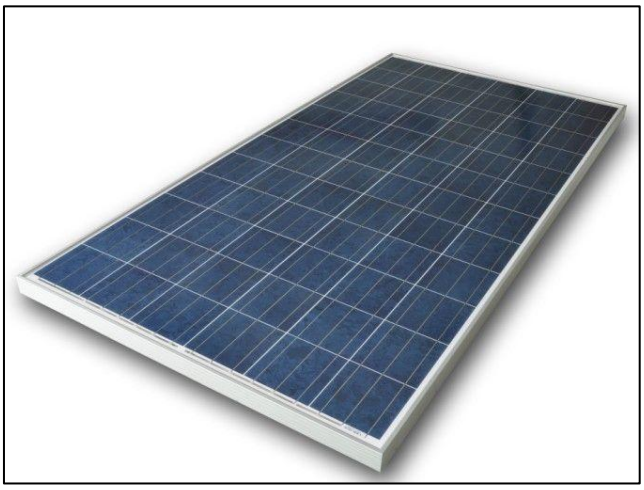

Figure 4.5: Poly-crystalline PV module

Table 4.5: Specifications of the PV module

Item	**Specification**
Place of origin	Malaysia
Brand name	EPV
Model no	LB250QM-60
Materials	Polycrystalline silicon
Size	1570 x 940 mm
Size of a cell	153 x 153 mm
Area of a cell	0.0234 m^2
Total Area of PV cell	1.4 m^2
Number of cells	6 × 10 = 60
Maximum power	250W
Open circuit voltage (V_{oc})	37.8V
Short circuit current (I_{sc})	8.73A
Voltage at $P_{max.}$ (V_{mpp})	30.6V
Current at $P_{max.}$ (I_{mpp})	8.17A
Maximum system voltage	1000V
Maximum series pause rating	10A
Operating temperature	-40°C - ±85°C
Standard testing condition (STC)	1000W/m^2, AM 1.5, 25°C
Tolerance	±3%
Weight of PV module	20 kg

4.6.1.2 Thermal collector for experimental study

Thermal part of a PV/T system is simply a solar thermal collector that receives heat from the PV back surface. The collector is attached to the PV module back side by means of thermally conductive adhesives. Generally, an absorber plate is used in between the PV back surface and the flow channel. However, in the present research, a novel design of thermal collector without absorber plate has been introduced. Four configurations of flow channels have been designed, namely, parallel plate flow channel, pancake flow channel, parallel square pipe flow channel and serpentine flow channel.

The parallel-plate flow channel that has been used for experimental investigation is shown in Figure 4.6. Both top view and isometric view have been presented for more clarity. The dimensions of the channel are dictated by the size of the PV module, which is 1570 mm in length and 940 mm in width. In order to accommodate the channel on the PV back surface to avoid the electrical junction box, the length of the channel is kept 1370 mm and the width 920 mm. The gap between the plates, i.e., height of the channel has been numerically optimized to 30 mm.

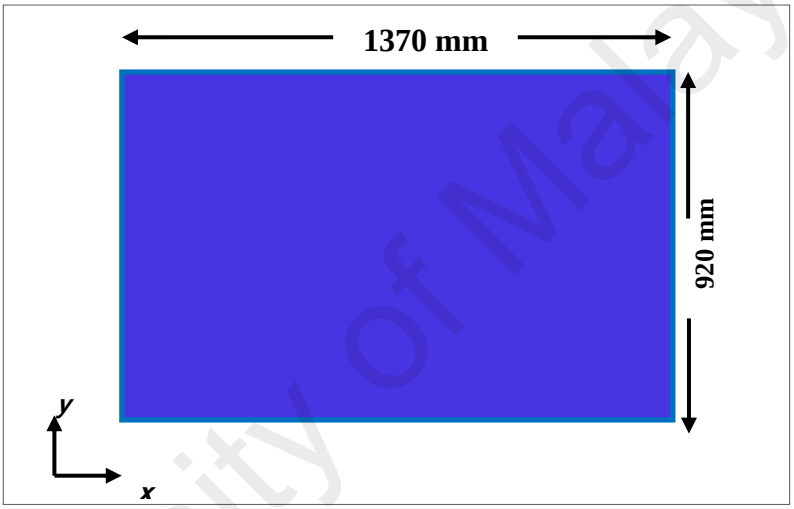

(a) 2D view

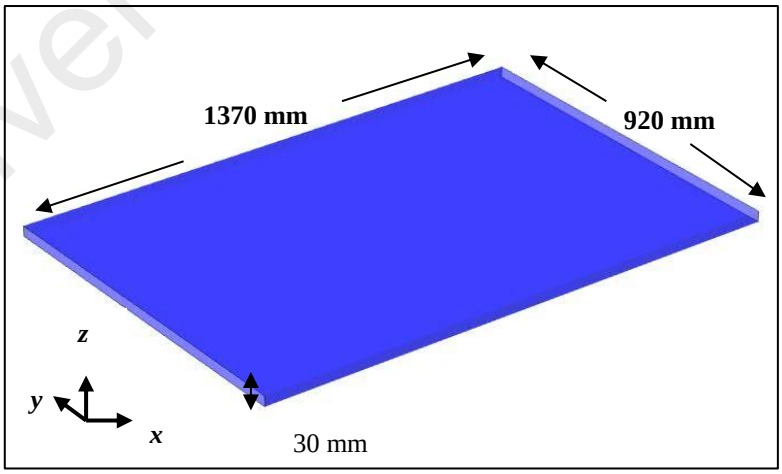

(b) 3D view

Figure 4.6: Parallel plate flow channel

4.6.1.3 Thermal collectors for numerical study

Apart from the parallel-plate flow channel, three other collector designs without absorber plate have been introduced and investigated numerically only. The first one out of three flow channel is a novel design and named as 'pancake flow channel' (Figure 4.7). It is actually a coil shaped circular pipe with an outer diameter of 940 mm which is dictated by the breadth of the PV module. The radial pitch, i.e., the distance between two consecutive coils is numerically optimized as 94 mm. So, the number coils is 4.7 with a total flow length of 8.5 m.

The parallel pipe configuration (Figure 4.8) has been chosen as one of the flow channel designs with cross section of the pipes to be square instead of circular as in case of conventional designs. The square shape of the pipes ensures quite a greater contact area with PV back surface as compared to the circular pipe which has only line contact. There are ten pipes (each 1.35 m long) in parallel at a distance of 94 mm to each other and connected by two header pipes (each 1.0 m long), all having the same cross section of 24 mm × 24 mm as optimized numerically.

The serpentine configuration (Figure 4.9) is a popular design for flow channel. There are several configurations in serpentine flow channel design. In this research, single loop, parallel configuration has been designed which offers a large coverage area with simplicity in design. The pipe is circular in cross section with an inside diameter of 24 mm. The bend is made as arch shaped with a radius of 50 mm and gap between two consecutive arms is optimized as 50 mm. The total flow length is 11.1m.

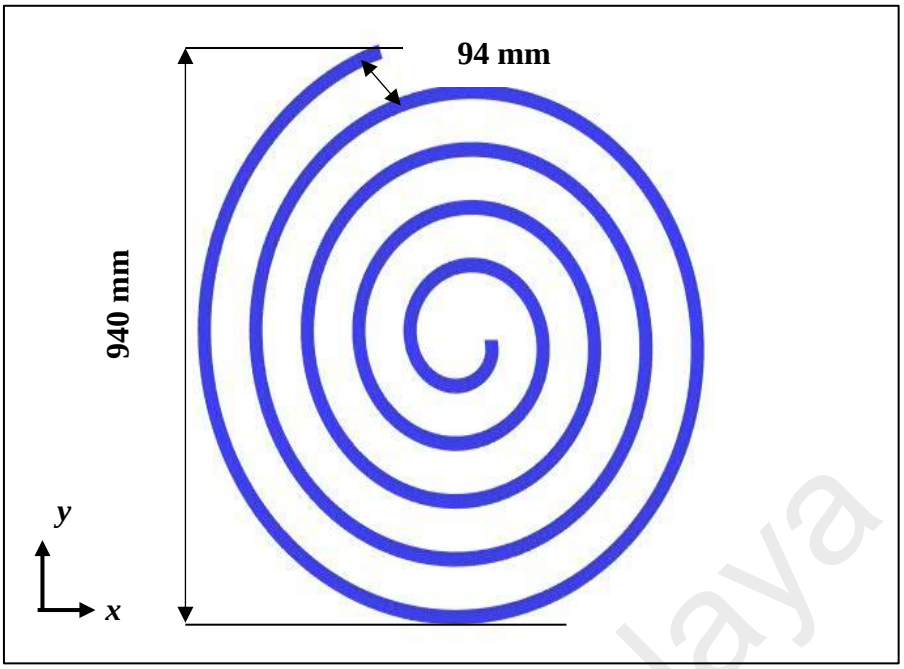

(a) 2D View

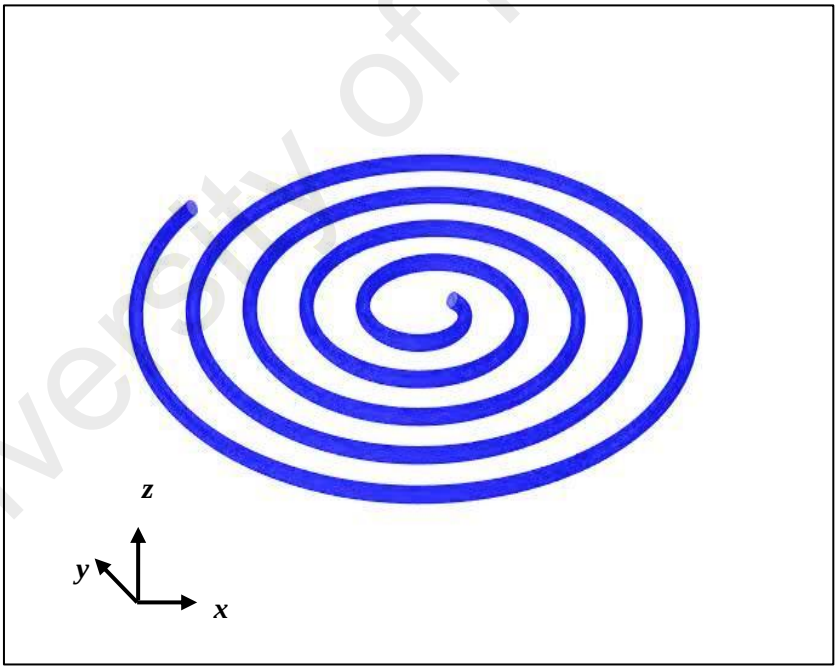

(b) 3D view

Figure 4.7: Pancake flow channel

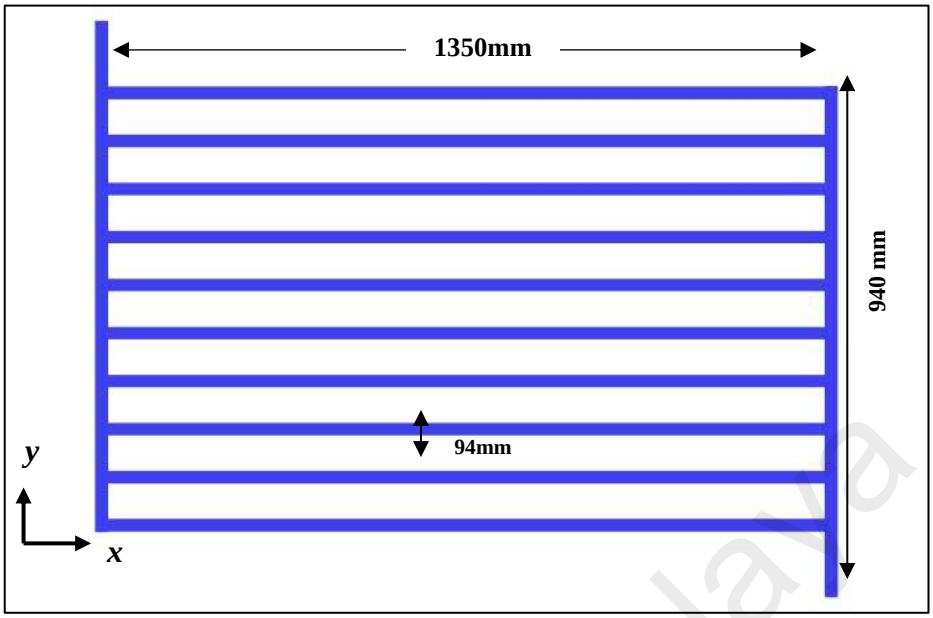

(a) 2D View

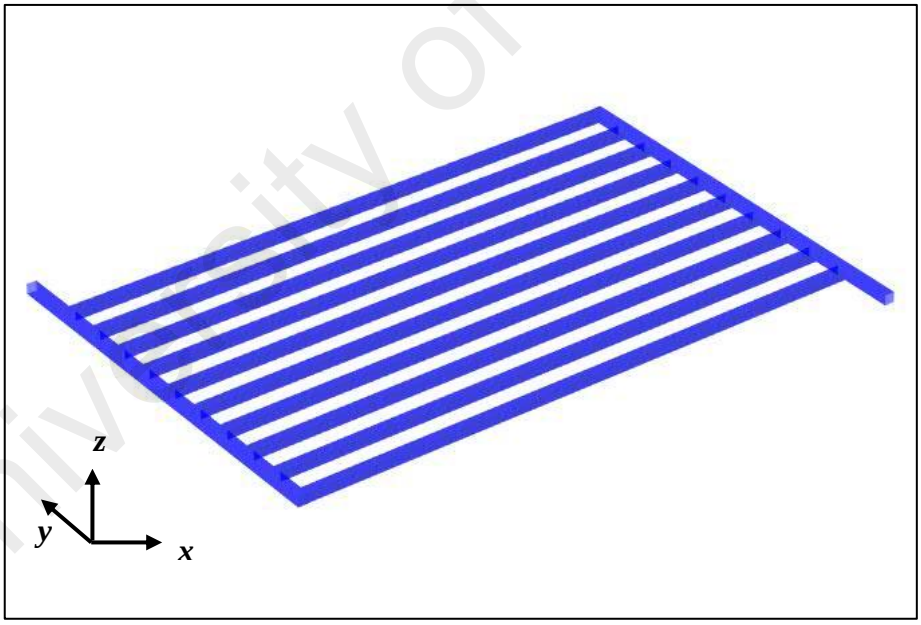

(b) 3D View

Figure 4.8: Parallel square pipe flow channel

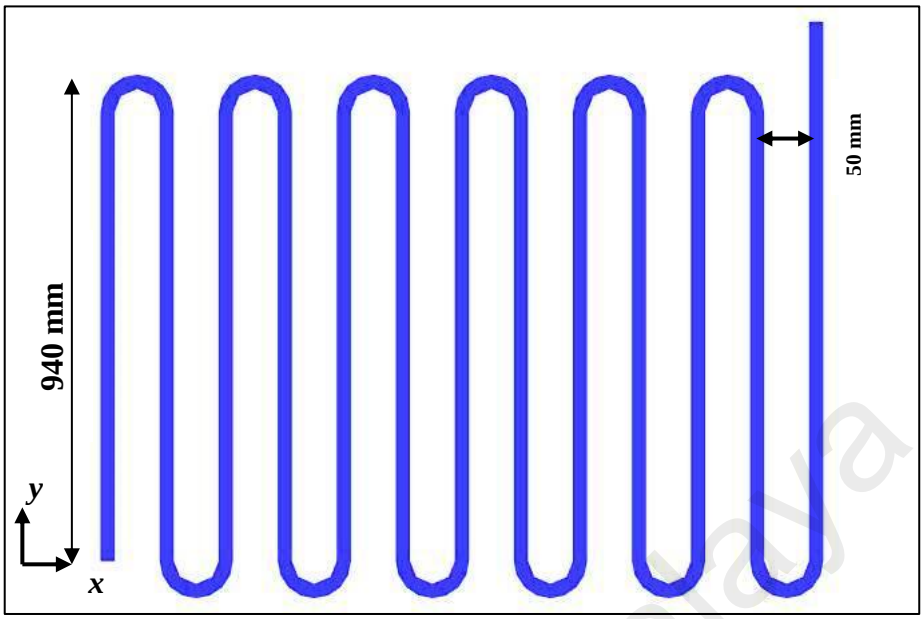

(a) 2D View

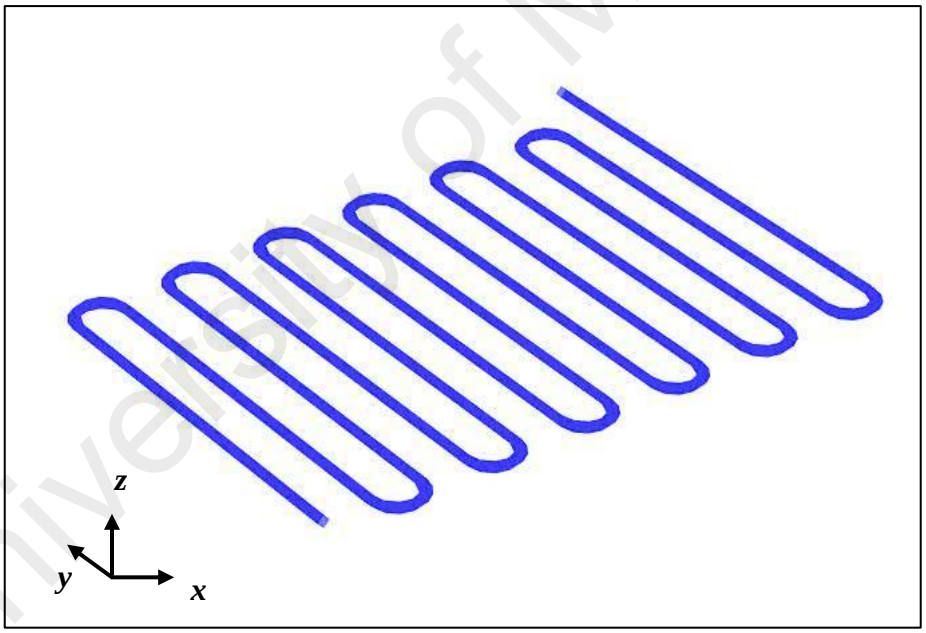

(b) 3D View

Figure 4.9: Serpentine flow channel

4.6.2 Instrumentation and Control

The experimental set up is built to test the effect of one or more independent variables on the behavior of several dependent variables. The control mechanisms are designed so as to regulate the independent variables and the instrumentations are set in

accordance the requirement to measure the dependent variables. The independent variables involved in the present study are inlet flow velocity, incident solar irradiation, water inlet temperature and ambient temperature while the dependent variables are electrical and thermal energy. Therefore, the following instrumentation and control have been used in the present experimental work.

4.6.2.1 I-V tracer

An *I-V* tracer (Figure 4.10) is used to measure the current-voltage relationship (*I-V* curve) of photovoltaic modules. The *I-V* tracer Nasa 2.0 used in the present experimental study is developed at UMPEDAC, University of Malaya, Malaysia. It is used for measuring and controlling short circuit current (*Isc)*, open circuit voltage (*Voc*), maximum current (*Im*), maximum voltage (*Vm*) and maximum power (*Pmax*) generated by module. This *I-V* tracer can trace power up to 2000 watt.

Figure 4.10: *I-V* tracer

4.6.2.2 Pyranometer

Pyranometer is used (Figure 4.11) to measure solar irradiance (radiant flux, W/m^2) on a plane surface. It can measure the global radiation, i.e., the blend of beam radiation and diffuse radiation from the hemisphere above the device. Basically, there are two types of pyranometers, viz, thermopile pyranometer which covers the total spectrum

range (300 nm to 2800 nm) of solar radiation on earth surface and photodiode-based pyranometers which can sense radiation in the range of 400 nm to 1100 nm. The later ones, also known as silicon pyranometer, show less uniform response. However, the measurements of silicon pyranometer are as faithful as the first-class thermopile pyranometer in visible solar spectrum which controls the photoelectric effect.

A silicon pyranometer of LI-COR brand, USA, model PY82186 has been used in this experiment to measure the insolation of the Sun. It is capable of measuring irradiation from 0 to 1280 W/m^2 within the spectral range of 300 nm to 1100 nm and can operate well from 40^{o}C to 75^{o}C temperature.

Figure 4.11: Pyranometer (LI-COR, Model: PY82186)

4.6.2.3 Flow meter

The flow meter (Figure 4.12) used in this experimental set up to measure the flow rate of the heat transfer fluid (HTF) is a variable-area meter (also known as rotameter). The measuring range of the flow meter is 16 L/h to 160 L/h with a resolution of 8 L/h. As water is employed as the HTF in the experimental study, rotameter of model LZB-10B is selected to ensure the use with fluids having specific gravity 1.0 at normal operating temperature range. The basic independent or control variable in this experimental study is water inlet velocity. Although differential gate valve has been

used for gross level flow control, the precise control of flow velocity is achieved by the flow control knob of the flow meter.

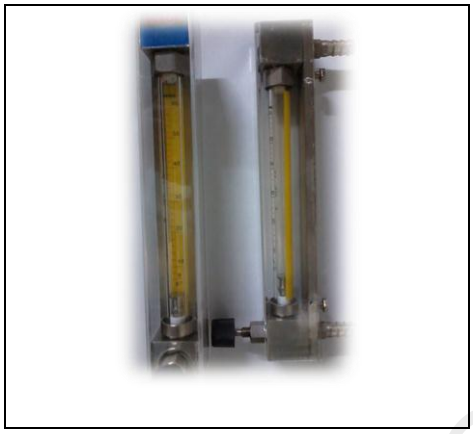

Figure 4.12: Flow meter (Model: LZB-10B)

4.6.2.4 Thermocouple

The type K thermocouple probe has been used to measure the inlet and outlet temperatures of water along with top and bottom surface temperatures of the PV module. Type K thermocouple is the most rugged in temperature measurement with the widest measuring range. This thermocouple is a bimetal wire of chromel (90% nickel and 10% chromium) and alumel (95% nickel, 2% manganese, 2% aluminum and 1% silicon).

Figure 4.13: K-type thermocouple

4.6.2.5 Data logger

The solar experimental data are stochastic by nature and the experiments are run for a whole day or even for days together. So, there is a need for continuous data acquisition in order to follow the real trend of a particular variable. A digital data logger of brand Data Taker, model DT80 (Figure 4.14) has been used to measure and store different temperatures and irradiation level continuously for a long period of experimental run. The real-time data is viewed and downloaded through a web based graphical user interface that defines basic measurement tasks. Logged data is then extracted by a USB memory device or downloaded using the web interface into files ready for import into spreadsheets and data analysis tools.

Figure 4.14: Data Taker DT80

4.6.3 Experimental Procedure

Performance of a PV/T-water system with a novel thermal collector design without absorber plate has been experimentally investigated. Parallel plate configuration of the thermal collector has been selected out of four collector designs. Two prototypes have been constructed, one made of aluminum and the other one of copper. The flow channels are then attached with two separate but same size and rating of PV module by means of thermal paste. Elevation head from overhead reservoir tank to the PV/T module is employed to maintain the circulation of water through the collector. This

scheme of using elevation head for circulating water will save pumping energy which makes the system passive, in order to avoid the use of pump constructed and tested in different conditions and configurations to achieve a significant enhancement in efficiency.

The experimental setup is installed at Solar Garden, Level-3, UMPEDAC, Wisma R & D, University of Malaya, Malaysia. The complete experimental set-up with different instrumentation is shown in Figure 4.15.

The on-site data collection includes incident solar radiation, ambient temperature, PV panel top surface and back surface temperature, water inlet and outlet temperature and electrical current, voltage, power and wind speed. The experiments were carried out during the months from February to June 2016. The meteorological data is collected from the weather station installed at the Solar Garden for the days of experiment. The irradiation was measured by a LI-COR brand PY82186 model silicon pyranometer connected to a digital data logger of brand Data Taker DT-80 for continuous data acquisition. The K-type thermocouples were also connected to this data logger to get uninterrupted temperature data at a time from all the measuring points. The Nasa 2.0 model *I-V* tracer has been used to measure and record the short circuit current (I_{sc}), open circuit voltage (V_{oc}), maximum power (P_{max}) and fill factor (*FF*). A variable-area flow meter of model LZB -10B is used to control and measure the flow rate of water.

Data has been collected in every one minute from 8:00 am to 5:00 pm by both of the data acquisition devices. The measuring range and the least counts of the instruments are given in Table 4.5. The collected data has been analyzed with help of spreadsheet analysis software MS Excel. In order to investigate the effects of temperature, irradiation, cooling on the performance of the PV module, the results obtained from the spreadsheet have been plotted in Tecplot 10.

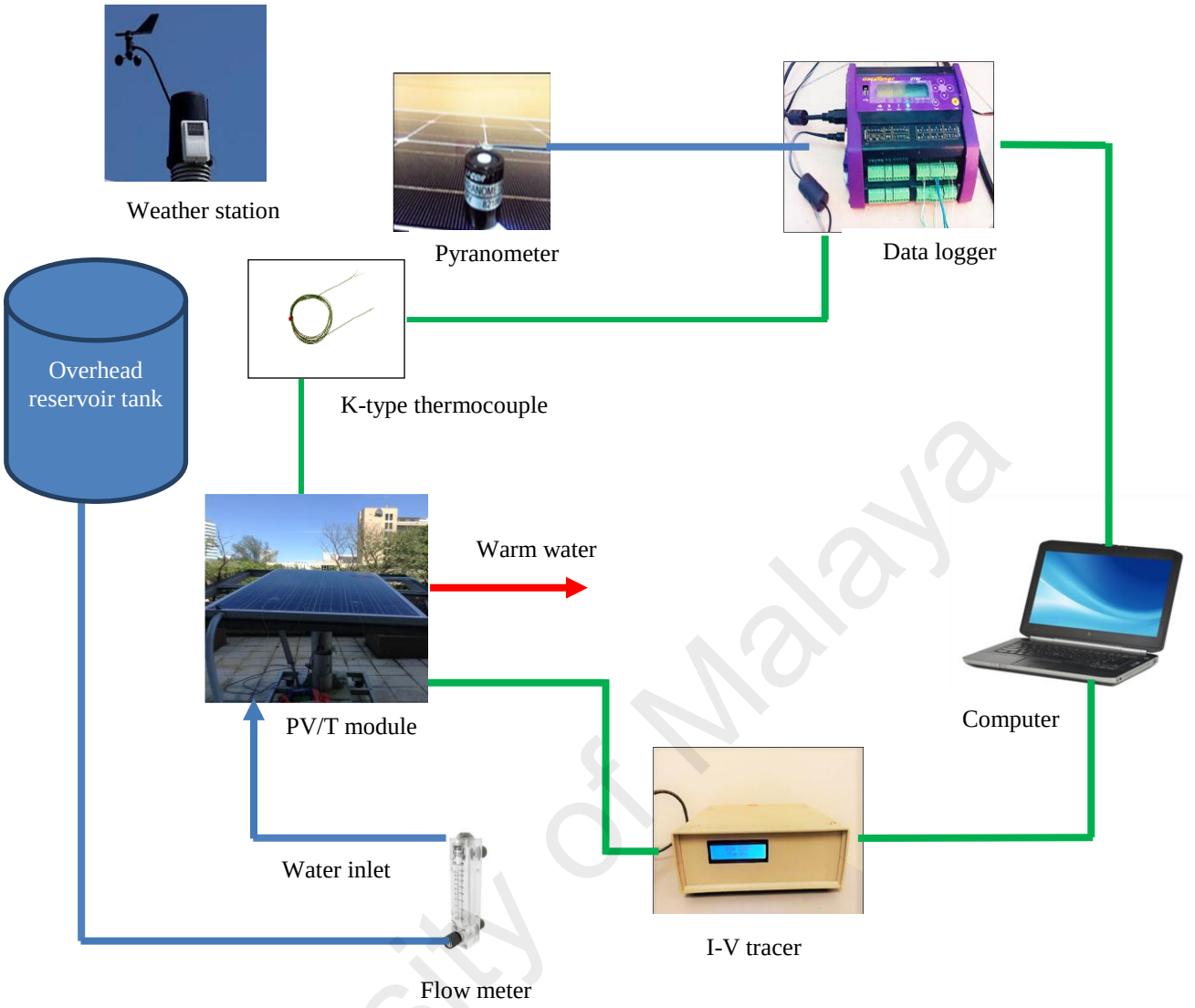

Figure 4.15: Instrumentation of the experimental set up

Table 4.6: Measuring range and least count of the measuring instruments

Instrument name	**Measuring range**	**Least count**
Pyranometer (LI-COR, Model: PY 82186)	0 to 1280 W/m^2	1.25 W/m^2
Flow meter (Model: LZB – 10B)	16-160 L/h	8 L/h
Type K thermocouple probe	– 200 to 1350^{o}C	0.1^{o}C

CHAPTER 5: RESULTS AND DISCUSSION

5.1 Introduction

The functioning of a PV/T collector is intrinsically dynamic. The excitations like solar irradiance and wind are transient in nature. Hence, a dynamic model is a predominant requirement for predicting working temperatures of the PV module and the heat-removal fluid when the irradiation is rapidly fluctuating. However, the difference between simulation outcomes using the steady-state and the dynamic models are trivial for particular time of the day under certain sky conditions and nature of radiation. In present research, the 3D steady-state model was found to perform almost as good as the more time-consuming 3D dynamic model considering the above mentioned conditions. In order to get an accurate prediction of the collector yield, it is necessary to generate the results when steady-state condition is established.

In the present research work, a 3D mathematical model has been developed numerically and validated experimentally. Hence the numerical model is employed to carry out performance evaluation of several newly developed designs of thermal collector. The thermal collector design excludes the conventional absorber plate; hence collector in present research is expressed by the term flow channel only. The numerical simulation was done using commercial finite element based software COMSOL Multiphysics®. The experiments were carried out on site under the typical weather condition of Malaysia. This chapter presents the results obtained from the numerical and experimental investigation in the following manner. In the present research four different configurations of thermal collector has been considered, all excluding the absorber plate; that is flow channel is the only part of the thermal collector. The first part of the analysis was a convergence study for the proposed numerical model and this was done by selecting Design 1 (parallel plate flow channel) as the representative

design, the numerical results of which have been validated by experimental results. After validation of Design 1, performances of the other designs have been evaluated by numerical simulation only. At the end, performance trends PV/T with every design of collector have been compared with each other to confirm an optimum design.

5.2 Justification of Exclusion of Absorber Plate

A novel design of thermal collector excluding absorber plate has been introduced in the present research. Thus thermal collector in this case is only the coolant flow channel that has been attached to the PV module backside by means of thermal paste only. This modification in the conventional thermal collector is justified by observing the performance of the PV/T with and without absorber plate.

Numerical simulation has been done under the conditions of water inlet and ambient temperature both at 27^{o}C, inlet velocity at 0.0007 m/ and irradiation level at 1000 W/m^{2}. The results show that the variation in electrical performance with and without absorber plate is negligible. However, the thermal as well as overall efficiency marginally differ due to this modification in thermal collector of the proposed model. As can be seen from Figures 5.1 (a) and 5.1 (b) thermal collector without absorber plate yields slightly better thermal performance; hence, thermal collector excluding absorber plate may offer a better solution for heat removal in PV/T module. Therefore, all further evaluations in the present research have been done without absorber plate for all the collector designs. This elimination of absorber plate will not only reduce the weight and cost, but also mitigate some technical issues like generation of leakage current in the PV/T system which is one of the reasons of potential induced degradation (PID).

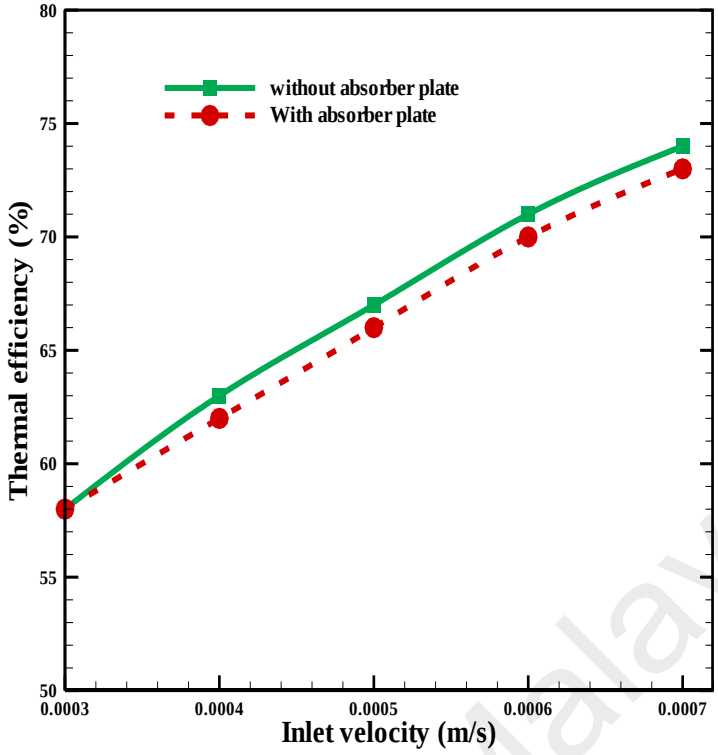

(a)

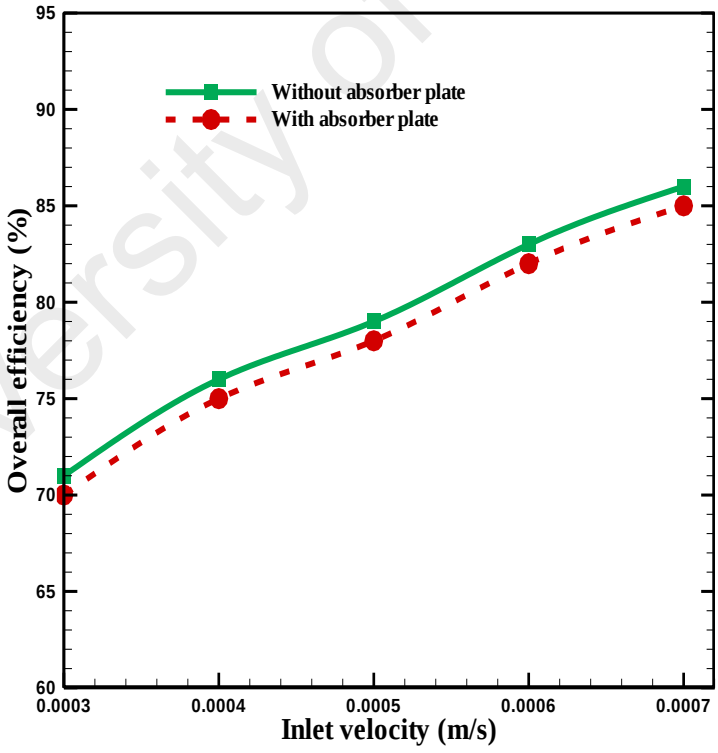

(b)

Figure 5.1: Comparison of PV/T performance with and without absorber plate

5.3 Experimental Validation

The mathematical model developed in the present research has been validated by experimental results in the following method. Design 1 (D1), that is, parallel plate flow channel has been selected for carrying out the experimental validation due to its geometrical simplicity and highest overall efficiency. The mathematical model has been employed to produce a numerical simulation of design1 (D1) in the environment of an FEM based software COMSOL Multiphysics®. The numerical results thus obtained from the simulation have been compared with those obtained from the corresponding experimental investigation of the same collector design. The daily average ambient temperature of Malaysia is 27^{o}C, but the temperature in peak hours of daytime usually varies between 33.5^{o}C to 35^{o}C with an average of 34^{o}C. In the present study, numerical investigations were carried out under this ambient condition (34^{o}C) with the inlet velocity from 0.0003 m/s to 0.0007 m/s at irradiation level 1000 W/m^{2}. The water inlet temperature was also taken same as peak hour average ambient temperature of Malaysia. This water temperature was selected to ensure that the cooling water may reach ambient temperature prior to enter the cooling channel to carry the heat away from the PV/T panel.

The numerical model has been validated by comparing the experimental results of thermal and overall efficiency with those obtained numerically. As can be seen from Figures 5.2 (a) and 5.2 (b), the experimental values of thermal and overall efficiencies are fairly comparable with the corresponding numerical values over the entire range of inlet velocity for both aluminum and copper channel. This slight difference is due the uncontrollable outdoor meteorological conditions like ambient temperature, water inlet temperatures and wind speed of the experimental site. Hence, both thermal and overall efficiency curves in Figures 5.2 (a) and 5.2 (b) are found to be at well agreement with each other qualitatively as well as quantitatively.

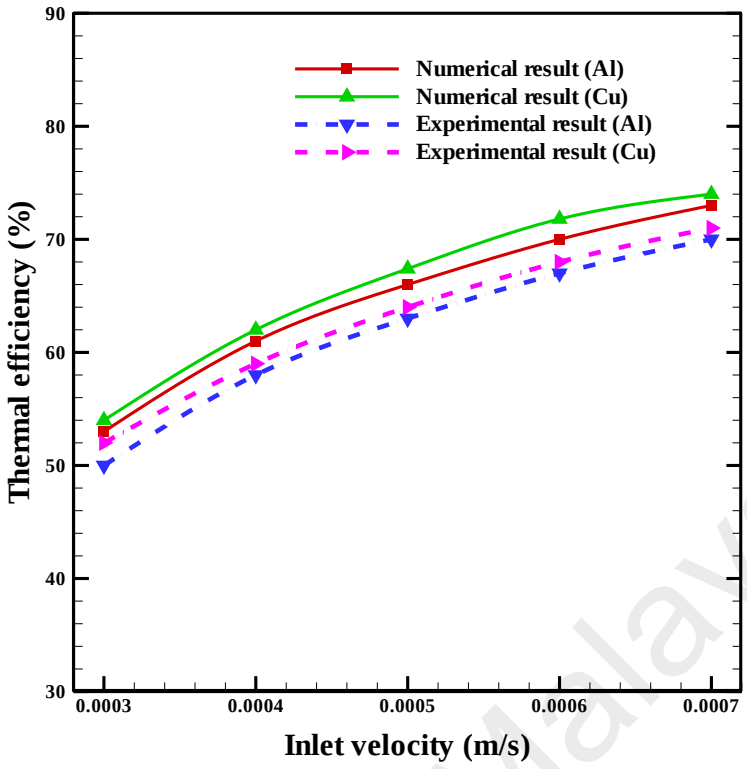

(a)

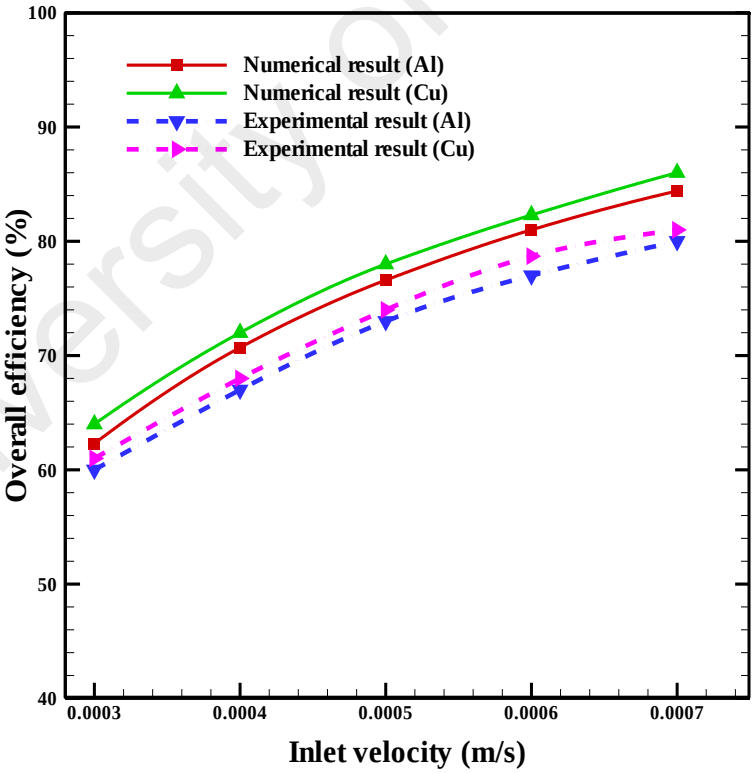

(b)

Figure 5.2: Validation of the experimental results by (a) thermal efficiency, (b) overall efficiency

The validity of the numerical model has further been assessed using the uncertainty analysis. The uncertainty between numerical and experimental results has been analyzed using root mean square percentage deviation (RMS) technique which is calculated using the following formula (Sobhnamayan et al., 2014):

$$\mathrm{RMS} = \sqrt{\frac{1}{N_{\exp}} \sum \left[\left(\frac{X_{num,i} - X_{\exp,i}}{X_{\exp,i}} \right) \times 100 \right]^2} \tag{5.1}$$

where $X_{num,\,i}$, $X_{exp;\,i}$ represent the numerical and experimental values, respectively, N_{exp} is the number of the experiments carried out.

The plots of thermal and overall efficiency as a function of inlet velocity (Figure 5.2 (a) and (b)) have been used to measure the uncertainty of this study. The RMS percent deviations for thermal efficiency are 4.97% for Al and 4.85% for Cu, while that for overall efficiency are 5.03% for Al and 5.42% for Cu. Sobhnamayan et al. (2014) validated a simulation model of PV/T-water collector with experimental results by using RMS percent deviations. The RMS error for thermal efficiency as obtained by the authors is in well compliance with that obtained in the present study. Hence, the experimental results of the present study fairly establishes the numerical model. Thus, the uncertainty analysis confirms the validity of the model with further cognition.

This compliance between the numerical and experimental results firmly establishes the validity of the present numerical model. So, it may be concluded that this mathematical model is worthy enough to predict the performance of the PV/T system with the proposed collector design to a good extent.

The PV/T collector with other flow channel designs in the present study has been developed with the same mathematical model based on the same physics which was employed in case of parallel plate flow channel (D1). Therefore, upon validation of the proposed mathematical model, it can now be employed to generate numerical simulation results for performing the parametric study of the PV/T module with other flow channel designs: pancake flow channel (D2), parallel square pipe (D3) and serpentine flow channel (D4).

5.4 Performance Evaluation of PV/T with Parallel Plate Flow Channel

5.4.1 Numerical Simulation Results

The numerical investigation has been conducted using dynamic simulation and the results are analyzed at steady state. The attainment of steady state is demonstrated in Figure 5.3 which shows that the PV cell and the water outlet temperature levels have become almost constant after certain period of time. At this steady state, variations of all the parameters become almost zero with respect to time. Further evaluations are performed at this particular steady-state condition.

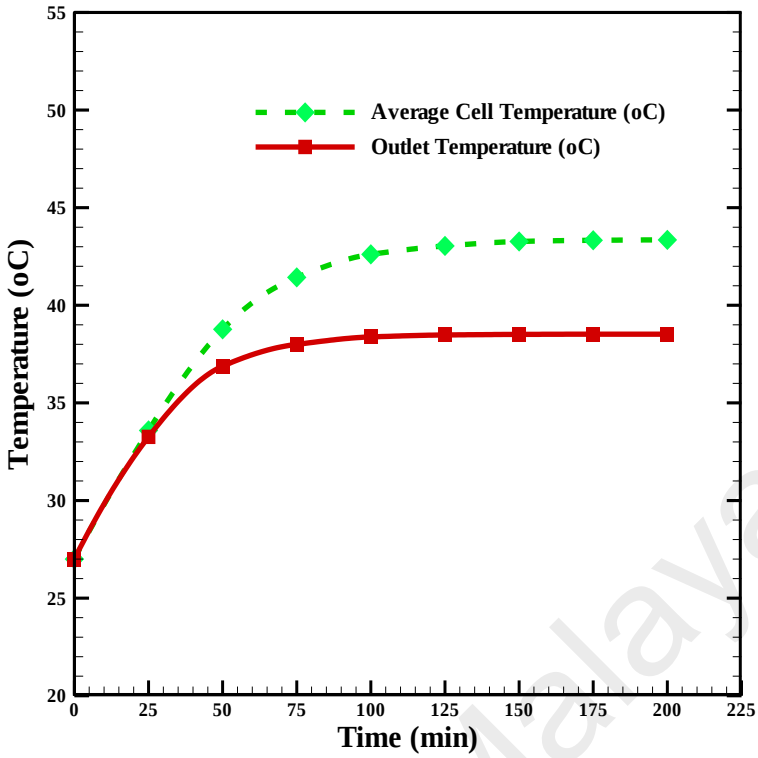

Figure 5.3: Attainment of steady state conditions in the simulation study

The effect of inlet flow velocity on the temperature distribution throughout the flow channel and the PV/T module has been demonstrated separately by numerical simulation 3D surface plots in Figures 5.4 and 5.5, respectively. Figures 5.4 (a) to (e) show the effect of inlet flow velocity on the temperature distribution throughout the flow channel for velocities ranging from 0.0003 to 0.0007 m/s, where the ambient and water inlet temperature was kept constant at 34^{o}C and irradiation 1000 W/m^{2}. Surface plot for aluminum channel are shown only as a representative demonstration. It can be observed that the maximum channel material temperature drops from 77^{o}C to 60^{o}C as the inlet velocity is increased from 0.0003 to 0.0007 m/s.

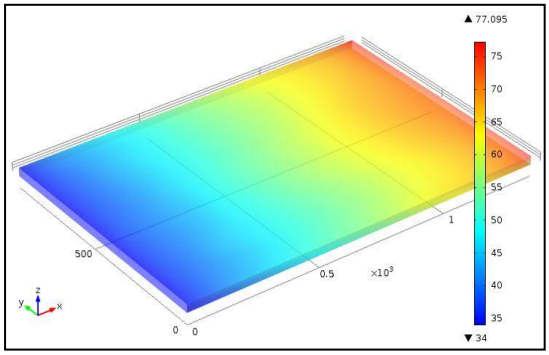

(a) U_o = 0.0003 m/s

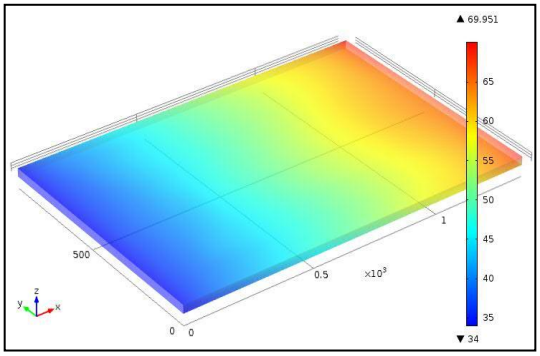

(b) U_o= 0.0004 m/s

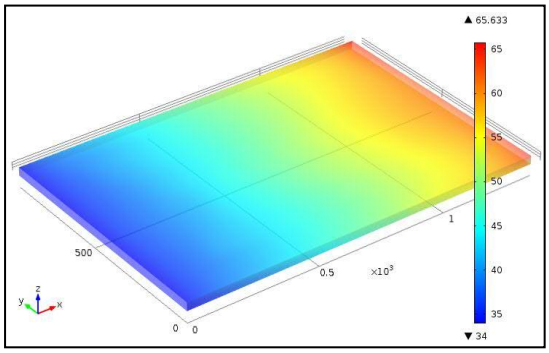

(c) U_o = 0.0005 m/s

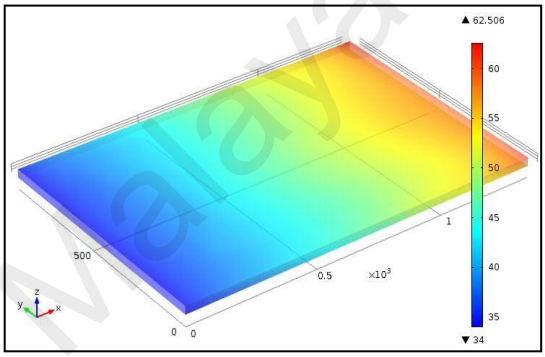

(d) U_o = 0.0006 m/s

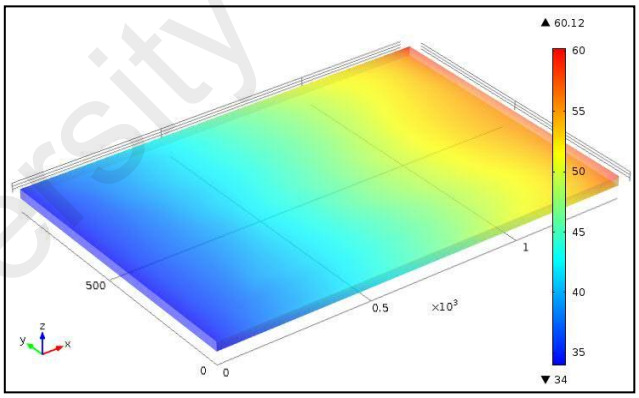

(e) U_o = 0.0007 m/s

Figure 5.4: 3D surface plot of temperature for flow channel at steady state

The temperature distribution throughout the PV/T module for inlet velocities from 0.0003 to 0.0007 m/s has been presented in Figures 5.5 (a) to (e). Within the range of the specified velocity, temperature of the materials of the module was reduced from

85°C (at 0.0003 m/s) to 70°C (at 0.0007 m/s). It is revealed from the above trend that for an increase in inlet velocity by 0.1 mm/s, module temperature decrease by 3.75°C which is very much ample for thermal regulation of PV module.

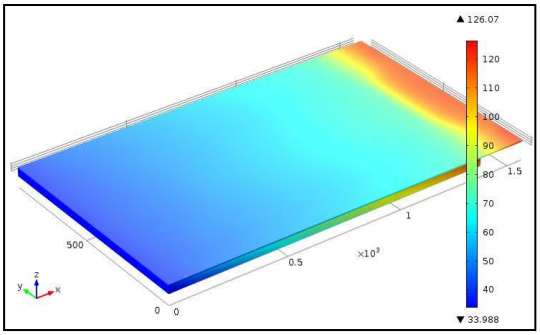

(a) U_o = 0.0003 m/s

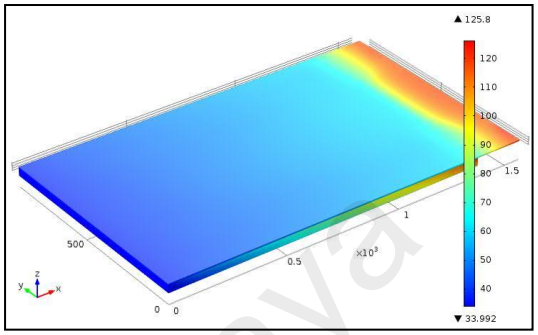

(b) U_o = 0.0004 m/s

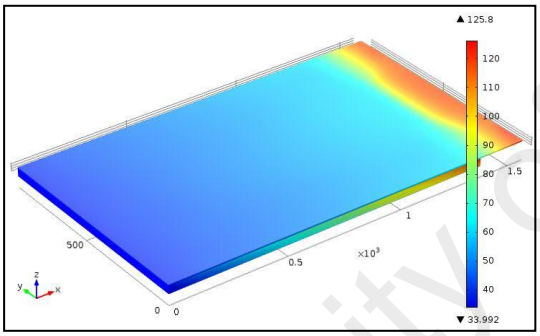

(c) U_o = 0.0005 m/s

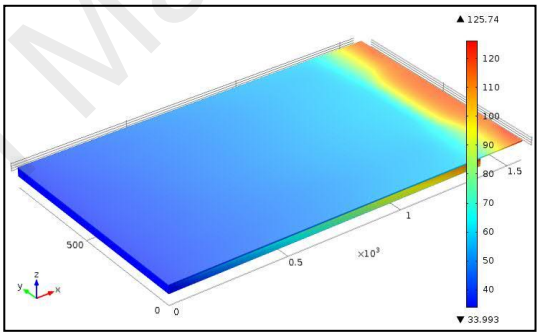

(d) U_o = 0.0006 m/s

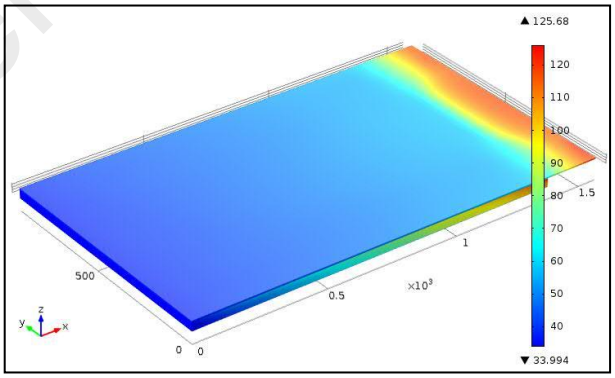

(e) U_o = 0.0007 m/s

Figure 5.5: 3D surface plot of temperature distribution throughout PV module

5.4.2 Experimental Results

The experimental investigation was carried out between the months of February to June 2016. However, experimental results have been presented (from Figure 5.6 to 5.8) here for a particular day of May 9, 2016 to illustrate a representative trend. The top and bottom surface temperatures as compared to the ambient temperature is shown in Figure 5.6. The outcomes for copper channel are given as a representative result. It can be noticed from the figure that both the top and bottom surface temperatures reach their peaks at the solar noon of 12:00 pm, the peak values being 72.5^{o}C and 63.3^{o}C, respectively. The ambient temperature remained almost the same at about 33^{o}C all along the day except the early morning time.

The electrical and thermal yields of the PV/T system have been shown in Figure 5.7 and 5.8, respectively. From Figure 5.7, it can be seen that the electricity production is the highest between 10:30 am to 11:30 am and the maximum electrical power output from the PV module is 107 W.

The thermal energy gain by the PV/T module throughout a particular day has been illustrated in Figure 5.8. It may be observed from the figure that maximum thermal energy gain occurs around 11:00 am to 1:30 pm. The highest thermal energy gain is about 678.5 W.

A comparative look into both figures reveals two facts; first, the highest gain in electrical and thermal energies does not necessarily occur simultaneously. Secondly, thermal output is about 6.5 times the electrical yield vindicating that PV/T systems can be a better replacement of the conventional solar thermal collectors with twofold yield.

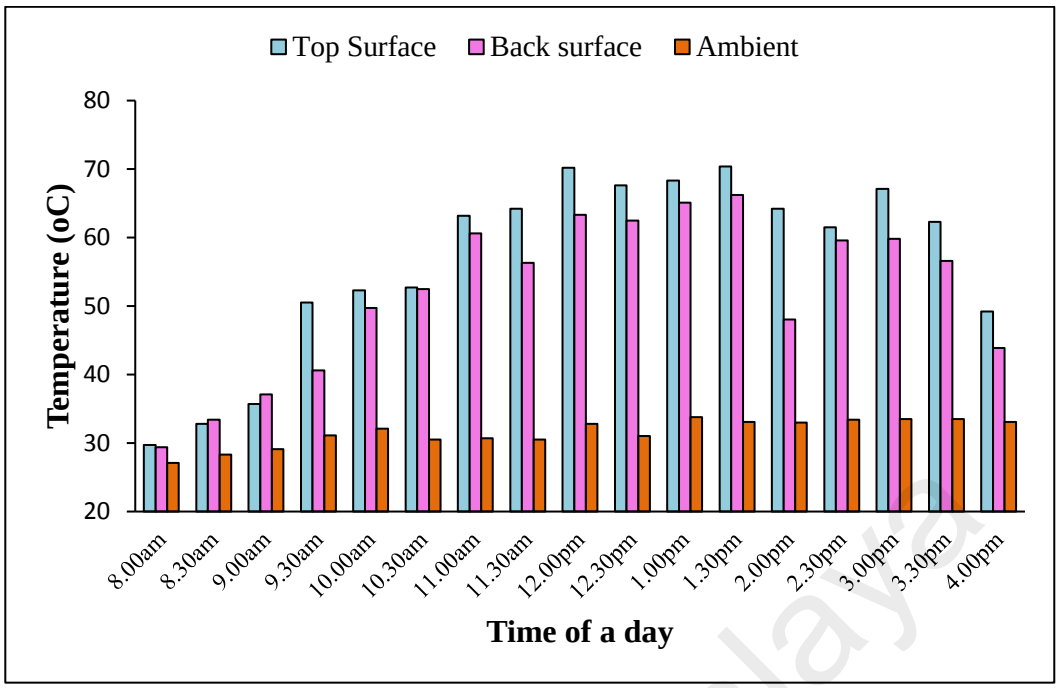

Figure 5.6: PV module top and bottom surface temperature and ambient temperature as a function of daytime (May 9, 2016)

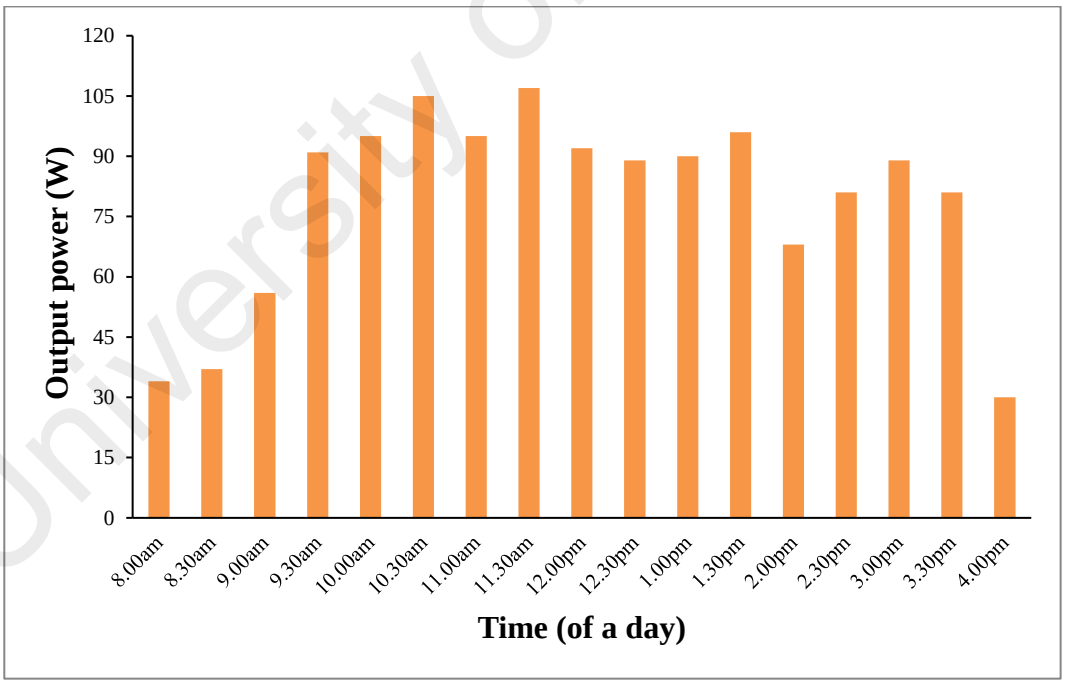

Figure 5.7: Electrical power output of the PV as a function of daytime (May 9, 2016)

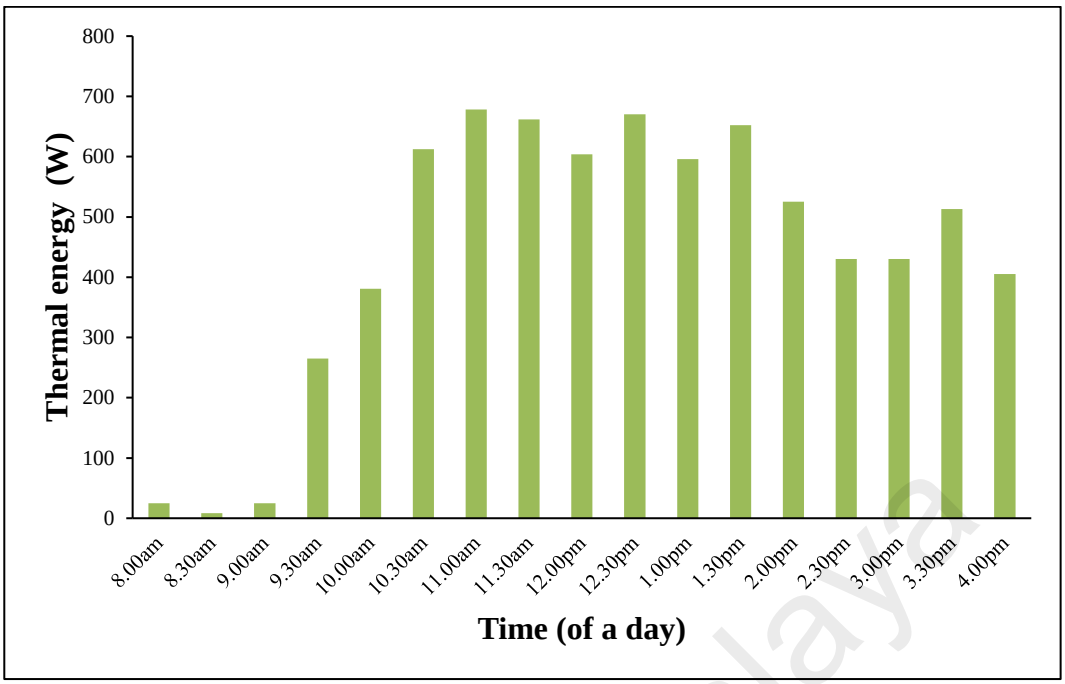

Figure 5.8: Thermal energy gain of PV/T module as a function of daytime (May 9, 2016)

5.4.2.1 Effect on inlet velocity

The effect of the inlet velocity on the performance of the PV/T system is shown in Figures 5.9 (a) to (d) under the condition inlet and ambient temperature 34ºC at irradiation level 1000 W/m^2 with inlet velocities from 0.0003 to 0.0007m/s. Figure 5.9 (a) shows that the average cell temperature decreases with increasing inlet velocity for both numerical (from 64.5ºC to 59.4ºC for aluminum and from 64.2ºC to 58.8ºC for copper) and experimental (from 66ºC to 60.5ºC for aluminum and from 65.3ºC to 59.9ºC for copper) cases. As the inlet velocity is increased more heat is removed from the module by convection which reduces the average cell temperature. The experimental values are somewhat higher than the corresponding numerical values for both aluminum and copper channels. This discrepancy between the numerical and experimental values is due to the uncontrollable outdoor ambient conditions of the experimental site where inlet temperature of water could not be maintained at certain level as in the case of numerical simulation. Figure 5.9 (a) also shows that in

experimental case, cell temperature achieved with copper channel is about 1.5^{o}C lower than that with aluminum channel. As the thermal conductivity of copper is almost double the aluminum, so heat removal with copper channel is more effective. Therefore, copper is better choice as thermal collector material from the viewpoint of reducing cell temperature. Figures 5.9 (b) shows the outlet water temperature also decreases with increasing inlet velocity for both numerical (from 54.3 ^{o}C to 45.7^{o}C for aluminum and from 53.6^{o}C to 44.6^{o}C for copper) and experimental cases (from 48.5 ^{o}C to 42.2^{o}C for aluminum and from 49 ^{o}C to 42.7^{o}C for copper). With the increase in flow velocity, rate of heat removal is also increased and less time is available for thermal accumulation, thereby decreasing the water outlet temperature.

Figures 5.9 (c) and (d) show the trend of output power and electrical efficiency as a function of water inlet velocity. Both output power and electrical efficiency are observed to rise with increasing water inlet velocity. The average cell temperature is reduced with increasing water velocity; as a result PV current drops marginally with noticeable increase in PV voltage. This, in turn, increases the output power and electrical efficiency of the module. For aluminum channel, the maximum PV output power obtained is 121.5 W numerically and 106W experimentally whereas the electrical efficiency achieved is around 11.2% for numerical and 10% for experimental case. On the other hand, for copper channel, the maximum PV output power attained is 123 W numerically and 108 W experimentally whereas the electrical efficiency achieved was about 11.5% for numerical and 10.2% for experimental case. It may be noticed that the experimental values of both output power and electrical efficiency are a bit lower than the corresponding numerical values. The reason behind these incongruities is due to the unrestrained ambient conditions that prevail in outdoor experiments. Rather ambient temperatures increases with irradiation level and wind speed also varied continuously in experimental site. Therefore, in experimentation cell temperature could not be reduced

that much as compared to the numerical results. Due to the higher cell temperature, the electrical efficiency as well as the overall efficiency drops below of the model predicted values.

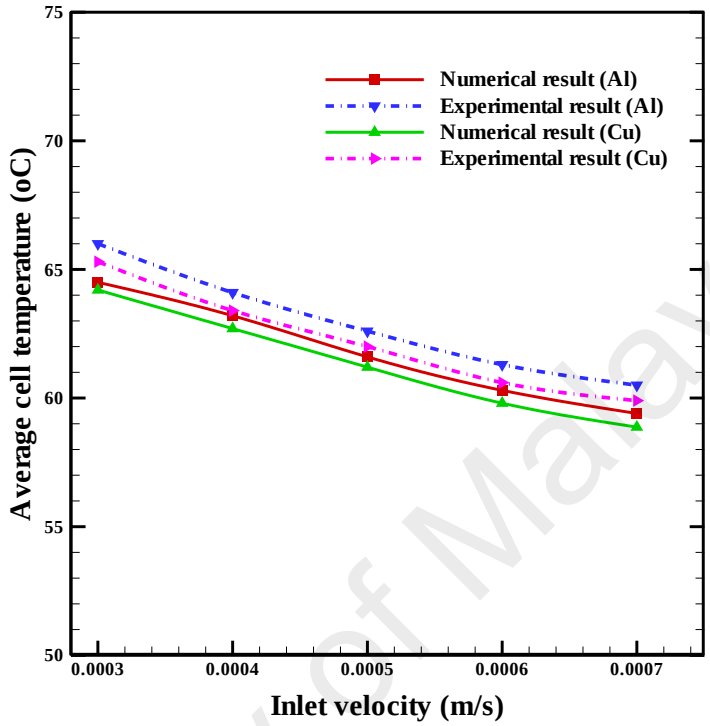

(a)

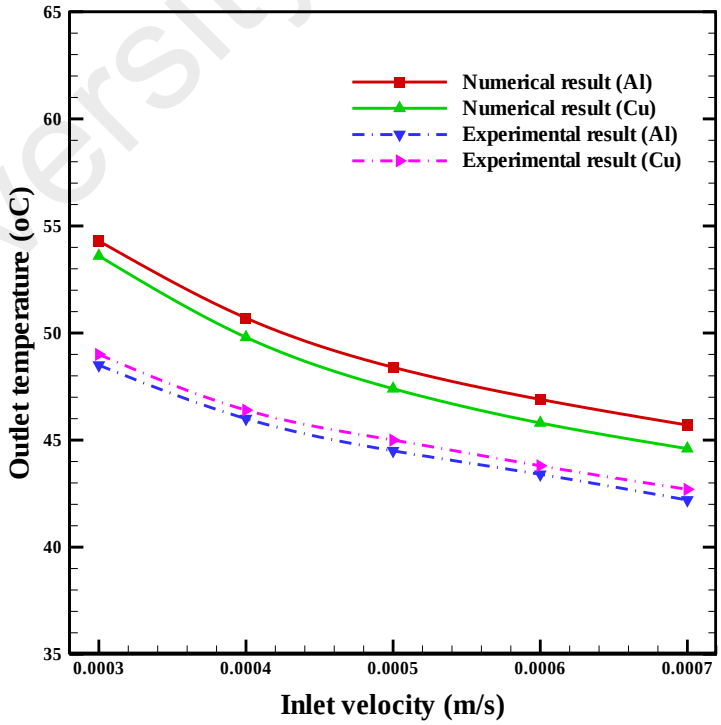

(b)

Figure 5.9: Effect of inlet velocity on the performance of PV/T at irradiation 1000 W/m^2

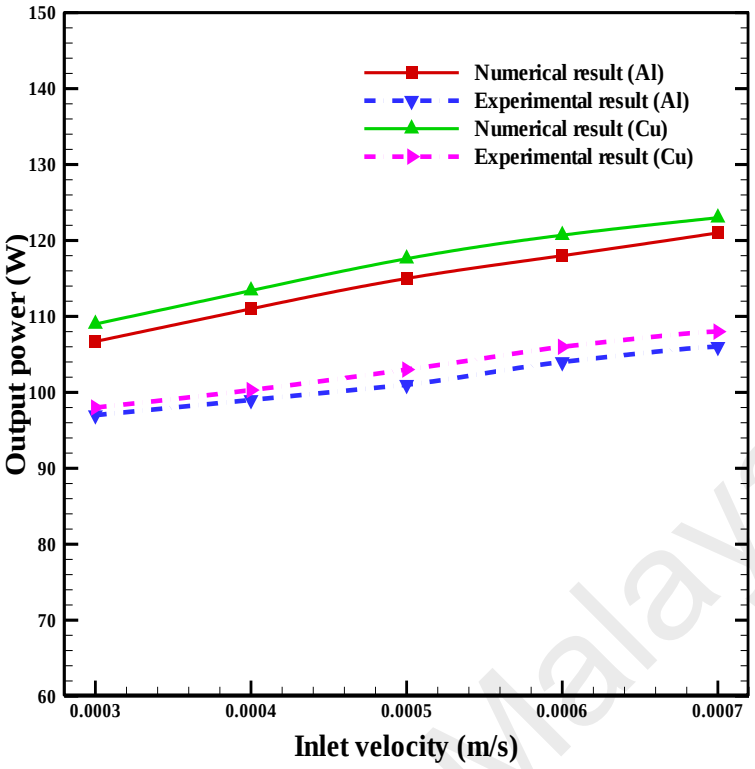

(c)

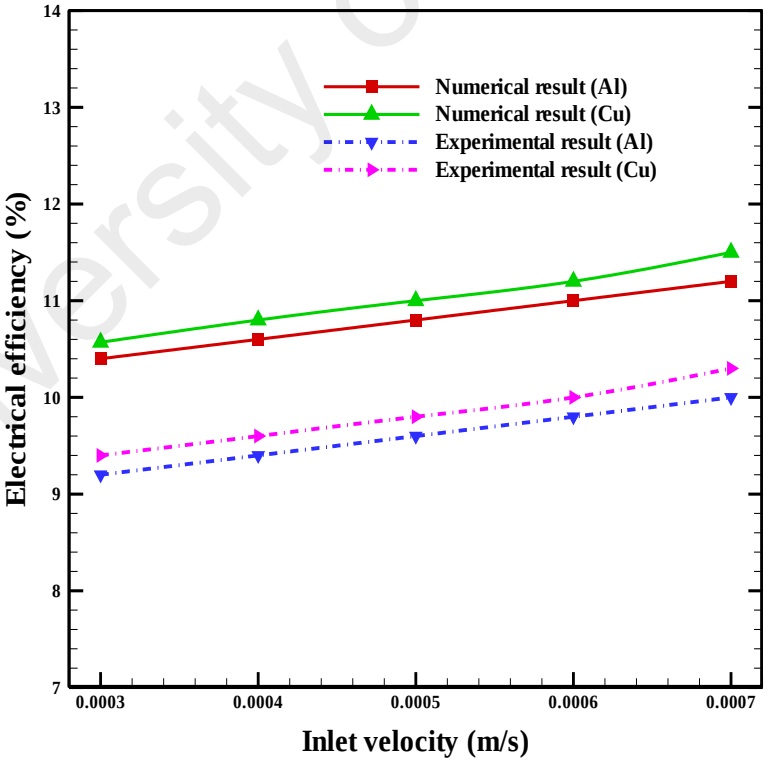

(d)

Figure 5.9, continued

The cell temperature has got significant impact on the electrical performance of the PV module. Figures 5.10 (a) and (b) show that both of output power and electrical efficiency decrease with increasing cell temperature. It is also revealed from the same figures that numerically a decrease in cell temperature by 6.5^{o}C for both of aluminum and copper channel, increase the output power by 14 W for aluminum and 14.5W for copper, while in experimental case, the output power increases 9 W for aluminum and 10 W for copper with decrease in cell temperature by 5.5^{o}C for both channels. For numerical case, the electrical efficiency increases by 0.9% for aluminum and 1% for copper with decrease in cell temperature by 6.5^{o}C for both of aluminum and copper. On the other hand in experimental case, this efficiency increases by 0.8% for aluminum and 0.9% for copper channel. The reason behind the above trend is due to the fact that a decrease in cell temperature causes significant increase in PV voltage with a slight decrease in PV current, which eventually increase the output power and electrical efficiency (Kumer & Rosen, 2011).

Table 5.1 shows the effect of decreasing cell temperature on electrical performance of PV/T system. The increase in output power and electrical efficiency for every 1^{o}C decrease in cell temperature for both aluminum and copper channel in case of numerical and experimental studies are given in the table to have a comparative picture. It is evident from the table that the rate of increase in electrical power and efficiency in experimental case is greater to some extent for both aluminum and copper channel. This is due to the fact that the ambient temperature and thereby water inlet temperature was much higher than the numerical set point. As the water inlet temperature becomes high, its cooling capacity gets lowered and cell temperature becomes high. As a result, the electrical performance in experimental case is inferior to that with numerical study.

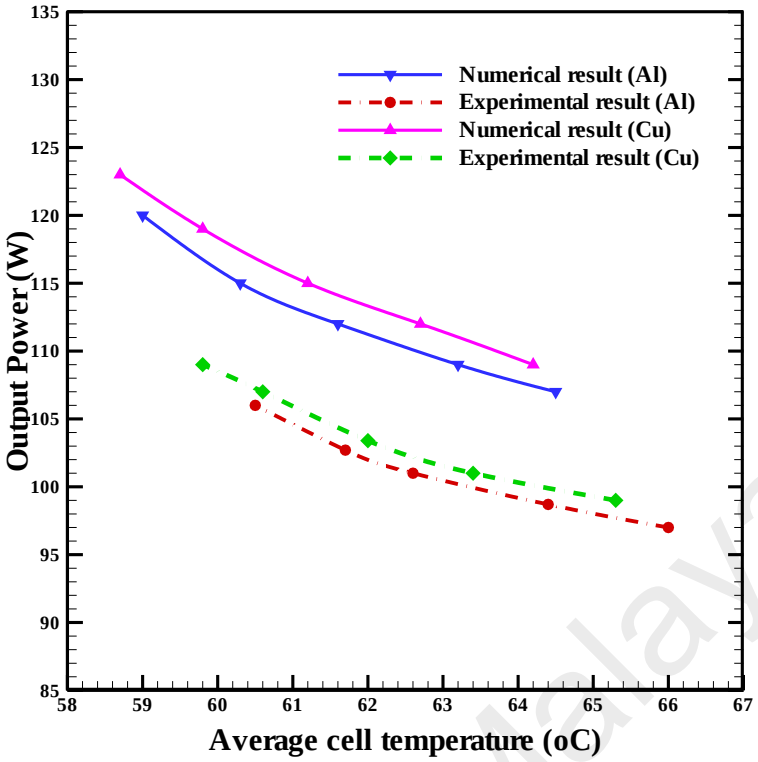

(a) Output power

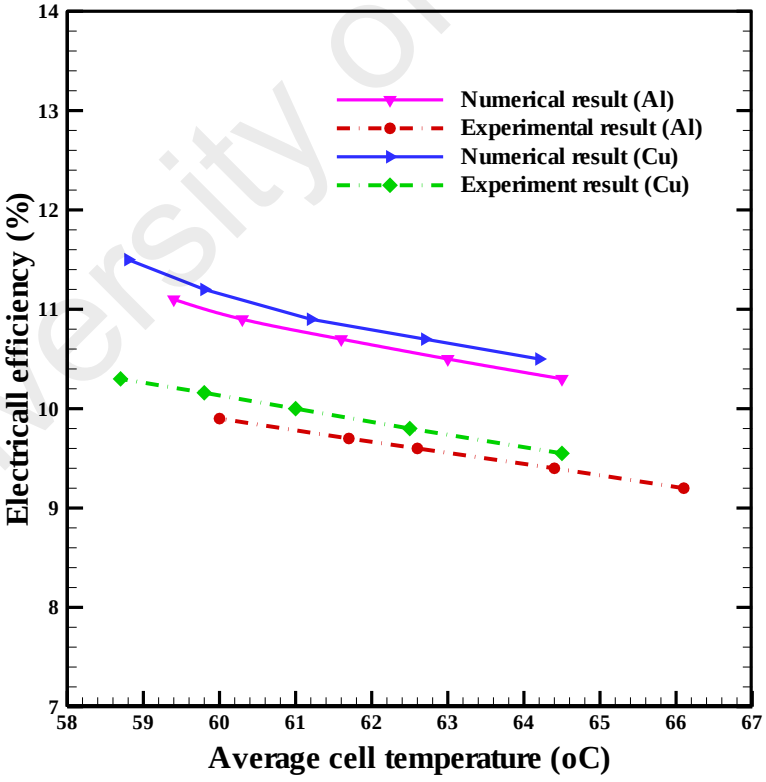

(b) Electrical efficiency

Figure 5.10: Effect of cell temperature on PV performance (a) output power, (b) electrical efficiency at irradiation level 1000 W/m^2

Table 5.1: Increment in electrical efficiency and output power per 1°C decrement in cell temperature

Performance parameter	Al		Cu	
	Numerical	**Experimental**	**Numerical**	**Experimental**
Electrical efficiency increase (%)	0.16	0.12	0.18	0.14
Output power increase (W)	2.4	1.6	2.5	1.8

5.4.2.2 Effect of irradiation

The influence of solar irradiation on the electrical performance of the PV module has been illustrated in Figures 5.11 (a) and (b). Figure 5.11 (a) shows for both numerical and experimental cases that output power increases with increasing irradiation level. The reason behind this increasing trend is that both current and voltage increase with irradiance where the increment rate of current is linear and much greater than the logarithmic increasing rate of voltage. As a result the output power increases almost linearly with irradiation (Fesharaki et al. 2011; Başoğlu & Cakir, 2016).

Figure 5.11 (b) shows that electrical efficiency decreases with increasing irradiation level for both numerical and experimental cases. As the irradiation level increases from 200 W/m^2 to 1000 W/m^2, electrical efficiency drops from 12.6% to 11.3% for numerical and from 12.2% to 10% for experimental case for aluminum and from 12.8% to 11.6% for numerical and from 12.4% to 10.3% for experimental case for copper channel. It may be noticed from Figure 5.11 (b) that the experimental electrical efficiency values are somewhat less than the numerical results. The relatively greater drop in efficiency in experimental investigation is attributed to unregulated outdoor experimental conditions which could not be governed according to the set points of the numerical study.

Another important issue which may be revealed from experimental study is that irradiations higher than a certain level do not produce favorable effect on electrical performance. From Figure 5.11 (a) it can be seen that although in numerical case the increment rate is almost constant, but in experimental case the incremental rate for gets decreased after 600 W/m^2 for both aluminum and copper channel. In addition, from Figure 5.11 (b) it can be observed that electrical efficiency rises near up to 600 W/m^2, and then drops gradually. Both of these trends imply that PV performance is much better at the irradiation level of 600 W/m^2 than at higher irradiances.

In Table 5.2 is given the effect of increased irradiation on electrical performance of PV/T system. The results for every 100 W/m^2 increase in irradiation level for both aluminum and copper channel in case of numerical and experimental studies have been tabulated. It is apparent from the table that although output power increases with increasing irradiation level, the electrical efficiency drops. The increment rate of output power in experimental case is less as compared to the numerical results, whereas the decline rate of electrical efficiency for experimental is greater than the numerical. Experimentally copper channel shows slightly better performance in terms of output power, while it suffers from relatively greater reduction in electrical efficiency than aluminum channel.

Table 5.2: Change in PV performance parameters per 100 W/m^2 increase in radiation

Performance parameters	**Al**		**Cu**	
	Numerical	**Experimental**	**Numerical**	**Experimental**
Output power increase (W)	11.5	10.0	11.6	10.1
Electrical efficiency decrease (%)	0.16	0.27	0.15	0.26

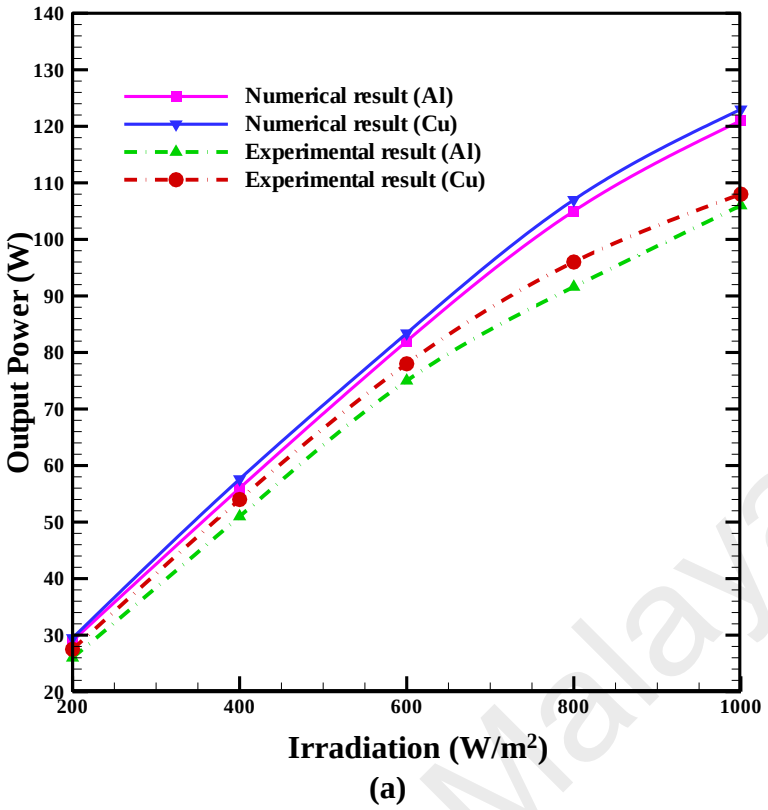

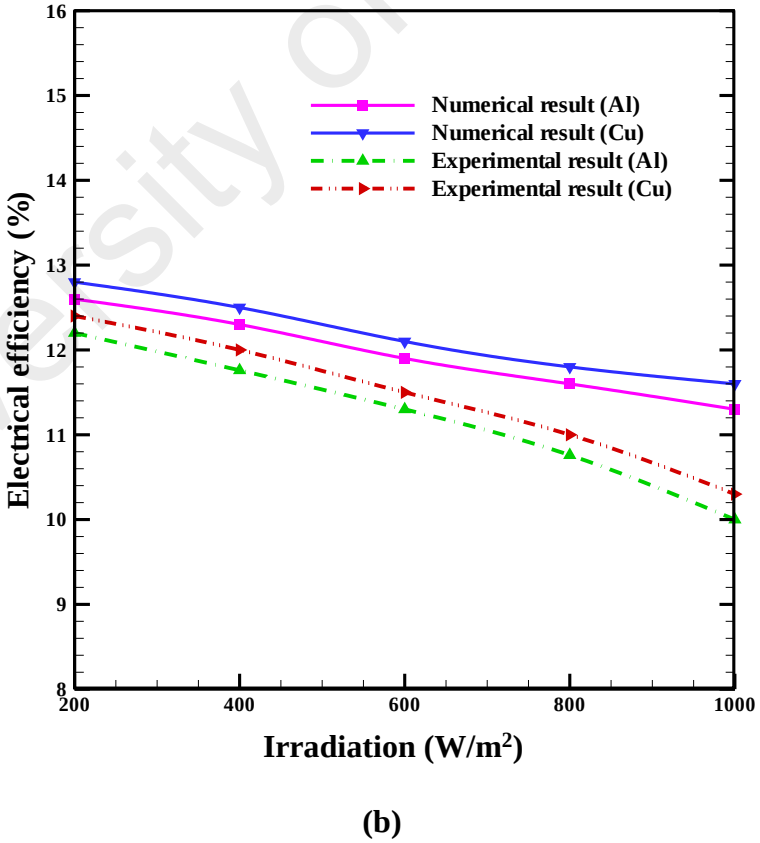

Figure 5.11: Effect of irradiation on PV performance (a) output power (b) electrical efficiency at inlet velocity 0.0007 m/s

5.5 Numerical Simulation Results with Different Collector Designs

Through experimental investigation on Design 1 (D1: parallel plate flow channel) the mathematical model has already been validated as discussed in section 5.2. Now, the same model is employed to perform numerical evaluation of the PV/T performance for all other flow channel designs, viz., pancake flow channel (D2), parallel square pipe (D3) and serpentine flow channel (D4). Numerical and experimental results of Design 1 (D1) show that among all other control parameters, the inlet velocity has the most noticeable effect on the temperature distribution of the PV/T module. Therefore, temperature distribution for the designs D2, D3 and D4 has been evaluated against the water inlet velocity only.

5.5.1 Effect of Inlet Velocity on Temperature Distribution Throughout the Flow Channel

The effect of the temperature distribution along the flow channels designs D2, D3, and D4 for aluminum is illustrated as 3D simulated surface plots in Figures 5.12 to 5.14. This evaluation has been done at a constant inlet and ambient temperature of 27^{o}C at irradiation level 1000 W/m^2. The inlet velocities were taken from 0.0009 to 0.05 m/s. In PV/T systems, the velocity of the heat transfer fluid is usually kept in the laminar flow in order to accumulate more heat from the PV module. Water temperature is strengthened with reduction in its velocity; however, flow rates that are too low will not remove heat effectively from the PV module. On the other hand, improvement in PV/T performance is limited to a certain higher flow rates, after which it may not enhance further. Therefore, optimized inlet flow velocity has a positive effect on the system performance to control the outlet temperature of water and achieve maximum energy saving. In addition, the choice of velocity range also depends on the particular design the flow channel of thermal collector. So, generally water inlet velocity in the flow

channel is optimized by trial and error method. In the present study, velocity range has been optimized so as to ensure that change in velocity do maximize the system efficiency. It has been observed numerically that below the inlet velocity of 0.0009 m/s the performance becomes near to that of non-cooled PV, while velocities above 0.05 m/s create no significant improvement in performance of the system. Therefore, in the present work fluid velocity range has been chosen in the range of 0.0009 – 0.05 m/s.

The 3D surface plots for aluminum channel are presented in this section as representative demonstration. The copper channel exhibits almost the same behavior and trend in temperature distribution.

Design 2 (Pancake flow channel)

From the Figures 5.12 (a) to (f), it can be observed that higher temperatures are obtained with very low velocities while temperatures fall gradually at higher velocities. Results show that the lowest channel temperature is obtained with the highest water inlet velocity of 0.05 m/s. On the other hand, when the inlet velocity is as low as 0.0009 m/s (refer to Figure 5.12 (a)), the maximum temperature occurs throughout almost the entire length (except the entrance) of the channel. This is due to the fact that with very low velocities of water heat transfer by convection becomes dime and the channel behaves almost like a heat sink in which waste heat from PV module back surface is dumped and accumulated due to very inferior heat removal rate. It can also be noticed that the portion of the outermost coils which are nearer to the entry section has got slightly lower temperature due to the effect of colder entrance of the first outermost coil.

As the inlet velocity is increased by ten times and reaches of the order of one thousandth meter per second (refer to Figures 5.12 (b), (c) and (d)), the convection heat transfer mechanism gets greater potency to take the heat away from the system which is

evident from the continuing lower temperature levels at higher velocities. However, with higher velocities an interesting trend is observed, that is, the temperature level in the innermost coils gets lowered compared to that in the outer coils. The reason behind this tendency may be explained by the phenomenon of heat transfer in curved flow paths.

Flow in curved pipes is greatly influenced by the centrifugal force that is generated due to change in flow direction. Curvature in pipes gives rise to a centrifugal force in the curved portion of flow field. This centrifugal force distorts the streamline flow and introduces a secondary flow in the curved section. This curvature induced secondary flow increase the convection heat transfer rate at the cost of pressure drop. In case of laminar flow, the heat transfer rate increase more significantly while the pressure drops moderately. Seyyedvalilu and Ranjbar (2015) also reported that heat transfer coefficient is augmented considerably by increase of coil curvature ratio. Authors asserted that as coil curvature is increased the torsional behavior of the flowing fluid becomes significant over linear behavior and this tends to induce more centrifugal force giving rise to secondary flow. This secondary flow facilitates more heat transfer in the curved flow paths and as a result at the same velocity temperatures in the more curved inner coils drops more rapidly than those in the less curved outer coils.

Salem et al (2015) also observed that Nusselt number (i.e., convection heat transfer) increases with increasing Reynolds number (i.e., flow velocity) and increasing centrifugal force with higher coil curvature ratio. Authors pointed out the same effect of centrifugal force behind this enhancement. This is evident from Figures 5.12 (e) and (f) where the convective heat transfer rate is seen to be accelerated further as the water inlet velocity enters in the range of one hundredth meter per second.

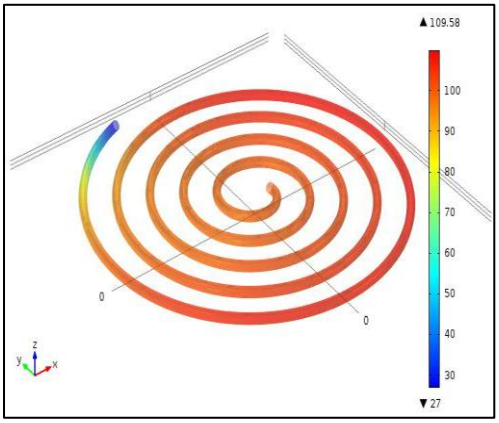

(a) U_o = 0.0009 m/s

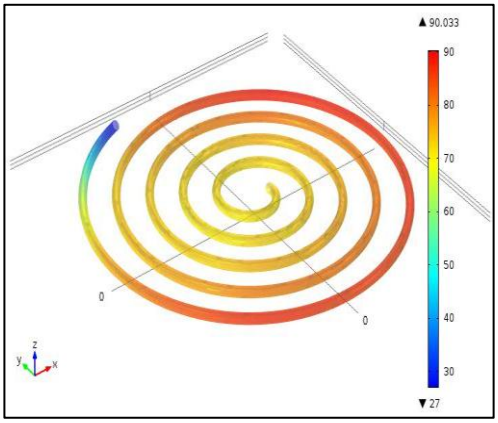

(b) U_o = 0.002 m/s

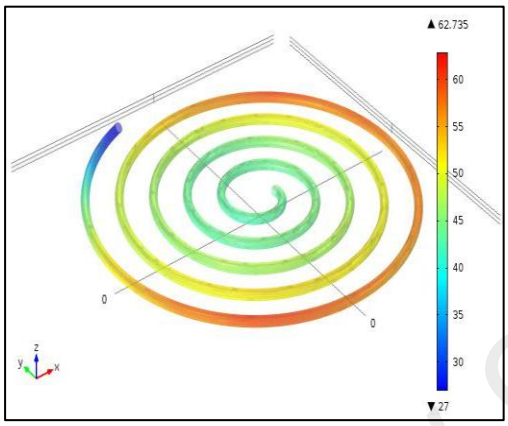

(c) U_o = 0.005 m/s

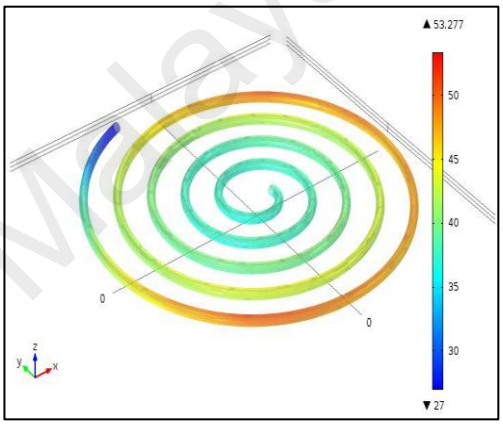

(d) U_o = 0.009 m/s

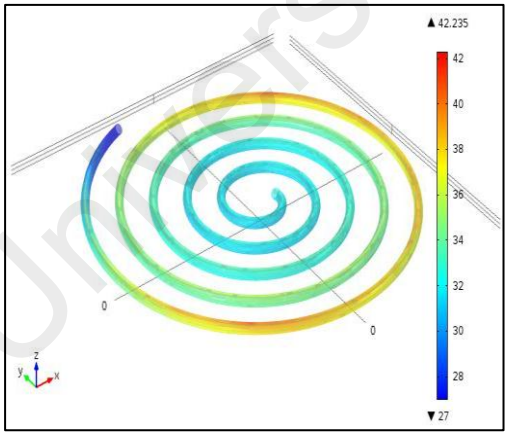

(e) U_o = 0.02 m/s

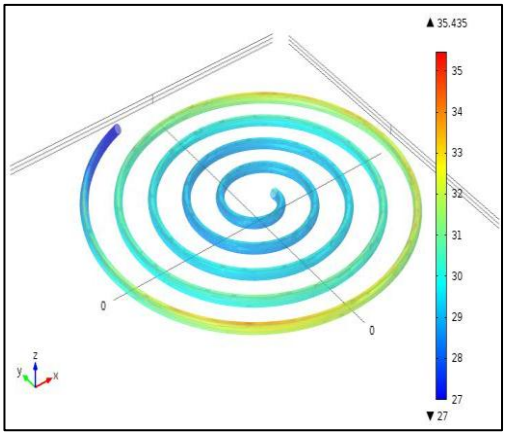

(f) U_o = 0.05 m/s

Figure 5.12: Effect of inlet velocity on temperature distribution throughout the pancake flow channel

In addition, it is very much revealing from Figure 5.12 (f) that at the highest inlet velocity, water outlet temperature approach very near to that of the ambient. A hybrid PV/T scheme requires a compromise between electricity and thermal yield. Water temperatures between 40 to 50^{o}C may be considered adequate and favorable for household and other applications. For pancake shaped channel, it has been found that such temperatures are obtained with an inlet velocity of 0.005 m/s.

Design 3 (Parallel square pipe flow channel)

The temperature distribution along parallel square pipe flow channel follows the same trend as observed for the pancake flow channel. Similar to the case of pancake flow channel, Figures 5.13 (a) to (f) show that channel temperature reduces progressively with increasing inlet velocity. At the lowest velocity of 0.0009 m/s (refer to Figure 5.13 (a)), the overall temperature of the channel material becomes the maximum. There is very little temperature difference among all the pipe branches along with the outlet header. This signifies that heat transfer is not that strong at very low velocity of water. At relatively higher velocities, the outermost branch pipe near the inlet is seen to have higher temperature compared to the next other branches. The reason behind this trend may be attributed to the energy losses that occur inside the pipe due to friction and change in fluid direction. The friction loss (also known as major loss) includes viscous friction as well as wall friction which increase linearly with length of the flow path. In addition, a substantial amount of energy is consumed when fluids experience a sharp change in direction which is known as minor loss.

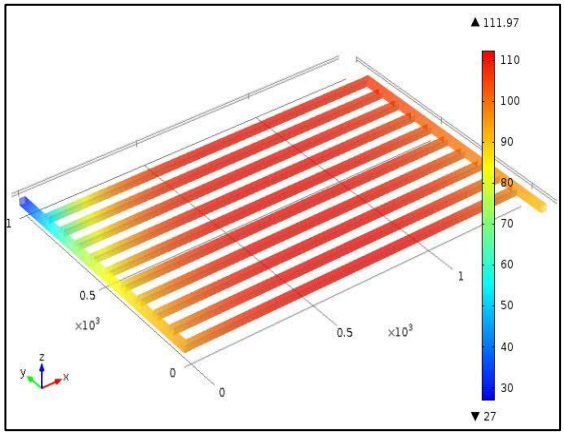

(a) U_o = 0.0009 m/s

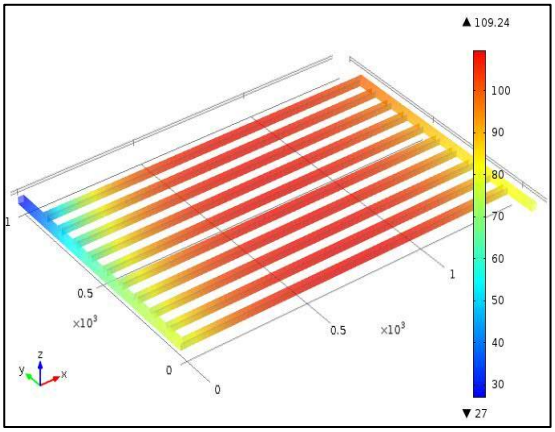

(b) U_o = 0.002 m/s

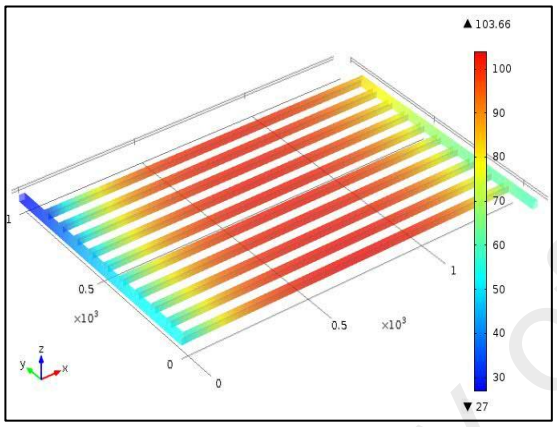

(c) U_o = 0.005 m/s

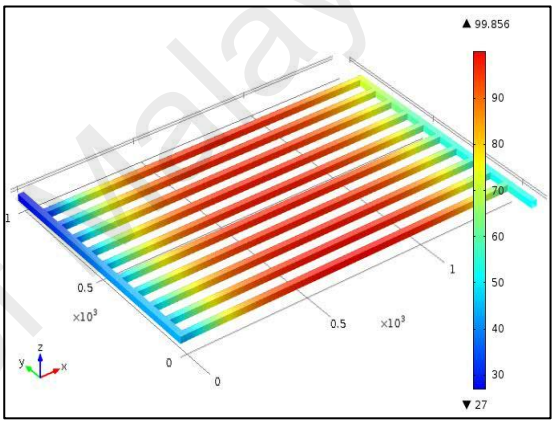

(d) U_o = 0.009 m/s

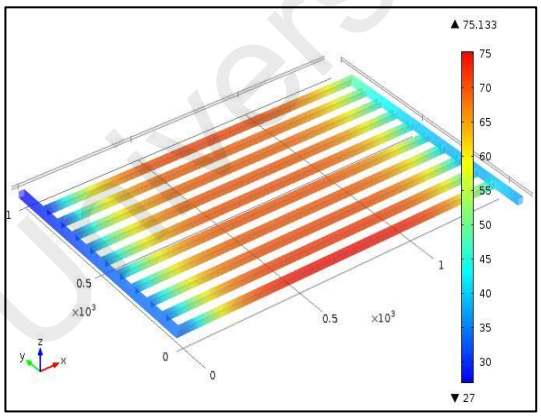

(e) U_o = 0.02 m/s

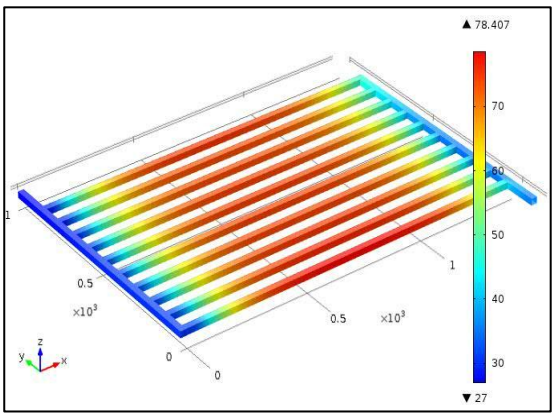

(f) U_o = 0.05 m/s

Figure 5.13: Effect of inlet velocity on temperature distribution throughout the parallel square pipe flow channel

Design 4 (Serpentine flow channel)

Unlike parallel pipe flow channel, the flow through the serpentine flow channel is not divided into several branches. So, temperature distribution throughout the serpentine flow channel is almost uniform from inlet to outlet of the channel. It may be observed from Figure 5.14 that the water temperature at both entry and exit loops of the channel is slightly higher than that at intermediate loops. Because of incessant heat transfer from the PV module backside the interior of the channel becomes hotter than the incoming cold water and the temperature difference is the highest at the entry loop. Likewise, the temperature difference between the interior of the last loop and circumambient is also high. On the other hand, after the first loop temperature difference between every two successive loops is lessened progressively. This high temperature differences at the entry (first) and exit (last) loop with surroundings facilitate to accumulate more heat than in the intermediate loops.

Figure 5.14 shows the temperature distribution throughout serpentine flow channel for various inlet velocities. Although the trend of temperature reduction with increasing velocity is the same as pancake and parallel square pipe channels, the rate of diminution in temperature is less with this configuration. The lowest temperature, that is achieved with the highest velocity, is greater than those attained with the other two flow channels. This is due to the longest traveling span for water in this channel design. As water travels through the extended path it gets time enough to accumulate more heat and then take it away. So, serpentine flow channel is better among the other channel design for cooling the PV/T module effectively which is illustrated in Figure 5.17.

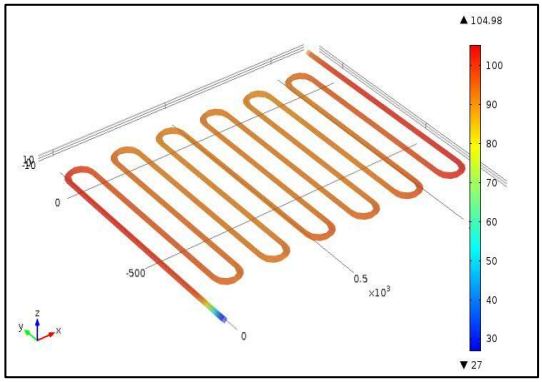

(a) U_o = 0.0009 m/s

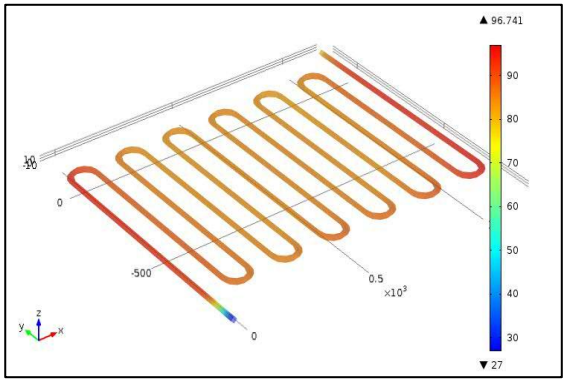

(b) U_o = 0.002 m/s

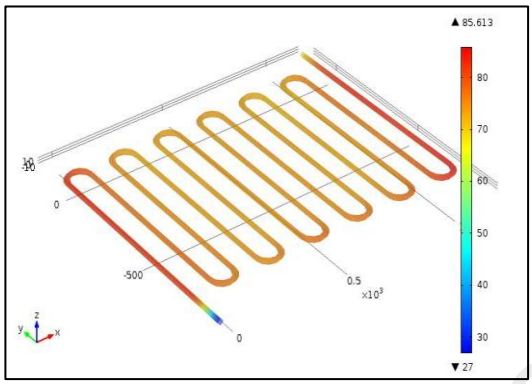

(c) U_o = 0.005 m/s

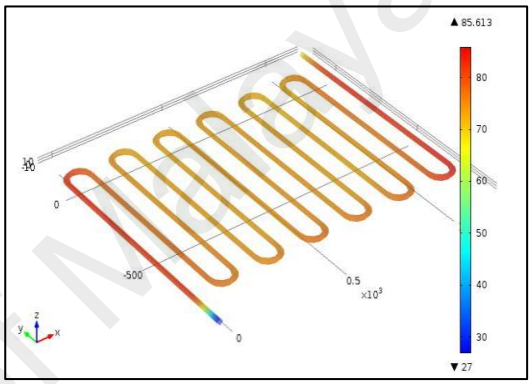

(d) U_o = 0.009 m/s

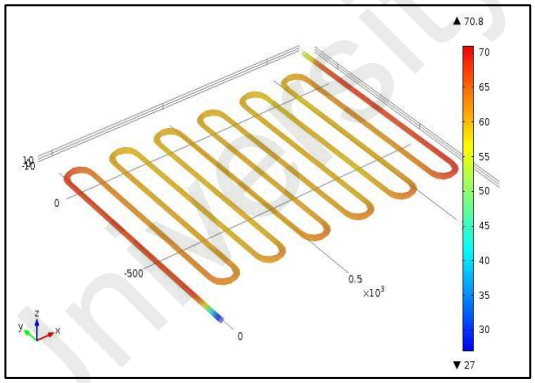

(e) U_o = 0.02 m/s

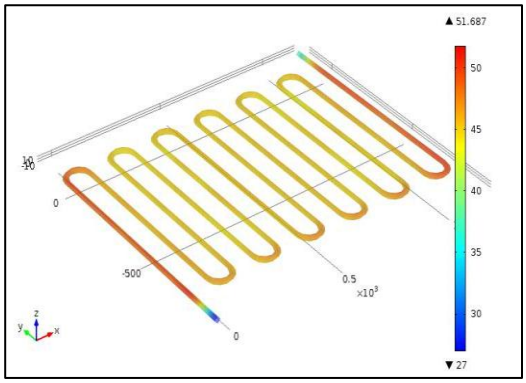

(f) U_o = 0.05 m/s

Figure 5.14: Effect of inlet velocity on temperature distribution throughout the sepentine flow channel

5.5.2 Effect of Inlet Velocity on Temperature Distribution Throughout the PV/T Module

The effect of water inlet velocity on the temperature distribution throughout the entire PV/T module including the flow channel for all three designs have been depicted in the 3D surface plots in Figures 5.15 to 5.17. The environmental conditions considered are: absorbed radiation 1000 W/m^2 and ambient temperature 27^oC. The operating parameters are: water inlet velocity from 0.0009 m/s to 0.05 m/s and water inlet temperature 27^oC. Representative numerical results for aluminum channel have only been presented in this section as the trend is similar for copper channel with slight differences in the magnitude of temperatures.

Design 2 (Pancake flow channel)

It is clearly evident from Figure 5.15 that temperature of the PV/T module, especially the portion directly in contact of the cooling channel, is gradually lowered with increasing water inlet velocity and it falls in the range of 40^oC at the highest velocity of 0.05 m/s. The temperature of the PV/T module is different from one part to another part because of non-uniform cooling within the system. Temperature of the central region of the PV/T module drops due to direct contact with cooling channel and the corner regions remains hotter (as can be noticed from the Figures 5.15 (a) to (f)) for being far from direct contact with the channel. As a result, the temperatures at corner portions of PV/T module are always higher than the central portion.

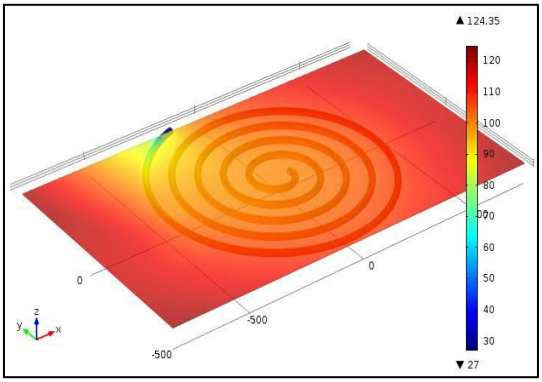

(a) U_o = 0.0009 m/s

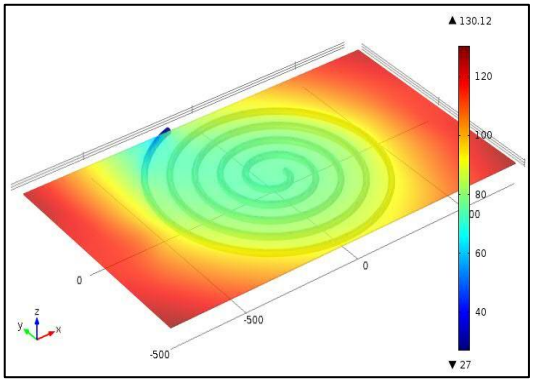

(b) U_o = 0.002 m/s

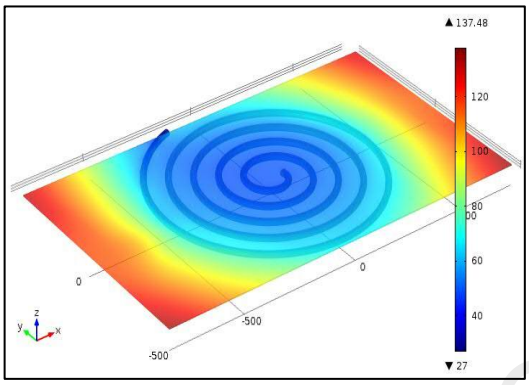

(c) U_o = 0.005 m/s

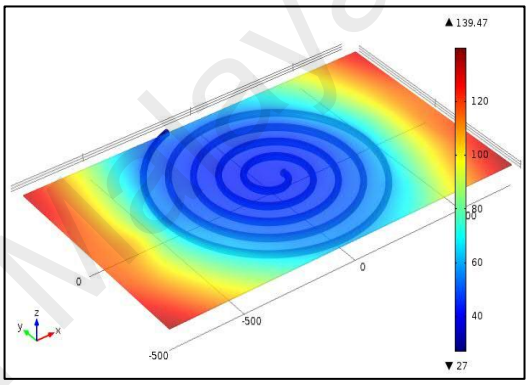

(d) U_o = 0.009 m/s

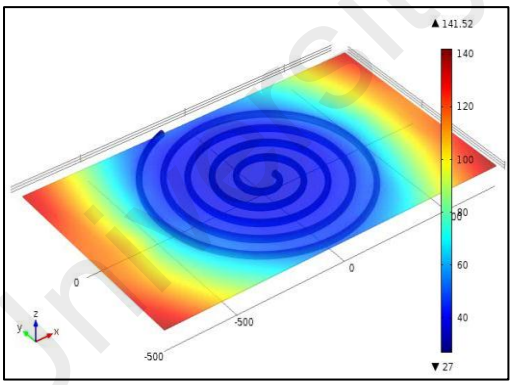

(e) U_o = 0.02 m/s

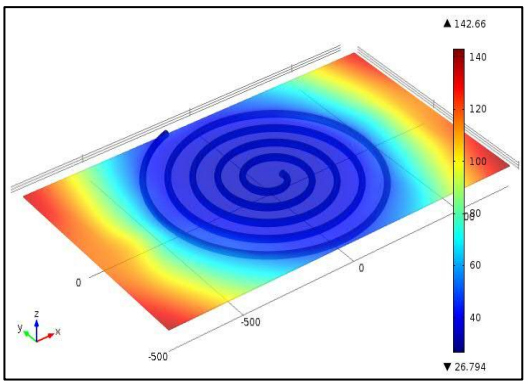

(f) U_o = 0.05 m/s

Figure 5.15: Effect of inlet velocity on temperature distribution throughout panel

Design 3 (Parallel square pipe flow channel)

The temperature distribution throughout entire PV/T module with parallel pipe flow channel is shown in Figure 5.16. Within the given velocity range, temperature of the panel material is observed to reduce steadily. The contact area between the square

channel and PV module back surface is the maximum among all other channel designs. So, this design enables more heat accumulation than parallel circular pipe flow channel in which there is only line contact with the PV module.

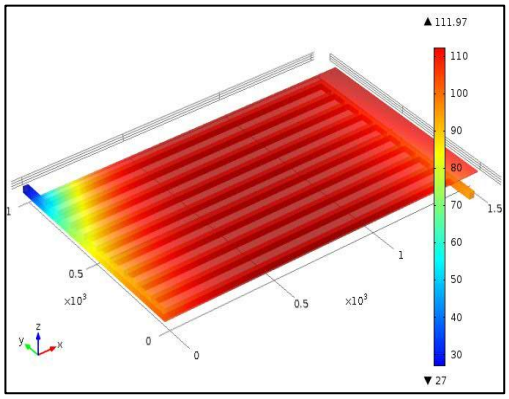

(a) U_o = 0.0009 m/s

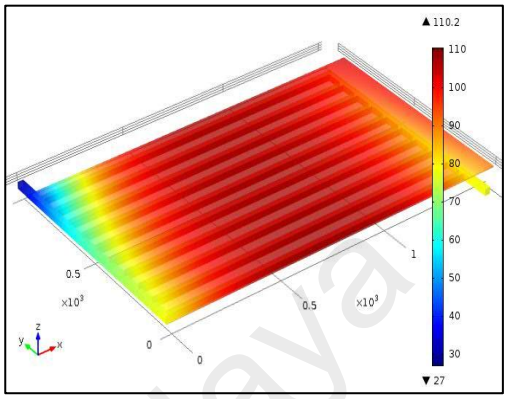

(b) U_o = 0.002 m/s

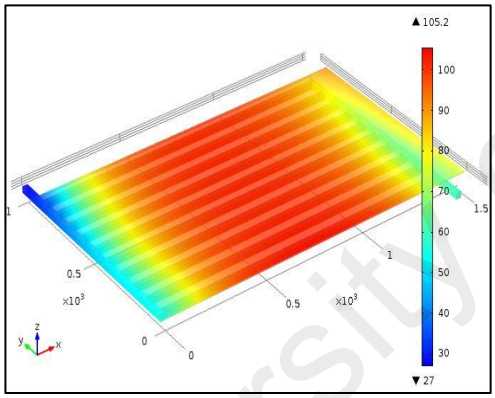

(c) U_o = 0.005 m/s

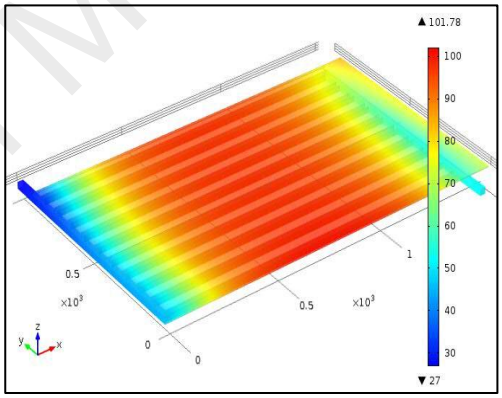

(d) U_o = 0.009 m/s

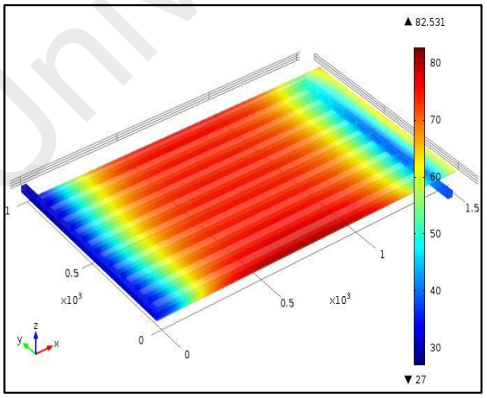

(e) U_o = 0.02 m/s

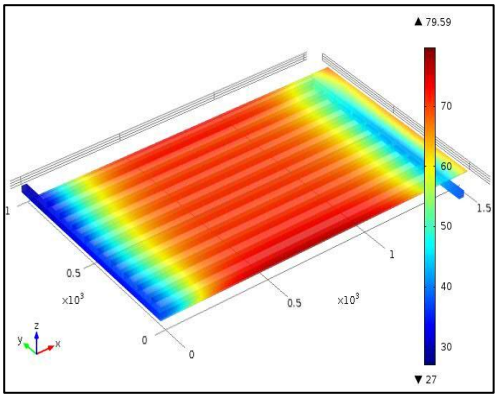

(f) U_o = 0.05 m/s

Figure 5.16: Effect of inlet velocity on temperature distribution throughout panel

Design 4 (Serpentine flow channel)

The temperature distribution all over the PV/T module with serpentine flow channel has been depicted in Figures 5.17 (a) to (f). From the 3D surface plots, it is noticeable that module temperature falls gradually with increasing water inlet velocity module. Results show that the highest reduction in PV/T module temperature is achieved with serpentine flow channel. This may be attributed to the greater coverage span of this design which facilitates to shave more heat. A notable point here is that such temperature profiles as presented in the Figures 5.17 (a) to (f) cannot be determined by simple one dimensional models as presented previous literatures (Tiwari & Sodha, 2006a; Sarhaddi et al., 2010). Furthermore, the 3D models so far developed are also unable to portray the total simulated depiction of the PVT collector. Because most of the models do not include all the layers of the PV module nor they incorporate the details of flow in the channel in the simulation study.

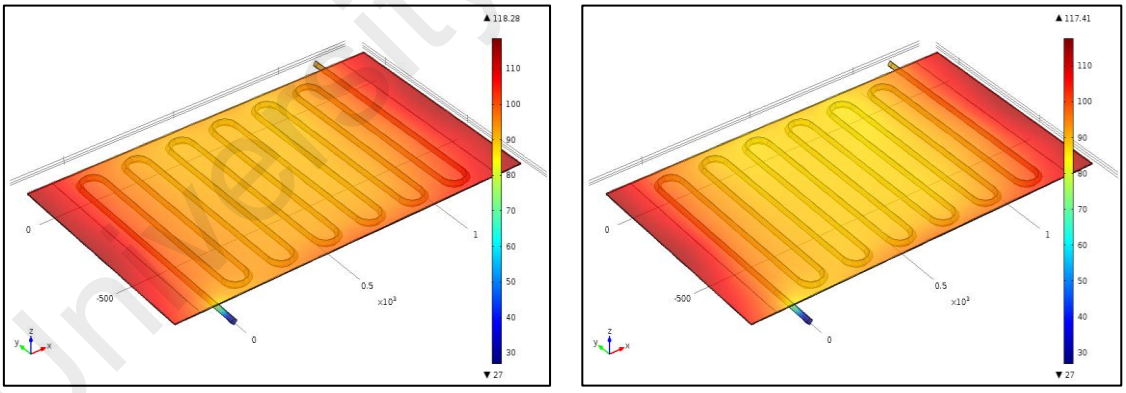

(a) U_o = 0.0009 m/s (b) U_o = 0.002 m/s

Figure 5.17: Effect of inlet velocity on temperature distribution throughout panel

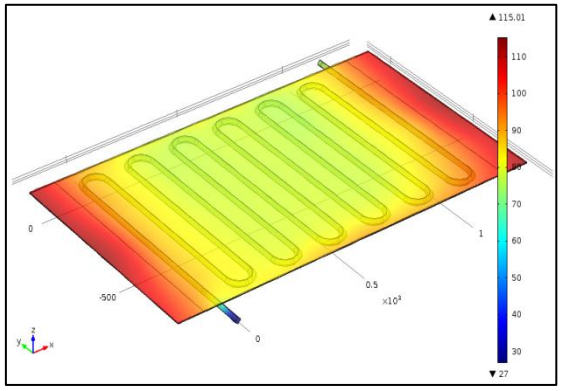

(c) U_o = 0.005 m/s

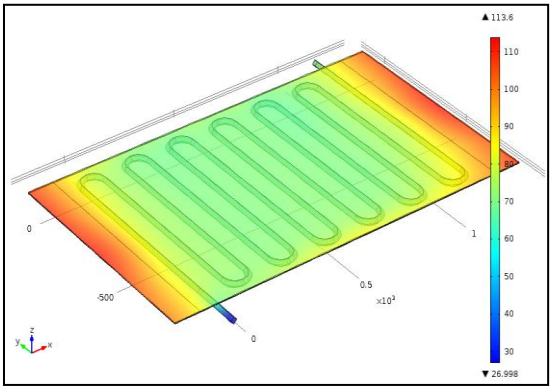

(d) U_o = 0.009 m/s

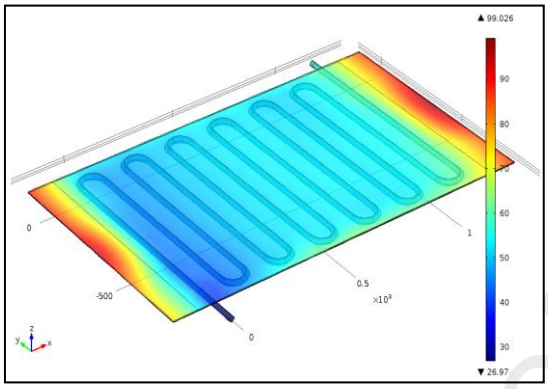

(e) U_o = 0.05 m/s

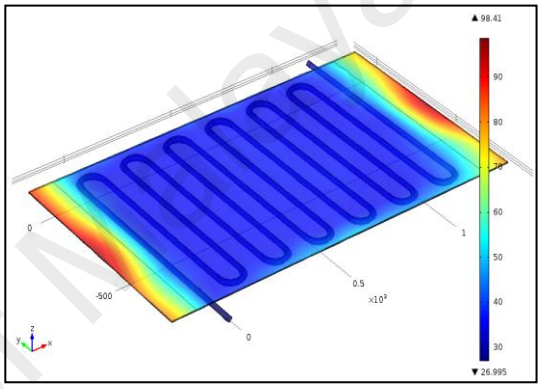

(f) U_o = 0.05 m/s

Figure 5.17, continued

5.5.3 Effect of Inlet Velocity

The effect of inlet water velocity on the performance of PV/T module has been investigated and the range of inlet velocities is taken from 0.0009 to 0.05 m/s, where the water inlet and ambient temperatures are kept constant at 27^{o}C with irradiation level constant at1000 W/m^2.

5.5.3.1 On cell temperature and water outlet temperature

Increasing water inlet velocity has got an assuaging effect on the solar cell and water outlet temperatures for both aluminum and copper channels as shown in Figure 5.18 (a) and (b). From Figure 5.18 (a), it is evident that PV cell temperature drops off gradually

with the increase in inlet velocity for all the flow channel designs. As the velocity increases, more volume of water pass through the channel allowing more heat to be removed from the module, resulting in a reduction in cell temperature. Results show that for aluminum and copper channels, a reduction in cell temperature of around 42^{o}C for the design D2 has been achieved as the inlet water velocity is increased from 0.0009 to 0.05 m/s. On the other hand, cell temperature is reduced by about 48^{o}C for the design D3 and by about 55^{o}C for design D4 in case of both aluminum and copper channels. At the highest velocity, the cell temperature reached its lowest value for the designs D4.

The heat removal capacity of water depends on its volume as well as the velocity at which it is taking away the heat. At higher water velocities, although the volume of water is more but it gets less time span to accumulate heat and take it away from the source, i.e., the PV module. The resultant effect lessens the rate of decrement of cell temperature at higher velocities, which is evident from Figure 5.18 (a). Another implication that is very much explicit from Figure 5.18 (a) is that channel material has very little impact on cell temperature as the values for aluminum and copper channel are almost the same for the entire range of inlet velocity for all the channel designs.

The outlet temperature of water drops with increase in inlet velocity. It can be observed from Figure 5.18 (b) that at very low velocities the outlet temperature level is very high especially for the design D2 with both Al and Cu. This is due to the fact that at very low velocities, the rate of heat removal through the channel is much less than the rates of heat gain from PV module, hence there occurs an augmentation of temperature at the outlet. As a result, the outlet temperature at very low velocities rise abruptly compared to that at higher inlet velocities. With the onset of a considerable level of inlet velocity, the outlet temperature falls steeply as the increased volume of water takes heat away at a greater rate. This tendency becomes relatively mild at higher velocities

because the heat removal rate grows so fast that the volume of water gets very less time to accumulate thermal energy. It can also be observed from the same figure that warm water of about 42.5°C (with design D2 at the inlet velocity of 0.005 m/s) to 52°C (with design D3 at the inlet velocity of 0.009 m/s) are obtained, which is suitable for household and other applications.

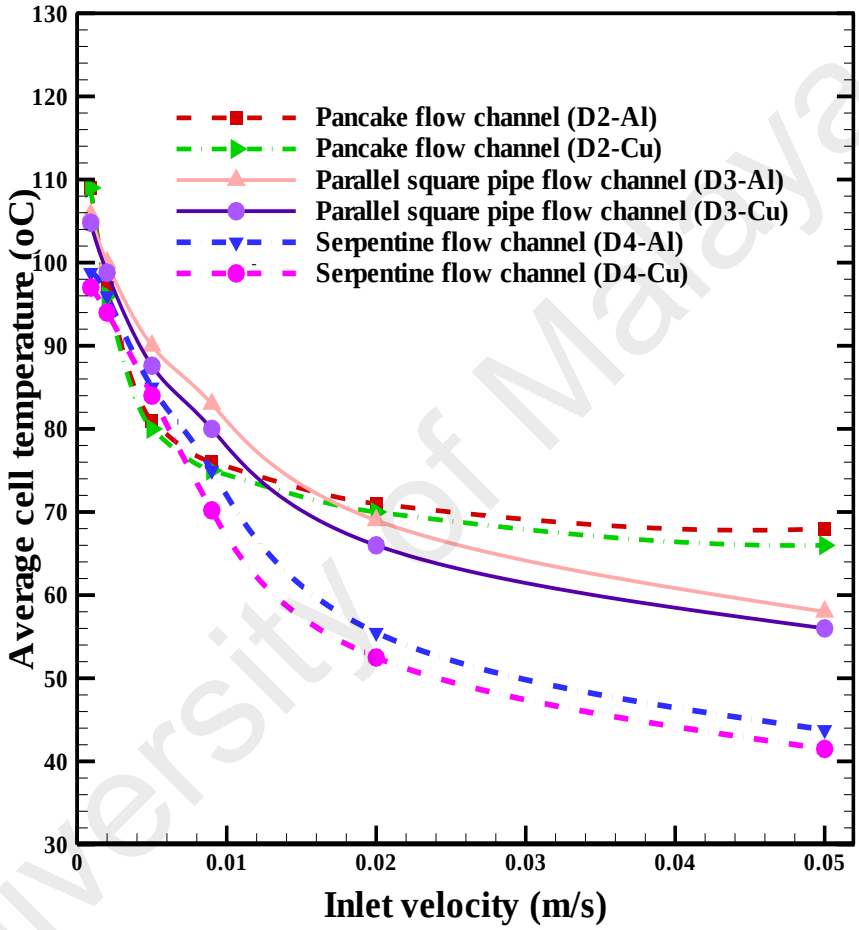

(a)

Figure 5.18: Effect of inlet velocity on (a) cell temperature and (b) water outlet temperature of the PV/T module for all designs with Al and Cu flow channels

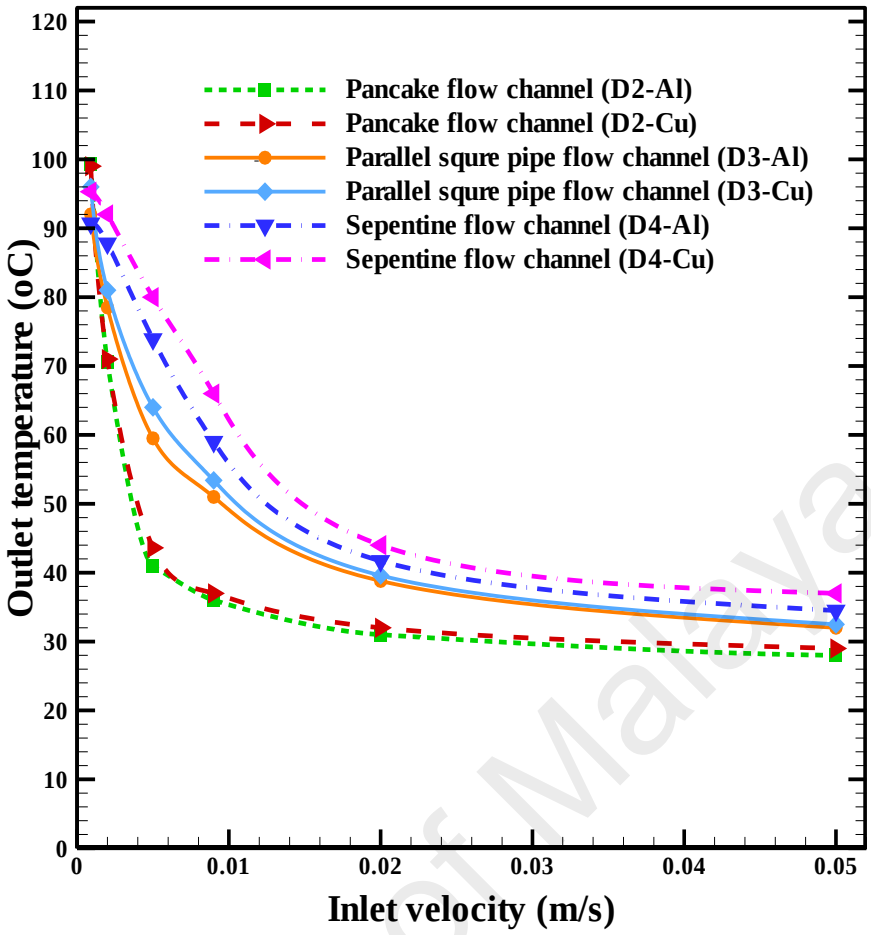

(b)

Figure 5.18, continued

5.5.3.2 On PV/T performance

The trend of output power, electrical efficiency and overall efficiency as a function of water inlet velocity has been illustrated in Figures 5.19 (a) to 5.19 (c). Figure 5.19 (a) and 5.19 (b) demonstrates that electrical efficiency and output power follows almost the same trend for all designs.

The output power enhances with increased water inlet velocity as shown in Figure 5.19 (a). Results demonstrate that a maximum electrical yield of about 125 W for aluminum and 126 W for copper channels is obtained with a water inlet velocity of 0.05 m/s for the serpentine pipe design (D4). Figure 5.19 (b) shows that electrical efficiency

with copper channel is a bit greater than that with aluminum channel which is more evident at higher velocities.

Figure 5.19 (b) shows that the electrical efficiency of serpentine flow channel design (D4) is the highest compare the other pancake flow channel (D3). This is due to the fact that with reduction in temperature the band gaps in the cells increase, thereby producing more electricity flow in the circuit which enhances its electrical conversion efficiency. It may also be noticed from the same figure that the efficiency augmentation rate becomes flat with higher inlet velocities. The maximum electrical efficiency of 12.3% with copper and 12% with aluminum is observed at the highest inlet velocity of 0.05 m/s of the serpentine flow channel design (D4).

For all the flow channel designs, it may also be remarked from as the thermal energy is also an output in case of hybrid PV/T applications; a compromise has to be made between the electrical power output and the water outlet temperature. In order to get warm water supply, the inlet velocity should be maintained somewhat lower than the velocity that yields the maximum electrical power. Thermal and overall efficiency, as can be observed from Figures 5.19(c) and (d), rise very steeply at lower velocities, and the rate of increment tends to become monotonous. The maximum thermal (63.5%) and overall (75%) efficiencies are achieved with serpentine (copper) flow channel (D4) among all three designs of D2, D3 and D4. However, the minimum thermal (26%) and overall (36%) efficiencies has been obtained from aluminum channel of pancake configuration (D2).

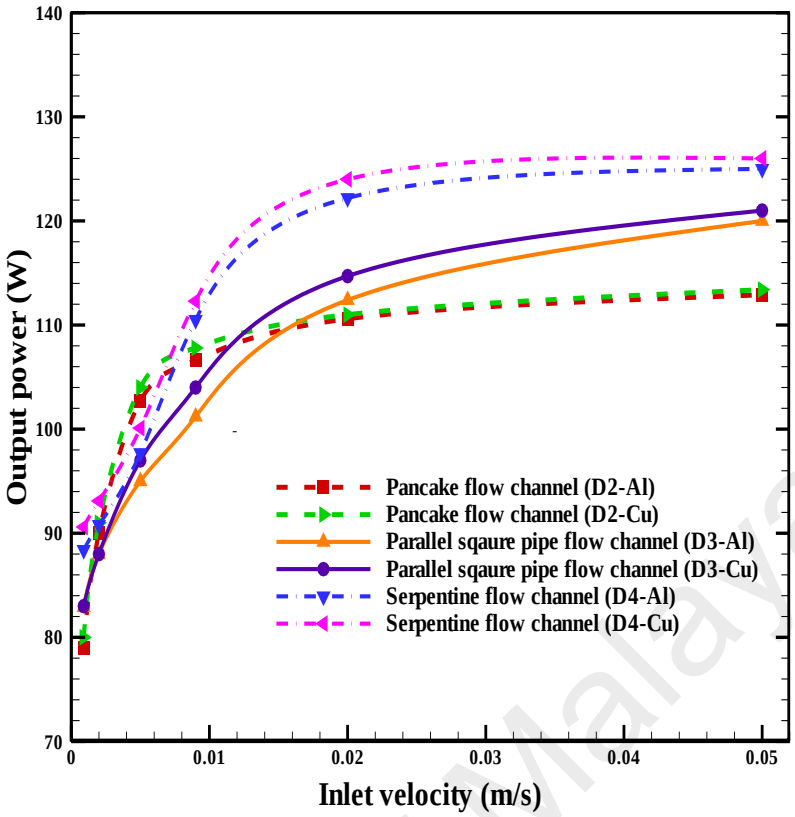

(a)

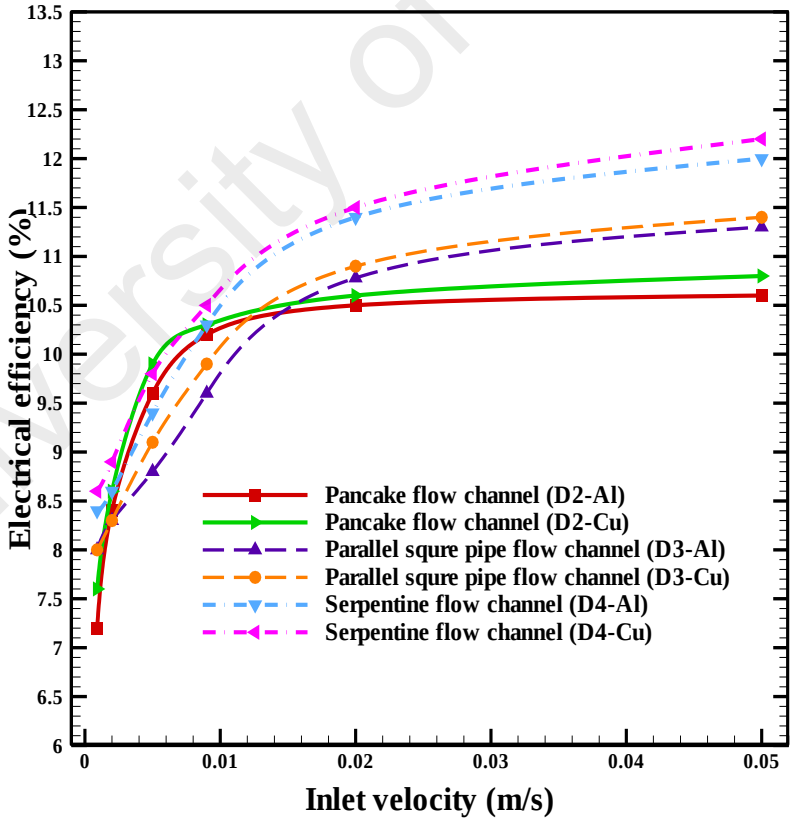

(b)

Figure 5.19: Effect of inlet velocity on the performance of PV panel for all designs with both Al and Cu flow channels

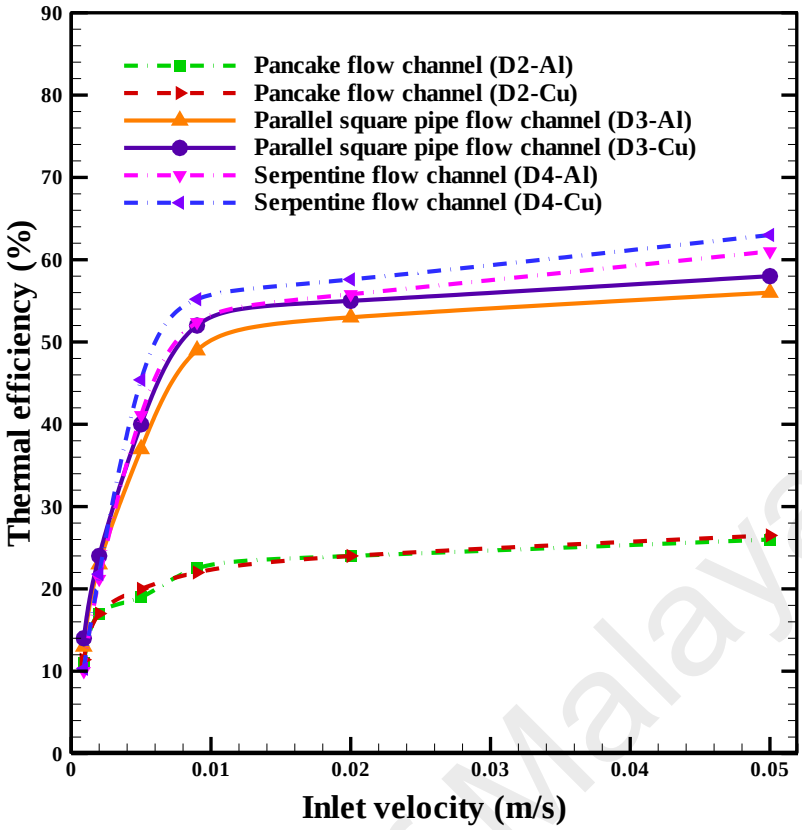

(c)

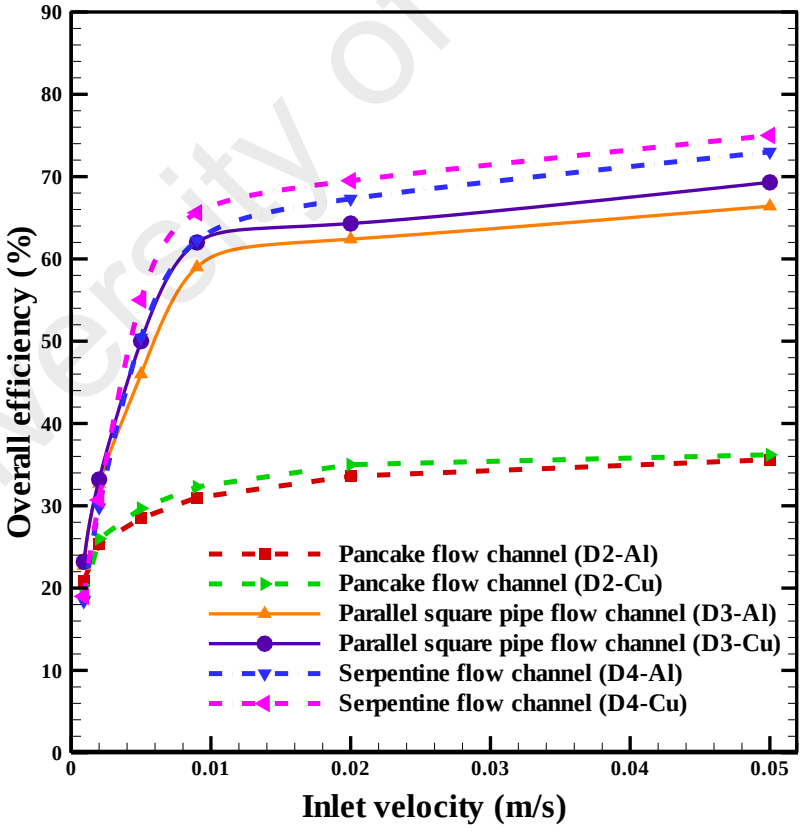

(d)

Figure 5.19, continued

5.5.4 Effect of Inlet Temperature on Overall Performance of PV/T Module

The PV/T performance at varying inlet temperatures has been presented in Figures 5.20 (a) to 5.20 (c). The range for inlet water temperature variation was taken 20 to 40^{o}C with the constant inlet velocity 0.005m/s and ambient temperature 27^{o}C at an irradiance level of 1000 W/m^{2}. As the water inlet temperature increases the electrical efficiency for the designs D2 (around 0.4% for both copper and aluminum channel), D3 and D4 (around 0.5% for both copper and aluminum channel) drops very slightly,

The thermal and overall efficiencies decrease for both aluminum and copper channels with increasing inlet temperature for all the designs with a D4 experiencing a substantial decline. Figure 5.20 (b) shows that the decrease in thermal efficiency of the PV/T module with channel designs D2 (by 13% for aluminum and 12.2% for copper channel) and D4 (by 16.8% for aluminum and 17% for copper channel) is less than that with the design D3 (by 22% for both aluminum and copper channel).

The overall efficiency of a PV/T collector is derived from the electrical and thermal performance of the system. Figure 5.20 (c) shows that decrease in overall efficiency of the PV/T module with channel designs D2 (by 12.8% for aluminum and 12.3% for copper channel) and D4 (by 19.2% for aluminum and 19% for copper channel) is less than that with the design D3 (by 22% for aluminum and 20.9% for copper channel).

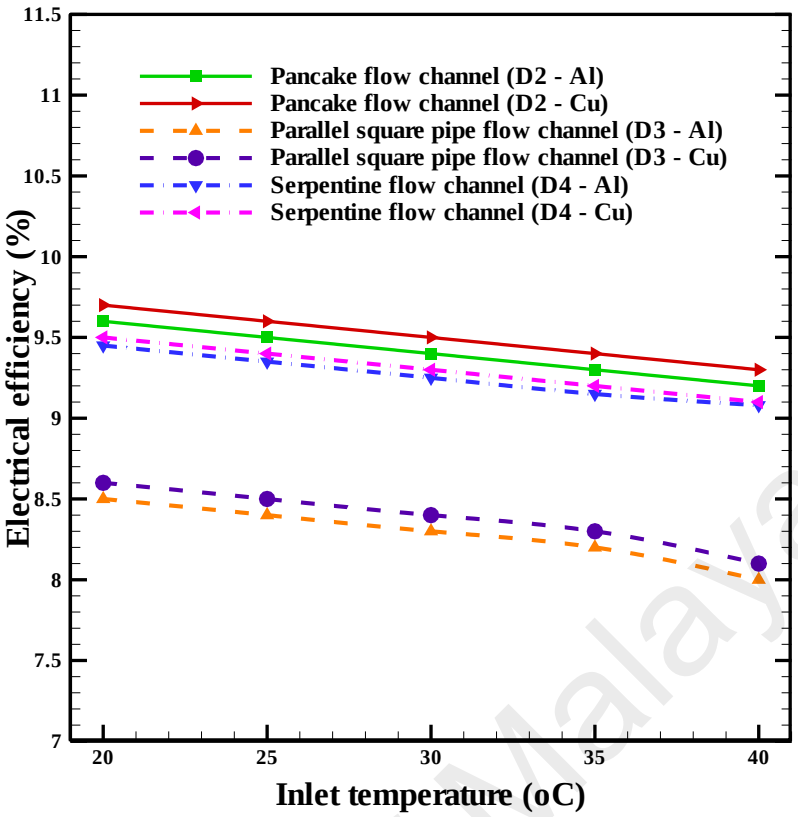

(a)

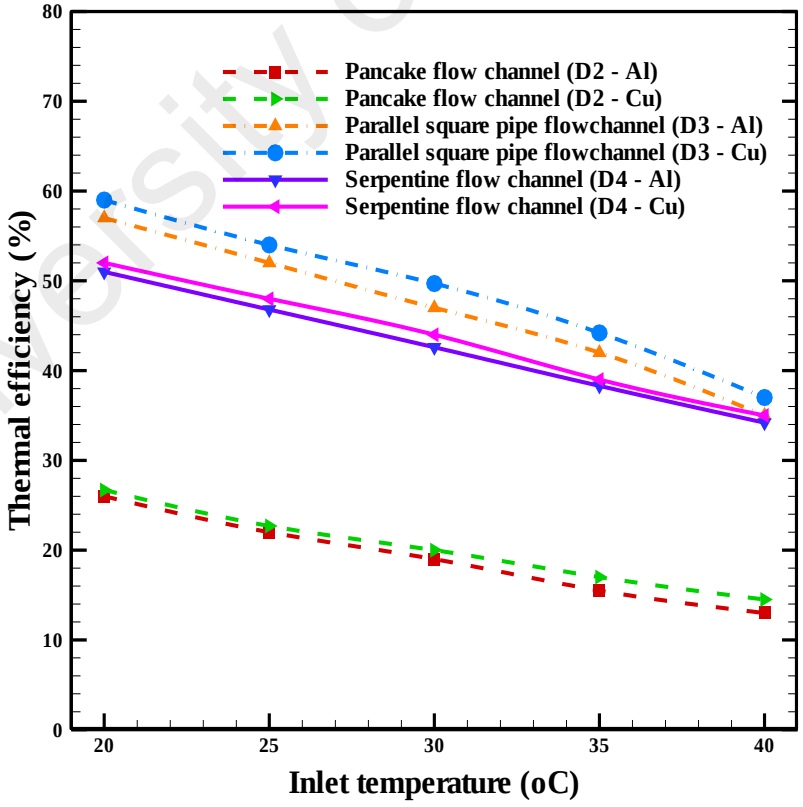

(b)

Figure 5.20: Effect of inlet temperature on PV/T performance for both Al and Cu flow channels

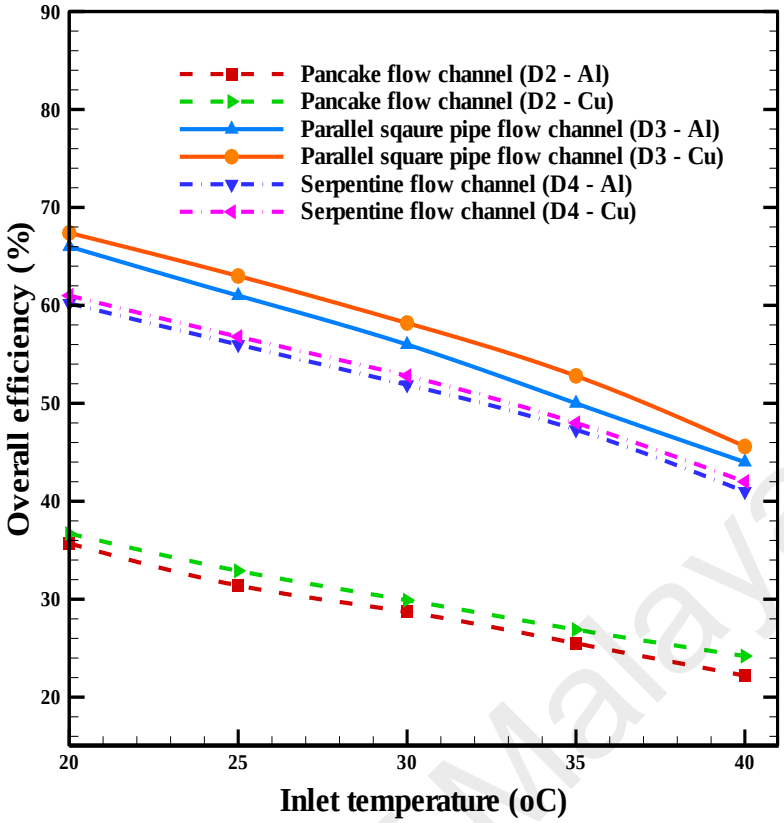

(c)

Figure 5.20, continued

5.5.5 Effect of Cell Temperature on Electrical Performance of PV Module

The impact of cell temperature on the electrical yield and its associated efficiency has been presented in Figures 5.21 (a) and 5.21(b) as water inlet velocity was varied from 0.0009 – 0.05 m/s. Figures show that both output power and electrical efficiency decrease with increasing cell temperature.

As the PV module temperature decreases, its output current decreases exponentially while the voltage increases linearly. As a result power output and the efficiency decrease almost linearly. Figure 5.21 (a) and 5.21 (b) shows an almost linear relation between the electrical performance and cell temperature, which totally complies with previous studies (Teo et al., 2012; Dubey et al, 2013).

By increasing the inlet velocity, the cell temperature decreases, thereby improving the electrical performance. Table 5.3 presents the summary of increment rate in output power and electrical efficiency per 1°C decrease in PV cell temperature at the irradiation level of 1000 W/m^2. It may be noticed from the table that the highest increment rate in both of electrical efficiency (0.08%) and output power (0.80 W) is achieved with aluminum channel of pancake configuration (D2).

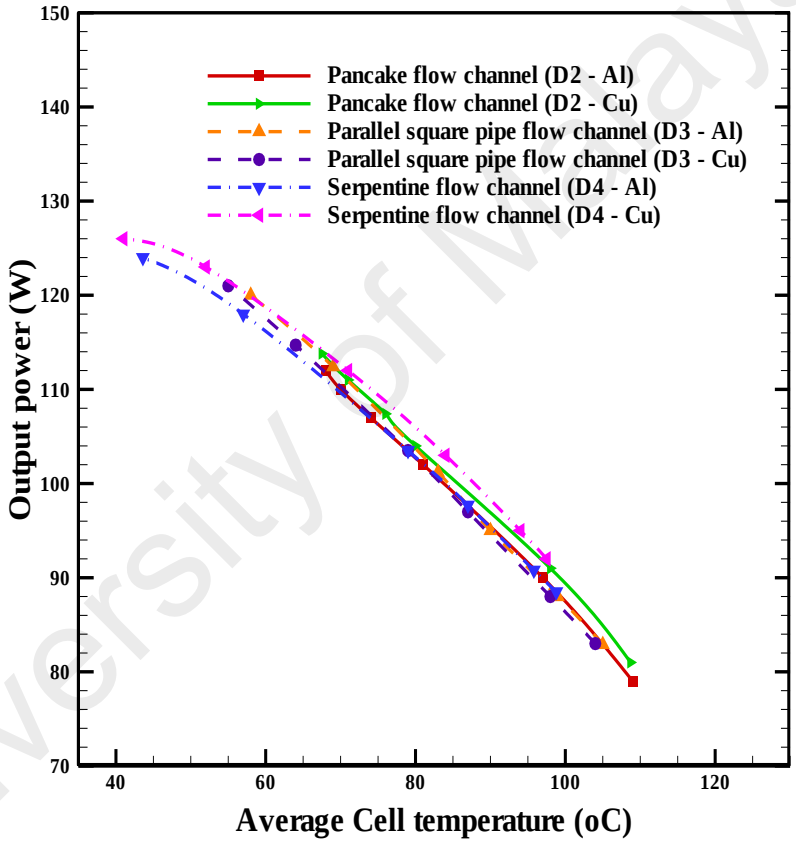

(a)

Figure 5.21: Effect of cell temperature (a) output power (b) electrical efficiency for both Al and Cu flow channels under cooling system

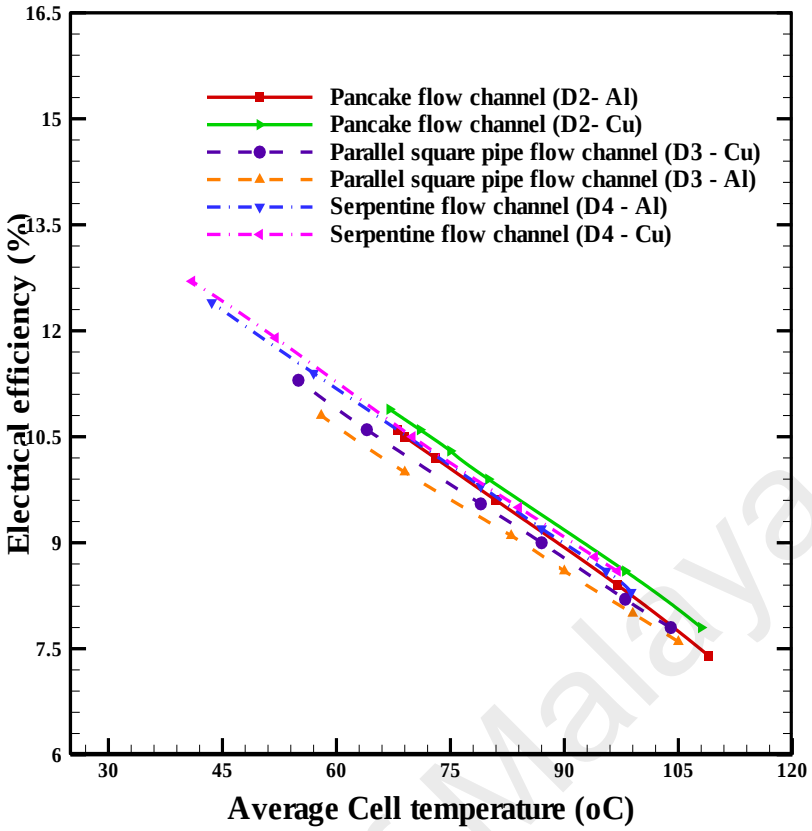

(b)

Figure 5.21: continued

Table 5.3: Increase in electrical efficiency and output power per 1°C increase of cell temperature

Performance Parameters	Design 2		Design 3		Design 4	
	Al	Cu	Al	Cu	Al	Cu
Electrical efficiency increment (%)	0.08	0.07	0.07	0.06	0.074	0.073
Output power increment (W)	0.80	0.79	0.79	0.78	0.64	0.61

5.5.6 Effect of Ambient Temperature on the Performance of PV/T

Due to rapidly changing weather, solar PV modules do not operate under normal operating conditions. The module works best in certain weather conditions. So the performance of a PV system depends on its basic characteristics and environmental issue. The ambient temperature is one such type of environmental issue that influences PV conversion process. The effects of ambient temperature on the performance of PV/T

system is shown in Figures 5.22 (a) to 5.22 (d). To investigate the effect of cooling on PV panel performance with various ambient temperatures (20^{o}C to 40^{o}C) are taken with the inlet temperature at 27^{o}C at irradiation level 1000 w/m^{2} at the inlet velocity 0.005m/s.

From Figure 5.22 (a)), it is observed that cell temperature increases with the increase of ambient temperature for all the flow channel designs; for D2 by 20.8^{o}C , for D3 by 22^{o}C and for D4 by 26.3^{o}C (both of aluminum and copper). Outlet temperatures also increase with increasing ambient temperature as shown in Figure 5.22 (b); for D2 by 21^{o}C for both of aluminum and copper; for D3 by about 22.8^{o}C for aluminum and copper; for D4 by 28.4^{o}C for aluminum and by 29.2^{o}C for copper.

A decrease in both the output power and electrical efficiency with the increase of ambient temperature is observed from Figure 5.22 (c) and (d). In case of design D2, Figure 5.22 (c) shows a decrease in output power by around 15 W for both aluminum and copper channel; while for D3 the drop is about 15.8 W for both aluminum and copper and for D4 around 22 W for aluminum and 21.3 W for copper. On the other hand, from Figure 5.22 (d), it is found that the drop in electrical efficiency for D2 is about 1.4% for both aluminum and copper; for D3 1.6% for aluminum and copper; for D4 around 2% for aluminum and copper channel. Cell temperature increases with increasing ambient and as a result electrical as well as overall performance falls substantially.

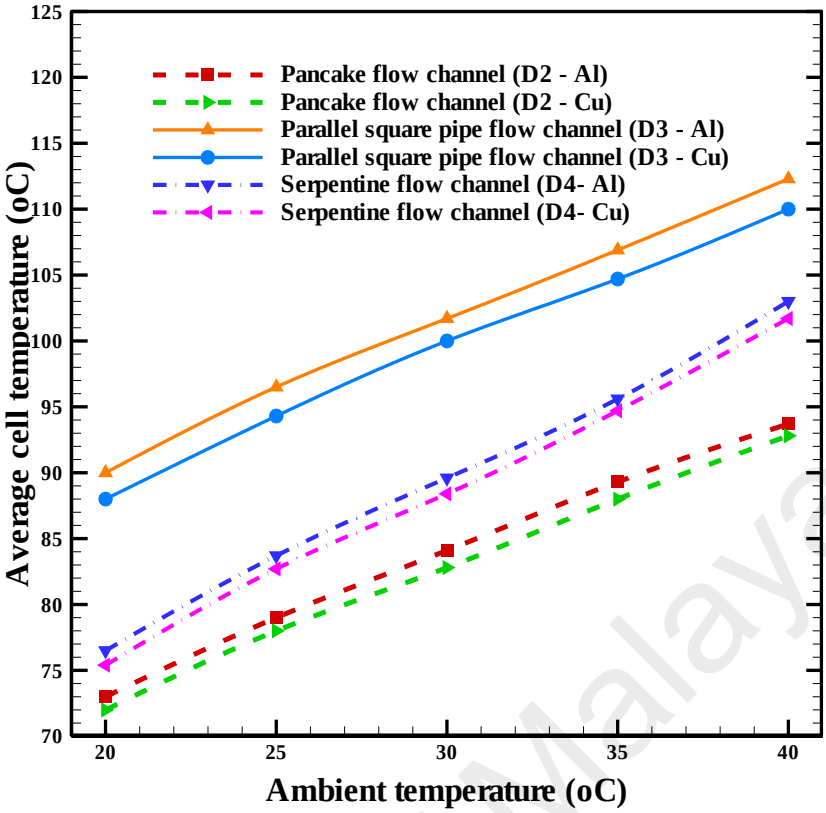

(a)

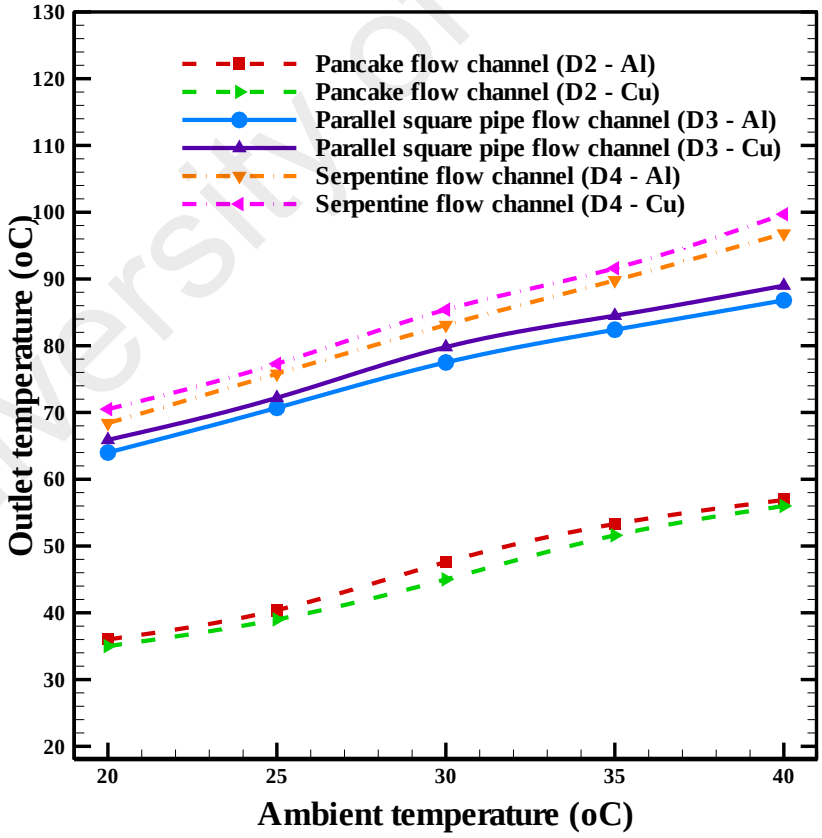

(b)

Figure 5.22: Effect of ambient temperature on the performance of PV/T panel for both Al and Cu flow channels

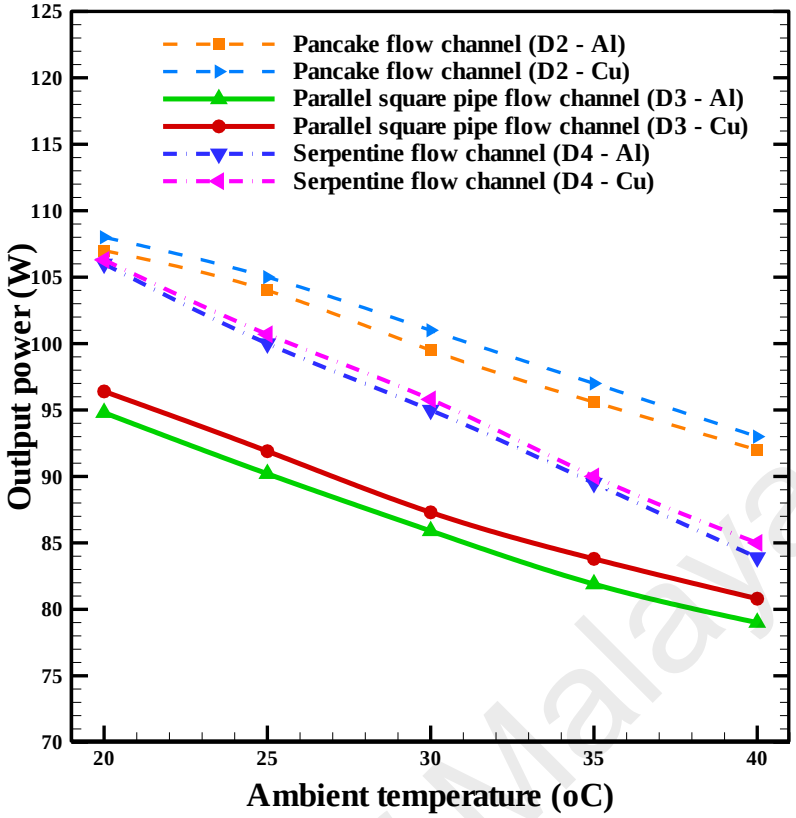

(c)

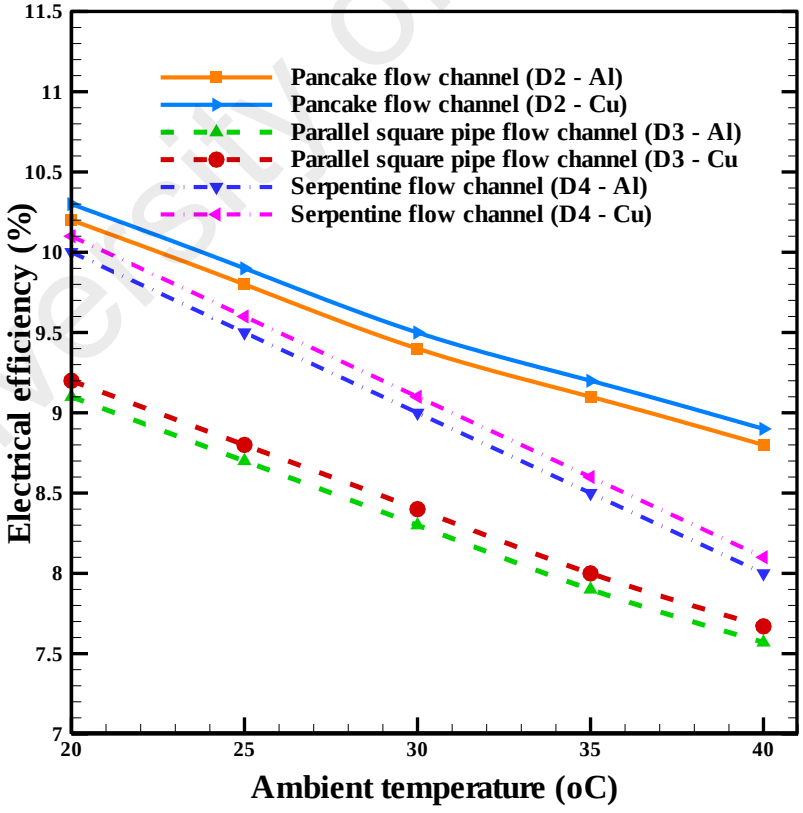

(d)

Figure 5.22, continued

5.5.7 Effect of Absorbed Solar Radiation on the Performance of PV/T

Another most effective environmental parameter that controls the performance of PV module is solar irradiation. The range considered for different parameters are: inlet velocity at 0.005 m/s, inlet temperature at 27^{o}C, irradiation level 200 to 1000 W/m^{2} and ambient temperature at 27^{o}C. All the investigations were done by varying a single parameter while keeping the others as constant. The results are shown in Figures 5.23 (a) to 5.23 (d).

It can be seen from these figures that the average cell temperature, water outlet temperature and output power increases while the electrical efficiency decrease with increasing irradiation level. PV efficiency decreases as PV temperature increases, mainly because a higher cell temperature decreases the voltage significantly (even though it increases the current by a very small amount).

From Figure 5.23 (a), it can be seen that cell temperature increases both of aluminum and copper by 43^{o}C for D2, by around 59 ^{o}C for D3 and by about 70^{o}C for D4. The water outlet temperature (refer to Figure 5.23 (b)) increases by about 12.7^{o}C (both aluminum and copper) for D2, by 37^{o}C (aluminum) and 41^{o}C (copper) for D3 and by around 67^{o}C for D4 (both aluminum and copper).

The output power increases as function of increasing irradiation level. From Figure 5.23 (c), it has observed that output power is increased by around 74.5 W for D2 (both aluminum and copper), by around 60 W for D3 (both aluminum and copper) and by around 50 W for D4 (both aluminum and copper). The electrical efficiency decreases with increased irradiation level. From Figure 5.23 (d) it may be seen that efficiency falls by around 3.2% for D2 (both aluminum and copper), by around 4.5% for D3 (both aluminum and 4.4% for copper) and by around 5.6% for D4 (both aluminum and copper).

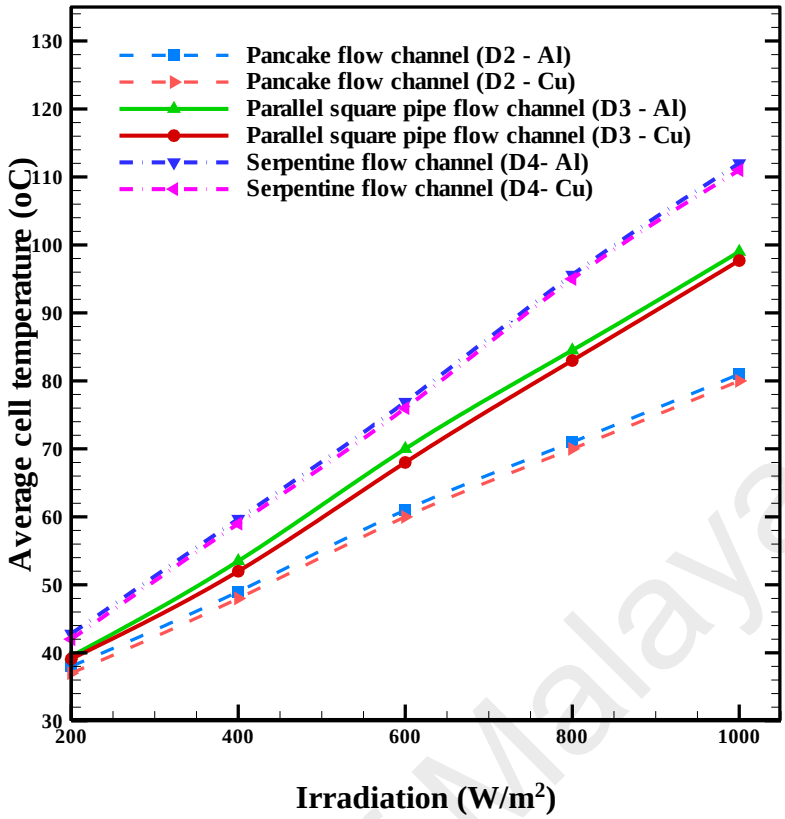

(a)

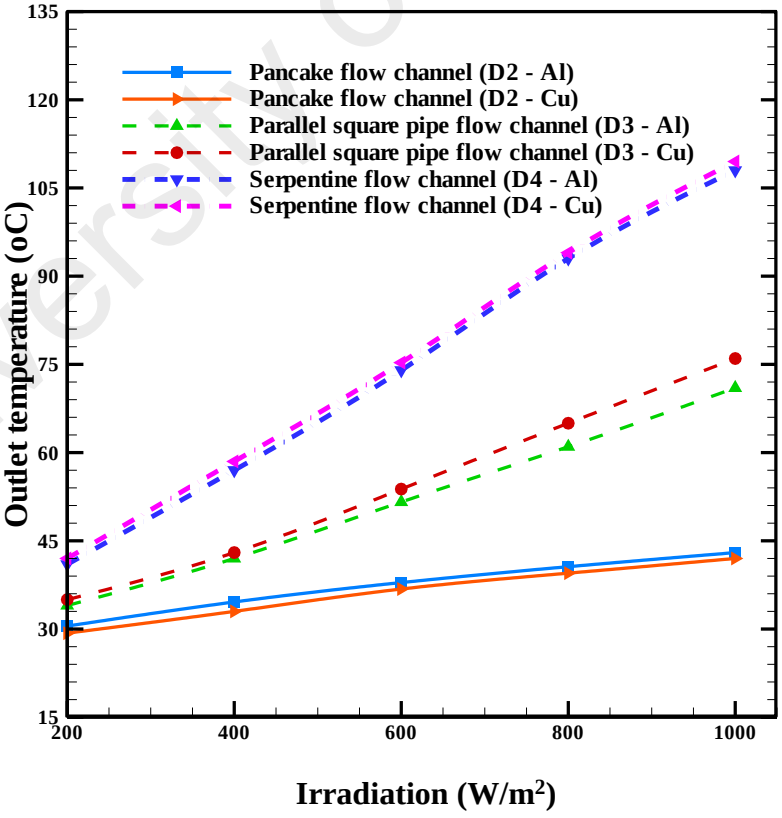

(b)

Figure 5.23: PV/T performance variation with absorbed radiation for both Al and Cu flow channels

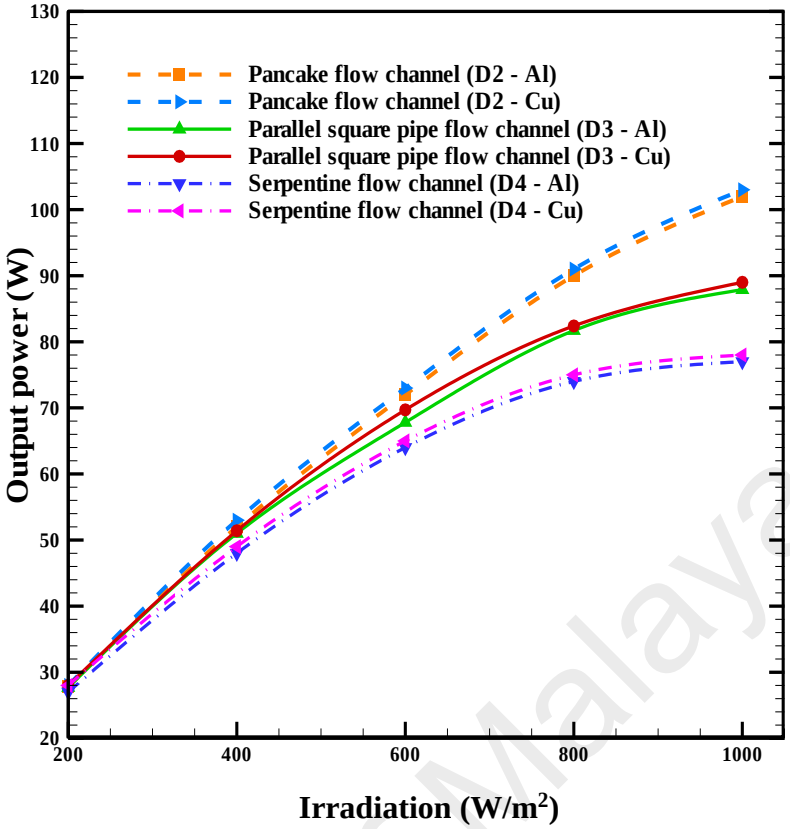

(c)

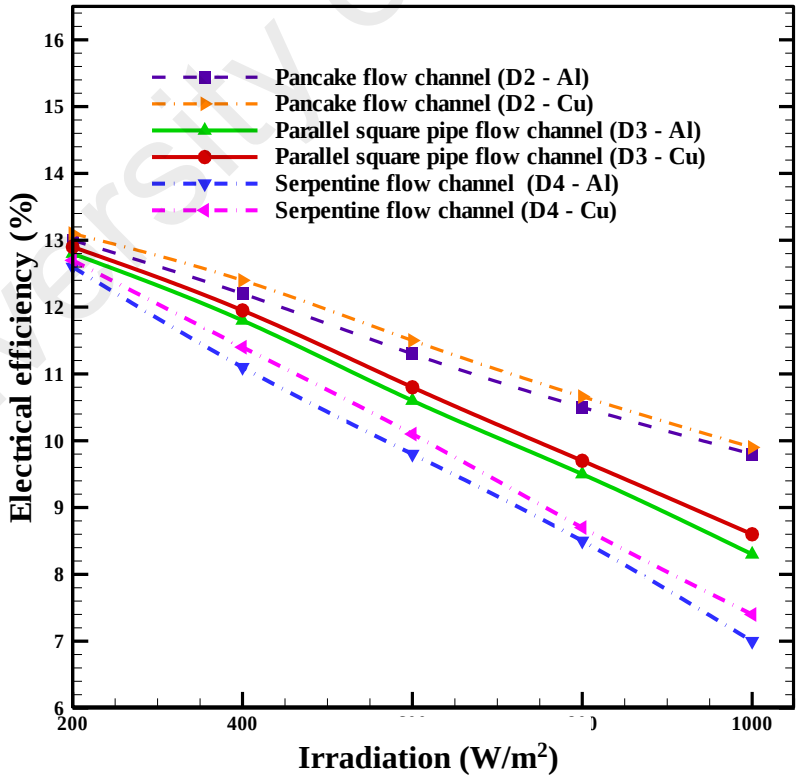

(d)

Figure 5.23, continued

5.6 A Compendium on Different Flow Channel Design

The temperature distribution and the electrical and thermal performances have been elaborately described in the preceding sections. In this section, a succinct summary of the PV/T performance with different thermal collector designs have been presented. The key performance parameters of the PV/T with flow channel design of D1, D2, D3 and D4 are tabulated in Tables 5.4, 5.5, and 5.6.

Table 5.4 tabulated the comparative values of different performance parameters of PV/T with different channel designs. Parallel plate flow channel (D1) produces the best performance among all other design. The highest output power of 129.2 W and the maximum electrical efficiency of 12.6% are achieved with copper channel of same flow design. Copper channel of parallel plate configuration (D1) produces the maximum thermal and overall efficiencies of 77% and 89%, respectively. Besides better performance, this design is simple and easy to manufacture. But it is relatively heavy weight and needs extra support to couple with the PV module.

Design 2, pancake flow channel (D2) shows the lowest electrical and thermal performance of all channel designs. This particular design is best suited for square PV modules where the arms of the square are equal to the outer diameter of the pancake flow channel. In case of conventional rectangular channels, two interconnected pancake flow channels may be placed on the PV module back surface. In this case the coverage area of channel will be more, which will help to improve both the electrical and thermal performance.

Table 5.4: Comparison in performance of PV/T with different collector designs (R = 1000 W/m^2, T_{in} = 27^{o}C and T_{amb} = 27^{o}C)

Performance parameters	**Design 1 Parallel plate**		**Design 2 Pancake tube**		**Design 3 Parallel square pipe**		**Design 4 Serpentine Tube**	
	Al	**Cu**	**Al**	**Cu**	**Al**	**Cu**	**Al**	**Cu**
Output power (W)	129	129.2	112.9	113.1	120	121	125	125
Electrical Efficiency **(%)**	12.3	12.6	10.6	10.8	11.3	11.4	12	12.2
Thermal Efficiency **(%)**	74	77	26	26.5	56	58	61	63
Overall Efficiency **(%)**	86	89	35.6	36.2	66.4	69.7	73	75

Design 4, serpentine flow channel offers an optimum compromise between the electrical and thermal performance. From Table 5.4 it can be seen that copper channel of serpentine pipe configuration yields an operative level of both electrical and thermal performance, which results into a considerable overall efficiency. As for comparative performance with different channel materials, Table 5.4 shows that material has got very minor impact on PV/T performance for all flow channel designs.

Enhancement in electrical performance as a function of reduction in cell temperature has been presented in Table 5.5. The increase in output power and electrical efficiency per 1^{o}C decrease in cell temperature is given in the table. It can be seen that output power improves the best (0.82W) with copper channel of parallel plate configuration (D1). From the viewpoint of increment in electrical efficiency per 1^{o}C decrease in cell temperature, D1 again shows the best performance with 0.11% increase with copper

channel. On the other hand, D3 (parallel squre pipe flow channel) shows less increment in efficiency (0.06% for copper) against per 1^{o}C decrease in cell temperature.

Table 5.5: Increase in electrical efficiency and output power per 1^{o}C decrease in cell temperature (R = 1000 W/m^2, T_{in} = 27^{o}C and T_{amb} = 27^{o}C)

Performance Parameter	**Design 1 Parallel plate**		**Design 2 Pancake tube**		**Design 3 Parallel square pipe**		**Design 4 Serpentine Tube**	
	Al	Cu	Al	Cu	Al	Cu	Al	Cu
Electrical efficiency (%) increase	0.076	0.11	0.08	0.07	0.07	0.06	0.074	0.073
Output power (W) increase	0.79	0.82	0.80	0.79	0.79	0.78	0.64	0.61

The variation in electrical performance parameters as a function of increased radiation has been summarized in Table 5.6. The table shows the change in efficiency and output power for every 100 W/m^2 increase in irradiation level. Electrical efficiency and output power behaves opposite with increasing irradiation; while the power rises, the efficiency gets reduced. The maximum rise in output power as a result of increased irradiation is achieved with Design 1 (D1, parallel plate flow channel) and the increment rate is almost the same (12.5 W), for both aluminum and copper channels. On the other hand increment rate in output power (6.3 W for aluminum and 6.4 W for copper channel) is the minimum in case of Design 4 (D4, serpentine tube flow channel).

From the viewpoint of loss in electrical efficiency per 100 W/m^2 increase in irradiation level, D1 again shows the best performance with only 0.16% drop with aluminum and 0.13% drop with copper channel. On the other hand, D4 (serpentine tube flow channel) suffers from a big drop in efficiency (0.7% for aluminum and 0.66% for copper) against increasing irradiation level.

Design 2 (D2, pancake flow channel) finds the middle ground between increment rate in output power (about 9.4 W for both aluminum and copper) and loss in efficiency (about 0.4% for both aluminum and copper). Therefore, this design may offer a sustainable performance against increased irradiation level.

Table 5.6: Change in electrical efficiency and output power per 100 W/m^2 increase in radiation (T_{in} = 27^{o}C and T_{amb} = 27^{o}C)

Performance Parameter	**Design 1 Parallel plate**		**Design 2 Pancake tube**		**Design 3 Parallel square pipe**		**Design 4 Serpentine Tube**	
	Al	Cu	Al	Cu	Al	Cu	Al	Cu
Reduction of Electrical efficiency (%)	0.16	0.13	0.4	0.41	0.56	0.54	0.7	0.66
Increment of Output power (W)	12.5	12.51	9.3	9.4	7.5	7.6	6.3	6.4

The comaparative performance study as presented in Table 5.4 to 5.6 shows that performance indicators are better for parallel plate flow channel among all four thermal collector designs. Therefore, parallel plate flow channel (design 1) is recommended as the best thermal collector design for PV/T applications.

CHAPTER 6: CONCLUSIONS AND RECOMMENDATIONS

6.1 Conclusions

Performance evaluation of PV/T modules with several newly designed thermal collectors has been carried out numerically using an experimentally validated mathematical model. The following inferences have been drawn from the present investigation:

- Four different configurations of thermal collectors for PV/T, namely parallel plate, pancake, parallel square pipe and serpentine pipe flow channels have been designed.
- A comprehensive 3D mathematical model for PV/T without absorber plate has been developed.
- The numerical model of PV/T with parallel plate flow channel has been validated by experimental investigation where the results were found to be in well agreement.
- As the elevation head has been employed to ensure passive cooling so no additional power is consumed to run the proposed system.
- Inlet velocity has been found to have the most prominent effect on PV/T performance among the control parameters.
- Maximum overall efficiency of the PV/T has been obtained with parallel plate configuration. For aluminum flow channel, the overall efficiency is 86%, while for copper flow channel this value is 89%. Electrical efficiency as well as output power was also found better for PV/T with parallel plate flow channel. The maximum electrical efficiency is about 12.3% for aluminum and 12.6% for copper channel and the output power values are around 129 W for aluminum and 129.2 W for copper channel.

- The water outlet temperature favorable for household and hospital applications (about 42^{o}C) was obtained with pancake flow channel.
- The highest rate of increase in electrical efficiency and output power for every 1^{o}C decrease in cell temperature has been obtained for parallel plate flow channel where the values are 0.12% and 0.81 W respectively.
- As for channel material, it has been observed that use of aluminum or copper have no significant effect on PV/T performance.
- Thermal performance of PV/T without absorber plate is found as good as PV/T with absorber plate. So the absorber plate may be discarded from thermal collector design for PV/T. This will reduce the weight and cost as well as alleviate some technical issues like leakage current generation in the PV/T system.

6.2 Recommendations for Further Works

The present investigation was inplemented to produce some new designs of thermal collectors for flat plate PV/T module and develop a three dimensional numerical model for water based flat plate PV/T system. Upon the achievement of the above mentioned outcomes, the following recommendations for future research works has been proposed hereby:

- In the present research, PV/T-water system considered for investigation, that is, water was only used as heat transfer fluid (HTF) in the thermal collector. It may be proposed that the performance of PV/T might be investigated incorporating nanoparticles in water at different proportions. Also, fluids with distinctive properties, such as, refrigerants and some types of oils may be employed as HTF in the PV/T and the performance may be evaluated thereby.

- Phase change materials may be employed in conjunction with water and any of the above mentioned fluids and the improvement in thermal performances may be studied thereby.
- In the present research, performance of PV/T collector with parallel plate flow channel has only been evaluated experimentally. Experimental investigations on the other designs proposed in the present study may be carried out.
- An all-inclusive exergy analysis of PV/T system may be carried out in order to ensure more efficient use of solar energy and optimize the system.

REFERENCES

Agrawal, B., & Tiwari, G. N. (2010). Optimizing the energy and exergy of building integrated photovoltaic thermal (BIPVT) systems under cold climatic conditions. *Applied Energy, 87(2),* 417-426.

Agrawal, B., & Tiwari, G. N. (2010). Optimizing the energy and exergy of building integrated photovoltaic thermal (BIPVT) systems under cold climatic conditions. *Applied Energy, 87(2),* 417-426.

Aktas, M., Ceylan. I., & Yilmaz, S. (2009). Determination of drying characteristics of apples in a heat pump and solar dryer. *Desalination 239,* 266-275.

Álvarez, A., Muñiz, M. C., Varela, L. M., & Cabeza, O. (2010). Finite element modelling of a solar collector. *Proceedings of International Conference on Renewable Energies and Power Quality*, ICREPQ'10, Granada, Spain.

Ammous, M., & Chaabene, M. (2014). Design of a PV/T based desalination plant: concept and assessment. *Proceedings of the International Renewable Energy Congress*, IREC '2014, Hammamet, Tunisia.

Anderson, T. N., Duke, M., Morrison, G. L., & Carson, J. K. (2009). Performance of a building integrated photovoltaic/thermal (BIPVT) solar collector. *Solar Energy, 83(4),* 445-455.

Annis, N. C., & Baur, S. W. (2011). Performance comparison of modular photovoltaic-thermal solar panels: *Proceeding of the GreenTech 2011: IEEE Green Technologies Conference (IEEE-Green),* Baton Rouge, USA.

Argiriou, A., Klitsikas, N., Balaras, C. A., & Asimakopoulos, D. N. (1997). Active solar space heating of residential buildings in northern Hellas - a case study. *Energy and Buildings, 26(2),* 215-221.

Backhurst, J. R., Harker, J. H., Richardson J. F., & Coulson, J. M. (1999). *Chemical Engineering Volume 1* (6th ed.). UK, Elsevier.

Bakker, M., Zondag, H. A., & van Helden, W. G. J. (2002). Design on a dual flow photovoltaic/ thermal combi panel: *Proceedings of PV in Europe – from PV technology to energy solutions*, Rome, Italy.

Başoğlu, M. E., & Çakir, B. (2016). Comparisons of MPPT performances of isolated and non-isolated DC–DC converters by using a new approach. *Renewable and Sustainable Energy Reviews, 60,* 1100–1113.

Bergene, T., & Løvvik, O. M. (1995). Model calculations on a flat-plate solar heat collector with integrated solar cells. *Solar energy, 55(6)*, 453-462.

Besheer, H. A., Mervyn S., Aggelos Z., Jayanta M., & Adrian P. (2016). Review on recent approaches for hybrid PV/T solar technology. *International Journal of Energy Research, 40(15)*, 2038–2053.

Bhargava, A. K., Garg, H. P., & Agarwal, R. K. (1991). Study of a hybrid solar system – solar air heater combined with solar cells. *Energy Conversion Management, 31(5)*, 471–479.

Böer, K. W., & Tamm, G. (2003). Solar conversion under consideration of energy and entropy. *Solar Energy, 74(6)*, 525–528.

Bouroussis, C. A., & Topalis, F.V. (2004). Optimization of potential and autonomy of a photovoltaic system for street lighting. *Word Scientific and Engineering Society Transactions on Circuits and Systems, 3(5)*, 1392–1397.

British Petroleum (BP). (2016). BP energy outlook: outlook to 2035. UK: Dudly, B.

Calise, F., d'Accadia, M. D., Vicidomini, M., Ferruzzi, G., & Vanoli, L. (2015). Design and dynamic simulation of a combined system integration concentrating photovoltaic/thermal solar collectors and organic rankine cycle. *American Journal of Engineering and Applied Sciences, 8(1)*, 100-118.

Carbon Trust. (2006). *Future marine energy. results of the marine energy challenge: cost competitiveness and growth of wave and tidal stream energy*. UK: Callaghan, J., & Boud , R.

Cattani, L. (2012). Numerical investigation of the convective heat transfer enhancement in coiled tubes. *Proceedings of the 2012 COMSOL Conference*, Milan, Italy.

Çengel, Y. (2003). *Heat transfer: a practical approach* (2nd ed.). Boston, USA, McGraw-Hill.

Charalambous, P., G. Maidment, G. G., Kalogirou, S. A., & Yiakoumetti, K. (2007). Photovoltaic thermal (PV/T) collectors: a review. *Applied Thermal Engineering, 27(2-3)*, 275-286.

Chow, T. T. (2003). Performance analysis of photovoltaic-thermal collector by explicit dynamic model. *Solar Energy, 75(2)*, 143 -152.

Chow, T. T. (2010). A review on photovoltaic/thermal hybrid solar technology. *Applied Energy, 87(2),* 365-379.

Chow, T. T., He, W., Chan, A. L. S., Fong, K. F., Lin, Z., & Ji, J. (2008). Computer modeling and experimental validation of a building-integrated photovoltaic and water heating system. *Applied Thermal Engineering, 28(11–12),* 1356-1364.

Chow, T. T., Pei, G., Fong, K. F., Lin, Z., Chan, A. L.S., & Ji J. (2009). Energy and exergy analysis of photovoltaic-thermal collector with and without glass cover. *Applied Energy, 86(3),* 310–316.

Coventry, J. S, & Lovegrove, K. (2003). Development of an approach to compare the 'value' of electrical and thermal output from a domestic PV/thermal system. *Solar Energy, 75 (1),* 63–72.

Cox III, C. H., & Raghuraman, P. (1985). Design considerations for flat-plate-photovoltaic/thermal collectors. *Solar energy, 35(3),* 227-241.

Danish Technological Institute, Solar Energy Centre. (2003). *Photovoltaic/thermal solar collectors and their potential in Denmark*. Copenhagen, Denmark: Bosanac, M., Sørensen, B., Katic, I., Sørensen, H., Nielsen, B., & Badran, J.

Davidsson, H., Perers, B., & Karlsson, B. (2010). Performance of a multifunctional PV/T hybrid solar window. *Solar Energy, 84(3),* 365-372.

Davis, M. W., Fanney, A. H., & Dougherty, B. P. (2001). Prediction of building integrated photovoltaic cell temperatures. *Journal of Solar Energy Engineering, 123(3),* 200-210.

de Vries, D. W. (1998). *Design of a photovoltaic/thermal combi-panel* (Doctoral thesis, Technische Universiteit Eindhoven). Retrieved from http://repository.tue.nl/ 1d4a2508-5c06-48ce-9c14-be2f22db6190.

Dobrzański, L. A., Szczęsna, M., Szindler, M., & Drygala, A. (2013). Electrical properties of mono- and polycrystalline silicon solar cells. *Journal of Achievement in Materials and Manufacturing Engineering, 59(2),* 67-74.

Dubey, S., & Andrew A. O. T. (2013). Testing of two different types of photovoltaic–thermal (PVT) modules with heat flow pattern under tropical climatic conditions. *Energy for Sustainable Development, 17(1),* 1-12.

Dubey, S., & Tiwari, G. N. (2009). Analysis of PV/T flat plate water collectors connected in series. *Solar Energy, 83(9),* 1485-1498.

Dubey, S., &. Tiwari, G. N. (2008). Thermal modeling of a combined system of photovoltaic thermal (PV/T) solar water heater. *Solar Energy, 82(7)*, 602-612.

Dubey, S., Sandhu, G., & Tiwari, G. (2009). Analytical expression for electrical efficiency of PV/T hybrid air collector. *Applied Energy, 86(5),* 697-705.

Dubey, S., Sarvaiya, J. N., & Seshadri, B. (2013). Temperature dependent photovoltaic (PV) efficiency and its effect on PV production in the world - a review. *Energy Procedia, 33*, 311 – 321.

Dunlop, E. D., Haverkamp, E., Sandberg, M., & Strobach, J. M. (1998). The energy balance of roof integrated hybrid photovoltaic modules. *Proceedings of the 2nd WCPEC,* Vienna, Austria.

Dupeyrat, P., Ménézo, C., Rommel, M., & Henning, H. M. (2011). Efficient single glazed flat plate photovoltaic–thermal hybrid collector for domestic hot water system. *Solar Energy, 85(7)*, 1457-1468.

Dye, S. T. (2012). Geoneutrinos and the radioactive power of the Earth. *Reviews of Geophysics, 50(3)*, 1-19.

Eck, M., Feldhoff, J. F., & Uhlig, R. (2010). Thermal modeling and simulation of parabolic trough receiver tubes. *Proceedings of the ASME International Conference on Energy Sustainability* Phoenix, Arizona, USA.

Eck, M., Uhlig, R., Mertins, M., Häberle, A., & Lerchenmüller, H. (2007). Thermal load of direct steam-generating absorber tubes with large diameter in horizontal linear fresnel collectors. *Heat Transfer Engineer 28(1)*, 42–48.

Eisenmann, W., & Zondag, H. (2005). PV Catapult/European collaboration for identification of pv research and markets opportunities, socio-economic studies, performance assessment and dissemination of PV and PV–thermal technology. *PVT workshop 2*, Germany.

Ekechukwu O. V., & Norton, B. (1999). Review of solar-energy drying systems III: low temperature air-heating solar collectors for crop drying applications. *Energy Conversion and Management, 40(6)*, 657-668.

Elbreki, A. M., Alghoul, M. A., Al-Shamani, A. N., Ammar, A. A., Bita, Y., …, Sopian, K. (2016). The role of climatic-design-operational parameters on combined PV/T collector performance: A critical review. *Renewable and Sustainable Energy Reviews, 57*, 602–647.

Ellabban, O., Abu-Rub, H., & Blaabjerg, F. (2014). Renewable energy resources: current status, future prospects and their enabling technology. *Renewable and Sustainable Energy Reviews, 39*, 748-764.

Energy Information Administration (EIA). (2016). International energy outlook 2016: with projections to 2040. Washington, DC, USA: John Conti.

Erdil, E., Ilkan, M., & Egelioglu, F. (2008). An experimental study on energy generation with a photovoltaic (PV)–solar thermal hybrid system. *Energy, 33(8)*, 1241-1245.

European Solar Thermal Electricity Association (ESTELA). (2016). Solar thermal electricity: global outlook 2016. Amsterdam, The Netherlands: Sven, T., Luis, C., & Ritcher, C.

Fesharaki, V. J., Dehghani, M., & Fesharaki, J. J. (2011). The effect of temperature on photovoltaic cell efficiency. *Proceedings of the International Conference on Emerging Trends in Energy Conservation*, Tehran, Iran.

Fesharaki, V. J., Dehghani, M., & Fesharaki, J. J. (2011). The effect of temperature on photovoltaic cell efficiency. *International Conference on Emerging Trends in Energy Conservation*, Tehran, Iran.

Florschuetz, L. W. (1975). On heat rejection from terrestrial solar cell arrays with sunlight concentration. *Photovoltaic Specialists Conference*, Arizona, USA.

Florschuetz, L. W. (1979). Extension of the Hottel-Whillier model to the analysis of combined photovoltaic/thermal flat plate collectors. *Solar energy, 22(4)*, 361-366.

Fraisse, G., Me´ne´zo C., & Johannes, K. (2007). Energy performance of water hybrid PV/T collectors applied to combisystems of Direct Solar Floor type. *Solar Energy*, *81*, 1426–1438.

Fu, H. D., Pei, G., Zhang T., Zhu, H. J., & Ji, J. (2012). Experimental study on a heat-pipe photovoltaic/thermal system. *IET Renewable Power Generation, 6(3)*, 129-136.

Fujisawa, T., & Tani, T. (1997). Annual exergy evaluation on photovoltaic-thermal hybrid collector. *Solar Energy Materials and Solar Cells, 47 (1 – 4)*, 135-148.

Gang, P., F. Huide, F., Tao, Z., & Jie, J. (2011). A numerical and experimental study on a heat pipe PV/T system. *Solar energy*, *85(5)*, 911-921.

Garg, H. P., & Adhikari, R. S. (1997). Conventional hybrid photovoltaic/thermal (PV/T) air heating collectors: steady-state simulation. *Renewable Energy, 11(3),* 363–385.

Geothermal Energy Association (GEA) (2016). Annual U.S. & Global Geothermal Power Production Report, USA: Matek, B.

Good, C. (2016). Environmental impact assessments of hybrid photovoltaic–thermal (PV/T) systems – A review. *Renewable and Sustainable Energy Reviews, 55,* 234–239.

Green, M. A., & Emery, K. (2016). Solar cell efficiency Tables. *Progress in Photovoltaics: Research and Applications, 24,* 905–913.

Guo, J., Simao L., Jose I. B., Stephen, D. W., & Alistair B. S. (2017). A review of photovoltaic thermal (PV/T) heat utilization with low temperature desiccant cooling and dehumidification. *Renewable and Sustainable Energy Reviews, 67,* 1–14

Hailu, G., Yang, T., Athienitis, A. K. & Fung, A. S. (2014). Computational fluid dynamics (CFD) analysis of building integrated photovoltaic thermal (BIPV/T) systems. *ASME International Conference on Energy Sustainability collocated with the ASME International Conference on Fuel Cell Science, Engineering and Technology*, Boston, Massachusetts, USA.

Hegazy, A. A. (2000). Comparative study of the performances of four photovoltaic/thermal solar air collectors. *Energy Conversion and Management, 41(8),* 861-881.

Heimsath, A., Platzer, W., Heß, S., Krüger, D., & Eck, M. (2009). Concentrating solar collectors for process heat and electricity generation. *FVEE.AEE*, 61-65.

Hendrie, S. D. (1979). Evaluation of combined photovoltaic/thermal collectors. *International Solar Energy Society Meeting*, Atlanta, USA.

Holman, J. P. (2010). *Heat Transfer* (10th ed.). USA, McGraw Hill

Hottel, H., & Whillier, A. (1955). Evaluation of flat-plate solar collector performance. *Transactions of the conference on the use of solar energy, 3(2).*

Huang, B. J., Lin, T. H., Hung W. C., & Sun, F. S. (2001). Performance evaluation of solar photovoltaic/thermal systems. *Solar Energy 70(5),* 443–448.

Hubbert, M. K. (2016). The present world energy situation. Retrieved from http://archives.datapages.com/data/gcags/data/008/ 008001/0012.htm.

Huc, N. (2014). Conjugate Heat Transfer. Retrieved from https://www.comsol. com/blogs/conjugate-heat-transfer/.

Ibrahim, A, Othman, M. Y., Ruslan, M. H., Alghoul, M. A., Yahya, M., Zaharim, A., & Sopian, K. (2009). Performance of photovoltaic thermal collector (PVT) with different absorbers design. *WSEAS Transactions on Environment and Development, 5(3)*, 321–330.

Ibrahim, A., Fudholi, A., Sopian, K., Othman, M. Y., & Ruslan, M. H. (2014). Efficiencies and improvement potential of building integrated photovoltaic thermal (BIPVT) system. *Energy Conversion and Management, 77*, 527-534.

Ibrahim, A., Othman, M. Y., Ruslan, M. H., Mat, S., & Sopian, K. (2011). Recent advances in flat plate photovoltaic/thermal (PV/T) solar collectors. *Renewable and Sustainable Energy Reviews, 15(1)*, 352-365.

International Energy Agency (IEA). (2011). Solar Energy Perspective. France: Philibert, C.

International Energy Agency (IEA). (2015). Energy technology initiatives: ocean - pilots, projects and potentials. Retrieved from http://www.iea.org /techinitiatives/renewableenergy/ocean/.

International Energy Agency (IEA). (2016). Renewable energy. Retrieved from https://www.iea.org/aboutus/faqs/renewableenergy/.

International Energy Agency (IEA). (2016). Wind energy: land-based and off-shore. Retrieved from http://www.iea.org/topics/renewables/subtopics/wind/.

International Hydropower Association (IHA). (2016). The 2016 hydropower status report: an insight into recent hydropower development and sector trends around the world. UK: Ken Adams.

Ji, J, Chow. T. T., & He, W. (2003). Dynamic performance of hybrid photovoltaic/thermal collector wall in Hong Kong. *Building and Environment, 38(11)*, 1327–1334.

Ji, J., Han, J., Chow, T. T., Hua, Y., Jianping, L., He, W. & Sun, W. (2006). Effect of fluid flow and packing factor on energy performance of a wall-mounted hybrid photovoltaic/water-heating collector system. *Energy and Building, 38(12)*, 380–407.

Joshi, A.S., Tiwari, A., Tiwari, G.N., Dincer, I., & Reddy, B.V. (2009). Performance evaluation of a hybrid photovoltaic thermal (PV/T) (glass-to-glass) system. *International Journal of Thermal Sciences, 48*, 154–164.

Kern Jr., E. C., & Russell, M. C. (1978). Combined photovoltaic and thermal hybrid collector systems. *IEEE Photovoltaic Specialists Conference*, Washington DC, USA.

Kim, J. H., Park, S. H., & Kim, J. T. (2014). Experimental Performance of a Photovoltaic-thermal Air Collector. *Energy Procedia, Proceedings of the 2nd International Conference on Solar Heating and Cooling for Buildings and Industry (SHC 2013), 48*, 888-894.

Kim, J. H., & Kim, J. T. (2012). Comparison of electrical and thermal performances of glazed and unglazed PVT collectors. *International Journal of Photoenergy, 2012*, 1–7.

Koech, R. K., Ondieki, H. O., Tonui, J. K., & Rotich, S. K. (2012). A steady state thermal model for photovoltaic/thermal (PV/T) system under various conditions. *International Journal of Scientific & Technology Research, 1(11)*, 1–5.

Krauter, S., & F. Ochs (2003). An integrated solar home system-history. *Proceedings of 3rd World Conference on Photovoltaic Energy Conversion,* Osaka, Japan.

Kreider, J. F., & Kreith, F. (1989). *Solar heating and cooling: active and passive design*. (2nd ed.). New York, USA: Hemisphere Publishing Corporation.

Kristual, M. A., & McDonnell, S. M. (1994). Drinking water temperature affects consumption of water during cold weather in ponies. *Applied Animal Behaviour Science, 41(3-4)*, 155-160.

Kumar, A., & Prasad, B. N. (2000). Investigation of twisted tape inserted solar water heaters—heat transfer, friction factor and thermal performance results. *Renewable Energy, 19(3)*, 379–398.

Kumar, A., Baredar, P., & Qureshi, U. (2015). Historical and recent development of photovoltaic thermal (PVT) technologies. *Renewable and Sustainable Energy Reviews, 42*, 1428-1436.

Kumar, R., & Rosen, M. A. (2011). Performance evaluation of a double pass PV/T solar air heater with and without fins. *Applied Thermal Engineering, 31*, 1402–1410.

Lalović, B., Kiss, Z., & Weakliem, H. (1986). A hybrid amorphous silicon photovoltaic and thermal solar collector. *Solar cells, 19(2)*, 131-138.

Li, G., Gang, P., Ji, J. Yang, M., Su, Y., & Xu, N. (2015). Numerical and experimental study on a PV/T system with static miniature solar concentrator. *Solar Energy, 120*, 565-574.

Liu, Y., Hu, P., Zhang, Q., & Chen, Z. (2014). Thermodynamic and optical analysis for a CPV/T hybrid system with beam splitter and fully tracked linear Fresnel reflector concentrator utilizing sloped panels. *Solar Energy ,103*, 191-199.

Lund, J. W., &. Boyd, T. L. (2016). Direct utilization of geothermal energy 2015 worldwide review. *Geothermics, 60*, 66-93.

Makki, A., & Omer, S. (2015). Performance analysis of heat pipe-based photovoltaic-thermoelectric generator (hp-pv/teg) hybrid system. Proceedings of Qatar Foundation Annual Research Conference, Qatar.

Marsh, A., J. (2011). Solar Radiation. *Natural Frequency*. Retrieved from http://naturalfrequency.com/wiki/solar-radiation

Mattei, M., Notton, G., Cristofari, C., Muselli, M., & Poggi, P. (2006). Calculation of the poly crystalline P/V module temperature using a simple method of energy balance. *Renewable Energy, 31(4)*, 553-567.

McAdams, W. C. (1954). *Heat transmission* (3rd ed.). New York, USA: McGraw-Hill.

Mekhilef, S., Saidur, R., & Safari, A. (2011). A review on solar energy use in industries. *Renewable and Sustainable Energy Reviews, 15(4)*, 1777-1790.

Modi, A., Fabian B., Jesper G. A., & Fredrik H. (2017). A review of solar energy based heat and power generation systems. *Renewable and Sustainable Energy Reviews*, 67, 1047–1064

Moradi, K., Ebadian, M. A., & Lin, C. X. (2013). A review of PV/T technologies: Effects of control parameters. *International Journal of Heat and Mass Transfer, 64*, 483–500.

Mortezapour, H., Ghobadian, B. Minaei, S., & Khoshtaghaza, M. H. (2012). Saffron drying with a heat pump–assisted hybrid photovoltaic–thermal solar dryer. *Drying Technology, 30(6)*, 560-566.

Nahar, A., Hasanuzzaman, M., Rahim, N. A., & Hosenuzzaman, M. (2014). Effect of cell material on the performance of PV System. *Advanced Materials Research, 1043*, 12-16.

National Aeronautics and Space Administration (NASA). (1980). Spectral distribution of solar radiation, Maryland, USA: Mecherikunnel, A. T., and Richmond, J. C.

National Renewable Energy Laboratory (NREL). (2015). *Photovoltaic-thermal: new technology demonstration.* San Francisco, CA, USA: Dean, J., McNutt, P., Lisell, L. Burch, J., Jones, D., & Heinicke, D.

National Solar Power Research Institute Inc. (NSPRI). (1998). *Fundamentals of photovoltaic materials.* San Francisco, CA, USA: Mah, O.

Nayak, S., Kumar, A., Mishra, J., & Tiwari, G. N. (2011). Drying and testing of mint (mentha piperita) by a hybrid photovoltaic-thermal (PVT)-based greenhouse dryer. *Drying Technology, 29(9),* 1002-1009.

Nemati, O., Candanedo, I. L. M., & Alan, S. F. (2016). Review of computer models of air-based, curtainwall-integrated PV/T collectors. *Renewable and Sustainable Energy Reviews,* 63, 102–117

Nikolaisen, P. I., & Ukeblad. T. (17 January 2015). 12 mega dams that changed the world. Retrieved from http://www.tu.no/artikler/12-megadammer-som-endret-verden/223528.

Othman, M. Y., Yatim. B., Sopian K., & Bakar, M. N. A. (2006). Double-pass photovoltaic-thermal solar air collector with compound parabolic concentrator and fins. *Journal of Energy Engineering, 132(3),* 116-120.

Palmer, K. F., & Williams, D. (1974). Optical properties of water in the near infrared. *Journal of the Optical Society of America, 64 (8),* 1107–1110.

Radziemska, E. (2003). The effect of temperature on the power drop in crystalline silicon solar cells. *Renewable Energy, 28(1),* 1-12.

Radziemska, E. (2003a). Thermal performance of Si and GaAs based solar cells and modules: a review. *Progress in Energy and Combustion Science, 29(5),* 407-424.

Rahman, M. M., Hasanuzzaman, M., & Rahim, N. A. (2015). Effects of various parameters on PV-module power and efficiency. *Energy Conversion and Managemen,*103, 348–358.

Ray, K. L. (2010). Photovoltaic cell efficiency at elevated temperatures. *Massachusetts Institute of Technology,* Retrieved from: http://dspace.mit.edu/bitstream/handle/1721.1/59937/676836192.pdf.

Rehena, N., & Alim, M. A. (2015). Thermal performance of nanofluid filled solar flat plate collector. *International Journal of Heat and Technology, 33(2),* 17-24.

Renewable Energy Policy Network for the 21st Century (REN 21). (2016). *Renewables 2016: Global Status Report*. Paris, France: Sawin, J. L., Seyboth, K., & Sverrisson, F.

Renno, C. (2014). Optimization of a concentrating photovoltaic thermal (CPV/T) system used for a domestic application. *Applied Thermal Engineering, 67(1-2),* 396-408.

Reynolds, O. (1883). An experimental investigation of the circumstances which determine whether the motion of water shall be direct or sinuous, and of the law of resistance in parallel channels. *Philosophical Transactions of the Royal Society, 174(0),* 935-982.

Riffat, S.B, Zhao, X., & Doherty, P.S. (2005). Developing a theoretical model to investigate thermal performance of a thin membrane heat-pipe solar collector. *Applied Thermal Engineering, 25(5-6),* 899 – 915.

Salem, M. R., Elshazly, K. M., Sakr, R. Y., & Ali, R. K. (2015). Experimental Investigation of Coil Curvature Effect on Heat Transfer and Pressure Drop Characteristics of Shell and Coil Heat Exchanger. *Journal of Thermal Science and Engineering Applications, 7(1),* 1100551-1100559.

Sandeep, K. P., & Irudayaraj, J. (2008). Introduction to Modeling and Numerical Simulation, Pennsylvania, USA: CRC Press.

Sandnes, B., & Rekstad, J. (2002). A photovoltaic/thermal (PV/T) collector with a polymer absorber plate: experimental study and analytical model. *Solar Energy, 72(1),* 63-73.

Sanvicente, E., Julien, G., Ménézo, C., & Bouia, H. (2012). Transitional natural convection flow and heat transfer in an open channel. *International Journal of Thermal Sciences, 63,* 87-104.

Sarhaddi, F., Farahat, S., Ajam, H., Behzadmehr, A., & Adeli, M. M. (2010). An improved thermal and electrical model for a solar photovoltaic thermal (PV/T) air collector. *Applied Energy, 87,* 2328–2339.

Schneider, H. (2013, May 8). World Bank turns to hydropower to square development with climate change. *The Washington Post*. Retrieved from https://www.washingtonpost.com/business/economy/world-bank-turns-to-hydropower-to-square-development-with-climate-change/2013/05/08/b9d60332-b1bd-11e2-9a98-4be1688d7d84_story.html.

Seyyedvalilu, M. H., & Ranjbar, S. F. (2015). The effect of geometrical parameters on heat transfer and hydro dynamical characteristics of helical exchanger. *International Journal of Recent Advances in Mechanical Engineering*, *1(4)*, 35-46.

Shahsavar, A., & Ameri, M. (2010). Experimental investigation and modeling of a directcoupled PV/T air collector. *Solar Energy, 84*, 1938–1958.

Shahsavar, A., Salmanzadeh, M., Ameri, M., & Talebizadeh, P. (2011). Energy saving in buildings by using the exhaust and ventilation air for cooling of photovoltaic panels. Energy and Buildings, *43(9)*, 2219-2226.

Shankar, A. U. (2016, June 21). Global Bioenergy Statistics 2016. Retrieved from http://www.besustainablemagazine.com/cms2/wolrd-bioenergy-association-publishes-global-bioenergy-statistics-2016/.

Siddiqui, M. U., Arif A.F.M., Kelley, L., Dubowsky, S. (2012). Three-dimensional thermal modeling of a photovoltaic module under varying conditions. *Solar Energy, 86, 2620–2631*.

Singh, G., Kumar, S., & Tiwari, G. N. (2011). Design, fabrication and performance evaluation of a hybrid photovoltaic thermal (PVT) double slope active solar still. *Desalination, 277(1–3)*, 399-406.

Skoplaki, E., & Palyvos, J. A. (2009). On the temperature dependence of photovoltaic module electrical performance: a review of efficiency/power correlations. *Solar Energy, 83(5)* 614-624.

Smith, D. R., Biringer. K. L., & Pritchard, D. A. (1978). Combined photovoltaic thermal collector testing. Sandia National Labs, Washington, USA.

Smith, J. M., Van Ness, H. C., & Abbott, M. M. (2005). *Introduction to chemical engineering thermodynamics*. Boston, USA: McGraw-Hill.

Sobhnamayan, F., Sarhaddi, F., Alavi, M. A., Farahat, S., Yazdanpanahi, J. (2014). Optimization of a solar photovoltaic thermal (PV/T) water collector based on exergy a concept. *Renewable Energy, 68*, 356-365.

Sodja, J. (2007). Turbulence models in CFD. *Presented in Seminar at Department of Physics, University of Ljubljana*, Ljubljana, Slovenia.

Sopian, K., Jin, G. L., Othman, M. Y., Zaidi, S. H., & Hafidz, M. (2011). Advanced absorber design for photovoltaic thermal (PV/T) collectors. *IASME/WSEAS*

International Conference on Energy, Environment, Ecosystems and Sustainable Development, Angers, France.

Sopian, K., Liu, H. T., Kakaç, S., & Veziroglu, T. N. (2000). Performance of a double pass photovoltaic thermal solar collector suiTable for solar drying systems. *Energy Conversion and Management, 41(4)*, 353-365.

Sopian, K., Yigit, K. S., Liu, H. T., Kakaç, S., & Veziroglu, T. N. (1996). Performance analysis of photovoltaic thermal air heaters. *Energy Conversion and Management, 37(11)*, 1657-1670.

Teo, H. G., Lee, P. S., & Hawlader, M. N. A. (2012). An active cooling system for photovoltaic modules. *Applied Energy, 90(1)*, 309-315.

Tiwari, A. & Sodha, M. S. (2006a). Performance evaluation of hybrid PV/thermal water/air heating system: a parametric study. *Renewable Energy, 31(15)*, 2460–2474.

Tiwari, A., & Sodha, M. S. (2006). Performance evaluation of solar PV/T system: an experimental validation. *Solar Energy, 80(7)*, 751-759.

Tiwari, A., & Sodha, M. S. (2007). Parametric study of various configurations of hybrid PV/thermal air collector: experimental validation of theoretical model. *Solar Energy Materials and Solar Cells, 91(1)*, 17-28.

Tonui, J. K., & Tripanagnostopoulos, Y. (2008). Performance improvement of PV/T solar collectors with natural air flow operation. *Solar Energy, 82(1)*, 1-12.

Tonui, J.K., & Tripanagnostopoulos,Y. (2007). Air-cooled PV/T solar collectors with low cost performance improvements. *Solar Energy, 81(4)*, 498–511.

Tripanagnostopoulos, Y., Souliotis, N. T., & Yianoulis, P. M. (2002). Hybrid photovoltaic/thermal solar systems. *Solar Energy, 72(3)*, 217–234.

Tsai, H. L. (2015). Modeling and validation of refrigerant-based PVT-assisted heat pump water heating (PVTA–HPWH) system. *Solar Energy, 122*, 36-47.

University of Colorado Technology Transfer Office (UCTTO). (2011), *Lowcost modular building-integrated photovoltaic–thermal collector*. Boulder Springs, Colorado, USA.

US Energy Information Administration (EIA). (2015). Solar thermal power plants. Retrieved from https://www.eia.gov/Energyexplained/?page=solar_thermal_power_plants.

van Helden, W. G. J., van Zolingen, R. J. C. & Zondag, H. A. (2004). PV Thermal Systems PV Panels Supplying Renewable Electricity and Heat. *Progress in Photovoltaics: Research and Applications*, *12*, 415–426.

van Sark, W. G. J. H. M., Meijerink, A., & Schropp, R. E. I. (2012) *Third Generation Photovoltaics*. Rijeka, Croatia: Intech.

Vats, K., Tomar, V., & Tiwari, G. N. (2012). Effect of packing factor on the performance of a building integrated semitransparent photovoltaic thermal (BIPVT) system with air duct. *Energy Buildings*, *53*, 159–165.

Vaxman, M, & Sokolov, M. (1985). Analysis of a free flow Solar collector. *Solar Energy*, *35*, 287-290.

Versluis R, Bloem, J. J., & Dunlop, E. D. (1997). An energy model for hybrid photovoltaic building facades. *European Photovoltaic Solar Energy Conference*, Barcelona. Spain.

Wall, S. (2016, August 4). PV/thermal; solar power wall - electricity + heating. Retrieved from http://solarwall.com/en/products/pvthermal.php.

Wolf, M. (1976). Performance analyses of combined heating and photovoltaic power systems for residences. *Energy Conversion, 16(1-2)*, 79-90.

Wu, S. Y., Zhang, Q. L., Xiao, L., & Guo, F. H. (2011). A heat pipe photovoltaic/thermal (PV/T) hybrid system and its performance evaluation. *Energy and Buildings, 43(12)*, 3558-3567.

Xing, J., Chao, X., Xue, H., Xiaoze, D., Gaosheng, W., & Yongping, Y. (2017). A review of the concentrated photovoltaic/thermal (CPVT) hybrid solar systems based on the spectral beam splitting technology. *Applied Energy, 187*, 534–563.

Yang, T., &. Athienitis, A. K. (2012). Investigation of performance enhancement of a building integrated photovoltaic thermal system. *Proceedings of the Canadian Conference on Building Simulation*, Québec, Canada.

Yang, T., &. Athienitis, A. K. (2014). A study of design options for a building integrated photovoltaic/thermal (BIPV/T) system with glazed air collector and multiple inlets. *Solar Energy*, *104*, 82-92.

Yang, T., &. Athienitis, A. K. (2015). Experimental investigation of a two-inlet air-based building integrated photovoltaic/thermal (BIPV/T) system. *Applied Energy, 159*, 70-79.

Zdrowski, J., Lilliestierna, N., Corbin, C. Zhai, J., & Brandemuehl, M. (2010). Building integrated photovoltaic/thermal collector panel design and test/developing a low cost modular building integrated photovoltaic/thermal collector for electricity and hot water. University of Colorado at Boulder — *College of Engineering and Applied Science.*

Zhang, X., Zhao, X., Smith, S., Xu, J., & Yu, X. (2012). Review of R & D progress and practical application of the solar photovoltaic/thermal (PV/T) technologies. *Renewable and Sustainable Energy Reviews, 16(1),* 599-617.

Zhang, X., Zhao, X., Xu, J., & Yu, X. (2013). Characterization of a solar photovoltaic/loop-heat-pipe heat pump water heating system. *Applied Energy, 102*, 1229-1245.

Zhao, X., Zhang, X., Riffat, S. B., & Su, Yaxin (2011). Theoretical study of the performance of a novel PV/e roof module for heat pump operation. *Energy Conversion and Management, 52(1),* 603-614.

Zondag, H. A, de Vries, D. W., van Helden, W. G. J., van Zolingen, R. J. C., & van Steenhoven, A. A. (2003). The yield of different combined PV-thermal collector designs. *Solar Energy, 74(3),* 253–269.

Zondag, H. A., van Helden, W. G. J., Bakkar, M., Affolter, P. Eisermann, W., Fechner, H., Tripanagnostopoulos, Y. (2005). PVT roadmap: a European guide for the development and market introduction of PVT technology. *European Photovoltaic Solar Energy Conference,* Barcelona, Spain.

LIST OF PUBLICATIONS AND PRESENTED PAPERS

Journals:

1. ***Afroza Nahar***, Hasanuzzaman, M., Rahim, N. A. (2017). Numerical and Experimental Investigation on the Performance of a Photovoltaic Thermal Collector with Parallel Plate Flow Channel under Different Operating Conditions in Malaysia. *Solar Energy*, *144*, 517-528.

2. ***Afroza Nahar***, Hasanuzzaman, M., & Rahim, N. A. (2017). A Three-Dimensional Comprehensive Numerical Investigation of Different Operating Parameters on the Performance of a Photovoltaic Thermal System with Pancake Collector. *Journal of Solar Energy Engineering*, *139*, 1-16.

3. ***Afroza Nahar***, Hasanuzzaman, M., Rahim, N. A., & Parvin, S. (2017). Effect of Reynolds Number and Prandtl Number on Heat Transfer Characteristics and Performance of Photovoltaic Thermal System. *Arabian Journal of Science and Engineering* (under review).

4. ***Afroza Nahar,*** Hasanuzzaman, M., Rahim, N. A., & Hosenuzzaman, M. (2014). Effect of Cell Material on the Performance of PV System. *Advanced Materials Research, 1043*, 12-16 (ISI/SCOPUS Indexed Publication).

5. ***Afroza Nahar,*** Hasanuzzaman, M., & Rahim, N. A. (2017). Advances in Photovoltaic Thermal Technology: An Overview on Thermal Collector Design (ready to submit).

Conferences :

1. ***Afroza Nahar***, Hasanuzzaman, M., Rahim, N. A. (2014). Concentrated Solar Thermal Based Power Generation, *Proceeding of the 2nd Power and Energy Conversion Symposium*, PECS,2014, University Technical Malaysia, Melaka, Malaysia, 12 May 2014, pp.135-140. (Non-ISI/Non-SCOPUS).

2. ***Afroza Nahar***, Hasanuzzaman, M., Rahim, N. A. (2015). Numerical Investigation of the Performance of Photovoltaic Thermal System Using Nanofluid. *International Conference on Power, Energy and Communication Systems*, IPECS 2015, 24th to 25th August 2015, Arau, Perlis, Malaysia.